UNIVERSITAT DE BARCELONA

Adhesion molecules and effector T cells subsets associated with female genital tract infection

Jamal Qualai

Adhesion Molecules and Effector T Cell Subsets Associated with Female Genital Tract Infection

Jamal Qualai

2023
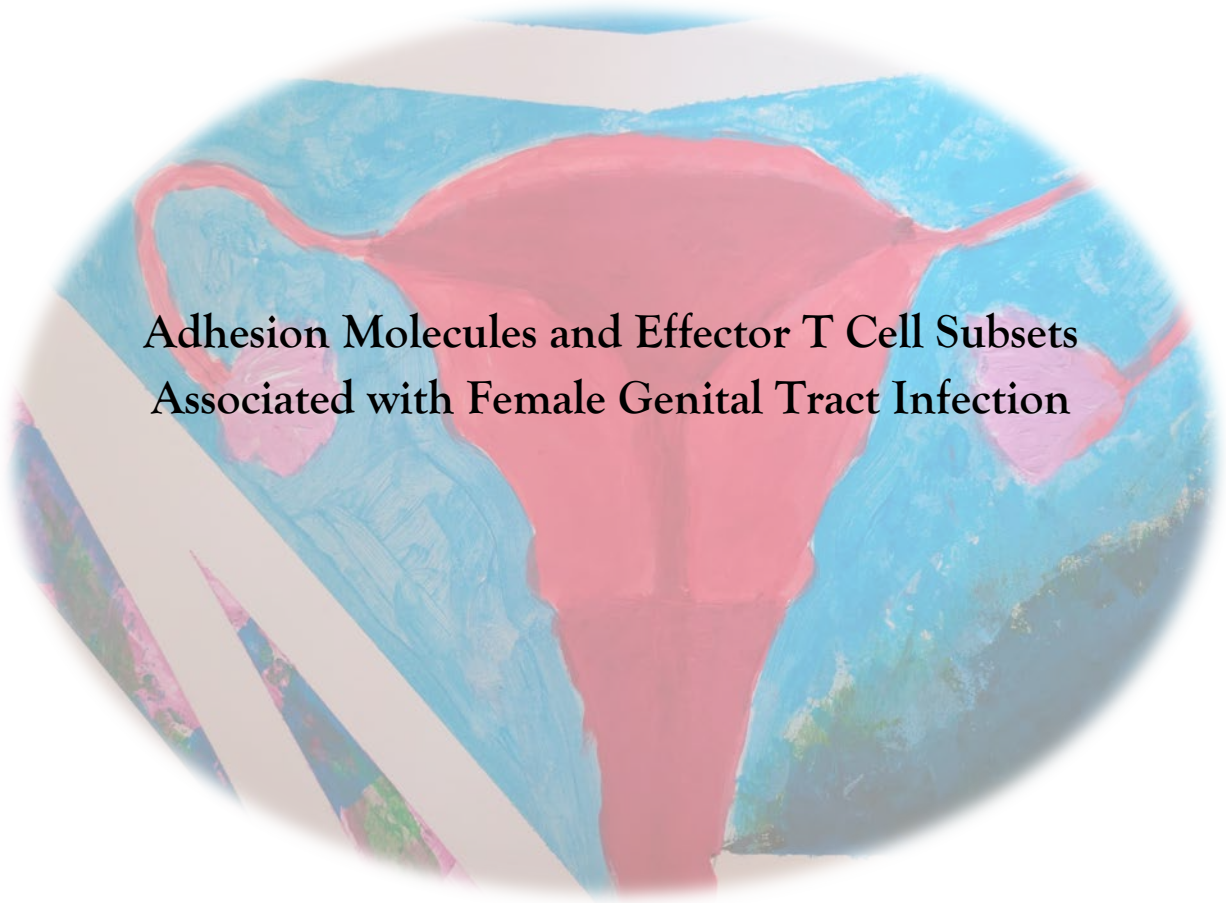
UNIVERSITAT DE
BARCELONA

Doctoral Program in Biomedicine

Adhesion Molecules and Effector T Cell Subsets
Associated with Female Genital Tract Infection

Doctoral thesis presented by Jamal Qualai Annan to qualify for the title of Doctor from
Universitat de Barcelona, 2023/2024

Doctoral student: Jamal Qualai Aannan

Director: Dra. Meritxell Genescà Ferrer

Tutor: Dr. Jorge Lloberas Cavero

Director: Dra. Meritxell Genescà Ferrer

Vall d'Hebron Research Institute (VHIR)

Infectious Disease Department

Tutor: Dr. Jorge Lloberas Cavero

Universitat de Barcelona, Faculty of Biology

Department of Cellular Biology, Physiology and Immunology

Immunology Section

Doctoral student: Jamal Qualai Aannan

Mucosal Immunology Unit,

German Trias i Pujol Institute (IGTP)

Jamal Qualai
15/05/2023 22:13 PM

Dedicated to my grandmother (Ma), my mother, my father,
my sisters and my nephews, with all my love.

Acknowledgment

La veritat és que no podia creure que arribo a escriure aquest apartat. El moment de fer-ho em sentia molt trist, perquè per mi és un comiat i conclusió d'una part de la meva vida molt llarga i plena d'acontexements, vivències, emocions i sobretot persones. Han sigut molts anys i les persones ha estat en aquest camí són moltes, axis que si m'oblido de tu, pèdon'm i gràcies.

Aquesta tesi doctoral ha estat dirigida per una dona, de temàtica en el camp de la salut de la dona. Mentre vas llegein aquest apartat veuràs que el 98% de les persones que han estat molt involucrades són dones. Axi, dedico aquest treball a totes les dones que han passat I estan en la meva vida.

Dono les gràcies a Txell, gràcies a ella he pogut arribar aquest punt. Li dono les gràcies per tot el temps que ha dedicat, el seu coneixement, l'acompanyament durant tota la tesi i sobretot la seva paciència. Em va obrir les portes del seu grup des de molt aviat, encara era estudiant de 4t de la carrera. Si m'he de recordar una emoció del primer dia que vaig parlar amb ella, seria l'alegria. Quan m'explicava el projecte m'ho explicava amb molt d'entusisme i elusió. Lo curios que fins avui, després de 7 anys segueixo veint el mateix quan parlem i potser això era el punt en comú bueno, això i ser una mica "cotilla" (això mateix ho diu Jon a la seva tesi, no m'ho invento!).

Gràcies a David el nostre tècnic i Jon el meu company de tota la part experimental. Encara me'n recordo el primer que m'ha dit Txell quan entraba Jon a trebllar amb nosaltres: " no el manis que tu t'agrada molt mandar" (té tota la raó). Amb en Jon era el meu primer intent de parlar castellà de manera fluida, dic intent perquè no ho aconseguia ni de conya. Li dono les gràcies per ajudarme amb tots els experiments, les grafiques i per moltes estones de terapia.

La part experimental de aquesta tesi doctoral s'ha fet a l'IGTP, lloc que tinc molts bons records i on he conegut persones molt maques. Persones que fins avui en dia mantenc una relació d'amistat. Dono les gràcies a Marc, Gerard i Iris que han estat en tota la part de citometria de fluxe. A Quim per ajudarme de manera molt dsinterasada a establirme en l'IGTP i en barcelona en genral. A les compis del lab: Noimi, Sara, Eva, Marina i vanesa.

Tota la part clinica i ITS s'ha fet en colaboracio amb ls servei de microbiologia de l'hospital germans trias i pujol. En especial dono les gràcies a Agueda, per enseñarme molt d'ITS i compartir amb mi tot el seu coneixement. Em sento molt agrait pels seus conseills i tot l'acompanyament que m'ha fet durant la meva estada. Dono les gràcies a Gemma per totes aquelles estones de riure i bon rollo que passavem entre experiment i un altre. També agraixo molt a totes les persones dels centres ASSIR que han participat en aquest estudi i sobretot a la Dra lopéz, la montse i l'Olga.

De les persones que han estat amb mi des del moment que vaig començar a escriure ha sigut la meva amiga Nina. Li dono les gràcies pels anims i l'enrgia positiva que em donava durant aquells moments d'ansietat i baxons. Puc dir amb veu molt alta, si no fos amb la seva ajuda dupto molt que hagi arribat a acabar d'escriure la tesi. Dono les gràcies a la meva amiga Victoria, amiga i ex compi de feina. Potser és la unica persona que en cada trucada em pregunta: i la tesi què?. Ha estat present en molts moments, sobretot durant 2 anys de covid fent guàrdies de 24 h!. Dono les gràcies a Jordi i Paula per escoltar-me i animar-me a seguir en els moments més baixos. Dono les gràcies a Vicent i Silvia per totes aquelles estones de caminar i xerrar, que per mi han sigut terapia. Dono les gràcies a la meva nova família de Qiagen, A Marta per ser tan bona companya i amiga, a Ana per dedicar una estona en cada reunió a preguntar-me què tal vaig amb la tesi, a Dani per treure'm molta feina i molts viatges i que pugui dedicar temps a escriure i corregir la tesi.

Estic arribant al final i potser és el més important. Dono les gràcies a la meva terapeuta Raquel que ha estat des del moment 0 fins ara i en tot aquest proces. Un procés que per mi ha sigut molt dur emocionalment i sense ajuda professional no ho hagués aconseguit. Aqui en el grup de psicòlogues dono les gràcies a Robert, per ser una persona molt important en una època de la meva vida i per totes aquelles teràpies . Dono les gràcies a Gina, l'amiga més exòtica que tinc. Aquestes tres persones han sigut el meu suport psicològic professional durant els set anys que ha durat aquest projecte.

Per acabar, dono les gràcies a la meva yaya, la meva mare, el meu pare, les meves germanes, les meves nebodes i nebots. Els hi dedico aquesta tesi amb tot l'amor i agraïments per acompanyar-me sempre.

Abstract

Common sexually transmitted infections like gonorrhea, Chlamydia, syphilis, and trichomoniasis are the leading cause of morbidity in developing countries. Adolescents and young women have the highest rates of STIs in developing countries. Pre-existing female genital tract infections affect the development and pathogenesis of other sexually transmitted infections, leading to long-term consequences such as pelvic inflammatory disease, cancer, and infertility. Efforts to develop vaccines against sexually transmitted infections have been hindered by the inability to measure immune responses in the genital tract. Effective vaccines should generate localized immune responses at potential exposure sites to provide faster and more robust infection control. Assays rely on blood samples to provide a complete picture of cellular traffic between lymph nodes and the mucosa, especially soon after infection. Studying and characterizing the homing profile of T cells becomes crucial to understanding mucosal immune responses against infections, and new methods to measure and manipulate immune responses are needed to develop effective STI vaccines. In this study, we examined how adhesion molecules are expressed by circulating effector T cells following mucosal infection of the female genital tract in mice and during symptomatic episodes of vaginosis in women. In a mouse model of Chlamydia infection, we observed preferential expression of CCR2, CCR5, CXCR6, and CD11c. However, during bacterial vaginosis in women, only CCR5 and CD11c were prominently expressed by effector T cells. We also investigated other homing molecules, like $\alpha 4\beta 1$ and $\alpha 4\beta 7$, previously suggested as essential for homing to the genital mucosa. Interestingly, these molecules showed differential expression in the patients. Surprisingly, CD11c, an integrin chain not commonly analyzed in the context of T cell immunity, was consistently elevated in all activated effector CD8+ T cell subsets studied. Additionally, CD11c expression was induced after systemic infection in mice, indicating that it is not exclusive to genital tract infection. Microarray analyses of activated effector T cells expressing CD11c from naïve mice revealed enrichment for genes associated with natural killer cells. Notably, flow cytometry analysis of murine CD11c+ T cells showed markers typically linked with non-conventional T cell subsets, such as $\gamma\delta$ T cells and invariant natural killer T cells. However, in women, the CD11c fraction of blood and cervical tissue mainly consisted of $\gamma\delta$ T cells and CD8+ T cells. These CD11c+ cells exhibited high activation levels and greater interferon (IFN)-γ secretion compared to CD11c- T cells. Moreover, circulating CD11c+ T cells in women correlated with the expression of multiple adhesion molecules, indicating a high potential for tissue homing. Our findings suggest that CD11c expression distinguishes a specific population of circulating T cells during bacterial infection, displaying innate capacity and mucosal homing potential. Furthermore, its increase in response to genital tract disorders may serve as a novel surrogate marker of mucosal immunity in women, offering potential applications in diagnostics and therapeutics. Further investigation is warranted to explore this potential thoroughly.

Abstract (Cat)

Les infeccions de transmissió sexual habituals com la gonorrea, la clamídia, la sífilis i la tricomoniasi són la principal causa de morbiditat als països en desenvolupament. Els adolescents i les dones joves tenen les taxes més altes d'aquestes infeccions. Les infeccions preexistents del tracte genital femení afecten el desenvolupament i la patogènesi d'altres infeccions de transmissió sexual, donant lloc a conseqüències a llarg termini com ara la malaltia inflamatòria pèlvica, el càncer i la infertilitat. Els esforços per desenvolupar vacunes contra les infeccions de transmissió sexual s'han vist obstaculitzats per la incapacitat de mesurar les respostes immunitàries al tracte genital. Les vacunes efectives haurien de generar respostes immunitàries localitzades als llocs d'exposició potencials per proporcionar un control de la infecció més ràpid i robust. Els assajos que es basen en mostres de sang proporcionen una imatge completa del trànsit cel·lular entre els ganglis limfàtics i la mucosa, especialment poc després de la infecció. Estudiar i caracteritzar el perfil de "homing" de les cèl·lules T esdevé crucial per entendre les respostes immunitàries de la mucosa contra les infeccions, a més a més, es necessiten nous mètodes per mesurar i manipular les respostes immunes per desenvolupar vacunes eficaces contra les ITS. En aquest estudi, es va examinar com s'expressen les molècules d'adhesió en les cèl·lules T efectores circulants després de la infecció de la mucosa del tracte genital femení en ratolins i durant episodis simptomàtics de vaginosi en dones. En un model de ratolí d'infecció per Chlamydia, vam observar l'expressió preferent de CCR2, CCR5, CXCR6 i CD11c. Tanmateix, durant la vaginosi bacteriana en les dones, només CCR5 i CD11c es van expressar de manera destacada per les cèl·lules T efectores. També vam investigar altres molècules d'homing, com $\alpha4\beta1$ i $\alpha4\beta7$, suggerides anteriorment com a essencials per a l'homing a la mucosa genital. Curiosament, aquestes molècules van mostrar una expressió diferencial en els pacients. Sorprenentment, CD11c, una cadena d'integrines que no s'analitza habitualment en el context de la immunitat de les cèl·lules T, es va elevar constantment en tots els subconjunts de cèl·lules T CD8$^+$ efectores i activades. A més, es va induir l'expressió CD11c després d'una infecció sistèmica en ratolins, cosa que indica que no és exclusiva de la infecció del tracte genital. Les anàlisis de microarrays de cèl·lules T efectores activades que expressen CD11c de ratolins naïfs van revelar un enriquiment per a gens associats a cèl·lules assassines naturals (NK). En particular, el anàlisi de citometria de flux de cèl·lules T CD11c+ murines va mostrar marcadors típicament vinculats amb subconjunts de cèl·lules T no convencionals, com ara cèl·lules T $\gamma\delta$ i cèl·lules T assassines naturals invariants (iNKT). Tanmateix, a les dones, la fracció CD11c de la sang i el teixit cervical consistia principalment en cèl·lules T $\gamma\delta$ i cèl·lules T CD8$^+$. Aquestes cèl·lules CD11c+ presentaven alts nivells d'activació i una secreció més gran d'interferó (IFN)-γ en comparació amb les cèl·lules CD11c-T. A més, les cèl·lules T CD11c+ circulants a les dones es van correlacionar amb l'expressió de múltiples molècules d'adhesió, cosa que indica un alt potencial per el "homing" cap a teixit. Els nostres resultats suggereixen que l'expressió CD11c distingeix una població específica de cèl·lules T circulants durant la infecció bacteriana, mostrant una capacitat innata i un potencial de "homing" cap a la mucosa.

A més, el seu augment en resposta als trastorns del tracte genital femení podria servir com a nou marcador substitut de la immunitat de la mucosa en dones, oferint aplicacions terapèutiques i altres potencials en diagnòstic. Es necessita investigació addicional per explorar aquest potencial a fons.

Content

List of Tables

List of Figures

Abbreviations

Ag	Antigen
AMP	Antimicrobial peptide
APC	Antigen-presenting cell
BV	Bacterial vaginosis
CAM	Cell Adhesion molecule
CD	Chron's disease
cDC	Classical dendritic cell
CLA	Cutaneous leukocyte antigen
CLEVER-1	Common lymphatic endothelial and vascular endothelial receptor 1
CM	Central memory
Cs	harge-switching synthetic particles
CT	Chlamydia trachomatis
CTL	Cytotoxic T lymphocyte
Cys	cysteine
DAMP	Damage-associated molecular pattern
DC	Dendritic cell
DP	Double-positive
EB	Elementary body
EM	Effector memory
EP	Epithelial cel
FBS	Fetal bovine serum
FGT	Female genital tract
FRT	Female reproductive tract
FSC	forward scatter
GALT	Gut-associated lymphoid tissue
GlyCAM-1	Glycosylation-dependent cell adhesion molecule-1
GM-CSF	Granulocyte-monocyte colony-stimulating factor
GPCR	G protein-coupled
GSEA	Gene Set Enrichment Analysis
GT	Genital tract
HBSS	Hanks' Balanced Salt solution
HEV	High endothelial venule
HIV	Human immunodeficiency virus
HMBPP	(E)-4-hydroxy-3-methyl-but-2-enyl pyrophosphate
HPV	Human papillomavirus

HSP60	Heat shock protein 60
HSV	Herpes simplex virus
HUGTP	University Hospital Germans Trias i Pujol
IBD	Inflammatory bowel disease
ICAM	intercellular adhesion molecule
IFNγ	interferon-gamma
IgA	Immunoglobulin A
IgSF	Immunoglobulin superfamily
IGTP	Germans Trias i Pujol Health Science Research Institute
ILC	Innate lymphoid cell
iNKT	Invariant T natural killer
IV	Intravenously
KLRG1	Killer Cell Lectin Like Receptor G1
LC	Langerhans cell
LFA-1	Lymphocyte function-associated antigen 1
LGT	Lower genital tract
LIF	leukemia inhibitory factor
LN	Lymph node
LP	Lamina propria
LPS	Lipopolysaccharide
LV	Lymphatic vessels
MAdCAM -1	Mucosal targeting cell adhesion molecule-1
MAIT	Mucosal-associated invariant T cell
MALT	mucosa-associated lymphoid
MaSigDB	Molecular Signatures Database
MHC	Major histocompatibility complex
MHCI	major histocompatibility complex class I
MIC	Transcription factor MIC
MOMP	major outer membrane protein
MR	Mannose receptor
MTB	Mycobacterium tuberculosis
ND	Normal donor
NK	Natural killer
NKG2A	NK group 2 member A receptor
NKT	Natural killer T cell
PAMP	Pathogen-associated molecular pattern

PBMC	Peripheral blood mononuclear cells
PBS	Phosphate-buffered saline
pDC	Plasmacytoid dendritic cell
PECAM	platelet-endothelial cell adhesion molecule
PI	Post-infection
PID	Pelvic inflammatory disease
PLGF	Placental growth factor
PS	Psoriasis
RB	Reticular body
RPMI	Roswell Park Memorial Institut
S-IgA	Immunoglobulin A secretory form
S1P	Sphingosine-1-phosphate
SD	Standard deviation
SIV	Simian immunodeficiency virus
SSC	Side scatter
STI	Sexually transmitted infection
TCR	T-cell antigen receptor
TEM	Effector memory T lymphocyte
TEMRA	terminally differentiated effector cells
TGF-β	Transforming growth factor-beta
Th	T-cell helper
TLR	Toll-like receptor
TNF	Tumor necrosis factor
Tregs	T regulatory cells
TRM	Resident's memory T lymphocyte
UC	Ulcerative colitis
UGT	Upper genital tract
VAG	Vaginally infected
VCAM-1	Vascular cell adhesion molecule 1
VEGF	Vascular endothelial growth factor
VLA-4	integrin very late antigen-4

0 Introduction

0.1 Mucosal immunology overview

The concept of mucosal immunity system refers to the local immune system that protects mucous membranes covering the aerodigestive and the urogenital tracts, as well as the eye conjunctiva, the inner ear, and the ducts of all exocrine glands against potential threats from the environment (1,2). These cells are accumulated in, or in transit between, various mucosa-associated lymphoid tissues (MALT), forming the most extensive mammalian lymphoid organ system together. It is considered a primary force that drives the development and stimulation of the entire immune system during evolution as well as in ontogeny. The mucosal immune system continuously interacts with antigens (Ag) contained in food, air, microbiota, and other immunogenic compounds. Cells involved in the mucosal immune system result from a selective evolutionary process creating specialized cells involved in Ag uptake, processing, presentation, and the production of innate and specific immune responses. Immune mechanisms occurring at the mucosal tissue have three significant functions: protection of the mucosal tissue against pathogens; avoiding blood circulation uptake of Ags like xenobiotics, foreign proteins, and external pathogens; finally, and perhaps the most critical function is the regulation of immune overresponse to all foreign compounds in case they cross the barrier to the systemic circulation (3).

0.1.1 Antigen uptake and presentation in local mucosal sites

0.1.1.1 Epithelial cells as the first mucosal barrier

Once a pathogen enters a mucosal site, several cell populations specialized in Ag uptake, processing, and presentation are activated to initiate the immune response. These mechanisms involve epithelial cells (EP), which beyond their role as a physical barrier, are closely related to local immune cells such as Ag presenting cells (APC) and mucosal-associated T and B cells, thus playing a critical role in mucosal induction sites (3,4). In addition, the epithelial barrier comprises different mechanisms involved in innate and adaptive responses (4–6).

Collaboration between EP and the underlying T, B, and dendritic cell (DC) cells is crucial in the immune response's inductive and effector phases. During pathogen invasion, EPs secrete various humoral factors of the innate system, regulatory cytokines, and chemokines (7,8). These secreted molecules affect myeloid and lymphoid cells' recruitment, activation, and differentiation. In addition, some cytokines produced by EPs in collaboration with T cells and the microbiota are essential for differentiating B cells toward synthesizing immunoglobulin A (IgA). IgA is the predominant immunoglobulin in mucosal secretions produced through EPs in secretory form (S-IgA). The mucosal epithelial barrier produces S-IgA (active form), adding peptide chains and glycans. These additives give S-IgA the ability to adhere efficiently to the bacterial wall and high stability (9,10).

0.1.1.2   Myeloid lineage cells as antigen-presenting cells

Neutrophils, monocytes, macrophages, and DCs form the myeloid cell lineage. This group of cells is responsible for monitoring the mucosa constantly, processing the external Ags, and emitting alarm signals to the rest of the immune cells. First, they phagocytize and destroy pathogens through acid and enzymatic digestion, then present Ags on the surface to educate the rest of the immune cell players. They can rapidly respond to pathogens using interactions that recognize highly conserved pathogen-associated molecular patterns (PAMPs) such us toll-like receptor (TLR) between others (11,12). The common myeloid precursor is formed during embryonic development in the yolk sac and later ends up in the bone marrow. Monocyte progenitors colonize various organs such as the liver, brain, skin, and lungs. Once they are in the tissue, they differentiate into resident macrophages. DCs can arise from bone marrow precursors but can also be derived from monocytes under inflammatory conditions. Additionally, neutrophils are differentiated from granulocytes as their precursor (13,14).

Monocytes are intermediate cells between bone marrow progenitors and resident phagocytes, although they are also associated with an effector function during inflammatory processes (15). In humans, three major types of monocytes are known based on the expression of CD14 and CD16, chemokines receptors, and integrins (16). Classical monocytes usually are $CD14^+CD16^-$, non-classical $CD14^{dim}CD16^+$ and intermediate $CD14^+CD16^+$(17). $CD14^{++}CD16^-$ or $CD14^{++}CD16^+$ monocytes are the precursors of macrophages and monocyte-derived DC; this differentiation occurs in response to infection or tissue injury (15). They are sources of inflammatory mediators such as nitric oxide, reactive oxygen species, and tumor necrosis factor (TNF). $CD14^{dim}CD16^+$ monocytes monitor blood vessels with remodeling and angiogenesis functions, in addition to early responses against external attacks (18).

A. Dendritic cells

DCs are mononuclear phagocytes with different phenotypes and functions. DC plays a crucial role in initiating and modulating the immune response. Their functions have been described in infectious diseases, autoimmunity, transplantation, and cancer. DC maturation involves exposure to PAMPs and damage-associated molecular patterns (DAMPs), causing changes in intracellular metabolic pathways, gene transcription, membrane proteins, and metabolic activity. In addition, DC's Ag presentation by the Major histocompatibility complex (MHC) receptor class I and II leads to the stimulation of T-cell receptors (TCR) of cytotoxic T lymphocytes (CTL) and helper T cells (Th), respectively (19).

DCs subset		Location	Surface markers		
cDCs	Mouse cDC1 (CD8α+)	Lymphoid organs	MHC-II+ B220− CD4− Ly6C−	CD8α+ CD11b lo CD11chi CD24hi	CD205+ (DEC-205+) CD207+ (Langerin+) CLEC9A+ XCR1+
	Mouse cDC1 (CD103+)	Lymphoid organs and non-lymphoid organs	MHC-II+ B220− CD8− CD86+	CD80+ CD11b+ CD11c+ CD24+	CD103+ CD205+ (DEC-205+) CD207+ (Langerin+) XCR1+
	Human cDC1 (CD141hi)	Lymphoid organs and non-lymphoid organs	CD11c lo CD45+	CD141hi (BDCA-3hi) CLEC9A+	XCR1+
	Mouse cDC2 (CD11b+)	Lymphoid organs and non-lymphoid organs	MHC-II+ F4/80− CD4+ CD11b+	CD11c+ CD24+ CD64+	CD103− CD172a hi (SIRPα hi) XCR1 lo/−
	Human cDC2 (CD1c+)	Lymphoid organs	MHC-II+ CD1a lo/+ CD1c+ (BDCA-1+) CD11c+	CD14− CD16− CD172a+ (SIRPα+)	XCR1− FcεRI+ CD207− (Langerin−)
pDCs	Mouse pDCs	Blood, lymph nodes and lymphoid tissues	MHC-II lo CD4+ CD11b− B220+	CD11c lo CD25lo CD38+ CD40−	CD43+ CD62L mid Ly6C hi
	Human pDCs	Blood and bone marrow	MHC-II lo B220+ CD1a− CD4+ CD11a+ CD11c− CD13−	CD14− CD38 lo CD16− CD18+ CD33− CD40 lo CD44+	CD54+ CD62L+ CD123+ (IL-3Rα+) CD127− (IL-7Rα−) CD303+ (BDCA-2+) CD304+ (BDCA-4)

Figure 1. Classification of DCs depending on their surface markers and anatomical location (adapted from (20))

DCs are highly heterogeneous and comprise two main subtypes (Figure 1). This differentiation is based on immunological functions, anatomical location, and phenotypic markers. All DCs express MCH II (HLA-DR), which increase during maturation (20). This lineage lacks CD3 and CD19/20 expression. The higher heterogeneity of DCs' is reflected by their anatomical locations (21). Diverse subsets are described in the literature: classical DCs (cDCs), plasmacytoid DCs (pDCs), monocyte-derived DCs, and other special populations, such as Langerhans cells and dermal DCs (22–24).

cDCs express CD11c and have two major subtypes, cDC1 expressing blood dendritic cell Ag 3 BDCA3/CD141/thrombomodulin and cDC2 type expressing blood dendritic cell antigen 1 (BDCA1)/CD1c. In addition, a new subtype named cDC3 has recently been described with a different molecular profile than the other two types (21). Subtypes 1 and 2 are very efficient cells for stimulating Ag-specific CD4 and CD8 T cells. Subtype 3 has been described in a tumor context in humans and mice. In contrast, pDCs express CD123 and CD303 (CLEC4 C/BDCA-2) and are specialized in producing type I interferons (IFN-

α and IFN-β) against viral infections. CD1c+ cDC2 is the most common subset in blood, while pDCs are frequent in the thymus and tonsils (22,25).

Unlike cDCs, pDCs are difficult to find in tissues and mucosa. pDCs circulate in the blood and can also be found in the peripheral lymphoid organs, and they are recruited to the mucosa soon after infection or during inflammation (22). In mucosa, different subtypes of DCs can be isolated: Langerhans cells located in the mucosal epithelium, and DCs located in the lamina propria, which may include dermal DCs and interstitial DCs. Langerhans cells are the most frequent DC subset on the mucosal surfaces of the anogenital tract, foreskin, and vaginal mucosa. In the intestinal mucosa, different populations of cDC can be isolated in humans and mice (26–28).

B. Macrophages

Macrophages have been described in different tissues of the human body. For example, they are found in the liver, the epidermis, the pulmonary alveoli, the uterus, the cervix, and breast milk. These cells have physiological functions related to metabolism, tissue repair, and vigilance against external attacks. Macrophages are susceptible to the tissue and cellular environment and respond to their signals. The two best-known macrophage subtypes are M1 and M2 (Figure 2) (29). M1 macrophages are proinflammatory and produce interleukin 6 (IL-6), IL-12, and TNFα; on the contrary, M2 macrophages have an anti-inflammatory profile participating in tissue repair processes. Differentiation and identification of macrophages as M1 or M2 is considered, by many authors, not accurate because of their versatility and changing phenotype (30,31). Other subtypes are described in the literature: CD169, tumor-associated macrophages, and the last ones described TCR[+]. All these populations differ in the expression of certain molecules, making them phenotypically and functionally unique (31).

Monocytes expressing C-X-C chemokine receptor type 1 (CX3CR1) and C-C chemokine receptor type 2 (CCR2) can be recruited to the mucosa. Once in mucosal sites, they differentiate into resident mucosal macrophages expressing different transcription factors, chemokine receptors, and TLRs (32). Macrophage phenotypes vary considerably depending on the local environment. For example, resident macrophages in the human intestinal mucosa express HLA-DR, CD13, CD33, and CD64 (as a specific macrophage marker that can be used to discriminate DCs from macrophages) but do not express CD11a, CD11b, CD11c, CD14, CD18, CD89, although these receptors are strongly expressed in human blood monocytes(33). There is controversy regarding the CD11b expression in macrophages since it has been described in intestinal mucosa only under inflammatory conditions (34,35). Together with DCs, macrophages play a vital role in promoting T cell recruitment through the secretion of chemokines in response to viral and bacterial infections (36).
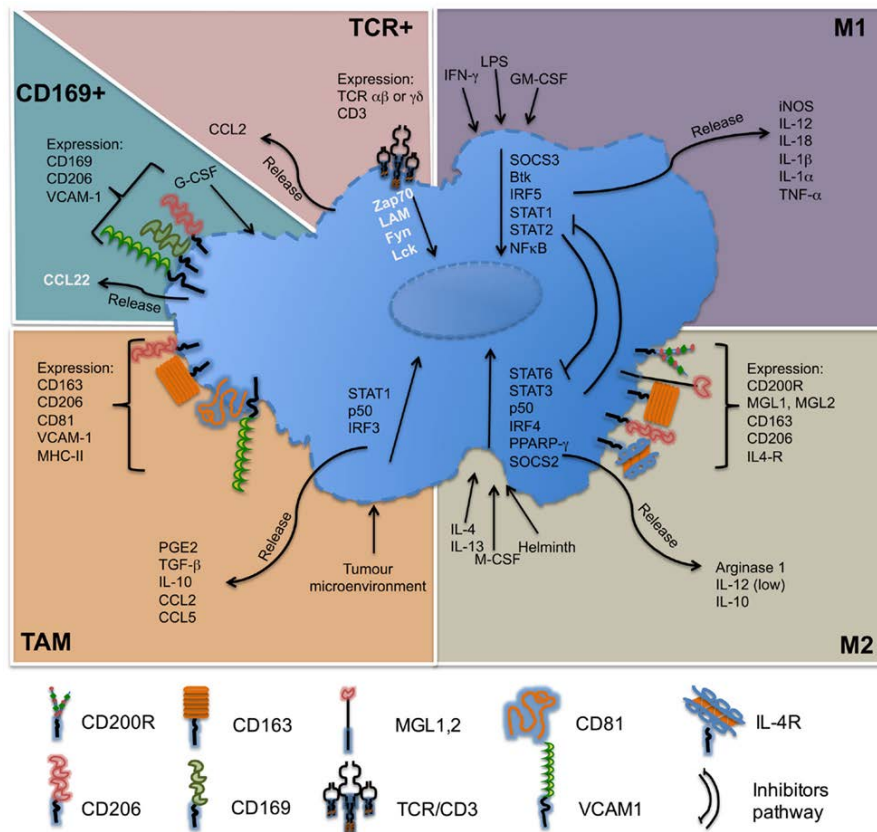
Figure 2. Functions and plasticity of different subtypes of macrophages (from (29))

C. Neutrophils

Neutrophils are part of the innate myeloid lineage, belonging to the granulocytes, and are characterized by an arsenal of cytotoxic factors that are released during inflammatory responses. However, unlike other myeloid cells, they have short life cycles, and their frequency changes between steady-state and inflammatory conditions. Neutrophils migrate from blood to the mucous membranes, and once they finish their function, the macrophages eliminate them.

0.1.2 Lymphocytes lineage as an effector immunity system in the mucosa

Different lymphocyte populations are implicated in protecting mucosal sites against viral and bacterial infections. After Ag presentation in the LN by APC, T, B, and other mucosal-specific lymphocyte populations are activated and migrate to the tissues for protection (4). In this section, the different populations of lymphocytes known in blood will be described, specifically, the CD4 and CD8 with their respective subtypes, in addition to the natural killer cells (NK) and other non-conventional T cell populations. In blood, other populations of lymphocytes are isolated (such as B cells) that we will not describe in this work.

0.1.2.1   CD4 and CD8 T Lymphocytes

CD4 and CD8 T cells represent heterogeneous populations with different phenotypes. Their differentiation is based on maturation and activation markers, chemokine receptors, cell adhesion molecules, and transcription factors (37).

T lymphocyte-mediated adaptive immune responses are crucial for protection against a range of pathogens, depending on the fast mobilization of T cells to infection sites. Naïve T cells are primed in the lymph nodes (LNs) by DCs, which induce clonal expansion and differentiation from naive to effector memory phenotype (38). Memory T cells can be divided into three classical functionally distinct phenotypes: effector memory T cells (EM) present in the blood, spleen, and nonlymphoid tissues; central memory T cells (CM) in lymph nodes, spleen, and blood (but scarce in nonlymphoid tissues) and finally, memory T cell subsets retained in tissues as non-circulating tissue-resident memory T cells (TRM) expressing CD103, and CD69 markers (Figure 3) (39). TRM mediates the best protective immunity to site-specific infections compared to circulating memory subsets (40). Circulating memory T cell classifications are based on CCR7 and CD45RA. Likewise, EM cells have a phenotype CD62L– CCR7– CD45RA– CD45RO+, CM cells are CD62L+ CCR7+ CD45RA– CD45RO+ (37,41–45).

Memory T cells are heterogeneous and follow a differentiation hierarchy after activation. Signal intensity and/or magnitude of activation create other phenotypes that are less abundant. In blood, we can also find the T memory stem cells (SCM) with multipotent and higher proliferative capacity with CD45RA+CD45RO− profile, expressing high levels of the co-stimulatory receptors CD27 and CD28, IL-7 receptor α-chain (IL-7Rα), CD62L and CCR7 (38,40,46). This characteristic gives them the capacity to differentiate into other subsets, including CM and EM. In the other extreme of differentiation, we find terminally differentiated effector cells (TEMRA) (38) . This subset is considered to be short-lived and terminally fated with an EM phenotype, low expression of CD127 and higher expression of Killer Cell Lectin Like Receptor G1 (KLRG1) (38). Other subtypes are found in the blood: Memory T cells with Naïve Phenotype, Peripheral Memory T cells, and Long-Lived Effector Cells (38). In this work, we will focus on the classically known memory phenotypes.
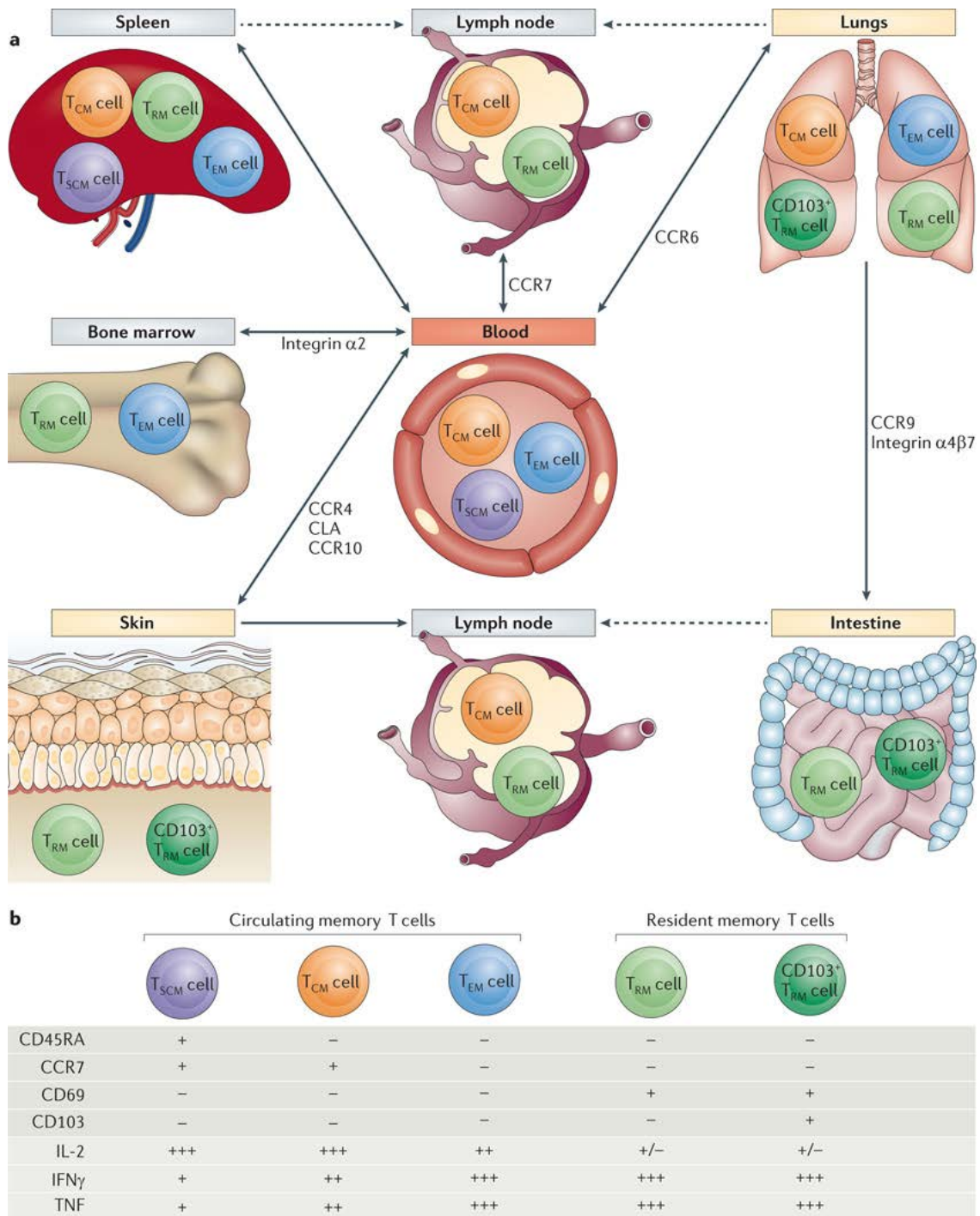
Figure 3. Distribution and migration patterns of classical human memory T cells (a) with phenotypic characterization (b) (39)

Naive cells are activated in the LNs by DCs and acquire an effector phenotype for their circulation into the blood and then homing to the tissue. Regarding the activation of T lymphocytes, different markers have been described that can be classified as receptor proteins, chemokine receptors, adhesion molecules, and other costimulatory receptors. One of the early activation markers in the blood is CD69 (47,48). MCH II isotypes (HLA-DR, HLA-DQ, and HLA-DP) are considered markers of activation in the blood that are overexpressed 3-5 days after infection, and for this reason, it is considered a late marker of

T lymphocyte activation (49,50) . Other activation markers have been described in the literature, such as CD38, CCR5, CD49d, and CD29 (49,51).

The polarization of CD4 and CD8 lymphocytes results in a lineage with specific and complementary functions between them and other immune system cells Figure 4. During the positive selection process, detecting Ags presented by the major histocompatibility complex class I (MHCI) or class II (MHCII) by the rearranged TCR decides the destiny of the CD4 or CD8 lineage, respectively (52). Roughly CD4 T cells are differentiated as T helper cells (Th) and CD8 T cells as cytotoxic T cells (Tc) (52). Figure 4 summarizes the function and markers of the different Th and Tc subtypes originating after activation by an APC.
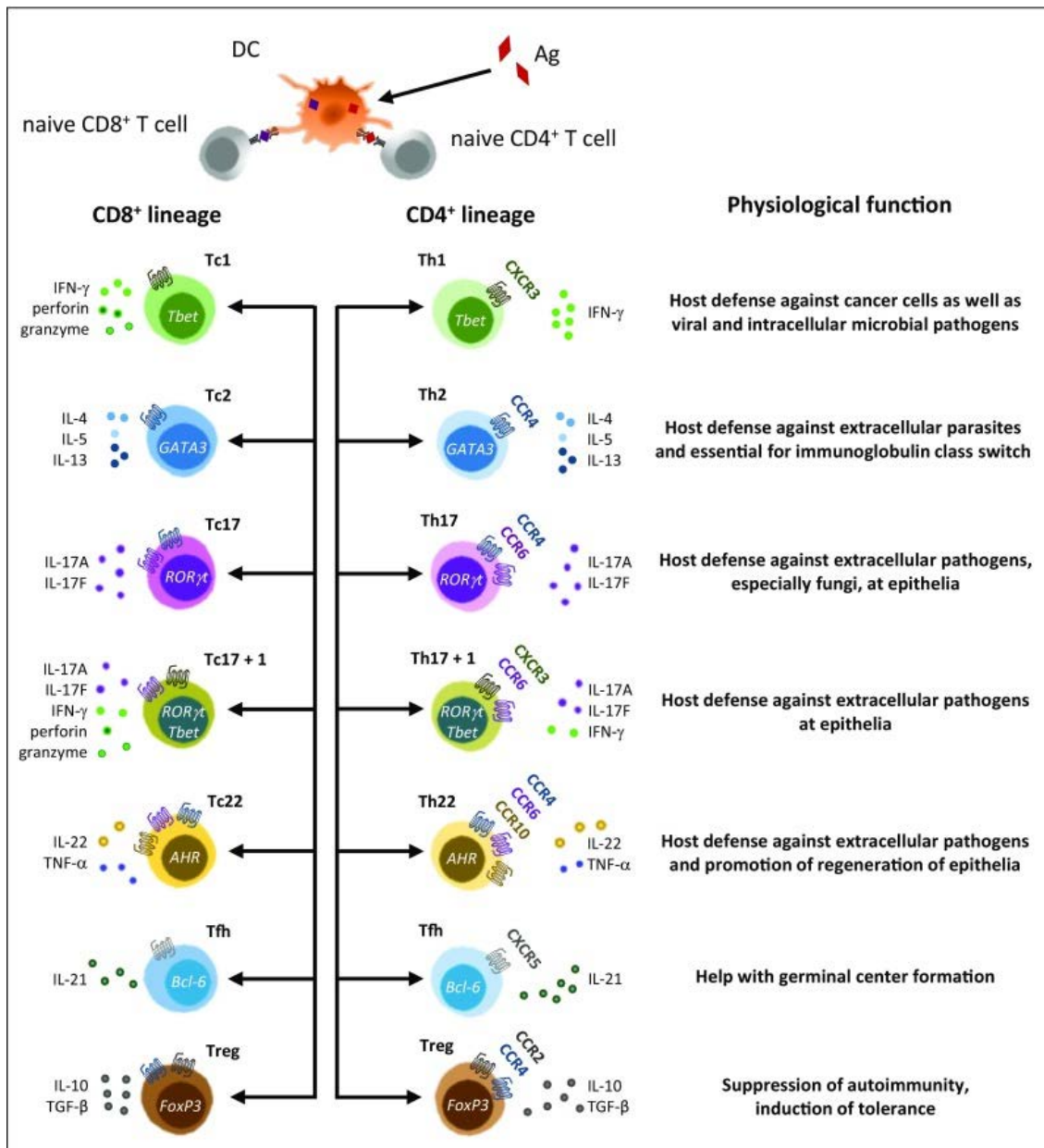
Figure 4. CD4 and CD8 T cell lineage after priming and their functions (52)

A. Effector CD4 T Lymphocytes

CD4 cells can differentiate into Th profiles based on the expression of CXCR3 and CCR6. CXCR3+CCR6−, CXCR3-CCR6−, and CXCR3-CCR6+ characterize Th1, Th2, and Th17 populations, respectively (10). Furthermore, they are regulated by transcriptional factors such as Tbet, RORγt, GATA3, AHR, Bcl6, and Foxp3 (53,54).

Th1 cells eliminate intracellular bacteria and viral infections. In addition, activated Th1 cells acquire the capacity to produce IFNγ in response to IL-12 and IFNγ and preferentially express chemokine receptors such as CCR5 and CXCR3 that drive them to mucosal effector sites (54,55).

Th2 cells are known for their role in the defense against intestinal parasites. During infection, EC produces lymphopoietin that attracts APC to the site, initiating a Th2-type response against parasites. In addition, APC produces IL-4, which activates the Th2 response through IL-4 and IL-13 production (55). In the context of Th2 homing, the CCR4 receptor is closely related to their activity in the skin mucosa. Among the various T-cell subsets, CCR4 is predominantly expressed by Th2 cells, cutaneous lymphocyte antigen (CLA)-positive skin-homing T cells, and T regulatory (Tregs) cells. Thus, CCR4 attracts much attention for its potential clinical applications in diseases involving these T-cell subsets (54,55)

The Th17 population produces IL-17-A and IL-17-F, which promote the recruitment of neutrophils to clear extracellular bacteria and fungi (56,57). Th17 is differentiated from Th2 by CCR6 expression. In addition, in Crohn's disease (CD), Th17 and Th1 express CCR9 homing receptors to migrate to the intestinal lamina propia (LP) (58).

Other subsets, like Tregs, are crucial for the induction of tolerance to the local microbiota in the mucosa and play an essential role during tumoral responses. Additionally, it is worth highlighting the role of Th22 as epithelial repairers and their collaboration with Th17 as innate regulators of antimicrobial responses and mucosal integrity (55).

B. Effector CD8 T lymphocytes

Cell-mediated immunity involves activated cytotoxic effector CD8+ T-cells, which recognize antimicrobial peptide-expressing cells associated with MHC-I and induce apoptosis in the infected cells using granzymes and perforins, among other mechanisms (59).
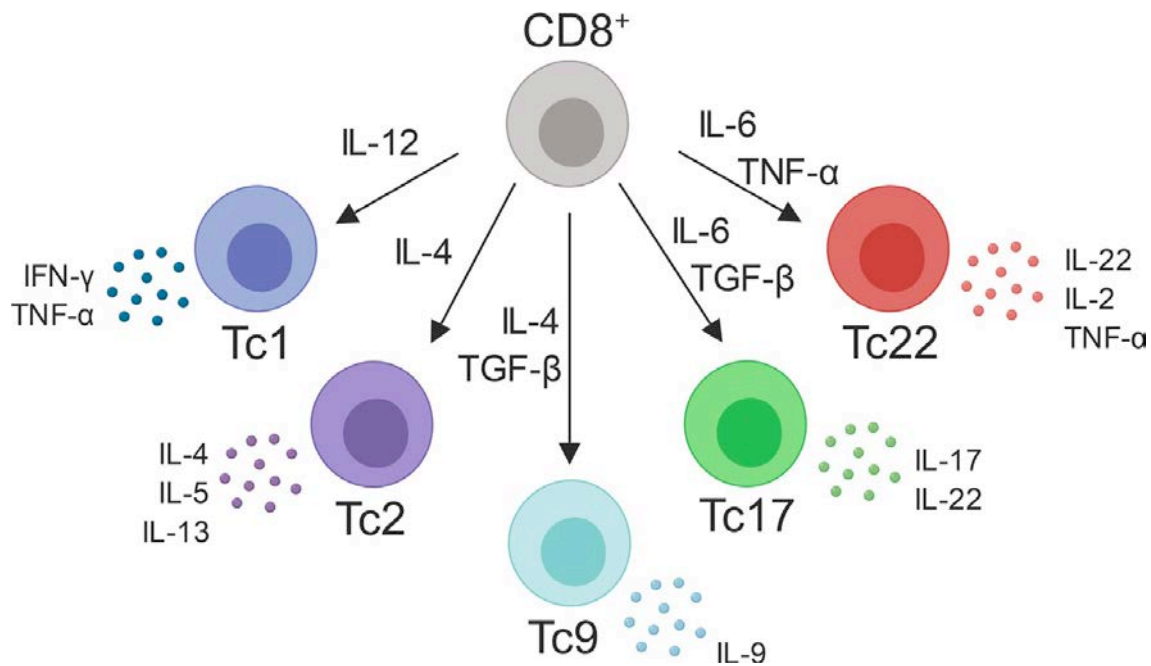
Figure 5. Cytotoxic CD8 T cell subtypes and their IL profile (60)

CD8 cells were classically considered uniform cells limited to secreting IFN-γ and granzyme B protease. However, a great diversity of Tc CD8 cells is currently known. In addition, there are cytotoxic profiles that reflect the Th CD4 phenotypes. The polarization of Tc CD8, like Th CD4, is done under the effect of a cocktail of cytokines. A transcription cascade induced by exposure to polarizing cytokines which will define the lineage phenotype (52,60,61).

The Tc1 CD8 lineage embodies the cytotoxic cells classically known for their extraordinary capacity to kill tumors and infected cells. They differ in their high production of perforins, granzyme B, IFN-γ, and TNF. The action of IL-12 generates the induction of the Tc1 phenotype (60).

The Tc2 CD8 lineage includes cells with cytotoxic capacity; however, they are known for producing IL-4, IL-5, IL-13, granzyme B, and minor production of IFN-γ. IL-4 induces the polarization of this subtype. These cells have been described in the context of allergies and respiratory tract infections (60).

Tc17 CD8 cells are known for their high production of IL17A, IL-17F, and IL-22. However, they do not have an efficient cytolytic capacity since they produce little granzyme B. The Tc17 profile is induced by IL-6 and transforming growth factor-beta (TGF-β) (also enhanced by IL-1β, IL-21, and IL-23). This phenotype has been described in skin tissue, tumor environments, and in response to fungal infections (60).

The Tc22 profile is known for its high cytotoxicity and closely resembles its Th17 counterpart. Its phenotype is quite controversial since it produces IL-22 as well as IL17. Their differentiation occurs thanks to the action of IL-6 and TNF. Tc22 activity is related to tissue repair (like Th22), inflammation, and viral infections in mucosal tissues (60).

Other CD8 polarizations, such as regulatory CD8 and follicular CD8, have functions similar to those corresponding to the CD4 T helper counterpart. Finally, the last described profile is Tc9 CD8 cells. They are known for feeble cytotoxic effects and polarization under the action of IL-4 and TGF-β action (60).

0.1.2.2   Natural Killer

NK cells are lymphocytes with an innate activity and spontaneous ability to kill cells. NK cells represent between 5 and 20% of circulating lymphocytes in the blood. Two main types of NK cells can be differentiated: the conventional ones that circulate in the blood and are the most studied since it is easy to access them, and NK cells residing in tissues and organs such as the liver, the uterus, the kidneys, lungs, lymph nodes, and thymus. NK cells in blood present two major phenotypes: CD3−CD56bright CD16− and CD3−CD56dim CD16+, the latter being associated with mature NKs. CD56dim cells are associated with great cytotoxic activity and are the most abundant in blood, while those that express CD56bright are great producers of cytokines and are abundant in tissues. NK cells have an array of activating and inhibitory receptors. The balance between these receptors ensures these cells' cytotoxic functionality and tolerance to self-body Ags (62–64).

0.1.2.3   Unconventional T lymphocytes population associated with the mucosa

Additionally, to the classical population of T lymphocytes, mucosal tissue has a particular T cell population associated with immune surveillance and pathogenesis. Among these unconventional T cells, we find γδ-T cells, mucosal-associated invariant T cells (MAIT), and T natural killer (NKT), including invariant (iNKT) cells (65,66). MHC class Ib molecules restrict all these cells and migrate toward the tissues during the first stages of development (67,68). Once in the tissue, these cells are instructed and trained via exposure to molecules derived from the local microbiota and other environmental Ags (67,69). Although innate-like lymphocytes are less common in circulation than their conventional counterparts, they are more prevalent at mucosal barrier regions, where they exhibit quick and strong antimicrobial responses and are assumed to play a significant role in immunosurveillance. Unconventional lymphocytes express various pattern recognition receptors (PRRs), allowing them to recognize conserved microbial antigens quickly (68,69).

A. NKT and iNKT

NKT cells coexpress αβTCR from T lymphocytes and NK markers such as CD161 (in mice NK1.1). In addition, unlike conventional T cells, NKT recognizes glycolipids Ags presented in the CD1d receptor by an APC. Like NK, NKT cells produce granzyme and perforin, essential in the innate mucosal system (70).

Like the development of CD4 and CD8 T cells in the thymus and their branch off at the double-positive (DP) stage, NKT undergoes the same process and is positively selected through CD1d engagement. Finally, NKT finishes maturation in the periphery expressing an NK phenotype. NKT cells are present at the naïve stage in blood; after activation, this

population expresses NK cytotoxic markers and migrates to the affected site of the mucosa (homing). However, another subset of NKT cells, called invariant, differs in TCR receptors from classical T cells (71,72). iNKT cells, as occur to MAIT cells, vary on their TCRs, specifically in the Vα chain. For example, the TCR of the iNKT cell population in mice contains the Vα14 gene segment, whereas its human counterpart uses Vα24. Further, in mice, iNKT cells are CD4− CD8− or CD4+ single positive, which is similar to humans, except for a small population of iNKT cells expressing CD8αα homodimers (73,74).

iNKT cells are reactive against lipid Ags, recognizing self and other microbial Ags presented by CD1d. APCs and EP are crucial in presenting Ags for activating iNKTs in the mucosa. APCs constitutively express the CD1d receptor, especially CD11c DCs. After activation, iNKT cells produce Th1 and Th2 cytokines with higher cytotoxic potential (73,74).

B. Mucosal-associated invariant T cells

MAITs cells are similar to iNKT cells and display an invariant Vα chain. MAIT cells express CD161, a C-type lectin-like membrane receptor found on many NK and iNKT cells; also, they express other activating and inhibiting NK receptors. In humans, MAIT cells are mostly CD8αα, CD8αβ^{int}, or double negative cells. In peripheral blood, they display an effector/memory phenotype (CD45RA$^{−}$, CD45RO^{+}, CD95^{hi}, CD62L^{lo}) (72,75). MAIT cells are present in blood, liver, thymus, and tissues, such as in the LP of the intestines or the mesenteric lymph nodes. Depending on the location, MAIT cells express CCR9^{int}, CCR7, CCR5^{hi}, CXCR6^{hi}, and CCR6^{hi}, which indicate a higher potential for homing or being retained in the tissue (76).

C. γδ-T cells

γδ-T cells are nonconventional lymphocytes that also vary in their TCR receptors. In this case, they express γ and δ chains in their TCR, unlike the classical α and β chains of most T lymphocytes (77). Based on the Vδ chain, we can find two subsets of γδ-T cells. Vδ1+ T cells are located in epithelial tissues of mucosa such as the intestine, uterus, and lung; they are activated by peptidic ligands, stress-induced self-Ags, and glycolipids presented by CD1c and MHC class I chain-related receptors. In contrast, Vδ2+ T cells are present in a higher percentage in blood and respond to nonpeptidic molecules and phosphoantigens stimuli from stressed cells and microbial infections (78,79).

These cells are associated with the immune response against viruses, bacteria, and protozoa. They also play an essential role in orchestrating the immune response during inflammation, tumor surveillance, and autoimmune diseases. Their main functions are cytotoxic activity and the secretion of IFN-γ, IL-17, antimicrobial substances, and growth factors (80). In addition, γδ-T cells play a vital role against infections in the mucosa. For example, it has been described that they are capable of clearing skin protozoa parasites in humans (81). Their homing mechanism remains unclear but seems essential in mucosal infections (82).

0.2 Lymphocyte Trafficking to Mucosal Tissues

Cellular traffic between LNs and the tissues, including the mucosa, is dynamic, especially after infections. The movement of T lymphocytes after mucosal infection involves a sophisticated and finely tuned system through the expression of specific molecules that drive these cells to the appropriate tissues to clear the infection (83). The capacity of distinct subpopulations of T cells to traffic selectively into the compartment of initial Ag contact is termed 'homing.' T cells sensitized to Ag in mucosal inductive sites leave the site of Ag presentation in the mucosa, move through the lymphatics to enter the blood, recirculate, and ultimately re-enter mucosal tissues. Most of these cells re-enter their original site in the mucosa, differentiating into memory or effector lymphocytes (84,85). Then, memory T cells are retained in the tissue presenting higher reactivity for current and future conditions, most likely as TRM (85–87).

0.2.1 Lymph node trafficking

Adaptive immunity depends on T-cell migration and homing. T cells may move fast and quickly across great distances through blood arteries and lymphatic vessels (LV). They move through the lymphatic system in two different ways: LNs, where they exit into efferent lymphatics to return to the bloodstream, and outside tissues, where they exit the tissue through afferent lymphatics to move to draining LNs and back into the bloodstream (88,89). The lymphatic system comprises a network of blind-ended lymphatic capillaries in peripheral tissues, which merge into larger collecting arteries that drain into and via LNs. Lymph is returned to the blood vasculature through the thoracic duct, which merge into the subclavian vein after passing through tissue-draining LNs and joining contiguous collecting LVs (90).

0.2.1.1 Afferent and Efferent trafficking

Efferent lymph collected after passage through one or more LNs is composed of 90% of T lymphocytes in human and animal models. CD4+ T cells enter and recirculate through LNs more rapidly than CD8+ T cells, making them a significant cellular fraction in efferent lymph. In steady state, most cells collected in efferent lymph are naïve (90,91)owever, the composition change after antigenic stimulation in LN (90). There are frequently three distinct phases to the efferent lymph response that are triggered by antigenic stimulation of LNs: an initial "LN closure" in which lymphocyte output is reduced; a "recruitment phase" in which lymphocyte output rises above resting levels; and a "resolution phase" in which lymphocyte output and cellular composition return to basal levels (91).

αβ T lymphocytes are the most prevalent cell type in afferent lymph, specifically CD4+ T cells. However, the total cell number is less than in efferent lymph, where T cells have a TEM phenotype with increased expression of common T cell activation markers, adhesion molecules, and effector cytokines (90). Additionally, steady-state afferent lymph frequently contains DCs, monocytes, B cells, and a small number of granulocytes. During chronic

inflammation, CD4$^+$ and CD8$^+$ T cells substantially increase in efferent lymph; while their number does not change during acute inflammation (89,90).

0.2.1.2 T cell recirculation, egress, and retention in and out of lymph nodes

Through a multistep adhesion cascade, naive T cells enter from the blood to LN through the high endothelial venule (HEV) and go to T cell regions in the paracortex. T cell intranodal location, migration, and motility are regulated by the CCR7 and its two ligands, CCL19 and CCL21 (91,92). Naive T cells transmigrate into the cortical or medullary sinuses and leave through the efferent LV after spending some time looking for a particular antigen encounter. T cell egress from the LN into the efferent LVs is mainly mediated by CCR7, sphingosine-1-phosphate receptor 1 (S1PR1), CD69, and other adhesion molecules mechanisms (Table 1) (91).

Table 1. Molecular regulation of the T cells exits from LNs (adapted from (93))

Mechanisms	Role
S1PR1	S1PR1-deficient T cells are retained in LNs; disruption of the S1P gradient in LNs prevents T cell egress
CD69	CD69 expression induces S1PR1 internalization and degradation in T cells resulting in T cell retention in LNs (and tissues)
CCR7	CCR7−/− T cells egress more rapidly from LNs, whereas CCR7-overexpressing T cells are retained
CXCR4	Synergizes with CCR7 in retaining T cells in LNs
Leukocyte function-associated Ag 1 (LFA-1) and intercellular adhesion molecule 1 (ICAM-1)	CD4+ LFA-1−/− T cells egress more rapidly from LNs.
common lymphatic endothelial and vascular endothelial receptor 1 (CLEVER-1)	Blockade of CLEVER-1 reduces T cell binding to LN sinuses in situ. In vivo, involvement has not been confirmed thus far
Mannose receptor (MR)/L-selectin	Blockade of MR/L-selectin reduces T cell binding to LN sinuses in situ. In vivo, involvement has not been demonstrated thus far
α9 integrin	Blockade of LEC-expressed α9 reduces T cell egress from LNs

The sphingosine-1-phosphate receptor (S1PR) intervenes in diverse cellular processes, particularly S1PR1 expressed in T cells that have been described to mediate the egress out of LN. The natural ligand of S1PR1 is an endogenous sphingolipid called S1P. S1P protein is highly regulated by the action of kinases in tissue. S1P concentrations are greater in the blood and lymph than in lymphoid organs, causing a gradient across lymphoid EC that supports T cells to transmigrate into lymphatic sinuses and exit into efferent lymph (89–91). A high concentration of soluble S1P in circulation is capable of inducing S1PR1 internalization in T cells, leading to low S1PR1 expression by circulating T cells. Following the entry into LN sinuses via HEVs, T cells begin to upregulate S1PR1 (91). CD69 is an early T cell activation marker and is upregulated by various inflammatory mediators in T cells. It interacts with S1PR1, leading to its internalization and degradation. Recently activated T cells only transiently express CD69, but once they have undergone several rounds of division, they start to re-express S1PR1 and then egress from LN (88,89,91). As additional support for the role of S1PR in T cell egress, the downregulation of S1PR1 and

the expression of CD69 in TRM cells support their retention in the tissue (91). In addition to S1PR and CD69 mechanisms, the time that T cells spend in LNs is influenced by CCR7 expression levels. Activated T cells suppress CCR7 after recognizing an antigen, while fibroblastic reticular cells in the LN release CCL21 (88,91,94). T cells' expression of CCR7 encourages their retention in LNs, whereas egress signals from S1PR1 partially block CCR7-mediated retention. CXCR4 and CCR7 expressions work together in T cells to keep both resting and actived T cells in LNs (91).

Adhesion molecules and their integrin ligands play an important role in T cell entry into LNs, but not much is known about their role in T cell egress across lymphatic sinuses. LFA-1 has been suggested as having a role in delaying the egress of T cells across lymphatic sinuses, and mice lacking the major LFA-1 ligand intercellular adhesion molecule 1 (ICAM-1) lost this distinction (91). The lymphatic endothelial and vascular endothelial receptor-1 (CLEVER-1), the macrophage mannose receptor (MR), and its ligand L-selectin have been implicated in T cell migration across lymphatic sinuses. However, the in vivo involvement of these receptors in LN egress has not been demonstrated. A possible role for the integrin α9 subunit in lymphocyte egress from inflamed LNs has been reported (90). Tenascin-C (extracellular matrix component) binding to lymphoid EC-expressed α9β1 induces S1P production in lymphoid ECs, establishing a mechanistic link between α9 integrin expression and S1P1-mediated T cell egress. Antibody-based blockade of α9 or tenascin-C deficiency resulted in impairment of T cell egress from inflamed LNs (88,89,92).

0.2.2 Adhesion molecules and homing

Adhesion molecules known as CAMs comprise the following groups: integrins, selectins, cadherins, members of the immunoglobulin superfamily (IgSF), including lectins, as well as others, such as mucins. Their molecular structures and functions differ depending on the union with their ligand (Table 2). Integrins bind the extracellular matrix, while selectins and cadherins are responsible for cell-cell adhesion mechanisms. In addition, selectins and integrins are involved in T-cell rolling, which is the most critical step in homing mechanisms. Selectins allow cells to roll over the endothelium, starting the rolling cascade and activating the subsequent integrin to slow cell movement in order to enter the mucosa (95).

Selectins are involved in lymphocyte migration to peripheral LN and to the skin. Three types of selectins are expressed in mammal cells, L, P, and E. L-selectin is expressed in many types of immune cells' membranes, specifically naïve T cells, CM, and in the myeloid lineage. They bind ligands expressed by vascular endothelium. Contrariwise, P and E selectins are expressed by endothelial cells and interact with saccharide ligands expressed by immune cells; these molecules are over-expressed in inflammatory disorders(96).

Integrins are αβ heterodimers constituted by 18 α– and eight β-subunits that bind noncovalently to form 24 distinct forms. The α– and β-subunits are both type I transmembrane receptors and share structural resemblances, such as a large extracellular domain, a single transmembrane domain, and a cytoplasmic tail (97). T cells express two

main integrins: LFA-1 (L2, CD11a/CD18) binds to ICAM family proteins, whereas VLA-4 (CD49d/CD29) that binds to a variety of ligands, including VCAM-1. The elementary receptor-ligand interaction responsible for long-standing-term T cell-APC adhesion is LFA-1 binding to ICAM-1 (98,99). In addition to enhancing cell-cell adhesion, ICAM-1 engagement to LFA-1 sends specific intracellular signals (the so-called "outside-in signals") that lower the threshold dose of antigen required for complete T cell activation and influence T cell trafficking. VLA-4 is only expressed at detectable levels following T cell activation and is essential for T cell homing (99). Table 2 shows the most known integrins, ligands, and their distributions (100).

Table 2. Lymphocyte Integrins and Integrin Ligands (adapted from (100))

Integrins	Other Names	Integrin Ligands	Ligand Distribution
αLβ2	LFA-1, CD11a/CD18	ICAM-1, -2, -3, -5	Endothelium
			DCs, leukocytes
α4β1	VLA-4, CD49d/CD29	VCAM-1	Endothelium
		Fibronectin	Extracellular matrix
α4β7	LPAM-1	MAdCAM-1	Intestinal LP endothelium, HEV of MLNs and PPs
		Fibronectin	Extracellular matrix
αEβ7	HML-1	E-cadherin	Epithelium
α1β1	VLA-1, CD49a/CD29	Collagen	
α2β1	VLA-2, GPIa, CD49b/CD29		Extracellular matrix
α5β1	VLA-5, CD49e/CD29	Fibronectin	
α6β1	VLA-6, GPIc, CD49f/CD29	Laminin	

0.2.3 Chemokines receptors targeting T cell homing

Chemokines are molecules with chemoattractant capacity, with similar structures organized in three β-pleated sheets, a C-terminal α-helix, a free N-terminus, and disulfide bonds connecting two conserved cysteines (Cys) residues (101). There are four chemokine families based on the first two N-terminal Cys. CXC family, also called α, which contains one amino acid between the two conserved Cys in the N-terminal extreme; the CC family (or β), which shows two adjacent Cys; CX3C (or δ) and the C (or γ) families, which have three amino acids between its first Cys residues and a single cysteine residue in the N-terminus, respectively (102).
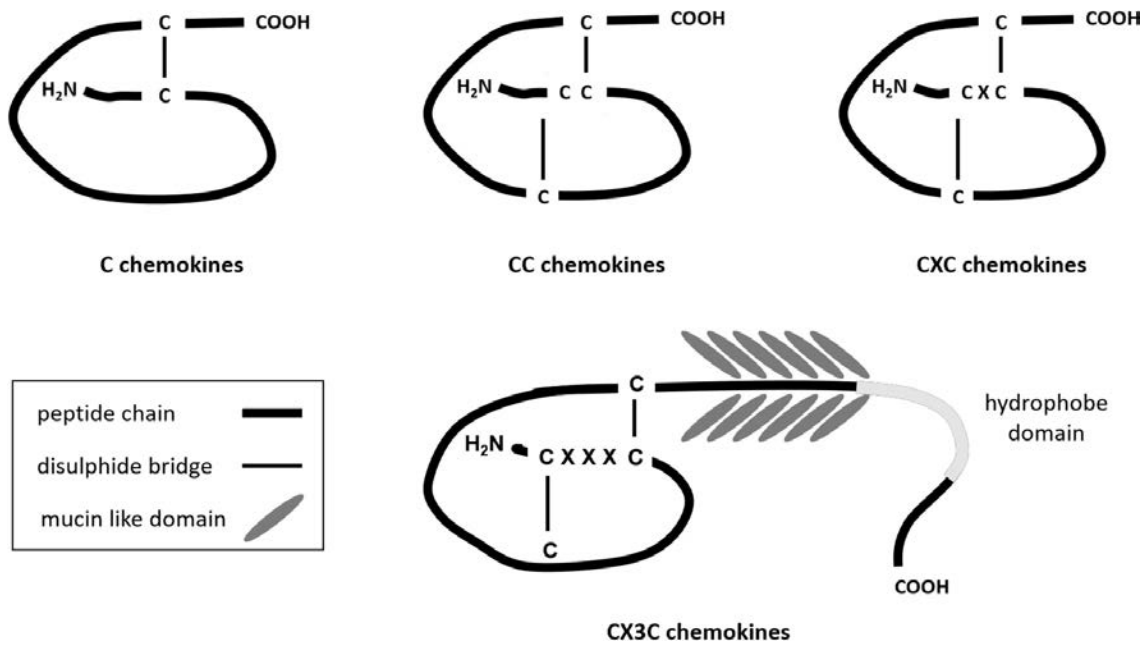
Figure 6. Molecular structure of the chemokine subfamilies (103)

Chemokine receptors are G protein-coupled receptors (GPCRs) with various downstream signaling pathways. There are two functional categories (104). The first is an inflammatory function, which is always associated with tissue damage or infection. Resident immune cells produce chemokines, which attract effector and innate cells over-expressing their receptors to the site. The second function is homeostatic, related to a healthy state of normal cell trafficking and strong immune surveillance. Chemokines receptors direct specific T cells populations from LN to the mucosal site, depending on the inflammatory process and the mucosal tissue (105).

Table 3. Immune function of chemokines receptors and their activating ligands (87).

Chemokine	Receptor	Key Immune Function
CXCL1		
CXCL2	CXCR2	
CXCL3		
CXCL5	CXCR2	Neutrophil trafficking
CXCL6	CXCR1, CXCR2	
CXCL7	CXCR2	
CXCL8	CXCR1, CXCR2	
CXCL9		
CXCL10	CXCR3	Th1 response; Th1, CD8, NK trafficking
CXCL11		
CXCL12	CXCR4	Bone marrow homing
CXCL13	CXCR5	B cell and Tfh positioning LN
CXCL16	CXCR6	NKT and iLC migration and survival
CCL1	CCR8	Th2 cell and Treg trafficking
CCL2	CCR2	Inflammatory monocyte trafficking
CCL3	CCR1, CCR5	Macrophage and NK cell migration;
CCL4	CCR5	T cell-DC interactions
CCL5	CCR1, CCR3, CCR5	
CCL7	CCR2, CCR3	Monocyte mobilisation
CCL8	CCR1, CCR2, CCR3, CCR5 (human); CCR8 (mouse)	Th2 response; skin-homing mouse
CCL11	CCR3	Eosinophil and basophil migration
CCL12	CCR2	Inflammatory monocyte trafficking
CCL13	CCR2, CCR3, CCR5	Th2 responses
CCL17	CCR4	Th2 responses, Th2 cell migration, Treg, lung, and skin-homing
CCL18	CCR8	Th2 response; marker AAM, skin-homing
CCL19	CCR7	T cell and DC homing to LN
CCL20	CCR6	Th17 responses; B cell and DC homing to GALT
CCL21	CCR6, CCR7	T cell and DC homing to LN
CCL22	CCR4	Th2 responses, Th2 cell migration, Treg
CCL24	CCR3	Eosinophil and basophil migration
CCL25	CCR9	T cell homing to the gut; thymocyte migration
CCL26	CCR3	Eosinophil and basophil migration
CCL27	CCR10	T cell homing to skin
CCL28	CCR3, CCR10	T cell and IgA plasma cells homing to the mucosa

As described in Table 3, chemokines receptors have more than one ligand with many immune functions, ensuring recruitment and high response regulation. During a pathological state, effector T cell functions depend on clonal expansion and the acquisition of patterns of adhesion and chemokine receptors crucial for specific tropism to the mucosa (84). For example, in the context of Th response in inflammatory sites, CXCR3-bearing Th1 cells are attracted to Stat1– dependent chemokines, CXCL9, CXCL10, and CXCL11. Conversely, CCR4– and CCR8-bearing Th2 cells move to the inflammatory site in the

mouse model of asthma via activation of Stat6-dependent chemokines, CCL1, CCL17, and CCL22 (87).

0.2.4 The multistep model of leukocyte migration

The leukocyte migration model involves several steps. First, the action of cell adhesion molecules and integrins is crucial for the process to be carried out efficiently and to complete the immune response to the target tissue. In addition, the activity of chemokines receptors has a coadjuvant role for their fine arrival to inflamed mucosa (87). The figure below shows the leukocyte multistage migration model.
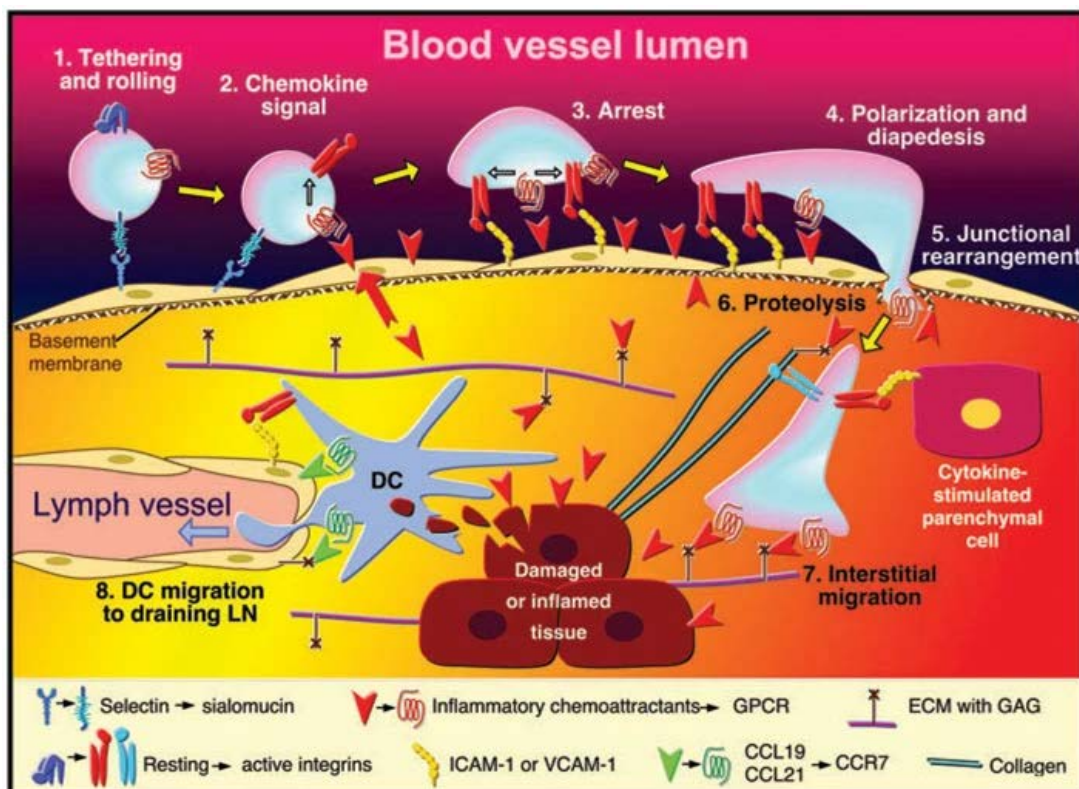
Figure 7. The action of chemokines, adhesion molecules, and integrin on the multistep model of leukocytes migration (106)

- Tethering and rolling: a transitory interaction between leukocyte selectins and their vascular ligands results in tethering, the previous step to start rolling. Tethering and rolling are first stabilized by the elongation of rear tethers as well as by cell-autonomous adhesive substrates termed slings (107) The inflamed target tissue begins to over-express selectins in the endothelium. The arrival of T-lymphocytes to the damaged tissue causes tethering as the first interaction, then rolling over the endothelium by the action of polysaccharide ligands and L-selectin receptors (108,109).
- Arrest: T cells become more activated during rolling and over-express integrins that mediate adhesion to the endothelium. Ig-like ligands stop and fix the adhesion of

leukocytes to endothelial cells, causing strong adhesion and preparing them for the next stage (108,109).

- Diapedesis: transmigration is mainly mediated by the binding of platelet-endothelial cell adhesion molecule-1 (PECAM-1), also called CD31, to integrins. The expression of CD31 in the intercellular junctions permits the diapedesis of leukocytes (107,109).

The multistep model of leukocyte migration has been well-validated in human and animal models. Deficiencies in leukocyte adhesion mechanisms result in recurrent bacterial and fungal infections and peripheral leukocytosis. These deficiencies include poor expression of β2 integrins, fucosilides, L-selectins, or impaired integrin activation (110). Thereby, leukocyte migration patterns during states of inflammation in different tissues is important to consider in the search for biomarkers and new therapeutic targets (93).

0.2.5 T cells homing to the mucosa in a pathological state

T-cell homing during mucosal disorders is crucial to clear the infection and return to homeostasis. However, homing may cause the contrary aspect in the context of chronic inflammation and autoimmune diseases by increasing tissue damage (111,112). Extravascular lymphocyte migration is not uncommon; lymphocytes are recruited to LN, tonsils, or Peyer's patches, tissues known as peripheral (or secondary) lymphoid organs, even in non-inflammatory circumstances for immunosurveillance (107). However, T cells increase significantly during inflammation in mucosal tissue, altering their phenotype (113,114). This section will discuss the homing mechanisms involved in the trafficking of T cells toward the mucosa during acute inflammation and autoimmunity.

0.2.5.1   Gut inflammation

According to the Word Health Organization (WHO) definition, inflammatory bowel disease (IBD) involves two types of conditions: Crohn's disease (CD), located along the digestive tract in patches, especially in the small intestine, just before reaching the colon; and ulcerative colitis (UC), affecting the entire colon and anus. Both disorders are characterized by chronic inflammation in the gastrointestinal tract, causing mucosal destruction (115).

DCs activate and print specific T cells to home to the gastrointestinal tract. This mechanism occurs in the gut-associated lymphoid tissue (GALT). The resulting T cell phenotype allows these cells to migrate and reside in the digestive tract. T cells specifically migrating to the small intestine express α4β7 integrin, α4β1 integrin, β2 integrin, and CCR9, whereas cells primed for colon migration show high levels of α4β7 integrin and GPR15. Briefly, T cells homing to the gut reach their target tissue through a chemotactic gradient. In the rolling phase, L-selectin and integrins (α4β7, α4β1) on T cells bind to their ligands expressed on endothelial cells: glycosylation-dependent cell adhesion molecule-1 (GlyCAM-1), mucosal targeting cell adhesion molecule-1 (MAdCAM-1) and vascular cell adhesion molecule 1

(VCAM-1), respectively. αEβ7 integrin retains gut T-cells by strongly binding to local ligands (116,117).

Currently, the α4β7 integrin and the CCR9 receptor represent attractive therapeutic targets for IBD patients (118). Furthermore, Th1 effector T-cells expressing CCR9 have been detected in patients with CD. CCL25-CCR9 interactions are pivotal in guiding T-cell entry into the small intestine (119). In animal models of Simian immunodeficiency virus (SIV), the loss of CD4+ lymphocytes with high expression of β7 is related to the total loss of intestinal CD4+ T cells. These findings confirm that the elevation of CD4+ α4β7+ T cells indirectly indicates disease development in these tissues (120).

0.2.5.2 Skin immunological disorders

Like other peripheral tissues, the skin plays a fundamental role as a physical barrier; it is exposed to contact with various Ags. CLA is considered a distinctive marker of T cells homing to the skin mucosa (121). For example, in the case of allergic dermatitis, CLA and CCR10 receptors participate in the trafficking of Th2 cells to the skin (122). In the context of psoriasis, the involvement of CCR4 has been described in addition to CLA and CCR10 (114). By blocking CCR10 and CCR4 and their CCL17 (TARC) and CCL27 (CTACK) ligands, CD4+ T cells cannot migrate to the skin mucosa in the mouse model of contact sensitivity (84).

According to the WHO, psoriasis is a chronic autoimmune skin disease caused by an accelerated cell cycle in EP. Around 2-4% of the population is estimated to suffer from this immune disorder. The involvement of T cells in developing this disease has been described in the literature. It has been reported that the production of IL-17 is highly involved in modulating gene expression in keratinocytes together with IL-22. Th17, Th1 cells, and CD8+ T cells (Tc17) are the leading players in the disease's pathophysiology (123). As an IL-17A-producing population, Vγ9Vδ2-positive T cells expressing CLA and CCR6 recirculate to the skin in patients with active flares (124).

In the context of viral skin infection, the dengue virus enters just when the mosquito bites the victim. Therefore, a highly specialized antiviral immune response is required to eliminate the virus in the infected mucosa. CD8 Tc1 cells are the specialized line against viral infections, intracellular pathogens, and cancer cells. CD8+ T cells with high migratory capacity towards the skin and specificity against dengue (reactive against pentamer NS3 27) have been described (125). These CD8+ cells express CLA in addition to CXCR3 and CCR5, molecules that direct the cells toward the inflamed mucosa (126,127).

0.2.5.3 Respiratory tract infections

The airways are in continuous contact with pathogens and other environmental Ags. The upper respiratory tract is the main route of entry, along with the digestive tract, for the various Ags exposed daily. For an Ag-exposed system, TRM are necessary for the rapid reaction against respiratory pathogens in addition to lung tissue-specific effector T cells (128).

Respiratory infections have allowed the study of lung-specific T-cells. For example, infections with *Mycobacterium tuberculosis* (MTB), *Bordetella pertussis*, influenza virus, or SARS-CoV-2 have permitted the analysis of specific cells with tropism towards the lung (129–131). T cells homing to the pulmonary tract overexpress the following chemokine receptors and cell adhesion molecules: block lipid transport-1(BLT-1), CCR1, CCR3, CCR4, CCR5, CCR6, CCR8, CXCR3, CXCR4, CXCR6, CD69, CD103, lymphocyte function-associated antigen-1 (LFA-1), CD162, or CD11a/CD18. The expression of these molecules differ between CD8 and CD4 T cell profiles (130,132–134).

For example, MTB infection increases the circulation of CD4+CXCR3+ T cells to the lung parenchyma. In parallel, the relationship of CD8+CXCR3+ cells with influenza virus infections has been described. CXCR3 receptors, jointly with CD49a integrin, are related to the traffic and retention of T-cells in the lung parenchyma. Currently, both CXCR3 and CD49a are used to evaluate the effect of vaccines against respiratory pathogens (135).

0.3   Female genital tract immunity and homing

The female genital tract (FGT) has two main functions: protection against different infections and reproductive function. Given its nature, this tissue is greatly affected by hormonal changes during the menstrual cycle. Two parts of the FGT are recognized, the upper genital tract (UGT), comprising the fallopian tubes, the uterus, and the endocervix. While the ectocervix, the vagina, and the vulva form the lower genital tract (LGT). Between the two parts, there is a transition zone called the transformation zone (Figure 8) (136).
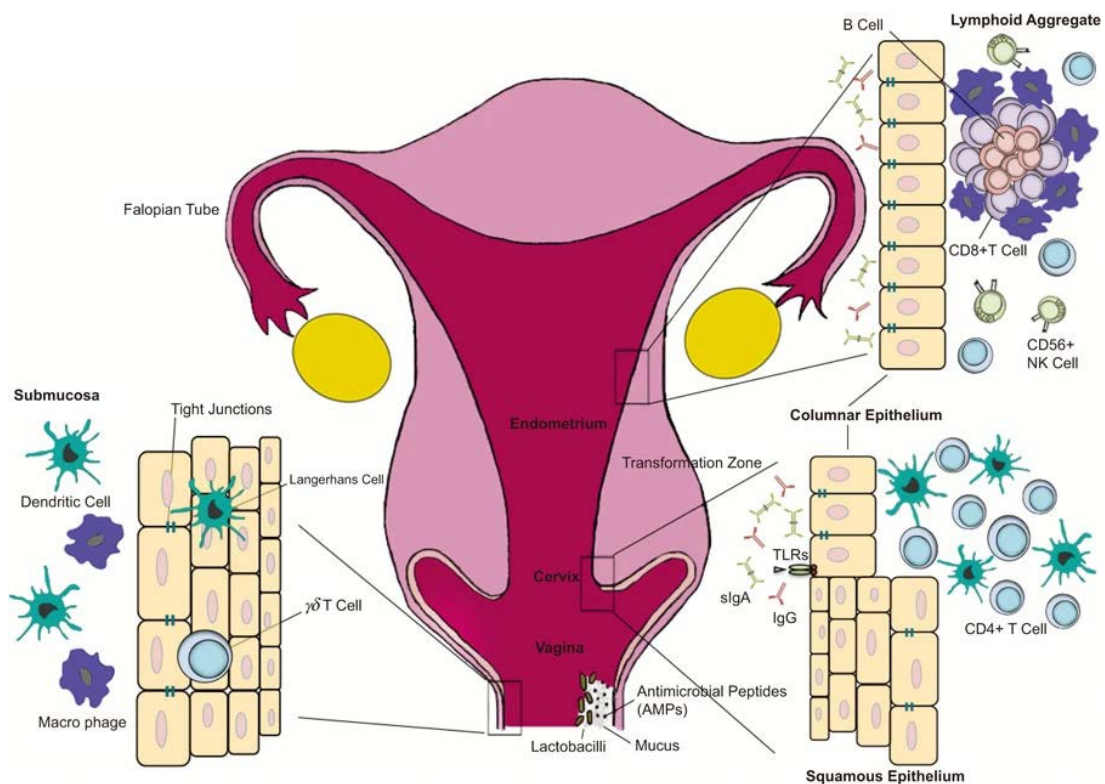
Figure 8. Anatomical and histological structure of female genital tract FGT, from (137)

The UGT comprises a single-layered columnar epithelium. While this could make this part more susceptible to infections, this anatomical section is protected by mucus and higher productions of mucins that play a mechanical role in trapping virus and bacterial pathogens (137). In addition, the columnar epithelium of the upper FGT constitutes only a tiny area of the total surface exposed to the infectious agents, which also reduces the chances of infection in this area (138,139).

The LGT includes the ectocervix and vagina, which are covered by a stratified squamous epithelium that forms a more protective barrier against infectious agents. This area is exposed to different external Ag (including viruses, bacteria, and parasites) (138,140,141). To avoid the entry of all these pathogens, EP establishes close junctions: desmosomes, tight junctions, and adherent junctions. This mechanism reduces the permeability of the epithelium, greatly hindering the transfer of any small macromolecules to the lower layers of the mucosa (136,137).

0.3.1 Immune functions of the female genital tract

The immunity of the FGT is very peculiar regarding function and regulation. FGT mucosa has evolved to deal with different pathogens, tolerate the vaginal microbiota, semen, and finally, an allogenic fetus for nine months. The immune system cells carry out these contradictory functions in the FGT, where proper regulation is vital for the physiological processes (139).

The functions of the FGT are influenced by the action of sex hormones resulting from the menstrual cycle. APCs' response and Ag presentation are highly sensitive to these hormonal changes. For example, vaginal immunization has more effect during the follicular phase (142,143). In general, the release of estradiol in the middle of the cycle, and the progesterone produced during the secretory stage, act by suppressing several immune functions in the mucosa. The effect of these two sex hormones is localized to the fallopian tubes and uterus (in the UGT), as well as the vagina and cervix (in the LGT) (139,143). During the secretory stage of the menstrual cycle, CD8+ cells are deactivated in the uterus but not in the LGT. On the other hand, CXCR4 and CCR5 are overexpressed on CD4+ T cells during the same phase. Estradiol and progesterone during the secretory phase suppress innate functions in the uterus and vagina, including NK and APCs' functions (136,144,145).

In the FGT, leukocytes are distributed in a dispersed but localized manner. Depending on the anatomical section, the immune cell composition, and proportions vary in the FGT. The predominant ones are T cells, macrophages/dendritic cells, NK cells, neutrophils, and mast cells (146).

Table 4. The frecuency of celular inmunity mambers across the FGT, adapted from (147).

	Cellular Immunity					
	T cells		NK cells	Monocytes and macrophages	DCs	Neutrophils
	CD4+	CD8+				
Myometrium	–	–	–	–	–	–
Fallopian tubes	+	+	+	+	+	++
Ovary	+	+	–	W	W	+
Endometrium	+	+	+	+	–	+
Endocervix	+	+	+	+	+	+
Ectocervix	++	++	+	+	+	+
Vagina	++	++	+	+	+	+

–: Negative; W: Weak, +: Medium; ++: High.

FGT lacks local lymphoid tissue as the primary induction site. Antibody-secreting cells have been found in the cervix, while CTLs have been found in both cervix and vagina (148). T cells are clustered in a distinct band below the epithelium and scattered in the epithelium and LP, while CD38+ plasma cells are present only in the LP. Still, lymphoid aggregates containing CD19+ and CD20+ B cells and CD3+, CD4+, and CD8+ T cells are present in the FGT (148). B cells play a vital role in the humoral immunity of the FGT. However, this study will focus on the effector cellular immune system. The following sections outline the different phenotypes of cellular immunity in the LGT.

0.3.1.1 Myeloid lineage in the FGT

FGT contains many hematopoietic cells, being CD14+ myeloid cells one of the most abundant cell types. These cells may also express CD11c+, associated with an interstitial dendritic cell or monocyte-derived phenotype or CD11c$^{dim/-}$, which could be related to a macrophage phenotype (11,12,21,26). In the cervical mucosa, classic CD11c$^+$ CD14 $^-$ DCs can also be found, and several other myeloid subpopulations with more specific functions, such as plasmacytoid dendritic cells (pDCs), which are mainly recruited from circulation during viral infections, or Langerhans cells, coexpressing CD1a and CD11c, which are responsible for carrying out antigenic surveillance. All these cells comprise between 10% and 50% of all leukocytes in the mucosal LGT, and play a key role as APCs that activate T cells (150–152). DCs and Langerhans cells generally activate Th2-type responses, while CD14$^+$ DCs and macrophages activate Th1 responses through TLRs (153).

The FGT mucosa mostly lacks MALT, so the priming of adaptive responses takes place in the draining LN (dLNs). However, cellular organizations that resemble inductive sites are found as endometrial lymphoid aggregates. This like-inductive site is located in the stratum basalis and composed of a B cell core surrounded by T cells and an outside halo of macrophages. During the secretory phase, this cell aggregate is bigger and contains more cell number; however, during the proliferative phase, cell number is decreased (154).

A. Dendritic cells in FGT

DCs are located in the LP of the FGT mucosa, while Langerhans cells (LCs) are abundant in the epithelium of the ectocervical mucosa. The role of these two phenotypes is to detect the entry of pathogens through the vaginal epithelium and maintain the integrity of the epithelium. DCs in the LGT populations are primarily negative for the resident cell marker CD103. This marker is shared between resident memory T cells and other resident leukocytes (147).DCs are in a resting state in the FGT mucosa; encountering different pathogens and inflammatory stimuli, such as exposure to bacterial lipopolysaccharides (LPS), activates their maturation. As a result of the stimulation, DCs overexpress the MCH-II complex and costimulatory molecules CD80 and CD86. The next step is migration to the secondary LNs, which are further activated by coupling their receptor CD40 to CD154 of Ag-specific CM T lymphocytes. Notably, the endometrium DCs present a tolerogenic phenotype with low expression of CD83 and CD86 and low stimulation via TLR3 and TLR4 (152,155–157).

B. Macrofages in the female genital tract

Macrophages belong to the APC family with similar functions to those of DCs, and they have a versatile role in FGT during pregnancy, infections, and tumor development (158,159). Macrophages are one of the most frequent types of immune cells in the endometrium and myometrial connective tissue, although they are also located in the cervicovaginal mucosa (160–163). They help with endometrial breakdown during the early phases of menstruation and tissue repairing during the later stages. Their levels stabilize during pregnancy and remain at approximately 20% of the leucocyte population (158,162). It is thought that implantation is an inflammatory process influenced by macrophage cytokine production. Macrophages produce IL-6 and IL-8 in response to extravillous trophoblast, which can increase placental invasion throughout the first trimester (158,159). In the context of STI, the role of the macrophage in type 2 immunity, including *Chlamydia*-specific Th2 response, was described (164).

In the endometrium, macrophages are highly influenced by the action of estradiol and progesterone. In the vagina, their frequency is mostly stable during the menstrual cycle (147,152,156). CD68+ macrophages are detected in all phases of the menstrual cycle. However, they increase progressively during the secretory phase. The maximum frequency of these cells is observed during menstruation, reaching 15-20% of the leukocyte population. These cells also express specific markers such as CD71, CD69, and CD54. The maximum activation of macrophages coincides with implantation, which suggests their vital role in this phase, secreting TNF-α, IFN-γ, IL-1, IL-6, IL-10, and IL-12 (152,157).

0.3.1.2   NK cells in the female genital tract

At the FGT, NK phenotype and number vary according to tissue location. For example, in the endometrium, these cells express CD9, CD69, and CD94, but little CD16, and are

negative for CD8 or CD57 markers. They also produce granulocyte-monocyte colony-stimulating factor (GM-CSF), IL-10, IL-8, and TGF-β1 (156).

Similarly to DCs and macrophages, NK cells are sensitive to sex hormones and increase to reach their maximum at the end of the secretory phase of the menstrual cycle. In addition, NK cells participate in the implementation of the zygote by producing vascular endothelial growth factor (VEGF), placental growth factor (PLGF), angiopoietin-2, and leukemia inhibitory factor (LIF) (147,152,156).

Regarding the homing profile, uterine NK cells express CXCR3, CCR5, and CCR7. During menstruation, the NK cells get attracted to ligands CCL4, CXCL9, and CXCL10 overexpressed in the endometrium. NK homing profile also involves VCAM-1 (147,152,156).

0.3.1.3 The adaptive immune system in the female genital tract

The adaptive immune response in the FGT is a pathogen-specific response, represented by activated T cells and antibodies secreted by Ag-specific B cells. T lymphocytes are found throughout the FGT in varying proportions. In general, within the leukocyte fraction of the FGT (comprising 2-10% of the cells), T cells represent 50% (165).

In the FGT, T cells are scattered below the epithelium and LP, with a strong presence of CD8+ T cells with a CCR7− profile; indeed, most of these cells belong to the TRM phenotype (166). Furthermore, these cells are organized into lymphoid structures in the endometrium. These structures have a nucleus with B cells surrounded by CD8+ T cells and some CD4+ T cells. A halo of macrophages surrounds these aggregates. The size of these lymphoid aggregates varies during the menstrual cycle, reaching its largest size at the end of the proliferative phase (just like macrophages and DCs). Postmenopausal women lack these cell aggregates, confirming the hormonal influence of these inductive site-like structures (156,167–169).

In the LGT, there is a strong presence of $CD3^+CD8^+$ cells with high cytotoxic and cytolytic capacity. Most frequently found in the transformation zone and endocervix, but also present in the ectocervix. In contrast, a much smaller number of immune cells are found in the vagina. In the case of inflammation or infection, the proportions of intraepithelial T lymphocytes change so that in cases of vaginitis and cervicitis, the total number of CD4+, CD8+ T cells, and APCs increase (138,160,162,163,170).

Estradiol and progesterone regulate the tissue environment via cytokines, chemokines, and growth factors, enhancing and suppressing critical components of the humoral, cell-mediated, and innate immune systems along the FRT (169,171). Both hormones change T cells' number and phenotype during the menstrual cycle. CD8 CTL is inhibited during the secretory phase in the endometrium as preparation for conception and tolerance to sperm and fetus. However, in LGT, the cytotoxic activity of CD8 is active during all phases of the menstrual cycle (169). CD4 T cells in the endometrium and endocervix are increased

during the secretory phase with higher expression of CCR5 with enrichment in activated and memory profiles(172,173).

A. Resident memory T cells

The TRM cell phenotype is present with high frequency in the FGT. Many studies have shown its involvement in surveillance and protection against pathogens. TRM cells are defined by the expression of CD69, CD103, and CD49a receptors, among others, that cause the retention of these cells in the mucosa. Additionally, TRM cells present low expression of egress markers such as S1PR1, CD62L, and CCR7 (174).

TRM cells play an essential role in the context of sexually transmitted infections (STIs), such as the human immunodeficiency virus (HIV) and the human papillomavirus (HPV) infection (175) . In recent years, its phenotype has been characterized throughout the FGT. Generally, the ratio of CD8+/CD4+ TRM cells is higher in the FGT, but in the vagina, the fraction of CD4+CD103+CD69+ T cells is very high. TRM CD4+ cells are essential and multifaceted in FGT entry against pathogens and tumoral processes (175).

CD8+ TRM cells close to the epithelium express CD103 and are characterized by high granzyme B and IFNγ production. On the contrary, the CD8+ cells in the stroma have low expression of CD103. Ag-specific CD8 cells are strategically localized in the FGT for long-term protection (176).

B. CD4+ T Cells

In the FGT, CD4+ cells are present at low frequency (in comparison to CD8+ T cells). These cells orchestrate the immune response and participate in many infectious processes. Currently, T cells with a Th1, Th2, and Th17 profile and other Tregs have been described in the female genital tract. Treg cells are the ones that control the activity of the rest of the CD4+ T cells. TGF-β and other cytokines regulate the differentiation of Th17 and Treg cells (152,156,177).

Within the T cell CD4+ population found int the FGT, the memory phenotype is the most abundant (167,168). They express the hallmark of tissue residency, CD69, and CD103. In addition to these markers, most CD4+ TRM cells are activated and express α4β7, CCR5, IL-17A, and IFNg (168,178,179). This phenotype is associated with productive HIV-1 infection, which may enhance and assist in disseminating the viral infection and other STIs in women (137,178,179). In contrast to humans, the CD4+ TRM cells in mice's vaginas decrease the risk for HSV infection (168).

C. CD8+ T Cells

In parallel to CD4+ T cells, the majority of CD3+CD8+ cells present in FGT are compatible with a TRM phenotype (175). These cells have the function of carrying out cytotoxic antiviral/intracellular responses. It has been reported that the activity of cytotoxic T cells in the uterus is inversely associated with estradiol and progesterone levels. During the

fertilization phase and embryo implementation, CD8+ T cell-mediated cytolytic activity is deactivated (147,152,169,180). FGT CD8 T cells exhibit activated phenotypes expressing CD38 and HLA-DR andD69 and CD103 (167,181–183).

0.3.1.4 Unconventional T lymphocytes populations in the female genital tract

Several populations of unconventional T cells (as previously described) lacking the αβ chain are found in the FGT. These cells are γδT cells, MAITs, and NKT (184).

In a healthy state, γδT cells are present at low frequency. This cell population is found at the UGT, especially in the endometrium, which is related to implantation and pregnancy. γδT cells are found in the intraepithelial compartment. In humans, the majority are Vγ6+ (IFN type I producers) (184,185). In addition to its cytotoxic activity and the secretion of antimicrobial substances and growth factors, this population promotes trophoblast invasion in the maternal decidua and regulates tolerance by suppressing its apoptosis (79,184). The vaginal flora and estradiol play a fundamental role in activating these cells which can be detected in the vagina in particular during FGT infections. γδT cells are modulated by the vaginal flora and may enhance susceptibility to STIs, since the decrease in these cells in the vagina after advanced bacterial vaginosis has been described. Indeed, the absence of γδT cells correlates with the susceptibility of women with bacterial vaginosis to HIV infection and other STIs (186,187).

MAIT and iNKT cells play an essential role in mucosa protection, linking innate and adaptive immunity (188). Both cells are found in the FGT, at low frequency, and distributed in different zones. MAIT cells in the FGT show EM and TRM profiles. They can produce IL-17 and IL-22 in response to bacterial infections, in addition to TNF and IFNγ (184,189). In contrast to blood-derived MAIT cells, FGT's MAIT cells release up to 22% more IL-17 in response to E. coli infection ex vivo but less TNF and IFNγ production (190,191). MAIT cells are located and distributed in several areas across the FGT, including the endometrium, endocervix, transformation zone, and ectocervix. Compared to CD4 and CD8 T cells, they are sporadically distributed throughout the FGT and located near and inside the glandular epithelium in the lamina propria of the endometrium near other T cells. To localize MAIT cells in the tissue, the double-staining for V7.2 and IL-18R is used (191,192). The function of MAIT cells in FGT is still under investigation. For example, they respond specifically against *N. gonorrhoeae*, showing an antimicrobial function in FGT (193,194). Compared to their circulatory and endometrium counterparts, MAIT cells in the placenta's intervillous region express larger quantities of IFNγ and granzyme B in response to microbial activation (192,195). They keep stable number during pregnancy and present an exceptional inflammatory response to riboflavin-producing bacteria (195).

iNKT cells share functions and some markers with MAIT cells, they are present in the FGT together with other T cells and NK subsets (184). iNKT in tissue expresses TRM profile, participates during pregnancy, and responds against STIs (192). The decidua-associated iNKTs play a special role in regulating immune homeostasis during pregnancy (192,196). iNKT interacts with extravillous and villous trophoblast cells expressing CD1d, which

increases with gestation (196). Elevated frequency of iNKT during pregnancy with Th1 cytokine (increased TNF and IFNγ production) contribute to higher pregnancy loss rates (196). Additionally, local NK cells start producing IFNγ, supporting the role of iNKT in pregnancy loss (192). In the context of STIs, mice models of genital infection with *Chlamydia muridarum* present iNKT with Th1 response against the pathogen. In contrast, prolonged exposure to chlamydia infection in FGT, iNKT cells cause oviduct dilation and fibrosis (197,198).

0.3.2 Female Genital Tract in the context of STIs

Sexually transmitted infections represent a major global health problem. The world health organization records 1 million cases of STIs per day worldwide. The 80% of these infections are represented asymptomatically, where 374 million new cases are estimated of the four most common STIs: chlamydia, gonorrhea, syphilis, and *trichomonas vaginalis*. As far as female sexual health is concerned, approximately 300 million women have an HPV infection, the leading cause of cervical cancer (199–202). HPV infection is directly associated with cervical cancer, causing more than 311,000 deaths yearly (203–206). According to data collected from the Spanish Women's Health Observatory and prepared with information from the Epidemiological Surveillance Network of the Carlos III Health Institute and the autonomous communities, up to 16.304 new cases of STIs were diagnosed in women in Spain in 2019 (207). During the period between 2015 and 2019, chlamydia increased by 480% in women. Syphilis, lymphogranuloma venereum, and hepatitis C infections increased by 129%, 178%, and 76%, respectively (207,208). It is important to note that there has been an increase of 5.6% in new HIV diagnoses, even though prior years show a marked decline in cases, which had really been stable for a decade at 400 to 500 new diagnoses per year for women. The latest numbers for CT infections in Spain are from 2021, which were 10.286 new infected women (207,208).

It is clear that STIs represent a threat to public health and have a direct impact on women's reproductive and sexual health. They cause infertility, cancer, and complications during pregnancy. Furthermore, STIs can have an impact beyond the infection itself since bacterial infections facilitate the acquisition of other STIs, such as HIV. Moreover, STIs such as gonorrhea and chlamydia are women's leading causes of pelvic inflammatory disease (PID) and infertility (152,205,209).

The epidemiology of STIs depends on many social and individual factors, characteristics of the pathogen, and available treatments. Currently, there are vaccine strategies against some STIs, such as HPV, and other prophylaxis treatments, as for HIV. However, considering that the number of cases continues to increase, more research is needed to understand the course of these infections and develop effective diagnostic and vaccine strategies (210,211). In this section, I will talk about some specific STIs, focusing on the pathogenesis and the immune response associated with these infections.

0.3.2.1 *Chlamydia trachomatis* infections

CT infection may cause multiple complications in the FGT partially because up to 80% of the infected women may have no symptoms (212). Prolonged residence of the pathogen in the FGT causes endometritis, salpingitis, or PID, leading to problems during pregnancy or even infertility. Furthermore, CT infection causes greater susceptibility to HIV infection and other STIs. In clinical practice, the infection is treated with macrolides antibiotics (mostly Azithromycin) (203,205,213,214). Like the resistance registered in other bacterial STIs, CT strains resistant to macrolides are beginning to be isolated. For all these reasons, developing effective vaccines against this bacterium is a topic of great interest for public health since it would save millions of euros currently used for antibiotic treatment, besides avoiding the problems associated with infection (152,215).

The CT reproduction cycle (Figure 9) in the FGT has two phases. First, an elementary body (EB) enters the columnar epithelial cell of the endocervix using a mechanism to remodel actin. Once inside, the EB differentiates into RB, which are metabolically active particles with a high reproductive capacity. At this point, there are two possible ways forward. The first is to enter a persistent reversible state; the second is to continue replication within the inclusion structure. The end of this phase is marked by differentiation back to EB and their exit by exocytosis or by causing cell apoptosis (115–117).
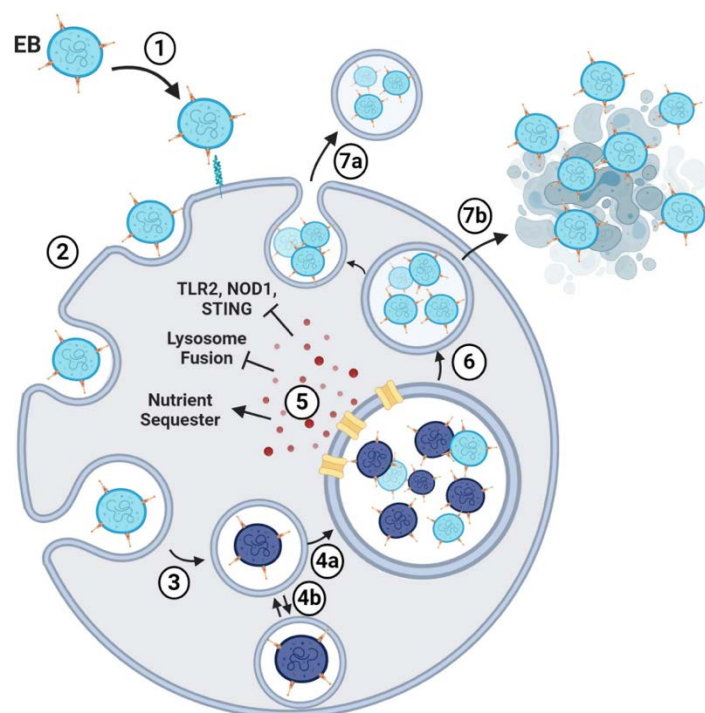

Figure 9. Phases of the reproductive cycle of CT; light blue: EN, dark blue: RB. (from (214))

The developmental cycle of CT directly affects the immune response by using several mechanisms to evade it (215,216):

- EB has low immunogenicity, expressing low levels of LPS on the surface (215,216).

- The inclusion proteins used by the EBs have a suppressive effect on the mechanisms namely TLR2, NOD1, and cGAS/STING which detect intracellular Ags and its presentation. In addition, the inflammatory response is blocked with suppression of CXCL10 and other transcription factors like NFκB and p65 (215,216).
- Suppression of cell apoptosis prevents Ag contact with the outside and ensures an environment that facilitates reproduction. These mechanisms, among others, include the degradation of the P65 protein (a tumor suppressor that induces apoptosis in affected cells) and the blockade of the pathways induced by caspases (215,216).

The immune response to CT infection in the FGT involves the innate and adaptive arms. Therefore, in the following points, we focus only on the cellular response mediated by innate cells and by T lymphocytes (215,216).

A. Innate response against CT

The innate response led by APCs, especially DCs, and the production of IFNγ has a crucial role in eliminating CT infection. The TLR2 pathway is involved in signal activation and binding to molecular patterns from CT. These molecules are usually proteins such as major outer membrane protein (MOMP) and heat shock protein 60 (HSP60) and secondary metabolites of bacterial DNA replication. One of the pathways related to nucleic acid derivatives (dsDNA, cyclic di-AMP, and cyclic di-GMP) is the STING pathway, which causes the production of IFNγ and IFN-β. NOD-like receptors, STING and TLR, are the major metabolic pathways involved in DCs activation after molecular patterns uptake and processing. Once activated, DCs secrete pro-inflammatory cytokines such as IL-6, TNF, CCR7, CXCL10, IL-1α, and IL-12. Moreover, IL-12 is crucial in protecting against CT infection by activating a Th1 response. In addition to TLR2 activity, TLR4 has been reported to activate monocytes in the context of CT infections (217–219).

B. Adaptive response against CT

Protection against CT infection involves cellular immune responses. In several human studies, a Th1 response by CD4+ T cells has been associated with a specific response against an active CT infection. The production of IFN-γ characterizes the inflammatory response by CD4+ and CD8+ T cells. Studies performed on vaginal fluids from infertile women with active CT infection have detected CD4+ and CD8+ T cells with the production of cytokines characteristic of Th1 and Th2 responses. CD4+ and CD8+ T cells isolated from the endocervix of women with active infection are HLA-DR+ primarily of a memory phenotype. In addition to IFN-γ production, other cytokines such as IL-12p70 (associated with differentiation to a Th1 profile) and CX3CL1 (a T-cell chemoattractant ligand) are detected. Of note, inflammatory environments with T cell-attracting cytokines are associated with an increased risk of HIV coinfection (214,215,220–225).

0.3.2.2 Bacterial vaginosis

The local microbiota of the FGT plays a significant role in regulating the immune response and protecting against STIs. Along with vaginal mucus, bacteria are a physical and mechanical trap against various pathogens (226–228). In the literature, the dominant presence of *Lactobacillus Crispatus* is associated with vaginal mucus and can trap even viruses such as HIV (229–233). In contrast, the presence of the bacterial species of *Gardnerella*, *Prevotella*, and Bacteroides in the context of bacterial vaginosis (BV) is associated with degraded vaginal mucus (due to the enzyme sialidase produced by these bacteria) and a high risk of contracting an STI. The vaginal flora comprises *Lactobacillus spp*, which includes *L. crispatus*, *L. gasseri*, *L. jensenii*, and *L. iners*. The presence of these bacteria lowers the pH of the vagina to 4.5, producing lactic acid, hydrogen peroxide, and other organic acids. The metabolites produced by the vaginal microbiota serve as bactericides and fungicides. An imbalance in the growth of these bacteria caused by an overgrowth of *Gardnerella vaginalis*, among others, is called bacterial vaginosis (234–238).

The etiology of BV is due to the metabolic activity of the *G.vaginalis* bacteria, degrading fatty acids and vaginal mucus, producing a characteristic "fishy" vaginal discharge. This metabolic activity increases the pH of the vagina and thereby multiplies the growth of anaerobic bacteria by 100 to 1000 times. BV diagnosis is performed using the Amsel test, analyzing the discharge's color, odor, and pH and the presence of bacterial biofilm in cervix EC (by light microscopy and KOH test) (147,152). BV represents a problem for public health with significant economic impact since it has a high cost associated with antibiotic treatment and facilitates the acquisition of other STIs. In addition, the prevalence of this infection reaches up to 60% in fertile women with various sexual partners. Therefore, characterizing the immune response against BV may help understand the mechanisms behind coinfections and g to design better treatment solutions (236,237,239).

Immune response in the context of bacterial vaginosis

BV is associated with subclinical inflammation, so bacterial overgrowth generates a pro-inflammatory response. PAMPs from *G.vaginalis*, in addition to degraded fatty acids, generate an immune response via TLR receptors on EC from the cervix. (152,156,235,236). The inflammatory response elicited by BV is accompanied by cytokine production. In several studies carried out on women, the high presence of *G. vaginalis* has been related to the high production of the cytokine IL-1β. *In vitro*, studies have shown that cervix EC produces IL-6 and IL-8 in the presence of anaerobic bacteria. However, these cytokines were not detected when the same cell line was cocultured with *lactobacillus* species. Moreover, TLR1, TLR2, and TLR3 pathways are downregulated under such conditions (240–242).

Regarding cellular response, studies carried out on sex workers have recorded the presence of CD4+ CCR5+ and CD4+CD69+ T cells in the cervix. In another study, healthy vaginal mucosa has been related to a lower presence of activated CD3+ populations such as CD3+HLADR+ or CD3+CD4+CCR5+ cells (144,147)—all these findings associate BV

with higher susceptibility to contracting other STIs, especially HIV. In parallel, women with BV often have CT and Gonorrhea coinfections (236,238,239,243).

0.3.3 Mice model for chlamydia infections

There are various mouse models of CT. These models are easy to handle and cheap to maintain, in addition to the existence of many knockout models for different studies. Female mice are susceptible to infection with CT and another species called *C.muridarum*. These two models have long been used for their similarity to FGT infection in women and due to the development of a similar immune response. The infection's complications are similar to humans, even though the mice develop a long-lived adaptive immunity against the infection (244–246).

0.3.3.1   C. muridarum model

Chlamydia muridarum infection affects the lung in mice, causing pneumonitis. In animal models, the pathogen is deposited intravaginally, resulting in an infection of the cervical epithelium, like CT infections in women. The propagation of *C. muridarum* starts in the LGT, going up to UGT towards the uterus and ovaries. The sequelae are very similar to those in women, infertility, fibrosis, PID, and interruption of pregnancy (244,246–248).

C. muridarum infection in mice lasts approximately 4 weeks and generally resolves naturally without antimicrobial therapy. Mice' age directly influences pathogenesis, strain, bacterial load, and hormone levels. Young mice in the luteal phase (presence of progesterone) are more susceptible to *C. muridarum* infection. Mice develop an adaptive protective immunity against *C.muridarum*; however, this does not occur in women. In the case of reinfection, mice take a short time to resolve it with no associated pathology (247).

The immune response in this model includes cells from the myeloid and adaptive lineages. DCs and macrophages are the first cells to infiltrate the genital tract (GT), followed by T lymphocytes. CD4+ T cells and B cells are critical elements for adaptive immunity against *C.muridarum*. CD4+ T lymphocytes predominate on the adaptive response; these cells are retained in the GT and continue to be detected after the resolution of the infection. Overall, the nature of the response is Th1, characterized by the production of IL-12 and IFN-γ. CD8+ T cells are present towards the end of infection but are not known to play an essential role in clearing the pathogen. Last, NK cells also infiltrate the GT towards the end of the infection, and they have been described as responsible for producing large amounts of IFN-γ in response to *C. muridarum* infection in mice (244–250).

0.3.3.2   C. trachomatis model

This model is characterized by a mild CT infection. More infective units are needed to elicit an inflammatory response in the GT of the mouse. Resolution takes less time than in the case of C. muridarum infection. Mice must be directly infected in the UGT to achieve complications, as in women (246,248,249).
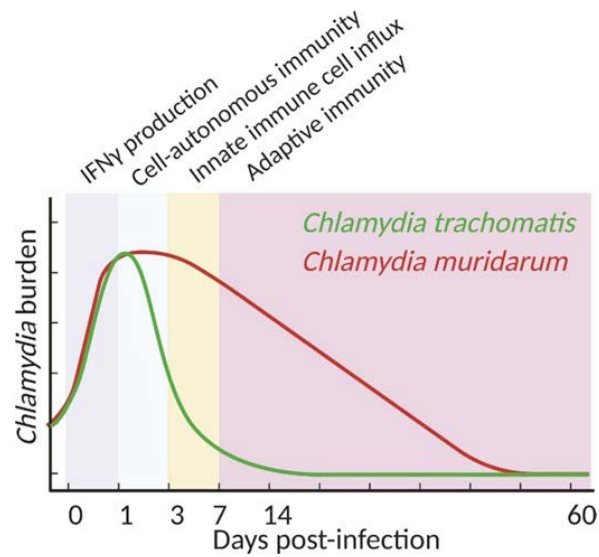
Figure 10. kinetics of CT and CM infection and immune response in mice

There is much controversy regarding the immune response to mice CT infection. The innate response is already sufficient to eradicate the infection in murine models (Figure 10). Unlike the C. *muridarum* model, this model does not require a response from CD4+ T cells for infection clearance. Last, in the CT model, bacterial load declines within 3 days without involving an adaptive response (247).

1 Antecedents and Objectives

1.1 Antecedents

Mucosal immunology studies immunity and defense mechanisms in tissues that directly interact with the external environment through a mucosal barrier. Continuous interaction with external Ags promotes the development and shaping of mucosal immune responses. As mentioned in this thesis, a wide variety of innate and adaptive immune phenotypes are represented in these mucosae. Importantly, these cells have distinct phenotypic and functional heterogeneity based on location and may strongly differ from blood phenotypes.

Celular trafficking between LNs and the mucosa is a complex and dynamic process, especially after infection. The capacity of distinct subpopulations of T cells to traffic selectively into initial Ag contact compartments is termed 'homing.' T cells sensitized to Ag in mucosal inductive sites leave the site of Ag presentation in the mucosa, migrate through the lymphatics to enter the blood, recirculate, and ultimately re-enter mucosal tissues. The lack of CCR7 expression allows us to identify T cell populations migrating to peripheral tissues (251). After recirculating to the original mucosal sites, most of these cells differentiate into resident memory and effector phenotypes. Thus, studying and characterizing homing profiles of T cell subpopulations on their way to tissues may help understand the type of immune response induced and established at the affected location. T cell homing studies have focused on the respiratory tract, gut, and skin to identify biomarkers and therapeutic targets for mucosal disorders associated with these peripheral tissues. However, the homing profile of T cells migrating towards the female genital mucosa is still poorly defined.

1.2 Hypothesis and Objectives

This project hypothesizes that lymphocytes induced by FGT infection traffic transiently in blood, expressing a specific set of homing markers. By isolating cells from blood soon after mucosal FGT infection during the brief period in which mucosal lymphocytes recirculate, it is possible to detect specific integrins, chemokine receptors, and other molecules responsible for lymphocyte entry into the FGT using differential transcriptomics analyses.

To identify specific trafficking molecules associated with effector T cells migrating to the FGT, which was the main objective, we developed the following specific objectives:

- Identify proteins and gene transcripts of molecules specific to T lymphocyte homing to the FGT using differential and integrative analyses from different groups of infected mice.
- Confirm and validate the expression of the selected candidates on circulating T lymphocytes in healthy patients compared to those with mucosal conditions.
- Characterize subpopulations of T lymphocytes with FGT-specific homing identity.

2 Methodology

2.1 Mice experiments

2.1.1 Ethics statement

For this project, samples from animal models were used in two separate studies. Samples from mice in the first study consisted of blood from a Chlamydia infection mouse model developed at the University of California, UC-Davis, by Dr. Stephen McSorley's team. The second study consisted of blood samples from uninfected mice generated in our laboratory at the Germans Trias i Pujol Institute, Badalona. For this purpose, the competent entities approved the ethical procedure in both countries.

For study 1: all mice were maintained following the Association for Assessment and Accreditation of Laboratory Animal Care International Standards and the guidelines in the Guide for the Care and Use of Laboratory Animals of the National Institutes of Health. The Institutional Animal Use and Care Committee of the University of California, Davis, approved these experiments (Protocol # 18299). For study 2: all animal procedures were approved and supervised by the Animal Care Committee of the Germans Trias i Pujol Health Science Research Institute (IGTP) and by the Department of Environment of the Catalan Government (approval number # 7066).

2.1.2 Animal models

2.1.2.1 Chlamydia muridarum infective stock

Chlamydia muridarum strain Weiss was purchased from ATCC (Manassas, VA) and propagated in HeLa 229 cells in Dulbecco's modified Eagle's medium (Life Technologies, Grand Island, NY) supplemented with 10% fetal bovine serum (FBS). *C. muridarum* EBs were purified by discontinuous density gradient centrifugation as previously described and stored at −80ºC (74). The number of inclusion-forming units of purified EBs was determined by infection of HeLa229 cells and enumeration of EBs stained with anti-Chlamydia major outer membrane protein antibody (provided by Dr. Harlan Caldwell).

2.1.2.2 Mouse experiments study 1

Eight weeks old C57BL/6 mice were purchased from The Jackson Laboratory (Bar Harbor, ME). For systemic infection, mice were intravenously (IV) injected in the lateral tail vein with $1x10^5$ *C. muridarum*. For vaginal infection, estrus was synchronized by subcutaneous injection of 2.5 mg medroxyprogesterone acetate (Greenstone, NJ). Seven days after, $1x10^5$ *C. muridarum* in 5µL sucrose/phosphate/glutamate buffer was deposited directly into the vaginal vaults with a blunted pipet tip (252). After that, 7, 10, and 14 days post-infection, blood was collected by retro-orbital bleeding. Immediately after collection, blood samples for cell sorting and validation analyses were air-shipped from the laboratory of Dr. McSorley (UC-Davis, CA) to the laboratory of Dr. Genescà (IGTP, Badalona, Spain). Samples arrived refrigerated and in good condition 48 hours later and were immediately processed.

Cell sorting study 1

Circulating CD62L⁻ CD44⁺ activated effector memory T cells. Cells were sorted from 7 days of Chlamydia-infected mice (VAG group) and six contemporary sham-treated mice (control group). Blood samples (~500 µl) were immediately lysed using an in-house red blood cell lysis buffer. After washing, cells were stained with antibodies against CD3-Vioblue (145-2C11), CD62L-PE (MEL-14-H2.100), and CD44-FITC (IM7.8.1; all from Miltenyi Biotec, Madrid, Spain) (Table 5). Cells suspended in cold FACS flow buffer (0.5% FBS-PBS with 0.5mM EDTA) were immediately sorted into 350 µl of chilled RLT buffer (QIAGEN, Valencia, CA) using a BD FACSAriaTM Cell Sorter (Flow Cytometry Platform, IGTP). Purity of sorted CD62L⁻ CD44⁺ activated TEM cells was >99%. Once sorted, samples were mixed for a minute (min), and after a short spin, the volume of RLT was adjusted (3.5:1 ratio of RLT to sheath fluid) using filtered tips. Next, samples were mixed, spun again, and frozen at −80°C.

2.1.2.3   Mouse experiment study 2

Six- to eight-week-old female C57BL/6 mice were bred in-house at the animal facility for the IGTP, Spain experimental models. Mice were kept in ventilated cages with sterile food and water ad libitum under specific-pathogen-free conditions. All animals were treated subcutaneously with 3 mg of Depo-Provera six days before euthanizing to homogenize the endocrine effects on immunity by synchronizing the menstrual cycle. All mice were euthanized with isoflurane (inhalation excess), and blood was immediately obtained by cardiac puncture.

Cell sorting study 2

Blood samples (~500 µl) were immediately lysed, washed, suspended in PBS, and incubated with Aqua vital dye to distinguish dead cells (Invitrogen, Burlington, ON, Canada). Cells were suspended in a staining buffer (1% BSA-PBS) and incubated with an Abs cocktail described in Table 5. Cells were suspended in a cold FACS-flow buffer and immediately sorted into CD3⁺ CD62L⁻ CD44ʰⁱᵍʰ CD11c⁺ and CD3⁺ CD62L⁻CD44ʰⁱᵍʰ CD11c⁻ using a BD FACSAria™ Cell Sorter. The purity of sorted cells was >99%. Each sample was sorted by collecting 300 cells directly into a refrigerated lysis buffer provided by the Institute for Research in Biomedicine (IRB, Barcelona, Spain) (74). Samples were immediately spun, heated at 65°C for 15 mins, and kept at 4°C until delivery to the Institute for Research in Biomedicine the following day for further RNA analysis.

Table 5. Abs cocktail for sorting experiment 2

Antibody	Fluorochrome	Clone	Volume	Manufactory
CD3	Vioblue	145-2C11	5 µl	Miltenyi Biotec[1]
CD4	APC-H7	GK1.5	3 µl	Miltenyi Biotec[1]
CD62L	PE	MEL-14-H2.100	5 µl	Miltenyi Biotec[1]
CD44	Brilliant Violet 570	IM7	5 µl	BioLegend[2],
CD11c	PE-Cy7	HL3	5 µl	BD Biosciences[3]

[1]. Miltenyi Biotec, Madrid, Spain; [2]. BioLegend, San Diego, CA; [3]. R&D Systems Inc., Minneapolis, MN

2.1.3 Gene expression experiments

Total RNA was isolated from cells using RNA easy Mini kit (QIAGEN). After a qualitative assessment of RNA integrity, samples were amplified using Whole Transcriptome Amplification 2 (Sigma-Aldrich, Madrid, Spain). We chose four samples in each group that qualified for microarray analyses, yet one sample from the VAG and control group was discarded as an outlier; thus, microarray analyses were performed in n=3 for the VAG group and n=3 for the control group (which were contemporary samples). The number of sorted cells in each group was similar (15,207 ± 2,339 cells for the VAG group and 20,793 ± 2,443 cells for the control group; not significant).

Affymetrix microarray hybridization was performed using the Mouse Genome 430 PM Strip platform. Image intensities were extracted using GeneAtlas System software (Affymetrix), normalized, and summarized using the Robust Multi-array Average algorithm. Differential gene expression analysis was assessed by fitting an empirical Bayesian linear model. Statistical significance in differential gene expression was computed with a false discovery rate multiple testing adjustment correction. We used the Limma package and the R statistical programming environment (253). The 'compute overlaps' function in the 'investigate gene sets web application [1] of the Molecular Signatures Database v4.0 (MaSigDB) was used to explore functions enriched among the top regulated genes defined as having a nominal (non-adjusted) p-value <0.005. The lists of gene symbols upregulated and down-regulated in infected versus uninfected samples were scrutinized for significant overlaps with a pathway (C2: CP, KEGG) and immunologic signatures (C7) in MaSigDB (79).

For study 2, additional bioinformatic analysis was done: NK-related γδTCR, iNKT CD4+, and iNKT CD4− specific gene sets (253) were tested by Gene Set Enrichment Analysis (GSEA) (79) for significant enrichment in CD11c+ cells.

---

[1] http://www.broadinstitute.org/gsea/msigdb/annotate.jsp

2.1.4 Flow cytometry analysis

This section describes the protocols used for flow cytometry in both mouse studies. Briefly, three main experiments were done in the following order:

- Confirmation and validation of the selected molecules from the microarray analysis in the Chlamydia mouse model
- Analysis of specific cell phenotypes in the tissue of mice infected with Chlamydia
- Analysis of specific cell phenotypes in the blood of mice infected with Chlamydia.

2.1.4.1   Confirmation of candidate molecules

Blood samples (~500 µl) were immediately lysed, washed, suspended in PBS, and incubated with Aqua vital dye to distinguish live from dead cells (Invitrogen, Burlington, ON, Canada). Following two more washes, cells were suspended in washing and staining buffer (1% bovine serum albumin-PBS) and incubated for 20 mins with a cocktail of pre-titrated anti-mouse Abs (Table 6).

Table 6. Abs cocktail for microarrays candidate molecules validation

Antibody	Fluorochrome	Clone	Volume	Manufactory
CD3	Vioblue	145-2C11	5 µl	Miltenyi Biotec
CD4	APC-H7	GK1.5	3 µl	Miltenyi Biotec
CD62L	PE	MEL-14-H2.100	5 µl	Miltenyi Biotec
CD44	Brilliant Violet 570	IM7	5 µl	BioLegend, San Diego, CA
CD11c	PE-Cy7	HL3	5 µl	BD Biosciences[1]
CCR5	FITC	CTC5	20 µl	R&D Systems Inc.
CXCR6	PerCP	221002	20 µl	R&D Systems Inc.
CCR2	APC	475301	6 µl	R&D Systems Inc.

1 BD Biosciences, San Jose, CA

All events were acquired in a BD FACSAriaTM Cell Sorter and analyzed with FlowJo vX.0.7 software (TreeStar, Ashland, OR).

Tissue and blood STAINING

Mouse tissues were harvested, and a single-cell suspension was prepared; Briefly, the mouse genital tract (vagina, cervix, uterine horns, oviducts), spleen, and draining lymph nodes dLNs were minced into small pieces and digested in 500 mg/L collagenase IV (Sigma) for 1 hour at 37 °C with constant stirring. Leukocytes were purified by percoll density gradient centrifugation (GE Healthcare), washed with FACS buffer, and stored on ice until use. Peripheral blood was collected by retro-orbital bleeding. Red blood cells were removed by ACK lysing buffer (Life Technologies). Leukocytes were washed with FACS buffer (PBS with 2% FBS) and stored on ice until use.

Single-cell suspensions from the spleen, dLNs, blood, and genital tract (GT) were prepared in FACS buffer and blocked with Fc block (culture supernatant from the 24G2 hybridoma, 2% mouse serum, 2% rat serum, and 0.01% sodium azide). Cells were stained with anti-

CD11b, F4/80, and B220-FITC together with MHC-II PerCP-Cy5.5 (dump channels), CD4-APC-eFluor780, CD8-Pacific Orange, CD44-Alexa 700 and CD11c-APC. All flow Abs were obtained from eBiosciences. Samples were acquired on an LSRFortessa flow cytometer and analyzed using FlowJo software (TreeStar).

2.1.4.2 T cell subset analyses

The Ab panel in Table 7 was used for T-cell subset analyses. Because of the low number of CD3$^+$ events in the genital tract (GT) of naïve animals, we analyzed some of the frequencies as % of the total number of events (i.e., CD3$^+$ or CD3$^+$ CD11c$^+$), while others, like the expression of specific molecules within the CD3$^+$ CD11c$^{+/-}$fractions, were analyzed as the % of the parent as we did for blood (i.e., CD3$^+$ CD11c$^{+/-}$TCR$\gamma\delta^+$). Boolean gating strategy was used for the simultaneous expression of different molecules, which were represented visually using Pestle (v1.7) and Spice (v5.3) software (provided by the National Institutes of Health) (87).

Table 7. Abs cocktail for T cell phenotype assessment from tissue and blood in mice experiment 2

Antibody	Fluorochrome	Clone	Volume	Manufactory
CD4	FITC	GK1.5	3 µl	eBiosciences[1]
CD8	FITC	53-6.7	3 µl	eBiosciences[1]
NKp46	PE	29A1.4	1 µl	Biolegend
CD49b	PE	DX5	3 µl	eBiosciences[1]
CD103	FITC	2E 7	1 µl	eBiosciences[1]
NK1.1	eFluor 450	PK136	3 µl	eBiosciences[1]
CD19	APC	MB19-1	2.5 µl	Biolegend
CD159a	APC	16A11	3 µl	Biolegend
CCR10	APC	248918	1 µl	R&D Systems
mCD1d	APC	PBS-57 tetramer	0.5 µl	NIH Tetramer Core Facility[2]
γδTCR	PE	eBioGL3	2 µl	eBiosciences[1]
CD11c	PerCP-Cy5.5	N418	5µl	eBiosciences[1]
CD3	Alexa700	eBio500A2	5 µl	eBiosciences[1]
CD11b	FITC	F4 80	3 µl	eBiosciences[1]
B220	FITC	RA3-6B2	0.5 µl	eBiosciences[1]
MHC-II	PerCP-Cy5.5	M5/114.15.2	1 µl	Miltenyi Biotec
CD4	APC-eFluor780	GK1.5	3 µl	eBiosciences[1]
CD8	Pacific Orange	53-6.7	3 µl	eBiosciences[1]
CD44	Alexa 700	IM7	2 µl	eBiosciences[1]
CD11c	APC	N418	5 µl	eBiosciences[1]

[1] eBiosciences San Diego, CA; [2] NIH Tetramer Core Facility, Emoroy University, Atlanta, GA

2.2 Human experiments

2.2.1 Ethics statement

Informed written consent was obtained from all participants, and the study protocols and questionnaires were approved by the University Hospital Germans Trias i Pujol (HUGTP, Badalona, Spain) Clinical Research Ethics Committee (reference numbers # EO-11-074 and # PI-14-070). The study was undertaken following the Declaration of Helsinki and the Good Clinical Practice requirements.

2.2.2 Participant enrolment and inclusion criteria for human blood and tissue samples

All participants from which blood was collected (age range: 20-40 years) were classified into the following different cohorts: normal donors (ND, n=13, 25±1 years old), psoriasis (PS, n=4, 34±3 years old), ulcerative colitis (UC, n=4, 28±3 years old), and BV (n=4, 31±4 years old). Healthy ND volunteers were recruited from the clinical trials unit of the University Hospital Germans Trias i Pujol (HUGTP, Badalona, Spain). Patient recruitment for the PS and UC cohorts was carried out in the related services of the Dermatology and Gastroenterology of the HUGTP. BV patients were recruited at the Attention to Sexual and Reproductive Health Unit from the Primary Health Care centers of Sabadell and Cerdanyola in Catalonia (Spain). An additional ND cohort (n=10, 27±4 years old) was enrolled for a specific T cell phenotype assessment.

Participants completed a questionnaire to detect possible exclusion criteria (other chronic or acute diseases, allergies or infections, immunosuppressive treatment, etc.) and to register menstrual cycle and birth control data. Patients in each cohort presented either an active burst (for PS and UC groups) or symptoms compatible with a recent infection within the last 7 days (for the BV group). Inclusion criteria for the PS group consisted of women with acute psoriasis *Vulgaris* that suffered a relapse of fewer than two weeks, with no treatment for at least six weeks. UC subjects were women with active ulcerative colitis: the extent of pathology was defined based on the Montreal classification (254) and the severity of the disease on the Mayo's Disease Activity Index (255). Only patients with an active burst (index >9) off immunosuppressive treatment were included. Lastly, untreated and symptomatic BV infections defined by Nugent scoring of >7 and suspected of *Gardnerella vaginalis* origin were confirmed by microscopic examination (which is considered by more than 20% of clue cells). Patients with other STIs were excluded.

Human cervical tissue was obtained from two sets of five healthy women (age 42-47) undergoing hysterectomy for benign indication at the HUGTP. After the Pathological Anatomy Service confirmed healthy tissue status, a separate piece from the ecto and endocervix, identified by anatomical localization, was delivered to the laboratory.

2.2.3 Flow Cytometry in blood samples from patient cohorts

Blood was collected and processed within 4 hours maximum. An ammonium chloride-based lysing reagent (BD Pharm Lyse, BD Biosciences) was used for erythrocyte deletion of 1 mL of blood. After washing, cells were suspended in PBS and stained with Aqua Dye (Invitrogen) for cell viability. Cells were rewashed, suspended in staining buffer, and divided into four tubes. The four assessed panels contained some common and specific Abs (Table 8). CD3$^+$ CD4$^-$ phenotype was considered CD8$^+$ T cells.

Table 8. Abs used for patients cohorts in flow cytometry study

Antibody	Fluorochrome	Volume	Manufactory
Common Abs			
CD3	eFluor 605	1µl	eBiosciences
CD4	Alexa 700	1µl	eBiosciences
CCR7	Horizon PE	0,5µl	BD Biosciences
CD38	Brillant Violet 421	1µl	BD Biosciences
HLA-DR	PerCP-Cy5,5	0,5µl	BD Biosciences
CD11c	PE-Cy7	1µl	BD Biosciences
Panel 1			
CCR2	PE	3µl	R&D Systems
CCR5	APC-Cy7	2µl	R&D Systems
CXCR6	APC	4µl	R&D Systems
CXCR3	FITC	3µl	BioLegend
Panel 2			
CD49d	FITC	4µl	BD Biosciences
β7	APC	2µl	BD Biosciences
CCR9	PE	3µl	BD Biosciences
CD29	APC-Cy7	2µl	BioLegend
Panel 3			
CD103	FITC	2µl	BioLegend
CD54	APC	0,5µl	BioLegend
CD49a	PE	0,5µl	BioLegend
CD29	APC-Cy7	2µl	BioLegend
Panel 4			
CD18	APC	4µl	BD Biosciences
CLA	FITC	10µl	BD Biosciences
CCR10	PE	2µl	BioLegend
CCR5	APC-Cy7	2µl	R&D Systems

For unconventional T cell subset phenotyping, an additional ND cohort was used. 1 mL of blood was lysed by ammonium Lysis Buffer (BD Pharm Lyse, BD Biosciences) and processed for staining. Leftover blood (~9 mL) was used to isolate peripheral blood mononuclear cells (PBMC) by density gradient centrifugation over the Ficoll gradient

(Biochrom AG, Berlin, Germany). Both cell suspensions were stained with the same Ab cocktail (Table 9).

Table 9. Unconventional T cell subset staining Abs

Antibody	Fluorochrome	Clone	Volume	Manufactory
CD3	eFluor 605	OKT3	2µl	eBiosciences
CD14	V450	MΦP9	2µl	eBiosciences
CD19	V450	HIB19	2µl	eBiosciences
CD11c	PE-Cy7	Bly6	2µl	eBiosciences
CCR7	PE-CF594	150503	1µl	eBiosciences
CD8-	V500	RPA-T8	5µl	BD Biosciences
NK1.1	PE	191B8	2µl	Milteny Biotec
γδTCR	FITC	11F2	20µl	Milteny Biotec
Vα7.2	APC	REA179	2µl	Milteny Biotec
Vα24	APC	6B11	5µl	BioLegend

For both experiments, cells were acquired using a BD LSRFortessa SORP flow cytometer (Flow Cytometry Platform, IGTP) and analyzed with FlowJo 9.3.2 software (TreeStar). Gates were drawn based on fluorescence minus one-controls.

2.2.3.1 PBMC activation and intracellular staining

PBMC were cultured in RPMI 1640 supplemented with 10% FBS and 40 µg/mL gentamycin. Stimulation was performed with 1µl (E)-4-hydroxy-3-methyl-but-2-enyl pyrophosphate (HMBPP, Sigma). After 18 h of activation, Brefeldin A (GolgiPlug, BD Biosciences) was added. Five hours later, cells were stained with an Ab mixt, described in Table 10. After surface staining, cells were fixed and permeabilized with Fix/Perm Kit (Invitrogen) and intracellularly stained with IFNγ-Alexa700 (B27). Data were acquired and analyzed as described before for blood.

Table 10. Abs for intracellular staining panel

Antibody	Fluorochrome	Clone	Volume	Manufactury
CD3	PerCP	OKT3	2µl	BD Biosciences
CD11c	PE-Cy7	B-Lye6	2µl	BD Biosciences
HLA-DR	PerCP-Cy5	G46-6	2µl	BD Biosciences
CD69	PE-CF594	FN50	5µl	BD Biosciences
γδTCR	PE	11F2	2µl	Miltenyi Biotec
IFN-γ	ALEXA 700	B27	2,5µl	Miltenyi Biotec

2.2.4 Cervical tissue digestion and flow cytometry

Human cervical tissue was obtained from two sets of five healthy women, which was collected in refrigerated RPMI 1640 medium (Cellgro, Manassas, VA) containing 10% FBS (Lonza, Basel, Switzerland), 500 U/mL penicillin, 500 µg/mL streptomycin, 5 µg/mL fungizone and 1 µg/mL gentamycin (Life Technologies). Tissue was processed within the next 12 h after surgery, and 8–mm^3 block dissection was performed as described (256). Tissue digestion of 5-9 pieces of ecto or endocervix with collagenase IV (Invitrogen) was immediately executed as described (256). Tissue blocks were then dissociated manually with a disposable pellet pestle and filtered through a 70µm-cell strainer (BD Biosciences). After centrifugation, the pellet was suspended in staining buffer (1% mouse serum and 1% goat serum in PBS) and stained with different combinations of Abs, described in Table 11. Data were acquired and analyzed as described for blood.

Table 11. Flow cytometry Abs mixt for cervical tissue study

Antibody	Dye	Clone	Volume	Manufactury
CD3	eFluor 605	OKT3	2µl	eBiosciences
CD14	V450	MØP9	2µl	BD Biosciences
CD11c	PE-Cy7	Bly6	2µl	BD Biosciences
CD8	V500	RPA-T8	5µl	BD Biosciences
HLA-DR	PerCP-Cy5.5	G46-6	2µl	BD Biosciences
CD69	Horizon PE	CF594	5µl	BD Biosciences
NK1.1	PE	191B8	2µl	Milteny Biotec
γδTCR	FITC	11F2	20µl	Milteny Biotec
Vα7.2	APC	REA179	2µl	Milteny Biotec
CD103	FITC	Ber-ACT8	3µl	BioLegend
Vα24	APC	6B11	5µl	BioLegend

2.2.5 Statistical analysis

Data are reported as the mean and the standard deviation (SD) for each group using Prism 4.0 software (GraphPad Software). For animal samples, statistical analyses were performed by Student's t-test or by Paired t-test when comparing the positive and negative fractions of the same sample. For all the other analyses in human samples, which did not pass the normality test ($p < 0.05$), non-parametric tests were employed.

2.3 Detailed protocols and buffer recipes

2.3.1 Mouse blood protocol

2.3.1.1   Solutions and buffers

- RBC Lysis Buffer (always used at RT):
    - 4.15 g NH_4Cl
    - 0.5 g $NaHCO_3$
    - 0.0186 g Disodium Ethylenediaminetetraacetic acid (EDTA)
    - 200 mL distilled H_2O
    - Sterile PBS
- Staining and Washing solution (SWB, 1 L): BSA 1g in 1 L PBS solution 1X
- FACS-Flow (PBS + EDTA 0.5mM) + 0.5–1% FBS. Use this buffer for cell suspension before sorting only.
- Notes: It is possible to use RPMI 1640, which contains serum as a staining buffer. Sodium azide is not needed as long as the incubation and the washes are done at 4°C. However, we have found that RPMI can increase the autofluorescence of cells and is not necessary for good viability (at least for human lymphocytes). Do not use RPMI for staining with avidin because its biotin will bind all the avidin.

2.3.1.2   Erythrocytes Lysis

1. Take 500 µl from mice blood.
2. Label 15 mL tubes necessary to separate blood in 250 µl fractions.
3. Add 5 mL of RBC lysis buffer (at RT) per 250 µL of mouse blood. Incubate 10 mins.
4. Spin the cells 5 mins at 400xg at 4°C and resuspend the pellet in 5 mL SWB to wash. Pool samples from the same animal in the same tube.
5. Spin the cells 5 mins at 400xg at 4°C and resuspend in 1 mL of SWB per each 500 µl of blood since we assume it corresponds to $1x10^6$.

2.3.1.3   Cell labeling for flow cytometry and sorting

1. Add 0.5µl of Aqua (dead cells staining). Incubate for 30 mins at RT, *protected from light. Note:* Because some mAb-fluorochromes and free amino acids in media can compete with amine-reactive dyes, all other surface stains should be added in a separate step to avoid the loss of dye effectiveness. In addition, PBS is used in this staining step, but all other wash steps can use media containing Fetal Bovine Serum or other enriched media containing amino acids.
2. Spin down 5 mins at 400xg, at RT.
3. Wash *twice* with 1 mL of PBS and centrifuge.
4. Resuspend 100 µL per 500µl of blood and add the corresponding Abs cocktail. Incubate for 20 mins at RT in the dark.
5. Add directly 2-3 mL of SWB and then spin down 5mins at 400x g, at RT.

6. Wash again with 2-3 mL and centrifuge.
7. Resuspend in FACS Flow: in 300 µL and keep cold.
8. Prepare RNAse-free Eppendorf with 350 µL of fresh RLT buffer and keep cold.

2.3.1.4   Cell sorting

1. Sort the sample as CD3$^+$ CD62L$^+$ CD44^{High} (these are the activated effector T cells of interest).
2. Sort all cells in the RLT Eppendorf (10,000-40,000 events): cap the tube, vortex for 1 min, and spin a few seconds to bring everything down.
3. Then, using a pipette with a sterile tip, measure the final volume.
4. Calculate the exact volume of the sample sorted into RLT. Adjust the amount of RLT to maintain a 3.5:1 ratio of RLT to sheath fluid using filtered tips. For example, if we now have 550 µL (µL of total volume, 200 µL of sheath fluid is dropped into the collection tube during the sort: 550 µl– 350 µl we had before. Then 3.5*200 µL =700 µL is needed as total, so add an extra 350 µl (700 µl-350 µl=350 µL) of chilled RLT into collected sample, and the final volume will be 900 µL (200 µL sheath fluid+700 µL RLT=900 µL). (from experience, 20.000 cells 350 µl, while 40.000 about 500 µl)

Notes: When sorting directly into RLT buffer, make sure to sort at a ratio of 100 µL of sort sample to 350 µL of RLT or a multiple of that. For low cell number samples, start with 350 µL of RLT. 350 µL of RLT can lyse no more than 5 million cells, 500 µL for 5-8 million cells. Use Eppendorf RNAsa free for every 2×10^6 cells. Pipette until there are no aggregates.

1. Cap the tube, vortex for 1 min, and spin to bring everything down. Freeze immediately on dry ice and store at –80°C.

2.3.2 Mouse tissue protocols

2.3.2.1   Buffers and reagents

- PBS 1mM EDTA 5% FBS (a minimum of 100 mL). Prepare EDTA PBS solution and autoclave.
- PBS 2% FBS. Prepare 0,8 mL FBS in 39,2 mL PBS (Cold).
- FACS-Flow (same as sorting): (PBS + EDTA 0,5mM) + 0,5-1% FBS. 0.5 mM EDTA (0,186 g/L) it dissolves easily in PBS (autoclave 20 mins at 131°C.)—store at RT. When you add 0,5–1% FBS, only on aliquots, keep at 4°C (1mL/100ml).
- On the day: prepare 1 ml of 2 mg/mL collagenase D (Roche) and 30 µg/mL DNase I in HBSS.
- HBSS (*11520476 Fisher Scientific*).
- 70–µm cell strainer (11883403 *Fisher Scientific*).
- Lineage FITC Abs or Isolating Kit (Stem cell).

2.3.2.2   mouse tissue staining Protocol

1. Preheat HBSS for digestion at 37°C.
2. Remove tissue pieces and place them into each Eppendorf.
3. Clean from fatty tissues and smash with the bottom syringe or cut with scissors.
4. Digest each tissue piece with A): 1 mL of 2 mg/mL collagenase D (Roche) and 30 µg/mL DNase I at 37 ° C for 30 mins in HBSS. Tissue pieces are collected in 0.5 mL of pure HBSS.
5. Add the pre-heated digesting mixtures, vortex, and leave in agitation at 37 ° C for 30 mins. Then, put the centrifuge at 4 ° C.
6. Add the mixture to a pre-heated 15 mL tube containing B) 5 mL of 1 mM EDTA PBS with 5% FBS. Incubate at 37 ° C for 5 mins.
7. Filter in a 70–µ m cell strainer to obtain single cells (smashing with pipette tip against filter) in a 50 mL conical tube on ice.
8. Centrifuge 1400 rpm 5 mins at 4 ° C. Work fast, keep cells cold, and use pre-cooled solutions.
9. Resuspend cells in 500 µl cold PBS containing 2% FBS (on ice).
10. Count cells: on a facs tube, place 30 µl of PBC (warm up a bit PBC and vortex well before taking them out) and then vortex the sample and add 30 µl to the same tube.
11. Calculate the number of cells and centrifuge again to adjust to 2,5 x10^6 cells per 100 µl of FACs Flow volume.
12. Take 100 µl (2,5 x10^6 cells) in a new FACS tube.
13. Incubate for 10 mins at 4 ° C in the presence of 5 µl of anti-CD16/32 Abs to block Fc receptors (FcR Blocking Mouse Ref. 130-092-575 Miltenyi).
14. Then immediately stained with Abs cocktail (24 µl each tube):
15. Incubate for 1 h on ice (in the dark).
16. Wash with FACS-Flow twice, centrifuge 1400 rpm 5 mins at 4 ° C.
17. Resuspend in 100 µl FACS Flow. Acquire 300.00 to 500.000 cells for each tissue piece.

2.3.3 Human blood staining

2.3.3.1   Homing panel staining protocol

1. Stain 100 µL of blood directly with the titrated amount of Ab.
2. Incubate for 15 mins, covered at RT.
3. Prepare 2 mL of Lysing Buffer: 200 µL (#555899) in 1,8 mL distilled sterile water at RT.
4. Add directly after the 15 mins. Vortex and leave for 5 mins at RT covered, after vortex again.
5. Incubate 5 mins more at RT covered.
6. Centrifuge 5 mins at 300-400xg at RT.
7. Wash and discard the supernatant and resuspend it in 3 mL PBS.

8. Centrifuge 5 mins at 300-400xg at RT.
9. Resuspend in 300 μL PBS.
10. Analyze in BD LSRFortessa™ Cell Analyzer immediately. Record the maximal events as maximal: 500.000 approx.

2.3.3.2 Unconventional T cell staining protocol

1. Separate 1 mL of blood and place it into a 50 mL conical tube.
2. Lyse with 9 mL of Pharmalyse® (1:10) at RT.
3. Incubate for 10 mins in the dark at RT, then spin down 7 mins at 400g, RT. Keep the tube on ice.
4. Wash with 10 mL SWB (cold) and spin down again. *Spin CD1d tetramer in a microcentrifuge at $14,000 \times g$ for 3 mins, at 4ºC.
5. Suspend in residual volume (50 μl aprox).
6. Add one test (0.5μl) of fluorescently-labeled tetramer to the cells and mix by pipetting.
7. Incubate at 4°C for 30 mins, shielded from light: in the refrigerator covered with foil.
8. Wash cells with 1mL SWB per tube.
9. Spin down 5 mins at 500xg 4ºC, then suspend in 100 μl.
10. Add the corresponding Abs cocktail.
11. Incubate tube on ice for 30 mins, shielded from light.
12. After 30 mins, add 1mL of SWB and spin down 5mins, 500xg at 4ºC.
13. Wash again with 1mL SWB and spin down.
14. Suspend the sample in 100 μl PBS.
15. Analyze in BD LSRFortessa™ Cell Analyzer immediately. Record the maximal events as maximal: 500.000 approx.

2.3.4 Cervical explant staining protocol

1. Set thermomixer at 37ªC.
2. With forceps, pick up the tissue blocks into a 1.7–mL Eppendorf tube containing 0.5 mL of RPMI–5% FBS.
3. Transfer up to 8 cervicovaginal tissue blocks.
4. Add 500 μl of collagenase IV (10 mg/mL) solution per tube containing the blocks to be digested.
5. Place the tubes in the Thermomixer and agitate at 400 r.p.m. for 30 mins.
6. Prewet and label one strainer-cap 12 × 75 tubes per experimental condition for analysis by addition of 500 μl of PBS.
7. Remove 500 μl of medium from the digestion tube with a pipette and transfer it to the appropriate strainer tube.
8. Carefully insert a disposable pellet pestle into the digestion tube and rotate the pestle while pulling it up and down without removing it from the tube. Proceed to two series of 20 rotations.

9. Transfer the content of the tube to the corresponding prewet strainer-cap tube.
10. Rinse the tube with 500 µl of PBS; pass through the strainer.
11. Centrifuge at 400xg for 5 mins at 16 °C; decant the supernatant.
12. Resuspend the pellet in 1 mL of PBS and centrifuge at 400xg for 5 mins at 16 °C; Decant the supernatant.
13. Resuspend the pellet in 500µl PBS for cell surface staining.
14. Prepare and label 12 × 75 tubes—also, the Ab mix.
15. Keep an aliquot (50–100 µl) of cell suspension (from Step 13) on ice.
16. Add 2 µl of Live–Dead fixable blue stain solution to the remaining 500 µl or 1–µl to the cell suspension aliquot.
17. Incubate at RT for 15 mins.
18. Add 500 µl of staining buffer.
19. Centrifuge at 400xg for 5 mins at 16 °C; decant the supernatant.
20. Resuspend the pellet in 0.5 mL of staining buffer.
21. Distribute 50–µl aliquots of cells into 12 × 75 FACS tubes containing specific volumes of the Abs mixes.
22. Incubate at RT for 20 mins.
23. Add 2 mL of staining buffer to the tubes containing cells to be stained.
24. Centrifuge at 400xg for 5 mins at 16 °C; decant the supernatant.
25. Fixation protocol:
26. Add 100 µl of PBS to each tube and vortex gently.
27. Add 100 µl of a 2% (wt/vol) formaldehyde solution in PBS and vortex gently.
28. Incubate at RT for 1 h.
29. Keep samples in the dark at 4 °C and acquire samples on flow cytometer BD LSRFortessa™ Cell Analyzer within 48 h.

2.3.5 PBMC protocol

1. Take 3 ml of blood from EDTA tube in sterile conditions.
2. Add 3 ml sterile PBS to make a total volume of 6 ml.
3. Spin down 15' at 900 rpm, at RT.
4. Remove the serum part (yellow).
5. Add 3ml approx of PBS to make a total volume of 6 ml.
6. Put 4 ml of Ficoll® in 50 ml conical tubs. Then carefully add the blood (from point 5) to each tube.
7. Spin down 30' at 720 g with Acceleration: 9/brake: 0
8. Take the leucocyte band (the white one) and put it in another 50 ml conical tube.
9. Wash with 10 ml PBS twice. Spin down 5' at 1400 rpm at RT.
10. Add 9ml PharmaLyse® 1:10. Incubate for 10 min in the dark at RT.
11. Spin down 5' at 1400 rpm at RT.
12. Wash with PBS and spin down again.
13. Suspend in 500 µl of PBS.
14. Take 50 µl by "reverse pipetting" and put it in Facs tube.

15. Add 50 µl by "reverse pipetting" from perfect count bottle after hard agitation it should be at RT.
16. From this point, you can start the stimulation protocol.

2.3.5.1   Stimulation of PBMC in vitro and intraceLlular staining

Before starting, it is necessary to count cells following the next steps

- Acquire at least 5000 Cells to see a defined population and verify that at least 1000 events have been acquired in the bead gate for the count to be statistically significant.
- In the same template, analyze acquisition and calculate the number of cells/ml according to the formula: Number of Cells (R2)/Number of FL2 Beads * Beads kit concentration (beads/ µl) *1000 = cells/ml

For culture procedure:

- Use c RPMI 1640 culture medium supplemented with 10% FBS and 40µg/ml gentamicin (Life Technologies)
- Suspend fresh PBMCs at 0.5x106 in 100 µl of culture medium
- Separate 1 tube to stain and analyze without culturing (baseline).
- Add 100 µl per well in each well (48 well plate).
- For stimulation, add 1 µl (E)-4-hydroxy-3-methyl-but-2-enyl pyrophosphate (HMBPP, Sigma) at a final concentration of 100 nM
- Incubate at 37ºC in 85º inclination (covered).
- After 18 hours of activation, Brefeldin A (SigmaGolgiPlug, BD) was added to the medium to reach a final 3.0 ug/ml concentration.
- 5 hours. Later, cells were stained following the previous intracellular staining protocol.

3 Results

Study 1. Identification of proteins and gene transcripts of molecules specific to T lymphocyte homing to the FGT using differential and integrative analyses from different groups of infected mice

3.1 Gene expression in mice

In order to define the transcriptomic profile of TEM cells (CD3$^+$ CD62L$^-$CD44$^+$ T) during early infection, the mouse model of *C. muridarum* infection was used. We compared two groups with 3 animals per group. The VAG group represents the group of vaginally-infected mice, and the control group represents the sham (simulating the infection by depositing physiological serum in the vagina). Blood was obtained 7 days post-infection (PI). The RNA samples extracted from blood were analyzed to assess their integrity before performing the microarray protocol. Microarray gene expression profiling was performed in collaboration with the Functional Genomics Core, Institute for Research in Biomedicine (IRB Barcelona).

As a first step, DAVID gene ontology tool was used for the functional analysis of the list of upregulated genes. First, fluorescence data were normalized and transformed to log2 values. After this step, a *t*-test was applied to compare gene expression between control and VAG groups. In addition to the *t*-test, the fold-change of the list of resulting genes was calculated, considering log values greater than 0.5 as significant. After applying the two filters, the gene list was uploaded to the online bioinformatic tool to classify the overexpressed genes into functional clusters. The first results obtained using the DAVID tool (Table 12) show clusters related to cellular and immunological functions. In summary, functions of transcription (11% of genes), cell cycle (7.6% of genes), regulation of programmed cell death (4.7% of genes), and a small fraction of genes related to cytokine signaling (0.9% of genes). The first data analysis invited the application of more sophisticated bioinformatics analysis using the Limma package and the R statistical programming environment. The second round of analysis was done under the supervision of Dr. Lauro Summoy from Genomics and Bioinformatics Group, Institute for Predictive and Personalized Medicine of Cancer (IMPPC), Can Ruti Campus, Badalona, Spain.

Table 12. Gene ontology chart for upregulated genes using DAVID platform

Category	Term	Count	%	P-Value	Benjamini
GOTERM_BP_FAT	Transcription	58	11	4.30E-02	6.90E-01
GOTERM_BP_FAT	Cell cycle	40	7.6	1.50E-07	2.60E-04
GOTERM_BP_FAT	Phosphorus metabolic process	33	6.2	2.50E-02	6.10E-01
GOTERM_BP_FAT	Phosphate metabolic process	33	6.2	2.50E-02	6.10E-01
GOTERM_BP_FAT	Protein localization	31	5.9	1.20E-02	4.50E-01
GOTERM_BP_FAT	Macromolecule catabolic process	28	5.3	1.10E-02	4.50E-01
GOTERM_BP_FAT	Cell cycle process	27	5.1	1.10E-02	9.10E-03
GOTERM_BP_FAT	RNA processing	27	5.1	6.60E-05	1.90E-02
GOTERM_BP_FAT	Cellular macromolecule catabolic process	26	4.9	1.50E-02	4.70E-01
GOTERM_BP_FAT	Protein transport	26	4.9	3.00E-02	6.30E-01
GOTERM_BP_FAT	establishment of protein localization	26	4.9	3.30E-02	6.50E-01
GOTERM_BP_FAT	regulation of apoptosis	25	4.7	8.90E-03	4.70E-01
GOTERM_BP_FAT	protein catabolic process	25	4.7	9.60E-03	4.60E-01
GOTERM_BP_FAT	regulation of programmed cell death	25	4.7	1.00E-02	4.60E-01
GOTERM_BP_FAT	regulation of cell death	25	4.7	1.10E-02	4.60E-01
GOTERM_BP_FAT	cell cycle phase	24	4.5	1.40E-05	5.90E-03
GOTERM_BP_FAT	death	24	4.5	8.10E-03	4.60E-01
GOTERM_BP_FAT	cytokine-mediated signaling pathway	5	0.9	5.60E-02	7.30E-01

Table 13. Functions enriched among the top upregulated genes in activated effector T cells from Chlamydia-infected versus uninfected mouse samples with Canonical pathways

Gene Set Name	# Genes in Gene Set (K)	Description	# Genes in overlap (k)	k/K	p-value	FDR q-value
REACTOME_SYNTHESIS _OF_DNA	92	Genes involved in Synthesis of DNA	7	0.0761	6.60E-08	7.02E-05
REACTOME_INTERFERON_ SIGNALING	159	Genes involved in Interferon Signaling	8	0.0503	1.87E-07	7.02E-05
REACTOME_ANTIVIRAL_MECHA NISM_BY_IFN_STIM._GENES	66	Genes involved in Antiviral mechanism by IFN-stim. genes	6	0.0909	2.03E-07	7.02E-05
REACTOME_S_PHASE	109	Genes involved in S Phase	7	0.0642	2.13E-07	7.02E-05
REACTOME_IMMUNE_ SYSTEM	933	Genes involved in Immune System	16	0.0171	6.15E-07	1.33E-04
PID_TCPTP_PATHWAY	43	Signaling events mediated by TCPTP	5	0.1163	6.29E-07	1.33E-04
REACTOME_CELL_CYCLE	421	Genes involved in Cell Cycle	11	0.0261	7.08E-07	1.33E-04
REACTOME_CYTOKINE_SIGNAL ING_IN_IMMUNE_SYSTEM	270	Genes involved in Cytokine Signaling in Immune system	9	0.0333	1.02E-06	1.69E-04
REACTOME_CELL_CYCLE_ MITOTIC	325	Genes involved in Cell Cycle, Mitotic	9	0.0277	4.66E-06	6.65E-04
REACTOME_DNA_STRAND_ELO NGATION	30	Genes involved in DNA strand elongation	4	0.1333	5.04E-06	6.65E-04
REACTOME_ACTIVATION_OF_T HE_PRE_REPLICATIVE_COMPL EX	31	Genes involved in activation of the pre-replicative complex	4	0.129	5.77E-06	6,92E-04
REACTOME_DNA_REPLICATION	192	Genes involved in DNA Replication	7	0.0365	9.38E-06	1,02E-03

K indicates the number of genes in the set from MSigDB. 1; b k indicates the number of genes in the intersection of the query set with a set fromMSigDB. 2; c k/K indicates the proportion of gene set genes in the query set. 3; d FDR corresponds to the false discovery rate.

The results were very similar to the ones obtained previously. Clusters of immune response genes were differentiated. The most significant clusters were: signaling via IFN (159 genes), immune response (933 genes), and signaling via cytokines (270 genes), in addition to other functional groups related to cell division and DNA replication (Table 13).

Several genes related to T cell homing were found in the list of genes with higher expression and fold change in the VAG group compared to the control group. The genes with the most interest in this sense were selected for subsequent validation by flow cytometry: CCR5, ITGAX, CXCR6, and CCR2 (Figure 11).

Probe Set ID	Gene Symbol	Gene Title	Fold Change	P.Value	adj.P.Val
1422259_PM_a_at	Ccr5	chemokine (C-C motif) receptor 5	3.64	0.01	0.56
1419128_PM_at	Itgax	integrin alpha X	2.93	0.02	0.58
1422812_PM_at	Cxcr6	chemokine (C-X-C motif) receptor 6	2.62	0.01	0.56
1421188_PM_at	Ccr2	chemokine (C-C motif) receptor 2	2.46	0.00	0.54
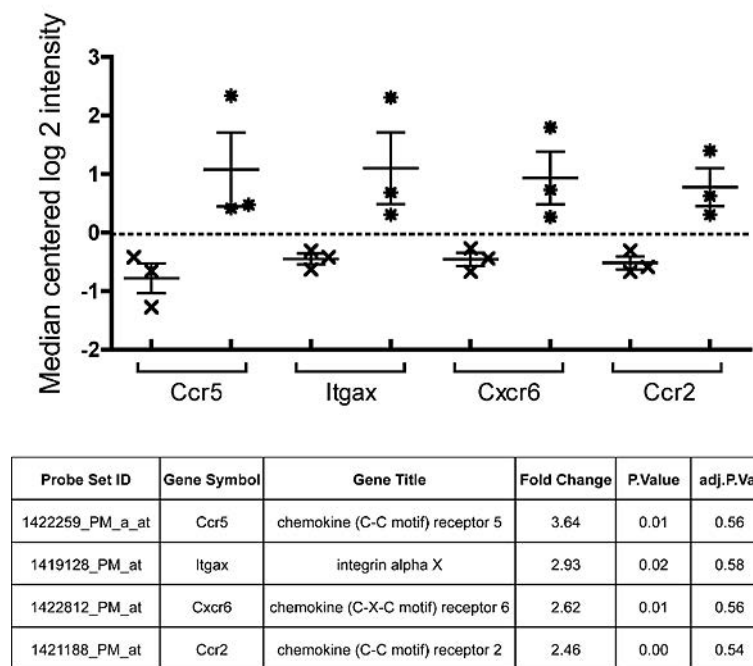
Figure 11. Adhesion molecule-related genes overexpressed in circulating activated TEM cells from vaginally Chlamydia-infected mice

Median centered log 2 intensity values derived from Affymetrix microarray hybridization experiments comparing non-infected 7 control mice (n=3, x symbol) vs. vaginally-infected mice (n=3, * symbol) for the CCR5, 8 Itgax, CXCR6, and CCR2 genes are shown. Fold change: average fold change of vaginally- infected vs. control mice. P value: nominal p-value. Adj p-value: false discovery rate adjusted 10 p-values.

3.2 Candidate molecules validation in *mice*

This section shows the confirmatory results of the findings obtained from the transcriptomics study. For this purpose, a panel of 10 colors was analyzed by flow cytometry. The results are shown separating four experimental groups: control, 7, 10, and 14 days PI. In each group, the CCR2, CCR5, CXCR6, and CD11c (Itgax) protein expression in CD4$^+$ and CD4– Live T cells (putative CD8$^+$) was evaluated.

As a general trend, the expression of the receptors studied reached its maximum at ten days PI. In most cases, a significant difference was shown between the control and VAG groups regardless of the PI days (Figure 12). There was also an increase in TEM (CD62L$^-$) cells in the VAG group versus controls. In addition, an exclusive increase in the frequency of

activated CD4$^+$CD62L$^-$CD44$^+$ T cells was recorded (from 5.2% in control animals to 12-19% in all conditions in the VAG group; p<0.01 in all the cases; Figure 12). On the other hand, CD8$^+$ T cells demonstrated a significant increase in both CD44$^+$ (from 8.7% to ~27%) and CD44$^-$ (from 6% to ~16%), 10 and 14 days PI (p<0.02 for all; Figure 12; e and f).
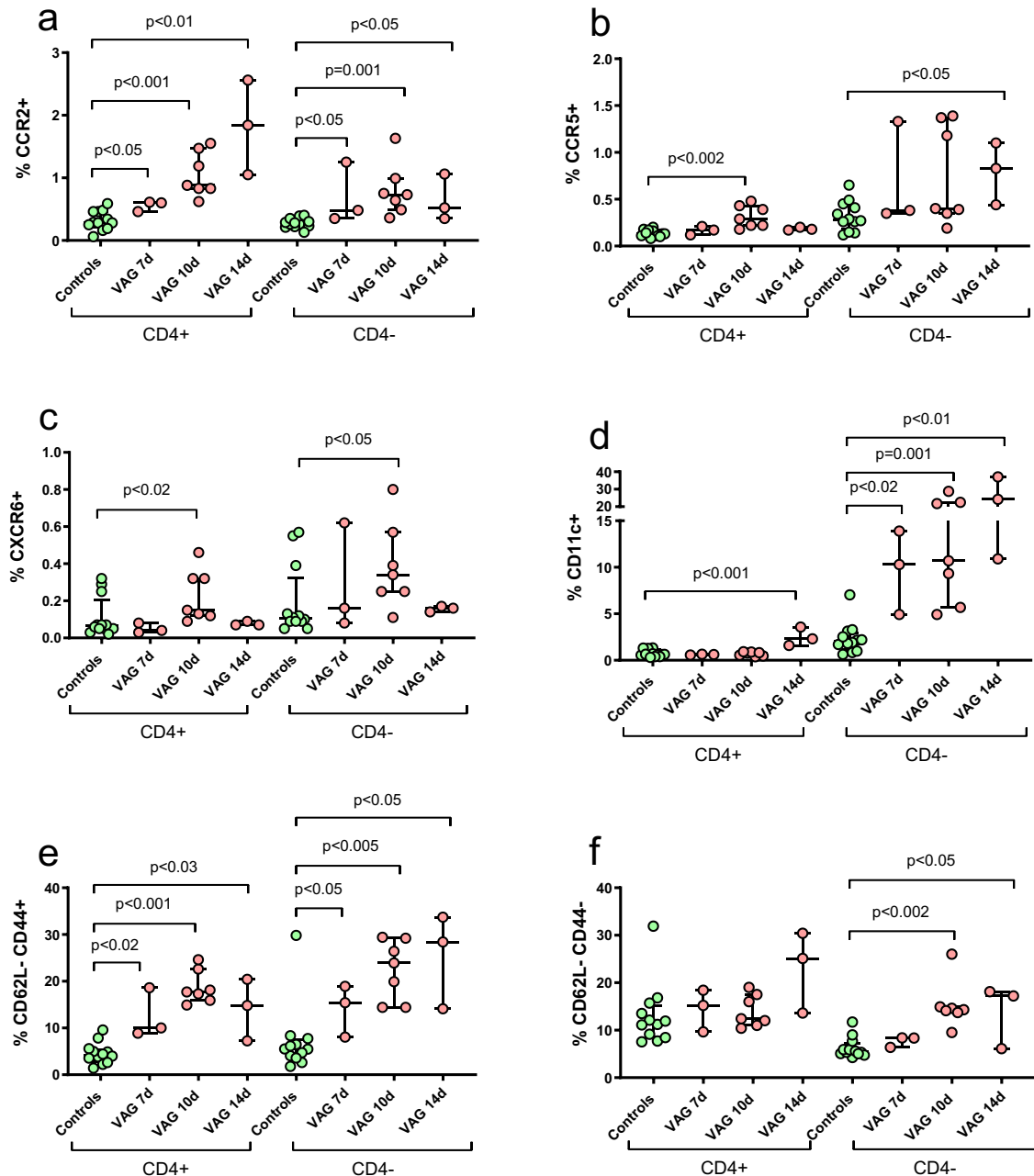
Figure 12. Kinetics of the frequency of adhesion molecules and effector T cells after vaginal infection in mice

The frequency of CCR5 (a), CCR2 (b), CXCR6 (c), CD11c (d), CD62LCD44+ (e), and CD62L- CD44- (f) was determined in T cells from blood by flow cytometry at 7, 10 and 14 days after vaginal infection with C. muridarum in mice. After gating on live CD3+ cells and CD4+ or CD4- (putative CD8+) T cells, the frequency of CCR5, CCR2, CXCR6, CD11c, CD62L- CD44+ and CD62L- CD44- was quantified. Each time point represents the median ± interquartile range of three or seven infected animals and all controls (n = 12).

When further analyzing the expression of selected targeted molecules, only the subset of activated TEM cells, CD4$^+$ CD44$^+$ TEM cells showed a significant increase in CCR2,

CXCR6, and CD11c at 10 and 14 days PI, and CCR5 only at 10 days PI (Figure 13: a, b, c, and d). In contrast, CD8$^+$CD44$^+$ TEM cells increased expression of CXCR6 at 7 days PI and CD11c at all PI times (Figure 13; e and g). Although the expression of these markers was also increased in the non-activated fraction of both TEM cell subsets, the magnitude of expression was much lower (Figure 13; b, d, f, and h). Therefore, all selected upregulated genes were confirmed by protein expression. In addition, while CCR2 and CCR5 were only increased in the CD4$^+$ TEM cell subset after infection, CXCR6 and CD11c expression were much more abundant in CD8$^+$ TEM cells (Figure 13; a, b, e, and f).
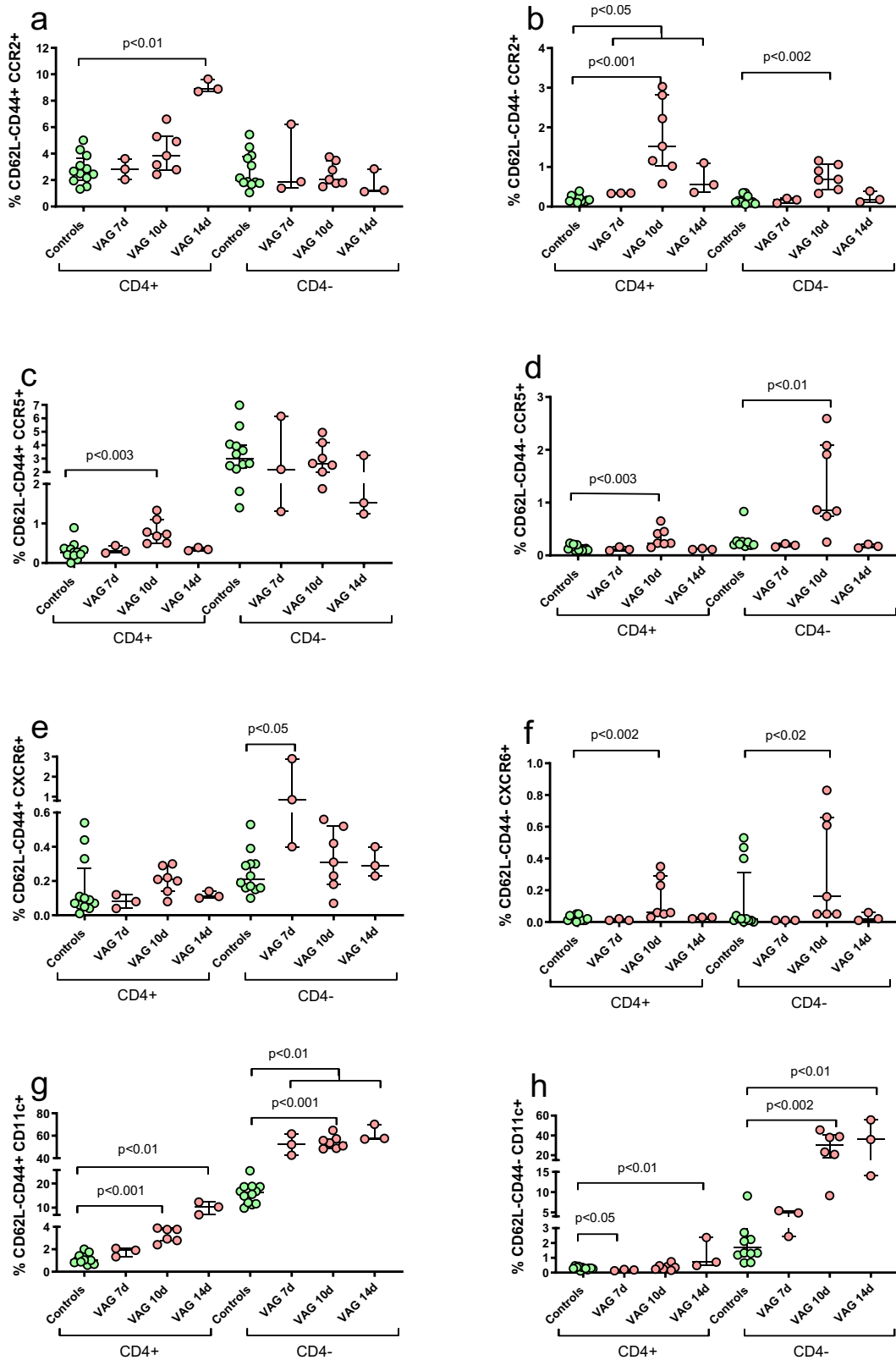
Figure 13. Kinetics of CCR2, CCR5, CXCR6, and CD11c expression after vaginal 1 Chlamydia infection in mice

The frequency of CCR5 (a, b), CCR2 (c, d), CXCR6 (e, f) 2, and CD11c (g, h) was determined in activated CD44+ (left graphs) and CD44- (right graphs) 3 effector memory T (TEM) cells from blood by flow cytometry at 7, 10 and 14 days after vaginal infections with C. muridarum in 4 mice. After gating on live CD3+ cells and CD4+ or CD4- (putative CD8+) T cells, the frequency of CCR5, CCR2, CXCR6, and CD11c was quantified in the CD62L- CD44+/CD44- T cell subsets. Each time point represents the mean 7 ± standard error of the mean of three infected animals and all controls (n=9).

Study 2. Confirmation and validation of the expression of the selected candidates on circulating T lymphocytes in healthy patients in comparison to patients with mucosal conditions

3.3 Validation of Homing Molecules in Women

3.3.1 Homing Molecules During Baseline Conditions

This section addresses the expression of relevant mucosal-homing markers in TEM cells. On top of validating the candidate molecules obtained in Study 1, we also added other known adhesion molecules relevant to some of the conditions studied. The study was done in 4 groups of patients. Briefly, 1) PS: Women with acute psoriasis *vulgaris* who experienced a recurrence of fewer than two weeks and did not receive therapy for at least six weeks; 2) UC: Women with active ulcerative colitis (index >9) after stopping immunosuppressive therapy; 3) BV: Infected women *Gardnerella vaginalis*, untreated, symptomatic, and classified by optical microscopy and Nugent score of >7. Additionally, we add a control group 4 named ND, represented by women without known immunological disorders, recent infections, or immunosuppressive treatment. Different mucosal homing markers were analyzed in peripheral blood in TEM CCR7$^-$CD4$^{+/-}$ cell populations (CD4$^-$ cells are considered putative CD8$^+$). In addition, the same markers were analyzed based on the expression of the cellular activation markers HLA-DR and CD38 (Figure 14).
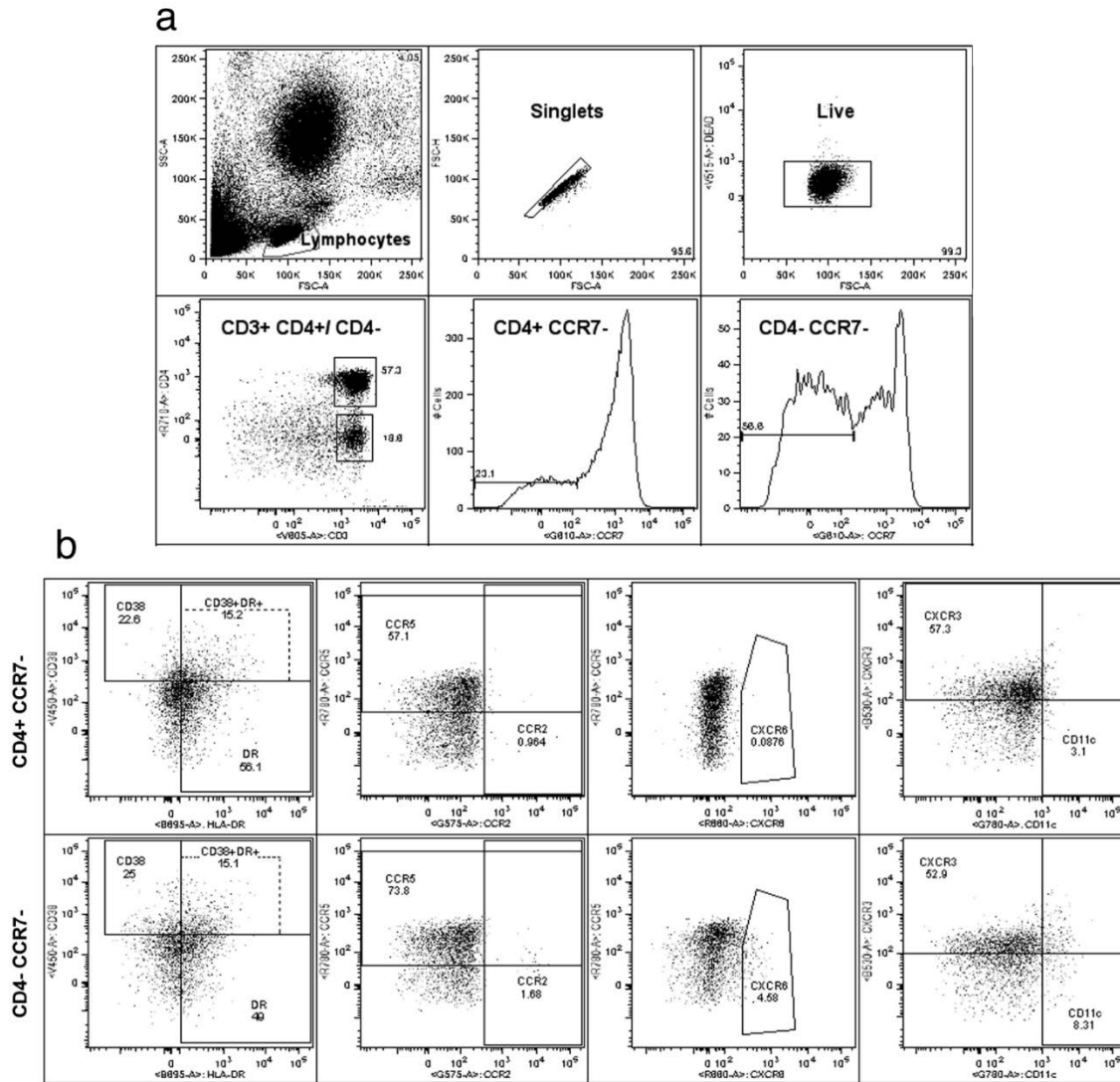
Figure 14. General gating strategy and homing markers assessment in circulating TEM cells from women

The overall gating strategy for a representative single 4 normal donor is shown. (a) General gating strategy for effector memory T (TEM) cells 5 consists of the following consecutive gates: lymphocytes, singlets, and live CD3+ T cells (top 6 rows); CD4+ and CD4- (putative CD8+) T cells, and the effector CCR7- fraction for each of 7 these subsets (bottom row). (b) Representative plots of molecules analyzed in TEM cells in 8 one of the panels are shown: activated CD38 and/or HLA-DR TEM cells, expression of 9 CCR5 and CCR2, expression of CXCR6, and expression of CXCR3 and CD11c for CD4+ 10 TEM cells (top row) and CD8+ TEM cells (bottom row).

Significant differences were observed between CD4+ and CD8+ T cells in the expression of different homing markers at baseline. CCR7-CD4+ T cells from blood expressed significantly higher levels of the chemokine receptors CCR2, CCR9, and CCR10, in addition to the integrins and cell adhesion molecules $\alpha 1 \beta 1$, $\alpha 7 \beta 4$, and CLA. In contrast, CCR7-CD8+ T cells expressed more CCR5 and CXCR6, in addition to $\alpha 4 \beta 1$ and CD11c (Figure 15). Finally, CD103 and CXCR3 did not show differences (Figure 16).
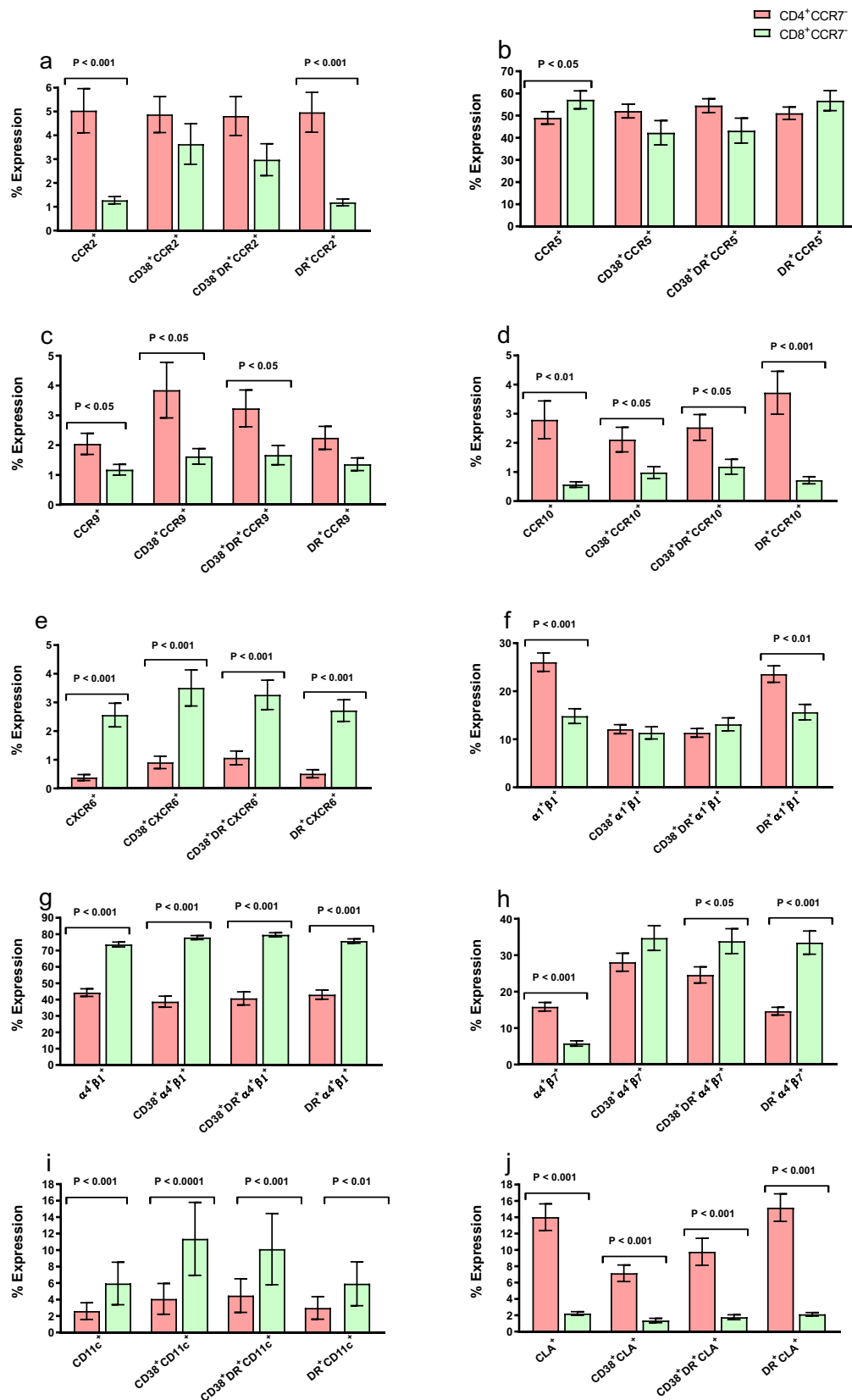
Figure 15. Comparison of adhesion molecule expression in CD4 and CD8 TEM cells from 12 healthy women

A comparison between the frequency of (a) CCR5, (b) CCR2, (c) CCR9, 13 (d) CCR10, (e) CXCR6, (f) α1β1, (g) α4β1, (h) α4β7, (i) CD11c and (j) CLA in CD4 14 (white bars) and CD8 (grey bars) effector memory T (TEM) cells was determined by flow 15 cytometry. The frequency of each molecule was analyzed in total CD3+ TEM cells, CD38+, 16 CD38+HLA-DR+, or HLA-DR+ activated fractions. Each bar represents the mean, ±standard error of the mean of healthy young women 18 (n=13).
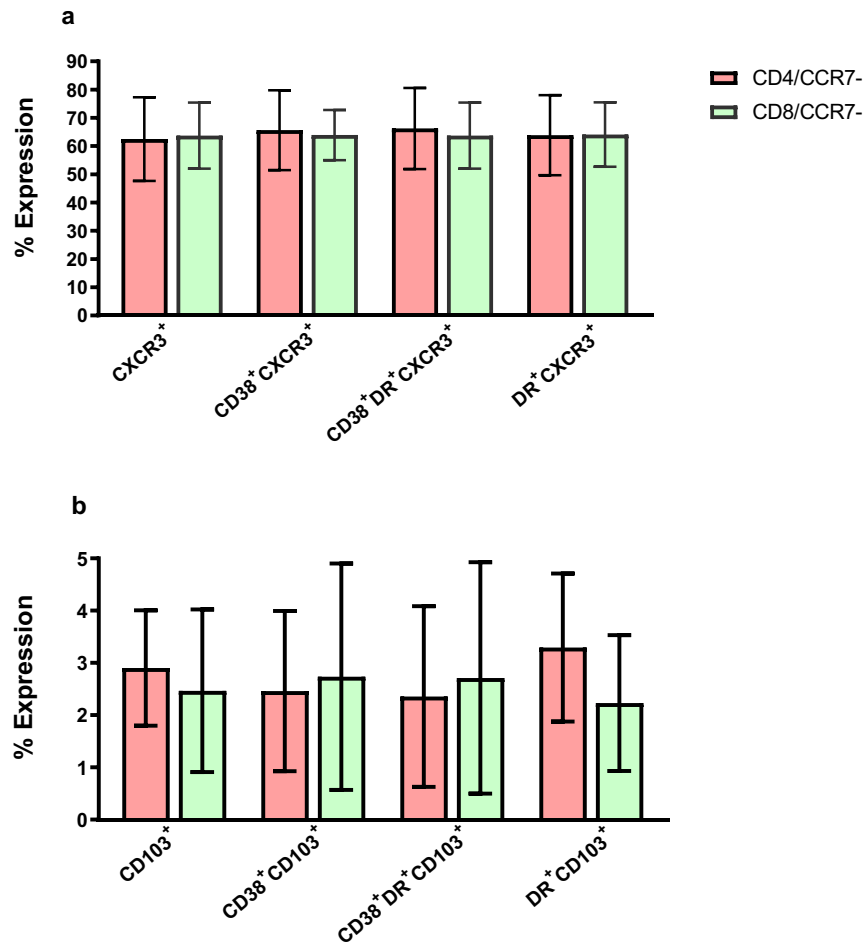
Figure 16. Comparison of CXCR3 and CD103 frequencies in CD4 and CD8 TEM cells from healthy women

A comparison between the frequency of (a) CXCR3 and (b) CD103 in CD4 (white bars) and CD8 (grey bars) effector memory T (TEM) cells was determined by Flow cytometry. The frequency of each molecule was analyzed in total CD3+ TEM cells and CD38+, CD38+ HLA-DR+ or HLA-DR+ activated fractions.

3.3.2 Homing molecules in ND vs. mucosal disorders

The frequency of activated $CD8^+$ and $CD4^+$ TEM cells (single $CD38^+$ or $HLA\text{-}DR^+$ and double $CD38^+$ $HLA\text{-}DR^+$) in each disorder was analyzed compared to the ND group (Figure 17). Of note, the overall frequency of $CD4^+$ T cells decreased in the BV group (from 57.4% in ND to 37.2% in BV; p=0.005, respectively; supplementary figure S1). Further, the different pathological groups showed the expression of at least one activation marker for $CD4^+$ and/or $CD8^+$ T cells. In this sense, both $CD4^+$ and $CD8^+$ T cells in the BV group showed significant differences for all markers compared to the control group. Likewise, in the PS group, there was an increase in the expression of HLA-DR in $CD4^+$ TEM cells compared to ND. In addition, CD38 and HLA-DR/CD38 double-positive cells increased in the UC group (Figure 17).
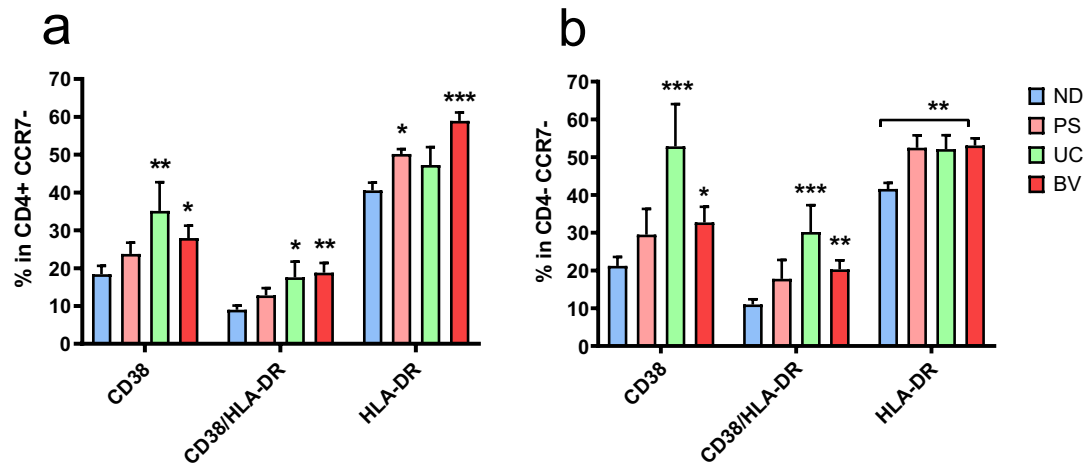
Figure 17. Comparison of activation markers in CD4 (a) and CD8 (b) TEM cells from different mucosal disorders

The frequency of activated CD38+, CD38+ HLA-DR+ or HLA-DR+ 9 CD4+ (a) and CD8+ (b) effector memory T (TEM) cells determined by flow cytometry is 10 shown for ND and the different groups of patients. General gating strategy 11 is shown in Fig 3. Each bar represents the mean ± standard error of the mean of healthy 12 young women ND; white bars, n=13), women with psoriasis (PS; grey bars, n=4), 13 ulcerative colitis (UC; checkered bars, n=4), and bacterial vaginosis (BV; dark bars, n=4).

The expression of chemokine receptors and adhesion molecules in CD4⁺ and CD8⁺ TEM cells was significantly different between mucosal disorders and ND (Figure 18). The BV group showed significant differences in the expression of the markers CD11c, CXCR6, and CCR10 in CD8⁺ T cells. For CD4⁺ T cells in the same group of patients, we detected differential expression for CCR2, CD11c, α4β7, and α4β1compared to ND. The most notable molecule in the other groups (PS and UC) was the CCR10 marker on CD8⁺ T cells.
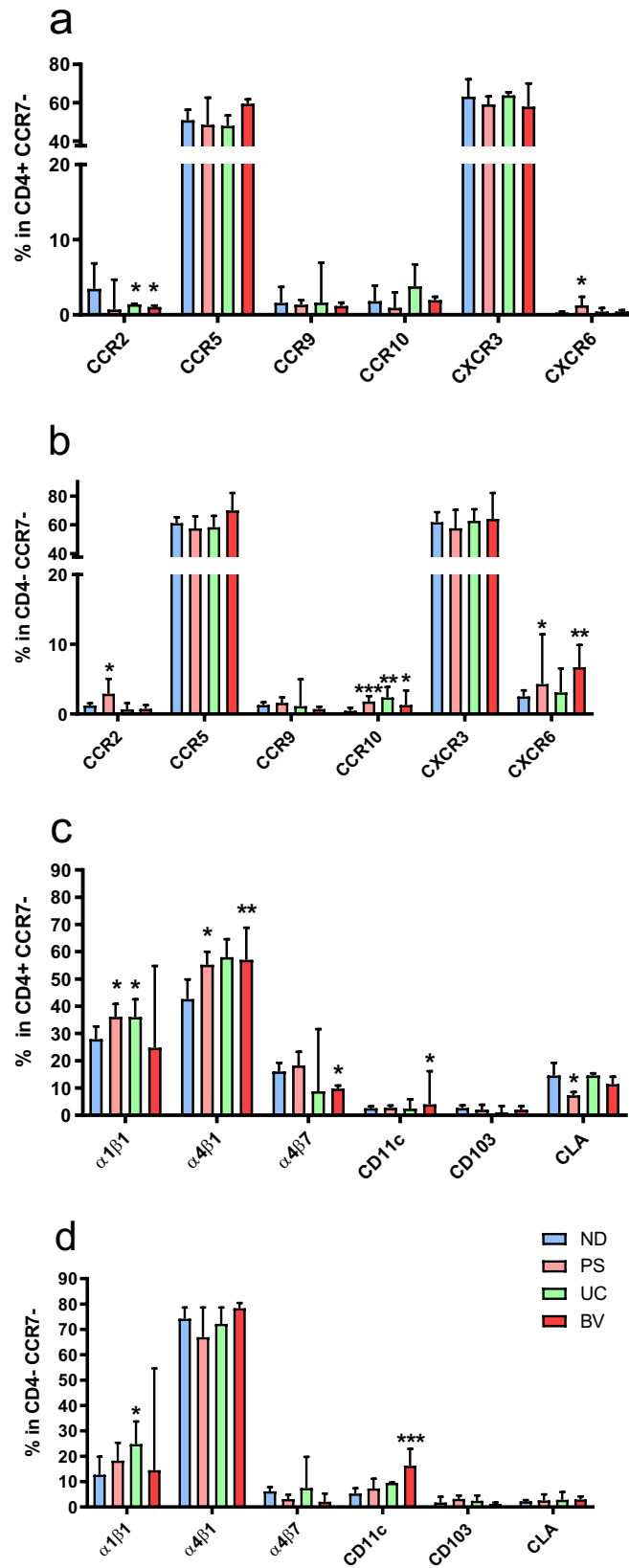
Figure 18. Comparison in the expression of adhesion molecules between the different mucosal disorders in TEM cells

Total expression of chemokine receptors in (A) CD4+ effector memory T (TEM) cells and (B) CD8+ TEM cells determined by flow cytometry is shown for normal donors (ND) and the different groups of patients. Total expression of integrins and other adhesion molecules in (C) CD4+ TEM and (D) CD8+ TEM cells determined by flow cytometry is shown for ND and the different groups of patients. The general gating strategy is shown in Figure 3. Each bar represents the mean ± standard error of the mean of healthy young women (ND; white bars, n=13), women with psoriasis (PS; grey bars, n=4), ulcerative colitis (UC; checkered bars, n=4), and bacterial vaginosis (BV; dark bars, n=4). P values indicate: *<0.05; **<0.01; ***<0.001.

After evaluating different molecules in total CD4$^+$ and CD8$^+$ T cells, we focused on studying their expression on the activated fraction since these cells might be the ones that migrate toward the mucosa (257) (Figure 19). Starting with the BV group, CD8$^+$ CD38$^+$ HLA-DR$^+$ TEM cells showed overexpression of CD11c and CXCR6 markers and decreased α4β7 compared to ND. Further, CD4$^+$ T cells showed higher expression of the α4β1 integrin in addition to the above markers. Of note, the decrease in α4β7 in TEM CD8$^+$ cells was common to all groups of patients compared to ND. For the PS group, the only significant changes within the CD38$^+$ HLA-DR$^+$ TEM cells were: a higher frequency of CXCR6 (as occurred in the BV group) in the CD4 and CD8 TEM cell fractions and a higher frequency of α1β1 in CD4$^+$ TEM cells. Last, the characteristic profile of the UC group in CD38$^+$ HLA-DR$^+$ TEM cells was: exclusive higher expression of CCR10 in CD8$^+$ TEM cells and increased α1β1 in CD4$^+$ TEM cells (as occurred in the PS group).
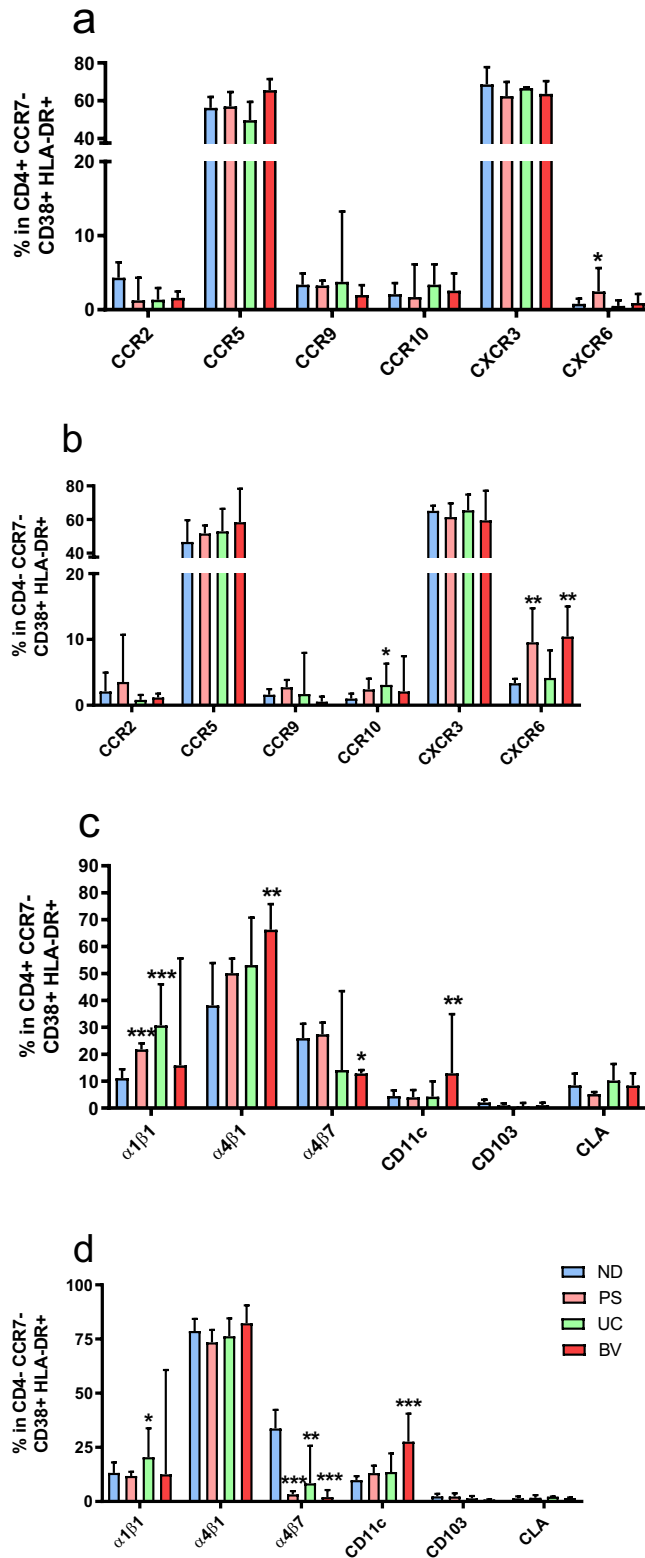
Figure 19. Comparison of adhesion molecule expression in CD38+ HLA-DR+ TEM cells from different mucosal disorders

Total expression of chemokine receptors in CD38+ HLA-15 DR+ (a) CD4+ effector memory T (TEM) cells and (b) CD8+ TEM cells determined by flow 16 cytometry is shown for normal donors (ND) and the different groups of patients. A total of 17 expressions of integrins and other adhesion molecules in CD38+ HLA-DR+ (c) CD4+ TEM and 18 (d) CD8+ TEM cells determined by flow cytometry are shown for ND and the different groups of 19 patients. The general gating strategy is shown in Fig 3. Each bar represents the mean X 20 standard error of the mean of healthy young women (ND; white bars, n=13), women with 21 psoriases (PS; grey bars, n=4), ulcerative colitis (UC; checkered bars, n=4), and bacterial 22 vaginosis (BV; dark bars, n=4). P values indicate: *<0.05; **<0.01; ***<0.001.

These results highlighted notable changes in the BV group for TEM cells. These changes are the exclusive increased expression of CD11c on CD4$^+$ and CD8$^+$ T cells and the higher expression of α4β1 on T CD4$^+$ cells. In other data (supplementary figure S2), there was a trend in total TEM CD4$^+$ cells towards a higher frequency of CCR5 in the BV group (59% vs. 49% in ND; p=0.076). In summary, increased CCR5, CXCR6, and especially CD11c expression on TEM cells in women with symptomatic BV was confirmed.

Study 3. Characterization of T lymphocytes with FGT-specific homing identity

3.4   CD11c expression as a candidate marker

3.4.1 Results in infected mice

This section was undertaken to study more in-depth the CD11c molecule and its association with genital tract infection. CD11c integrin expression on T cells appeared to be somewhat exclusive of T cell migration to the genital tract in humans and mice. To verify this, the first set of experiments was carried out in two new groups of infected animals: a group of mice infected with *C. muridarum* VAG and another group infected intravenously (IV). These new experiments were carried out to confirm that the increased expression of CD11c was exclusive to the productive infection in GT tissues and to rule out that it was not a consequence of a bacterial infection in general. It has been previously described (258) that IV infections induce pathogen replication in different systemic and mucosal tissues, including the spleen and lung.

An interesting finding was that, seven days after infection, the frequency of CD11c$^+$ cells on blood T cells was significantly greater in the IV group (median: 13.1% [IQR: 10.9-16.3]) than in any other group (median: 1.51%, [IQR: 0.9-2.2] in the controls or median: 5.23% [IQR: 3.4-8.4] in the VAG group) (Figure 20). Cell suspensions were collected from the genital tract from the control and VAG groups to assess the frequency of CD11c$^+$ T cells. Seven days after infection, the overall frequency of CD3$^+$ CD11c$^+$ in the vaginal tract increased from a median of 0.46% [IQR: 0.28-0.74] in the control group to a median of 4.43% [IQR: 2.68-5.33] in the VAG group, as shown in Figure 20.
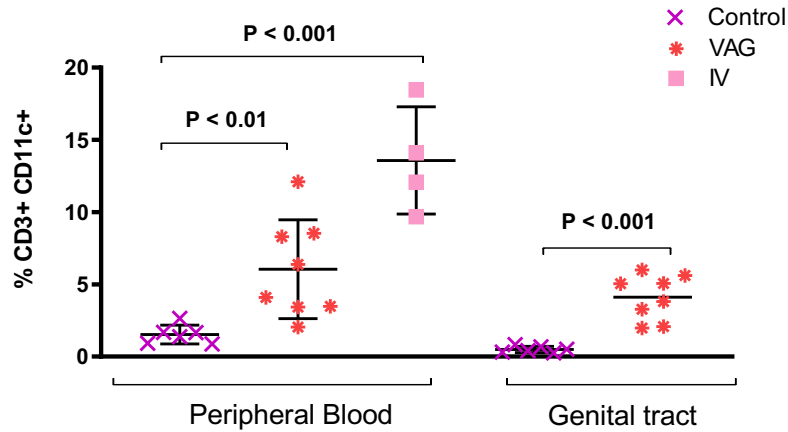
Figure 20. CD11c expression in T cells from blood and genital tract after vaginal or systemic Chlamydia infection

The frequency of CD11c in CD3$^+$ T cells was determined by flow cytometry 7 days after vaginal (VAG) or intravenous (IV) infection with C.muridarum in blood or genital tract from mice. Each time point represents the mean ± standard error of the mean of controls (n=6), VAG-infected animals (n=8), and IV-infected 8 animals (n=4).

Further evaluation of the frequency of CD11c$^+$ CD44$^+$ (activated) cells in different tissues was performed for the VAG group in comparison to the Control group at 14 days PI (Figure 21). In the spleen, the dLNs, the blood, and especially in the genital tract, most of these cells were CD8$^+$. Specifically, CD8$^+$ CD11c$^+$ CD44$^+$ cells were more frequent in all tissues from VAG compared to controls: 6.4% [IQR: 6.3–10] in the spleen, 1.9% [IQR: 1.5–2.1] in the dLNs, 23% [IQR: 15– 42] in blood and 53% [IQR: 46–53] in the genital tract. In contrast, the CD4$^+$ CD11c$^+$ CD44$^+$ population represented 0.37% [IQR: 0.47–0.85] of the CD4$^+$ cells in the spleen, 0.61% [IQR: 0.40–0.82] in dLNs, 0.83% [IQR: 0.17–0.41] in blood and 4.2% [IQR: 2.3–4.7] in the genital tract of the VAG infected mice. On days 7 and 14 PI, the expression of CD11c was increased in the FGT in correlation with that observed in the blood. Finally, the expression of CD11c was not specific to FGT infection since IV infection also expanded this cell population.
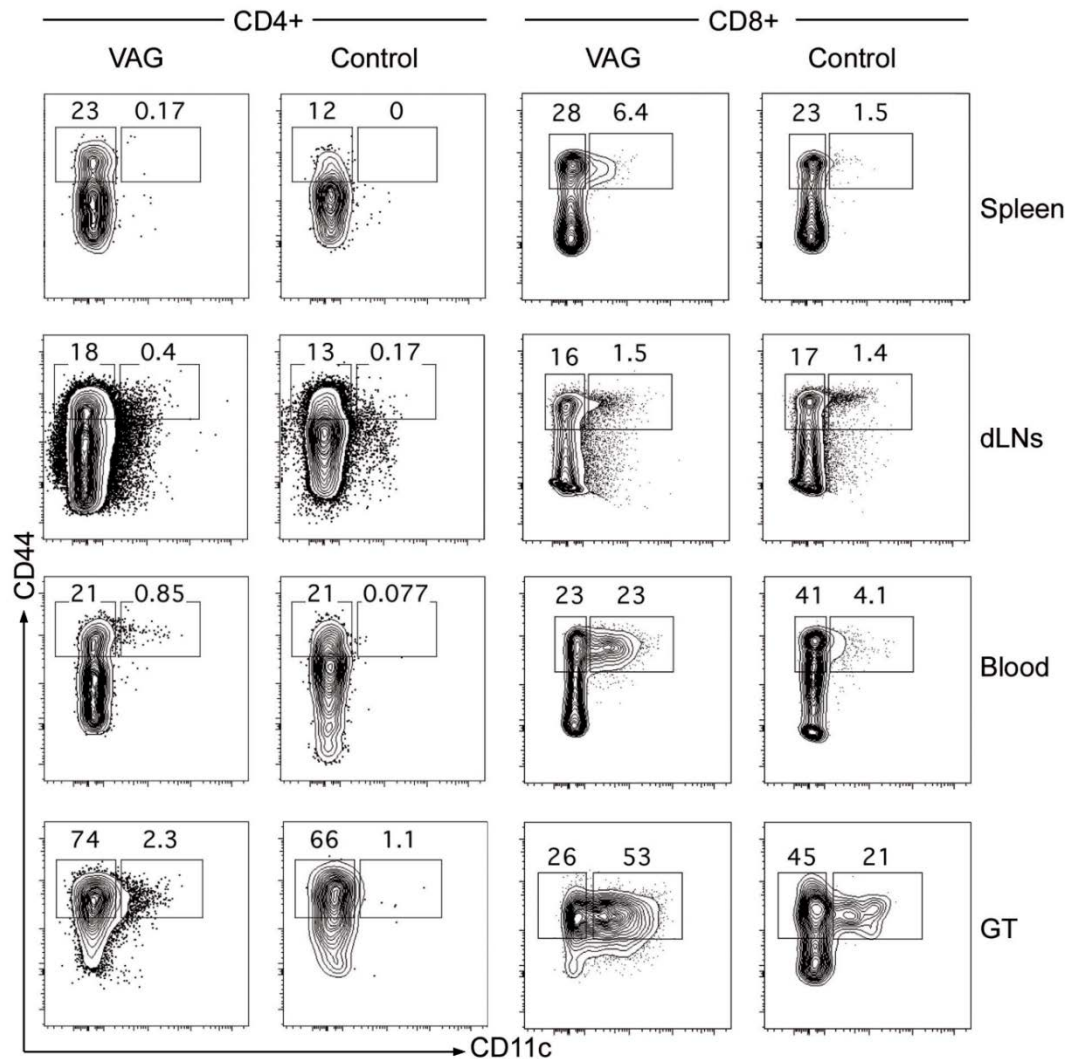
Figure 21. CD11c expression in activated CD4 /CD8 cells from different tissues after vaginal Chlamydia infection in mice

The frequency of CD44+ CD11c+ in CD4+ (left panels) and CD8+ cells (right panels) was determined by flow cytometry 14 days after vaginal (VAG) infections with C. muridarum in the spleen, draining lymph nodes (dLNs), blood and genital tract (GT) from mice. Examples from one infected and one control animal are shown.

3.4.2 Gene signature of CD11c⁺ T cells

Considering the previous results, we were interested in further understating the specific nature of CD11c⁺ TEM. Thus, as a first step, genes significantly over-expressed in purified CD3⁺ CD62L⁻CD44⁺ CD11c⁺ TEM cells were compared to CD3⁺ CD62L⁻CD44⁺ CD11c– from infection naive female mice. These results showed significantly overexpressed gene sets in CD11c⁺ cells. The most remarkable genes were between 2 and 8 times over-expressed in activated CD11c⁺ T cells compared to CD11c-T cells (Table 14). The list includes genes related to chemokine ligands, TLRs, complement, interferon, colony-stimulating factors, and genes related to NK cells. To evaluate the statistical significance of the list of genes obtained, these lists of genes were evaluated using the Gene Set Enrichment Analysis GSEA platform.

Table 14. Top upregulated genes in activated effector CD11c+ vs. CD11c– T cells in naive mice

Gene Symbol	Gene Title	Log Fold Change	Adjusted p Value
C3ar1	complement component 3a receptor 1	6.20	0.0081
C5ar1	complement component 5a receptor 1	5.80	0.0132
Ccl3	chemokine (C-C motif) ligand 3	7.04	0.0050
Ccl4	chemokine (C-C motif) ligand 4	5.23	0.0055
Ccl6	chemokine (C-C motif) ligand 6	7.19	0.0055
Ccl9	chemokine (C-C motif) ligand 9	6.39	0.0050
Cd244	CD244 natural killer cell receptor 2B4	3.75	0.0081
Cd8a	CD8 antigen, alpha chain	2.36	0.0490
Csf1	colony-stimulating factor 1 (macrophage)	5.98	0.0156
Csf1r	colony-stimulating factor 1 receptor	5.95	0.0077
Csf2ra	colony-stimulating factor 2 receptor, alpha, low-affinity (granulocyte-macrophage)	4.69	0.0240
Csf2rb	colony-stimulating factor 2 receptor, beta, low-affinity (granulocyte-macrophage)	7.74	0.0055
Csf2rb2	colony-stimulating factor 2 receptor, beta 2, low-affinity (granulocyte-macrophage)	6.66	0.0055
Csf3r	colony-stimulating factor 3 receptor (granulocyte)	2.36	0.0300
Gzma	granzyme A	3.66	0.0055
Gzmb	granzyme B	2.93	0.0490
H2-Aa	histocompatibility 2, class II antigen A, alpha	8.91	0.0050
H2-Ab1	histocompatibility 2, class II antigen A, beta 1	6.86	0.0065
H2-DMa	histocompatibility 2, class II, locus DMa	3.63	0.0063
H2-DMb1 /// H2-DMb2	histocompatibility 2, class II, locus Mb1 /// histocompatibility 2, class II, locus Mb2	4.46	0.0055
H2-DMb2	histocompatibility 2, class II, locus Mb2	4.76	0.0225
H2-Eb1	histocompatibility 2, class II antigen E beta	5.93	0.0121
Ifitm1	interferon induced transmembrane protein 1	6.42	0.0050
Ifitm2 /// LOC631287	interferon-induced transmembrane protein 2 /// interferon-induced transmembrane protein	5.09	0.0063
Ifitm3	interferon-induced transmembrane protein 3	6.20	0.0276
Klra2	killer cell lectin-like receptor, subfamily A, member 2	3.45	0.0258
Klrb1b	killer cell lectin-like receptor subfamily B member 1B	3.43	0.0253
Tgfbi	transforming growth factor, beta-induced	5.69	0.0050
Tlr7	toll-like receptor 7	2.47	0.0450
Tlr9	toll-like receptor 9	2.95	0.0065

The Gene Set Enrichment Analysis GSEA is a bioinformatic statistical method that analyzes whether a specific set of genes (up/down regulated) shows significant and concordant differences between two biological conditions, including phenotypes. The comparison is made with previously curated molecular signature databases from different publications and projects (Figure 22). This database encompasses annotated genes associated with conditions, phenotype, tissue, and cell type. In this study, a comparison was made with the C2 database: CP, KEGG, and immunologic signatures C7, a collection of genes from studies of metabolic pathways published in PubMed and sets of genes representative of the state of immune cells, respectively (259).
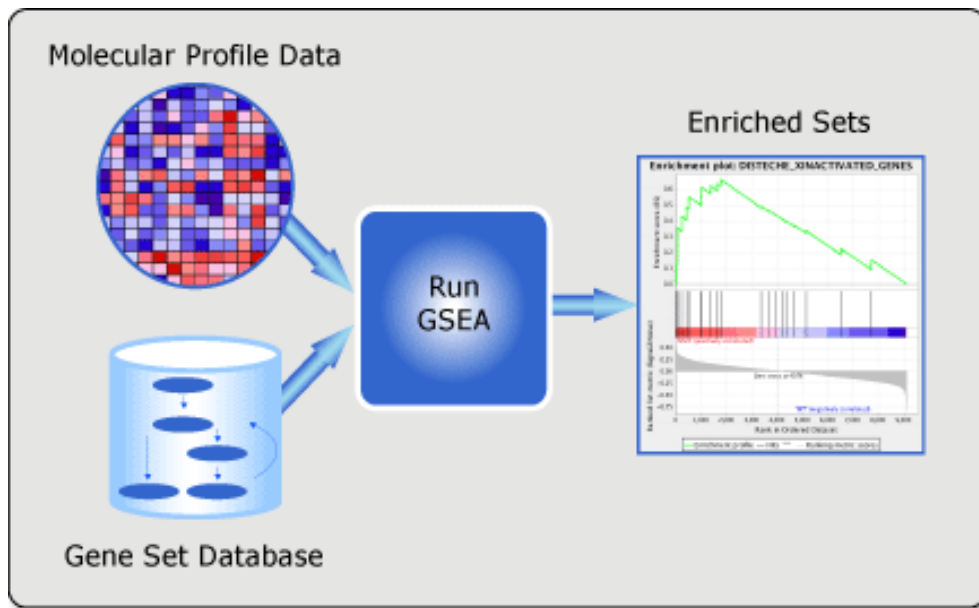
Figure 22. Gene Set Enrichment Analysis (GSEA) (from (260))

The list of genes overexpressed in CD11c⁺ T cells was used for GSEA analysis, comparing them with the MSigDB database ((C2: CP, KEGG) and immunological signatures (C7). Genes number involved in the molecular signature of NK was 100, representing the most significant number of all the sets analyzed (Figure 24). The enrichment plots (Figure 24) showed significant overlap with γδT, NK, and iNKT CD4– cell's molecular signatures. Analyzing the enrichment score (ES) (Figure 24), values of 0.89 stood out for the γδT signature (Figure 23; Figure 24), 0.80 for NKs, and 0.55 for iNKT CD4–.
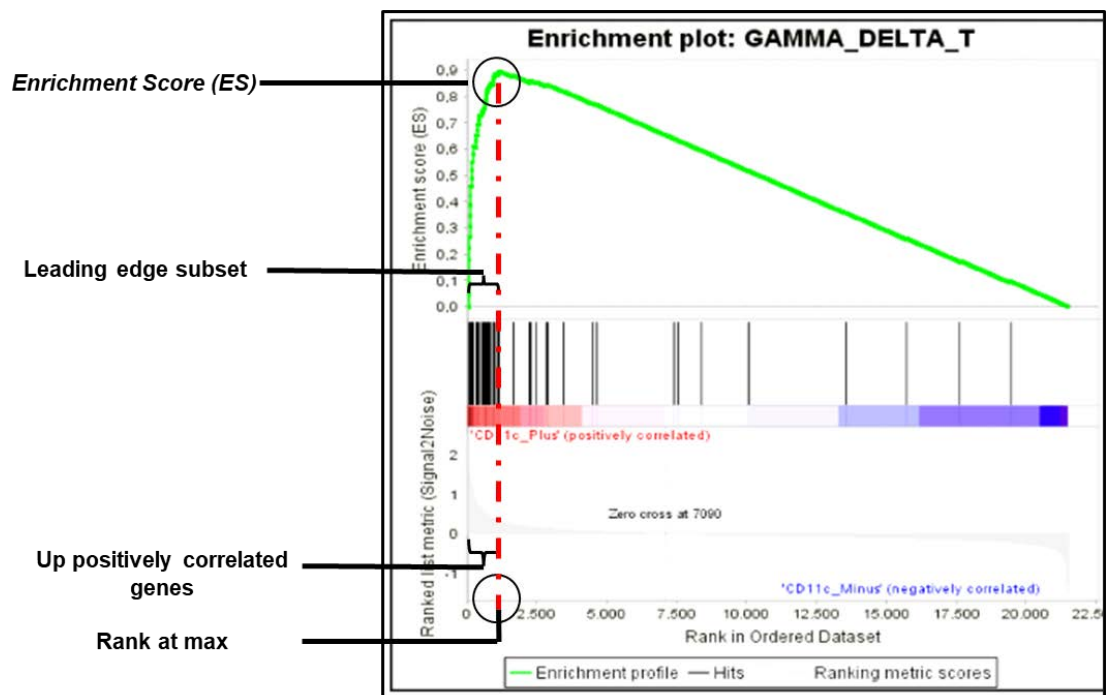
Figure 23. Example of enrichment plot of γδT cells signature and most valuable point for the analysis

Finally, the signature of iNKT CD4$^+$ also gave an acceptable enrichment profile but with a lower value of ES and fewer genes involved than in the other three profiles (Figure 24). The rank at max represents how concentrated the genes are before reaching the ES value. The larger this value is, the less statistical significance the result has. Thus, for the NK profiles, iNKT CD4$^-$ and γδT showed almost the same value. On the contrary, the iNKT CD4$^+$ profile showed a substantial rank at max value, which means that this result had limited significance (Figure 24). These data indicated that circulating T cells expressing CD11c$^+$ may include subpopulations of unconventional TEM cells with an innate profile, namely γδT and CD4-iNKT cells.
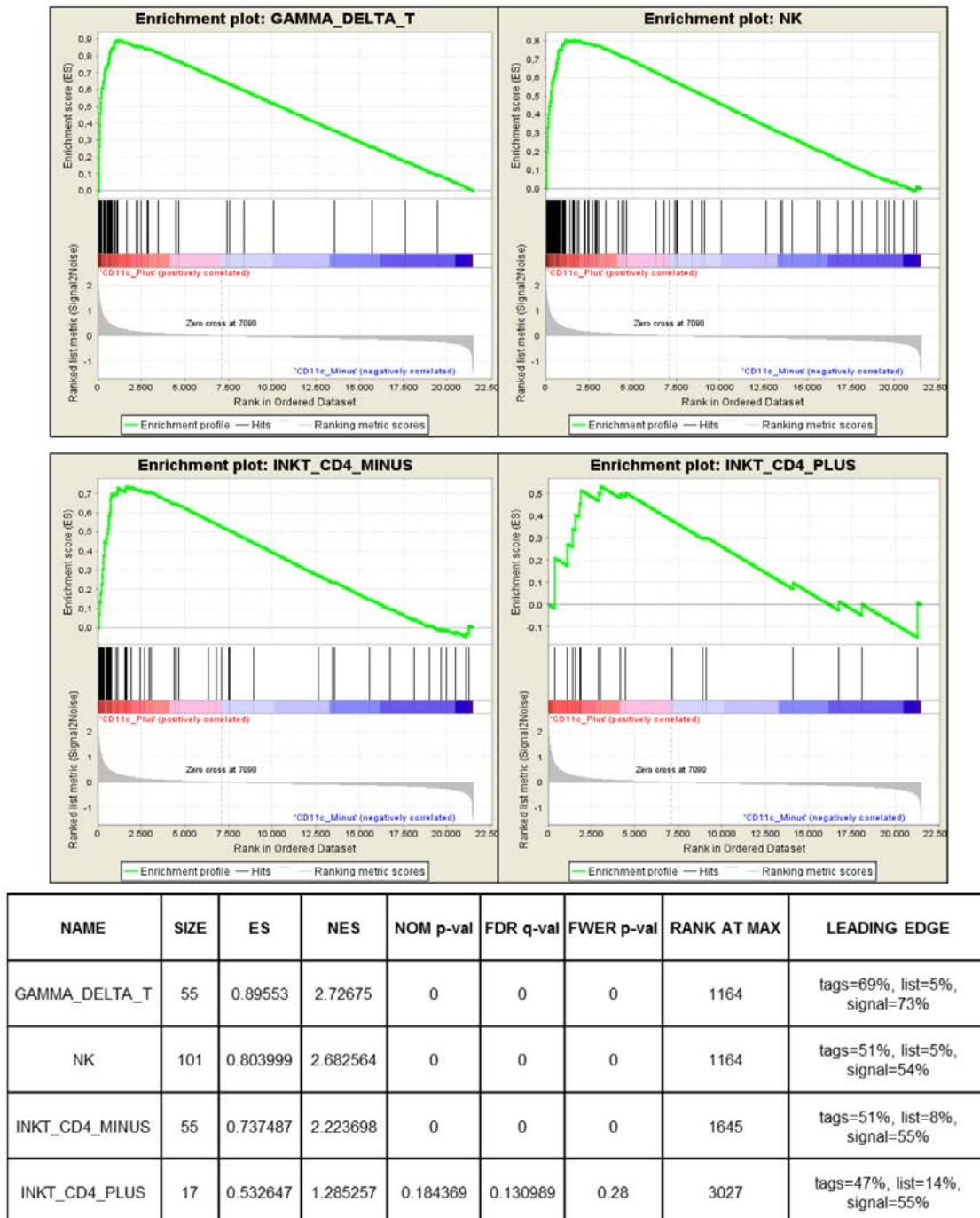
Figure 24. Enrichment analysis plot for the most significant molecular signature for TEM CD11c+ cells

NAME	SIZE	ES	NES	NOM p-val	FDR q-val	FWER p-val	RANK AT MAX	LEADING EDGE
GAMMA_DELTA_T	55	0.89553	2.72675	0	0	0	1164	tags=69%, list=5%, signal=73%
NK	101	0.803999	2.682564	0	0	0	1164	tags=51%, list=5%, signal=54%
INKT_CD4_MINUS	55	0.737487	2.223698	0	0	0	1645	tags=51%, list=8%, signal=55%
INKT_CD4_PLUS	17	0.532647	1.285257	0.184369	0.130989	0.28	3027	tags=47%, list=14%, signal=55%

3.4.3 CD11c⁺ T cells profile in Mice

The same animal model of chlamydial infection was used to study the phenotype of CD3$^+$CD11c$^+$ cells. Flow cytometry analysis was performed on blood and GT using different iNKT, NK, and γδT cell markers. Part of the gating strategy is shown in Figure 25, where different markers such as γδTCR, NK1.1, CD103, and CD8α were evaluated. These markers were analyzed in both the CD3$^+$CD11c$^-$ and CD3$^+$ CD11c$^+$ populations.

The gating strategy consisted of a selection of lymphocytes based on FSC versus SSC, followed by the exclusion of doublets and a selection of CD3$^+$ T cells. After selecting CD11c$^+$ or CD11c$^-$ T cells, the surface expression of the different markers was quantified.
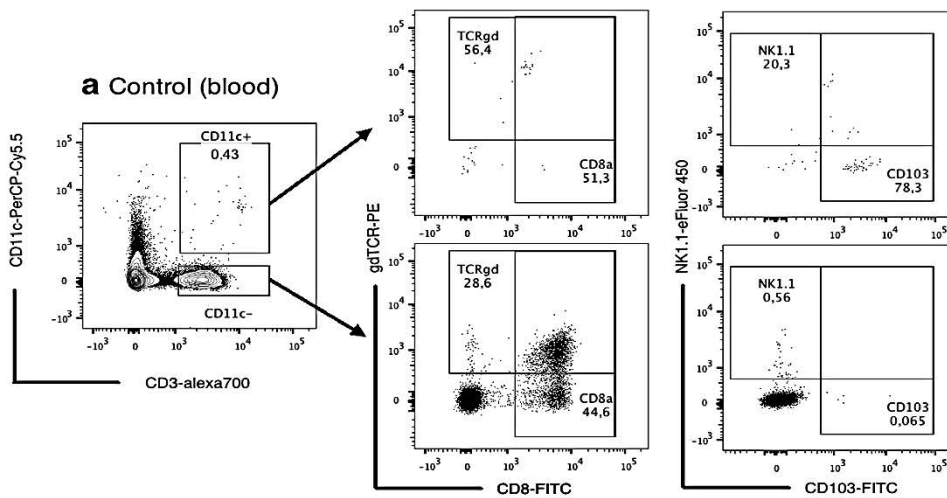
Figure 25. Part of the gating strategy is to evaluate T cell phenotypes in the blood and genital tract of mice by CD11c expression

As a general trend, seven days after infection, the frequency of T cells expressing CD11c$^+$ increased in tissue and in blood. The difference in expression of CD11c in tissue was higher compared to blood (data shown in results section 3.4.1 Figure 20).

In the GT, the total frequency of CD3$^+$ T cells increased dramatically from 2.0 ± 0.4% in the control group to 22.1 ± 9.5% in the VAG group (p = 0.0003), CD3$^+$CD11c$^+$ T cells in the GT increased from 0.5±0.2% to 4.1±1.6% 7 days PI (p=0.0001) (see section 3.4.1). Total CD4 expression remained stable, whereas CD3$^+$CD8$^+$ T cells increased significantly 7 days PI (from 0.9±0.3% to 13.7±4.7%; p<0.0001; data not shown).

3.4.3.1   NK1.1 and CD8α markers

The frequency of CD11c$^+$ T cells expressing CD8α in blood was similar before and after infection, while NK1.1 expression was markedly increased after infection (Figure 26 a and b). In contrast to blood, CD8 expression within CD11c$^+$ T cells was significantly increased in tissues after Chlamydia infection (p = 0.00005) (Figure 26; a). Further, NK1.1 was expressed at high levels by CD11c$^+$ GT T cells, already before infection. Conversely, the

expression of NK1.1 in CD3⁺ CD11c⁺ T cells, which represent 60% of the total at baseline, decreased PI (p=0.001) (Figure 26; b).
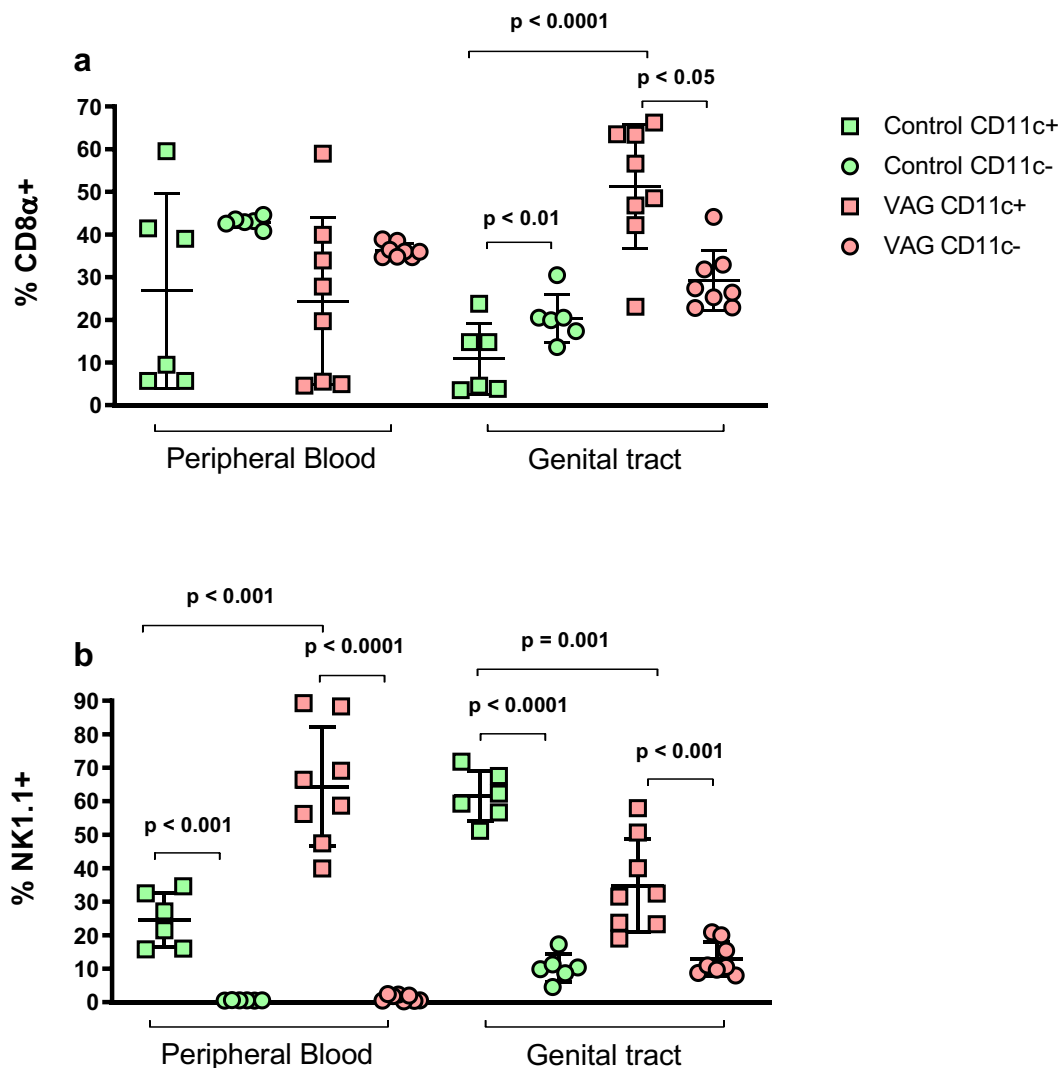
Figure 26. T cell phenotypes in blood and genital tract of mice by CD11c expression

Comparison of the frequency of (a) CD8α and (b) NK1.1 in CD11c+ (squares) and CD11c- (circles) T cells from the same individual. The gating strategy consisted of a lymphocyte gate based on FSC vs. SSC, followed by doublet exclusion and a CD3+ T cells gate. After gating on CD11c+ or CD11c- T cells, the surface expression of the different markers was quantified (see figure 25 for further details). Each bar represents the mean ± SD of control (white; n=3 or n=6) or vaginally (VAG)-infected mice (black; n=4 or n=8) seven days after infection. Data were analyzed using the paired Student's t-test.

3.4.3.2   Other NK cell markers

Since there was an enrichment for NK cell-related genes in our gene expression analyses, additional NK cell markers, including DX5, NKG2A, and NKp46, were also evaluated in the CD3⁺CD11c⁺ T cell population. Under basal conditions, more than 70% of CD3⁺CD11c⁺ T cells expressed DX5 and >20% NKG2A (which mostly co-expressed DX5, Figure 27). 7 days PI, the frequency of NKG2A within CD11c⁺ T cells decreased significantly (p=0.036), while the expression of DX5 remained identical (Figure 27). NKp46

expression was deficient in the control group and further decreased at 7 days PI (p=0.03; Figure 27).

There were other differences in CD11c$^+$ T cells from blood and GT: in blood, these cells were not particularly linked to CD8 but expressed DX5 in high proportions. While in tissue, DX5 was expressed at lower levels, and CD8 (and to a lesser extent CD8$^+$ NKG2A$^+$) increased significantly after infection (Figure 27).

NK cell markers in the GT were generally less frequent in CD11c$^+$ T cells than in the ones from blood. The exception was NKp46, expressed in 40% of these cells in GT (Figure 27). Contrary to blood, 7 days PI, the frequency of NKG2A within CD11c$^+$ T cells increased significantly (p = 0.006), while NKp46 decreased (p = 0.0009), and DX5 expression remained the same (Figure 27).
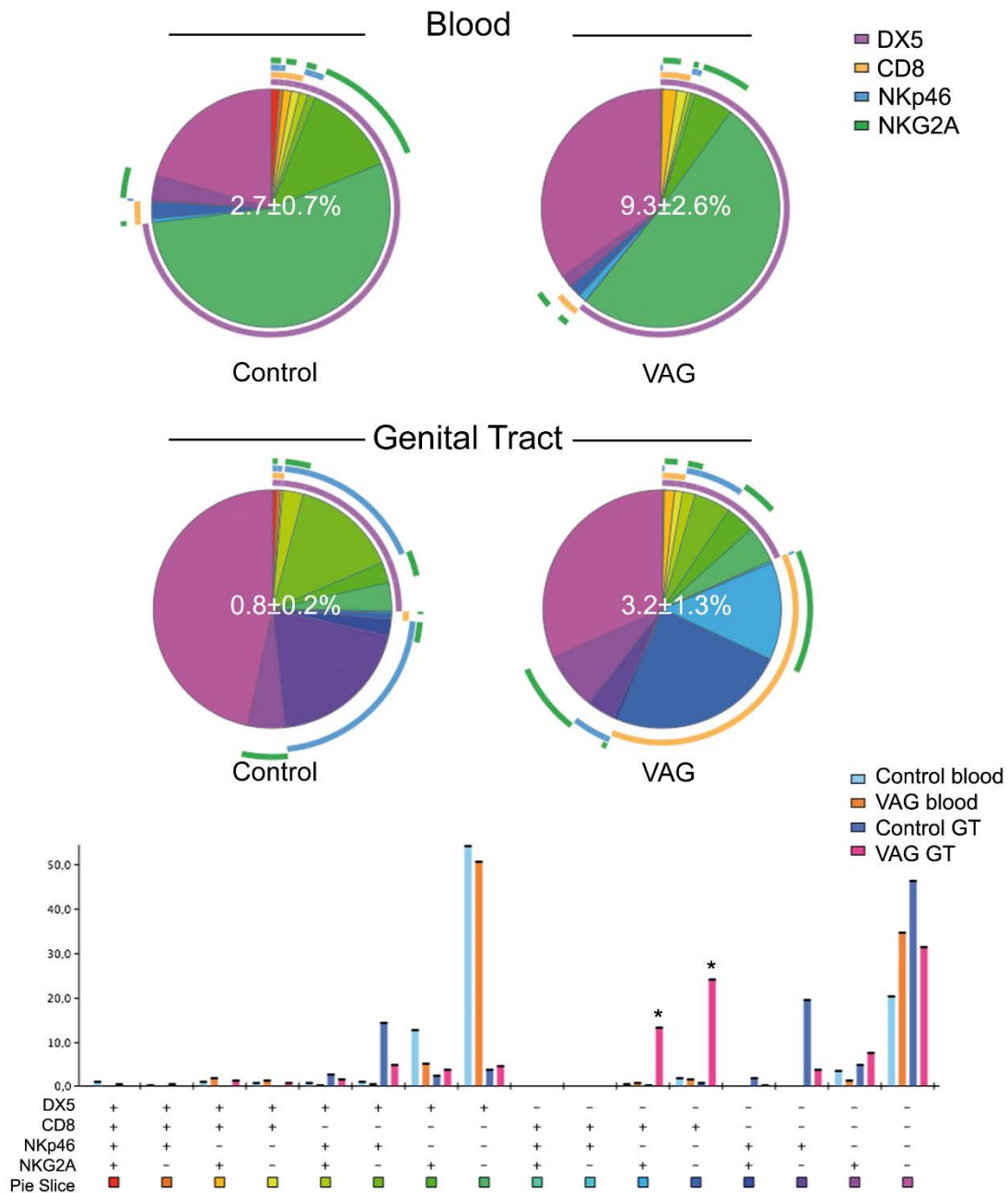
Figure 27. NK phenotypes were included in the CD11c+ T cell fraction after vaginal Chlamydia infection in mice's blood and GT

The frequency of the different subsets obtained from combining DX5, CD8α, NKp46, and NKG2A expression is displayed for each group as a pie chart and as a complementary bar graph. The gating strategy was performed as described in Materials and Methods. The frequency of CD11c positive cells in the T cell fraction as the mean ± SD is shown as a white number in the center of the pie chart for each group in the blood (top) and genital tract (GT, bottom). Each colored portion of a pie chart indicates the percentage of a specific subset detailed in the bar chart below. The arcs around the pie show the molecule or combination of molecules to which those proportions correspond (see color legend indicating DX5, CD8α, NKp46, and NKG2A). *Indicates p<0.05 by Student's t-test analyses only for values >5% of the total CD11c+ T cells in vaginally (VAG)-infected mice seven days after infection (n=4) compared to control (n=3) animals.

3.4.3.3 iNKT and γδT cells markers

We also addressed molecules employed to identify unconventional γδT cells and iNKT phenotypes. The total blood count of iNKT or γδ T cells did not change after vaginal infection; however, it was increased in the GT of infected mice (p < 0.003; data not shown). When comparing the CD11c$^+$ and CD11c$^-$ subsets, there was an apparent abundance of these unique T cells in the CD11c$^+$ fraction in both tissues (Figure 28, a and b). Thus, under physiological conditions, CD11c$^+$ T cells consisted almost exclusively of CD1d–tetramer$^+$ cells and a high proportion of γδ T cells. Among the CD3$^+$CD11c$^+$ T cells in the blood, 27-39% of them were iNKT, and 50-60% were γδ T cells, and this frequency did not change after vaginal infection (Figure 28, a and b). However, the frequency of CD1d-tetramer$^+$ cells in the CD11c$^+$ T-cell fraction was reduced in GT after infection (Figure 28, a).
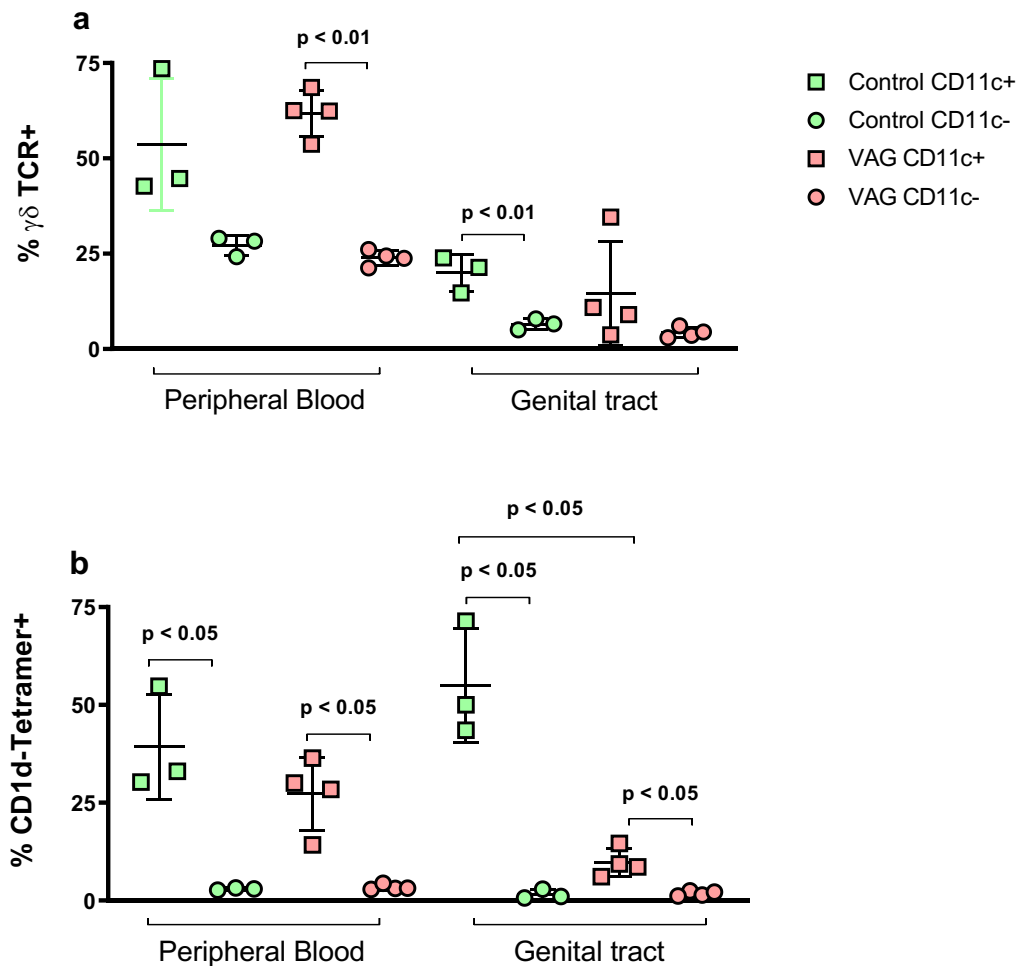
Figure 28. T cell phenotypes in blood and genital tract of mice by CD11c expression

Comparison on the frequency of (a) γδ TCR and (b) CD1d-Tetramer in CD11c+ (squares) and CD11c- (circles) T cells from the same individual The gating strategy consisted of a lymphocyte gate based on FSC vs. SSC, followed by doublet exclusion and a CD3+ T cells gate. After gating on CD11c+ or CD11c- T cells, the surface expression of the different markers was quantified (see figure 25 for further details). Each bar represents the mean ± SD of control (white; n=3 or n=6) or vaginally (VAG)-infected mice (black; n=4 or n=8) seven days after infection. Data were analyzed using the paired Student's t-test.

The CD11c⁺ T cell fraction presented unconventional T cell markers in blood and GT (Figure 29; b and c). Under basal conditions, the CD3⁺CD11c⁺ T cell fraction included almost exclusively all iNKT cells and high proportions of γδT cells, the latter remaining PI in blood and GT; however, iNKT cells decreased mainly in the GT. When performing boolean gate analyses of these markers together with CD8 and NK1.1 (Figure 29), It became clear that γδT and NK1.1⁺ cells were part of the significant subset enriched in blood. Further, the increase in the CD3⁺CD11c⁺ population detected in the GT was mostly associated with a CD8⁺ phenotype (Figure 29).
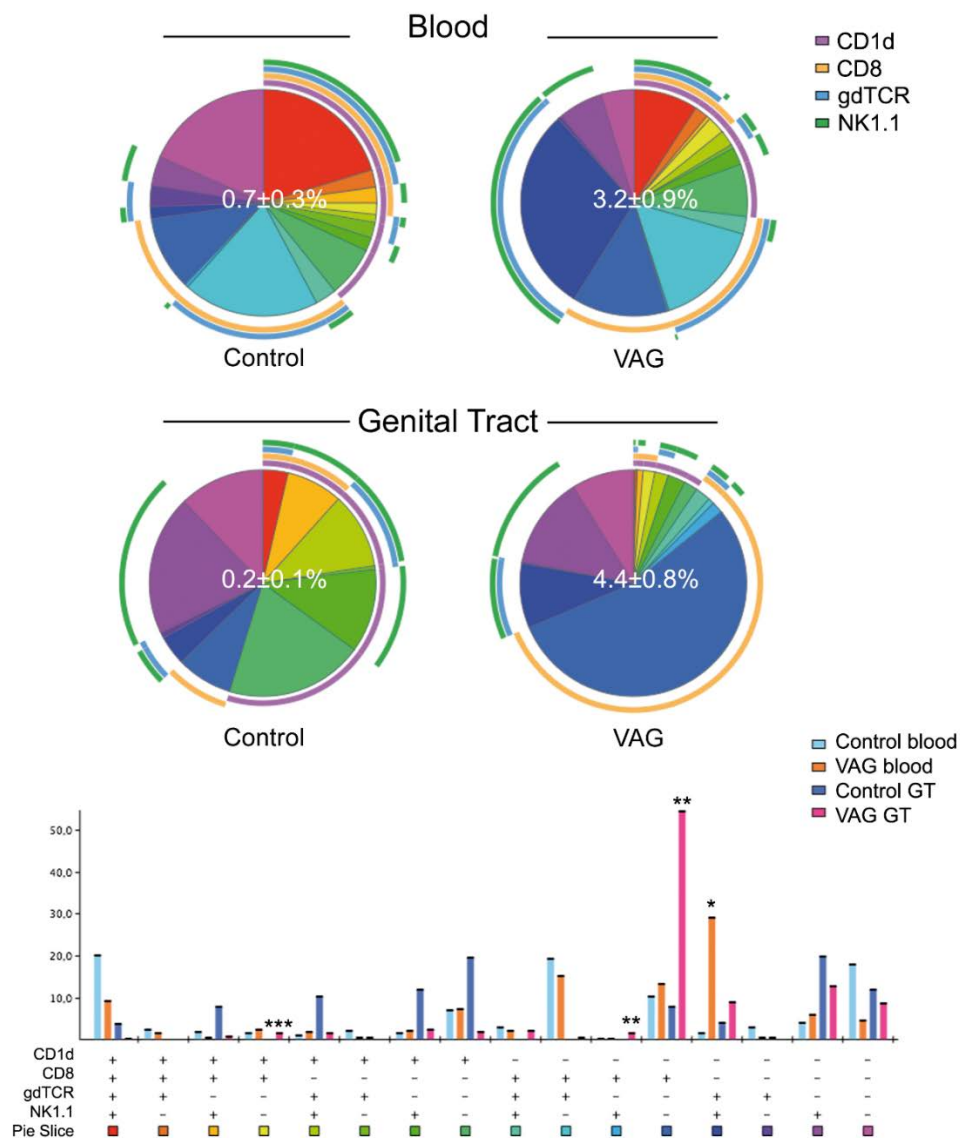
Figure 29. Unconventional phenotypes were included in mice's CD11c+ T cell fraction after vaginal Chlamydia infection

The frequency of the different subsets obtained from combining CD1d-tetramer, CD8α, γδTCR, and NK1.1 expression is displayed for each group as a pie chart and a complementary bar graph. The gating strategy was performed as described in Materials and Methods. The frequency of CD11c positive cells in the T cell fraction as the mean ± SD is shown as a white number in the center of the pie chart for each group in the blood (top) and genital tract (GT, bottom). Each colored portion of a pie chart indicates the percentage of a specific subset detailed in the bar chart below. The arcs around the pie show the molecule or combination of molecules to which those proportions correspond (see color legend indicating CD1d-tetramer, CD8α, γδTCR, and NK1.1). *Indicates p<0.05 by Student's t-test analyses only for values >5% of the total CD11c+ T cells in vaginally (VAG)-infected mice seven days after infection (n=4) compared to control (n=3) animals.

3.4.3.4 Homing markers

According to earlier research in a mouse model of colitis (261), the CD11c$^+$ CD8$^+$ Tregs are CD8 α $^+$ CD103$^+$ NK1.1$^-$ in the small intestine but CD8 α^- CD103$^-$ NK1.1$^+$ in the colon. We looked at the expression of various markers, including CCR10, which would represent CD11c$^+$ T cell trafficking into the GT. The vaginal tract expresses CC-chemokine ligand 28, and B lymphocytes that are homing there also express CCR10 (262). Thus, the expression of CD103 and CCR10 in blood and GT was analyzed (Figure 30).

In GT, the co-expression of CD103 and CD11c was already very high during basal conditions, and only CD11c-expressing T cells also expressed CD103 before and after infection (p<0.01) (Figure 30; a). The same trend was observed in blood, where the CD103 marker was highly expressed in CD11c$^+$ T cells. It should be highlighted that the basal condition exhibits the largest differential expression of CD103 between CD11c$^+$ and CD11c− (p>0.001) (Figure 30; a).

When we compared the expression of the CCR10 marker in circulating CD11c T cell fractions, we found that CD11c$^+$ were the only ones expressing this molecule. In blood, this chemokine receptor was only present in a marginal percentage of CD11c$^+$ T cells, but following infection, CCR10 was approximately 7-fold higher in the positive than in the negative CD11c fraction (p = 0.018; (Figure 30; b). T cells from GT did not shown notable differences in GT (Figure 30; b).
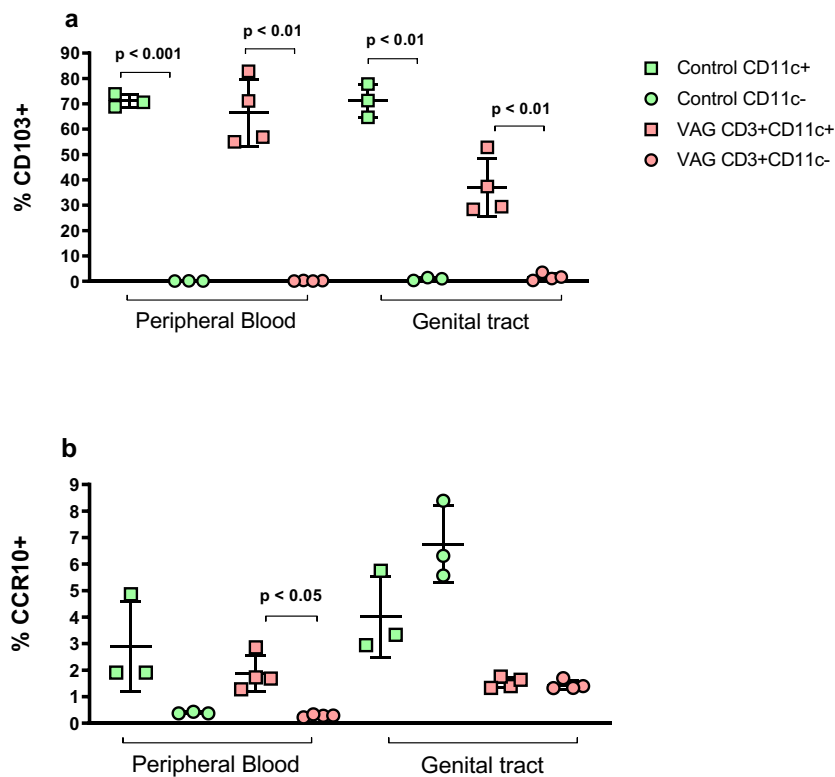
Figure 30. T cell phenotypes in blood and genital tract of mice by CD11c expression

Comparison of the frequency of (a) CD103 and (b) CCR10 in CD11c+ (squares) and CD11c- (circles) T cells from the same individual. The gating strategy consisted of a lymphocyte gate based on FSC vs. SSC, followed by doublet exclusion and a CD3+ T cells gate. After gating on CD11c+ or CD11c- T cells,

the surface expression of the different markers was quantified (see figure 25 for further details). Each bar represents the mean ± SD of control (white; n=3 or n=6) or vaginally (VAG)-infected mice (black; n=4 or n=8) seven days after infection. Data were analyzed using the paired Student's t-test.

When simultaneously representing the expression of these markers, it was evident that CD11c$^+$ T cells in blood mostly presented a CCR10-CD8α-CD103$^+$ NK1.1$^-$ phenotype (~47%) at baseline; however, in the GT, this profile was less frequent (~32%), since the CD103$^+$ NK1.1$^+$ phenotype was equally frequent (Figure 31). In the VAG group, circulating CD11c$^+$ T cells showed an evident expansion of CD103$^+$ NK1.1$^+$ CD8α$^-$ cells (p=0.056). While in the GT, the CD8α$^+$ CD103$^-$ NK1.1$^-$ cells were the ones that increased (p<0.002; Figure 31). These results do not coincide with Tregs phenotypes previously described in animal models of UC, where CD11c$^+$ CD8$^+$Tregs cells were CD8α$^+$ CD103$^+$ NK1.1$^-$ in the small intestine, and CD8α$-$ CD103$-$ NK1.1$^+$ in the colon (261)(13).
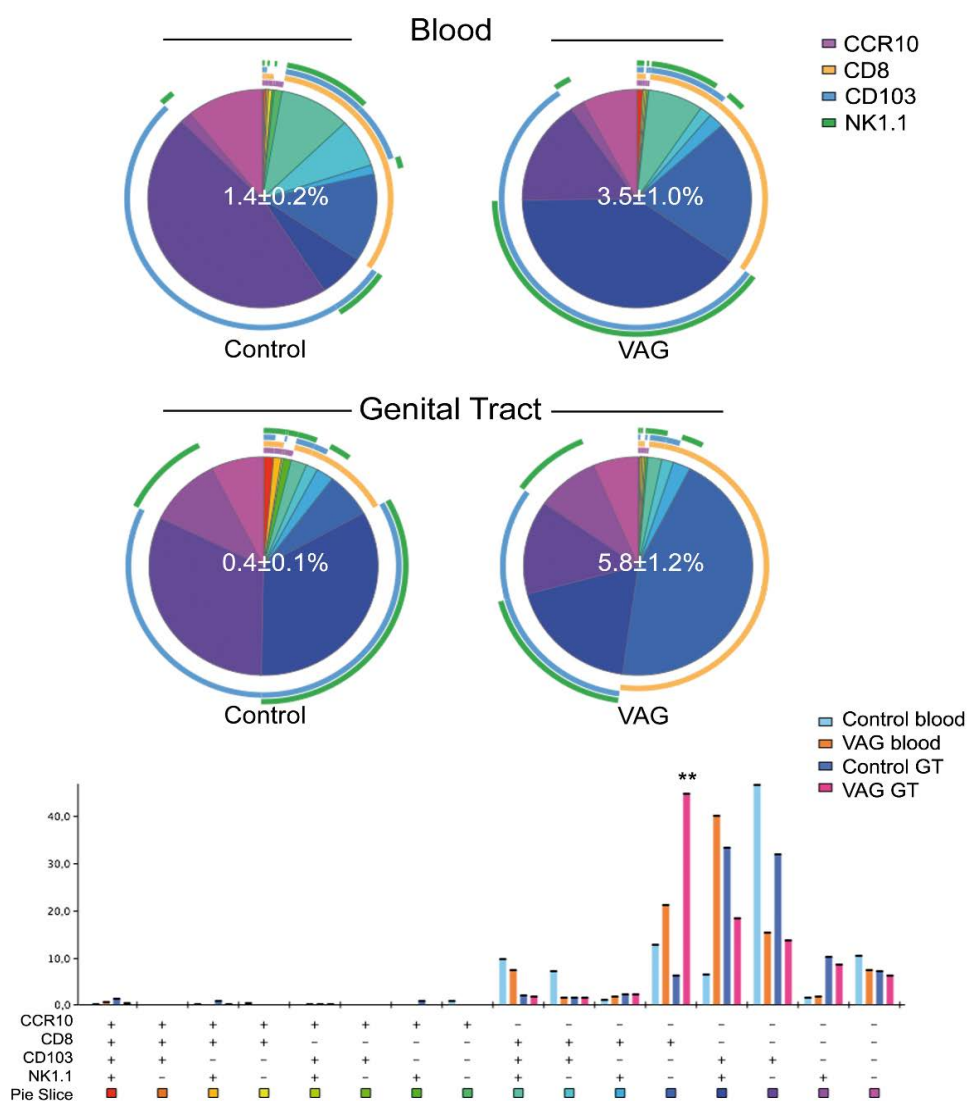
Figure 31. Adhesion molecules included in the CD11c+ T cell fraction after vaginal Chlamydia infection in mice

The frequency of the different subsets obtained from combining CCR10, CD8α, CD103, and NK1.1 expressions is displayed for each group as a pie chart and as a complementary bar graph. The gating strategy was performed as described in Materials and Methods. The frequency of CD11c positive cells in the T cell fraction as the mean ± SD is shown as a white number in the center of the pie chart for each group in the blood (top) and genital tract (GT, bottom). Each colored portion of a pie chart indicates the percentage of a specific subset detailed in the bar chart below. The arcs around the pie show the molecule or combination of molecules to which those proportions correspond (see color legend indicating CCR10, CD8α, CD103, and NK1.1). *Indicates

p<0.05 by Student's t-test analyses only for values >5% of the total CD11c+ T cells in vaginally (VAG)-infected mice seven days after infection (n=4) compared to control (n=3) animals.

3.4.4 CD11c$^+$ T cell profile in women

We then examined CD11c expression in CD3$^+$ CD4$^{+/-}$ and CCR7$^{+/-}$ T cells from healthy young women (normal donors, ND) and found an enrichment of this marker in the CCR7$^-$ CD4$^-$ fraction (Figure 32).
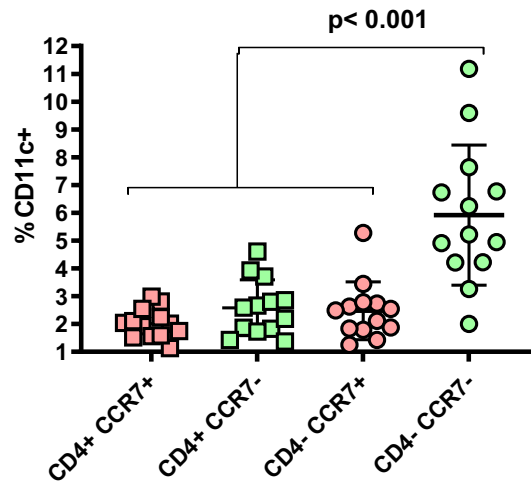

Figure 32. CD11c expression in circulating T cells from healthy young women

CD11c+ cells were analyzed by flow cytometry in the CD4+ CCR7+/- and CD4- CCR7+/- CD3+ T cell subsets. The gating strategy consisted of the following consecutive gates: lymphocytes, singlets, live CD3+ T cells, CD4+ or CD4- T cells, CCR7+ or CCR7- and CD11c+. Each bar represents the mean ± SD of normal donors (n = 13). Data were analyzed by the Kruskall-Wallis test with Bonferroni post-test correction.

Besides the phenotypes analyzed in mice, the anti-Vα7.2 antibody was included to determine MAIT cells, which show high expression of CD161 (human homolog of NK1.1) and are associated with the FGT mucosa (12,14). Therefore, each phenotype was analyzed in circulating CD3$^+$ CCR7$^-$ T cells, and we compared their expression in CD11c$^+$ cells (1.9±0.7%) versus CD11c$-$ (35.4±10.0%) by a paired non-parametric T-test. To ensure that we did not miss the detection of any infrequent populations by blood processing, we compared whole blood and PBMC staining (Figure 35). The gating strategy to perform these analyzes excluded CD19$^+$ and CD14$^+$ cells, which in other experiments contaminated the CD11c$^+$ T cell fraction (Figure 34).

3.4.4.1 Blood

The only subsets significantly enriched in the CD11c$^+$ fraction were CD8$^+$ (48.3±16.5% vs. 33.7±6.6%) and $\gamma\delta$TCR$^+$ (27.3±11.7% vs. 12, 0±4.2%) (Figure 35; a). CD161 expression was maintained at 55% in both subsets (Figure 35; a), while MAIT cells (Vα7.2+ CD161^h) were low in the positive fraction (Figure 35; a)

Of note, $\gamma\delta$T cells accounted for 5.7 ± 2.7% of total CD3$^+$ T cells in blood, and the frequency of CCR7-CD11c$^+$ in this subset was approximately ~10%, of which ~78 % were CD161$^+$ and ~18% were CD8$^+$ (Figure 33). Indeed, CD161 was similarly high on $\gamma\delta$T cells

regardless of CD11c expression, but CD8 expression was doubled in the CCR7-CD11c+ fraction of γδT cells compared to total CD3+ γδTCR+ T cells (p=0.039; Figure 33). Finally, in CD8+ T cells, which represented 28.8±7.7% of T cells, CCR7-CD11c+ represented ~3.5% of cells, in which CD161 was enhanced compared to total CD3+ CD8+ T cells (43% vs. 28%; p=0.023; Figure 33).
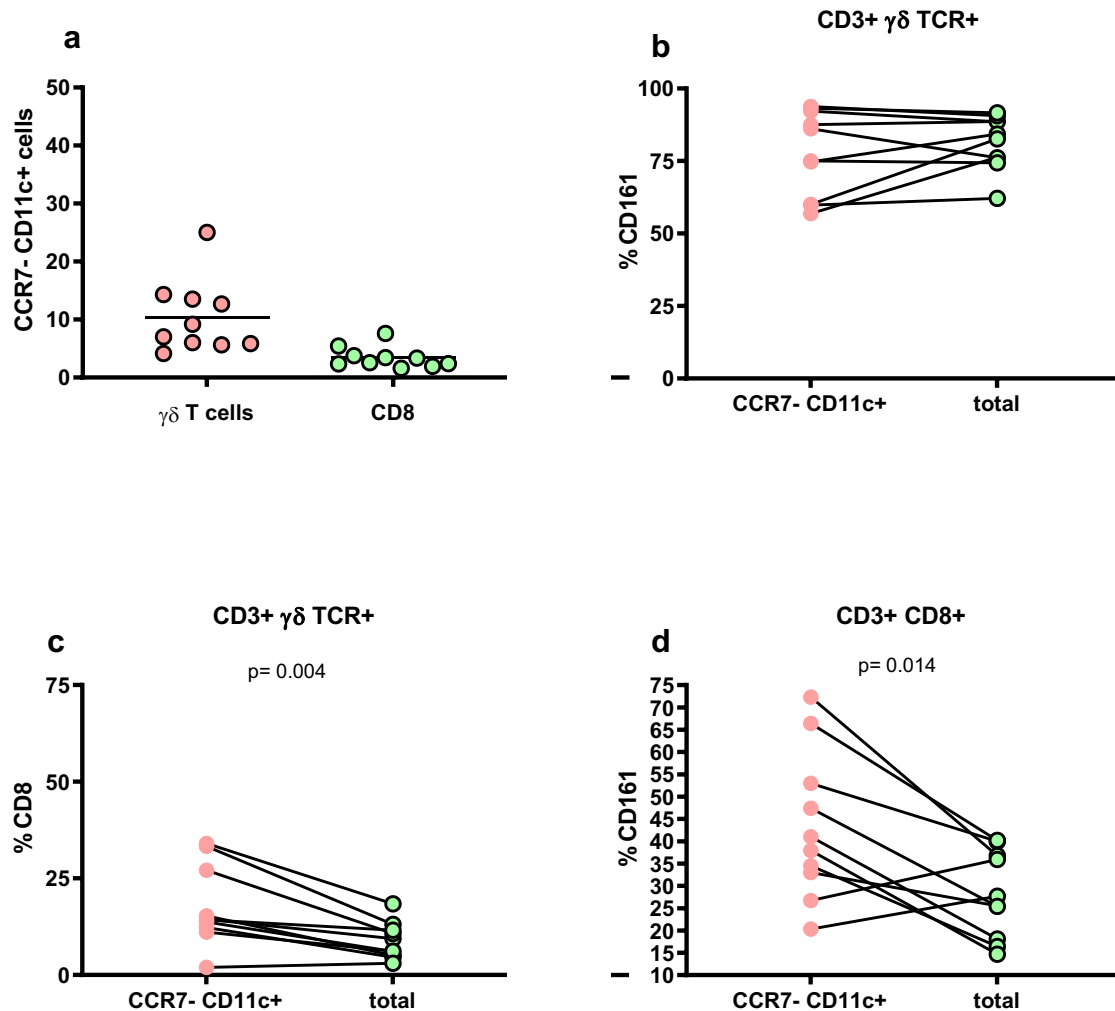

Figure 33. γδTCR+ and CD8+ T cells phenotype based on CD11c expression in blood from healthy women

The percentage of CD11c in γδTCR+ and CD8+ T cells is shown in (a). A comparison of the expression of CD161 and CD8 in CD11c+ γδ T cells vs. total γδ T cells from the blood is shown in (b and c). A comparison of the expression of CD161 in CD11c+ CD8+ T cells vs. total CD8+ T cells from the blood is shown in (d). Data were analyzed using Wilcoxon matched-paired signed-ranked test.

3.4.4.2   PBMC

When analyzing the differences between TEM CD11c+ and CD11c− cells after PBMC processing, in general, they were similar to whole blood, except for MAIT and iNKT, which lost significance (Figure 35; b). Thus, circulating CD11c+ TEM cells represent at least two different populations in healthy women: a subset of γδT cells with their high constitutive expression of CD161 and enriched expression of CD8, and a subset of CD8+ T cells with high expression of CD161. However, this phenotype was not associated with the MAIT or iNKT lineages.
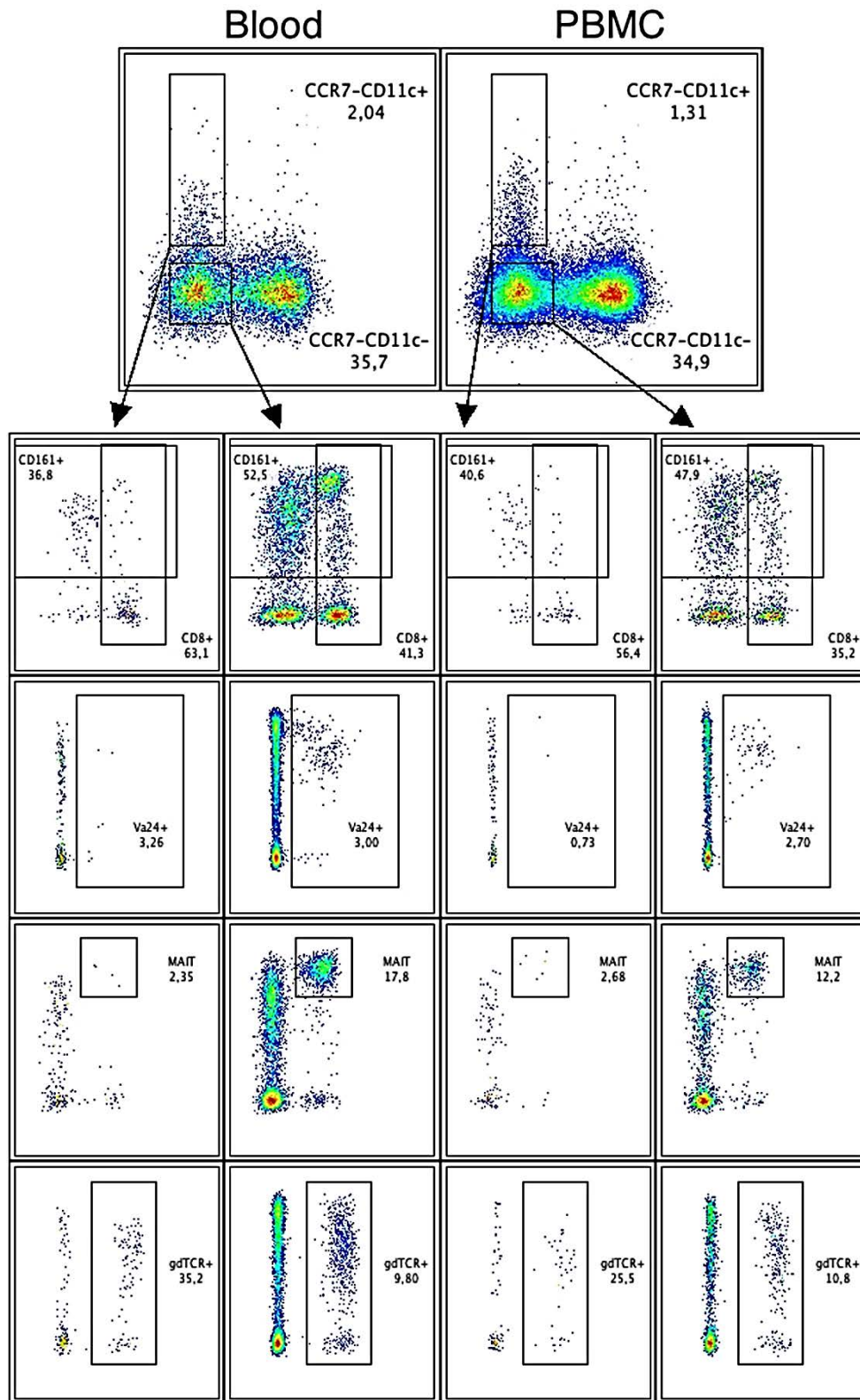
Figure 34. Example of gating strategy to study unconventional T cell subsets in CCR7– CD11c+/–

Example of the frequency of CD161, CD8, Vα24, MAIT, and γδTCR in the CD11c+ and CD11c-, CCR7- CD3+ T cell fractions on fresh blood (left) and processed PBMC (right) from the same individual.
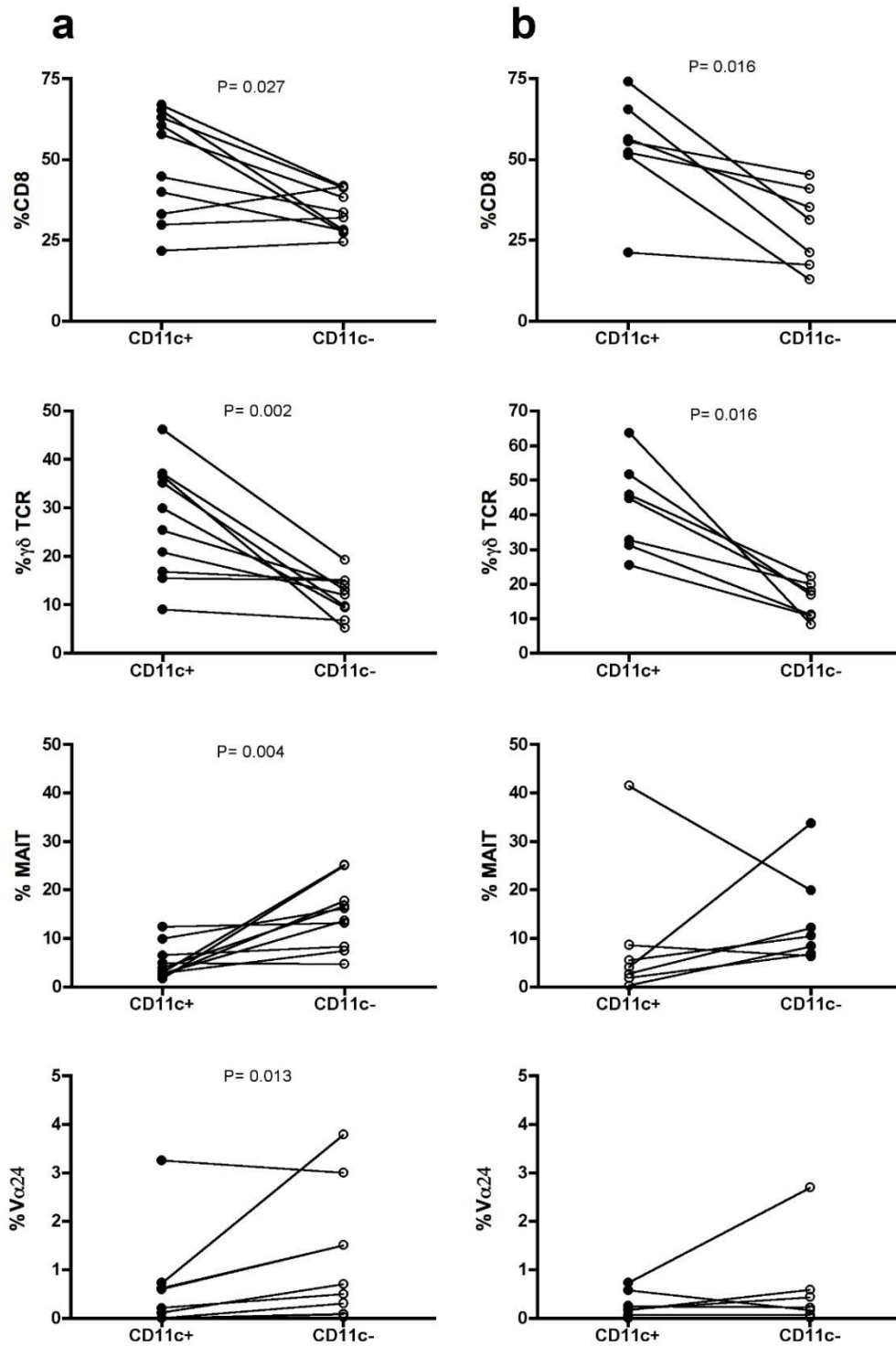
Figure 35. Comparison of specific phenotype frequencies based on CD11c expression in a) blood samples and b) PBMC from healthy women

(a) Fresh blood (n=10) and (b) PBMC (n=6). Comparison of the frequency of CD8, γδTCR, MAIT, and iNKT (Vα24) in CD11c+ and CD11c-, CCR7- CD3+ T cells from the same individual. (a) Fresh blood (n=10) and (b) PBMC (n=6). The gating strategy consisted of the following consecutive gates: lymphocytes, singlets, live CD14- CD19- CD3+ T cells, and CCR7- CD11c+ or CD11c- T cells. Data were analyzed using the paired Student's t-test.

3.4.4.3 Human cervical tissue

The same populations studied in blood were also studied in the GT of women. For that, cervical samples from women undergoing hysterectomy were processed. Before beginning the study, the effect of enzymatic digestion by collagenase on the expression of the different study markers was evaluated. As previously described (263), the loss of CD56 expression and a drastic reduction of CD19, CD20, and CCR7 staining were confirmed. On the other hand, the expression of: CD3, CD8, CD14, CD16, CD161, $\alpha\beta$TCR, $\gamma\delta$TCR, Vα7.2, Vα24, CD11c and HLA-DR was not modified. Since the majority of CD3$^+$ T cells in these tissues are CCR7– (>95%), this marker was excluded due to the negative effect observed by the digestion process. Applying the gating strategy shown in (Figure 36; a), CD11c expression in CD3$^+$ CD14-T cells represented an average of 3.3 ± 1.5% for the ectocervix and 3.7 ± 2.5% for the endocervix (Figure 36; b). Thus, these tissues were grouped to increase statistical significance. This way, the proportion of $\gamma\delta$TCR was >9% in CD11c$^+$ vs ~1% in CD11c$^-$ and the proportion of CD8 was 59% in CD11c$^+$ vs 46% in CD11c$^-$ (P<0.006 for both).
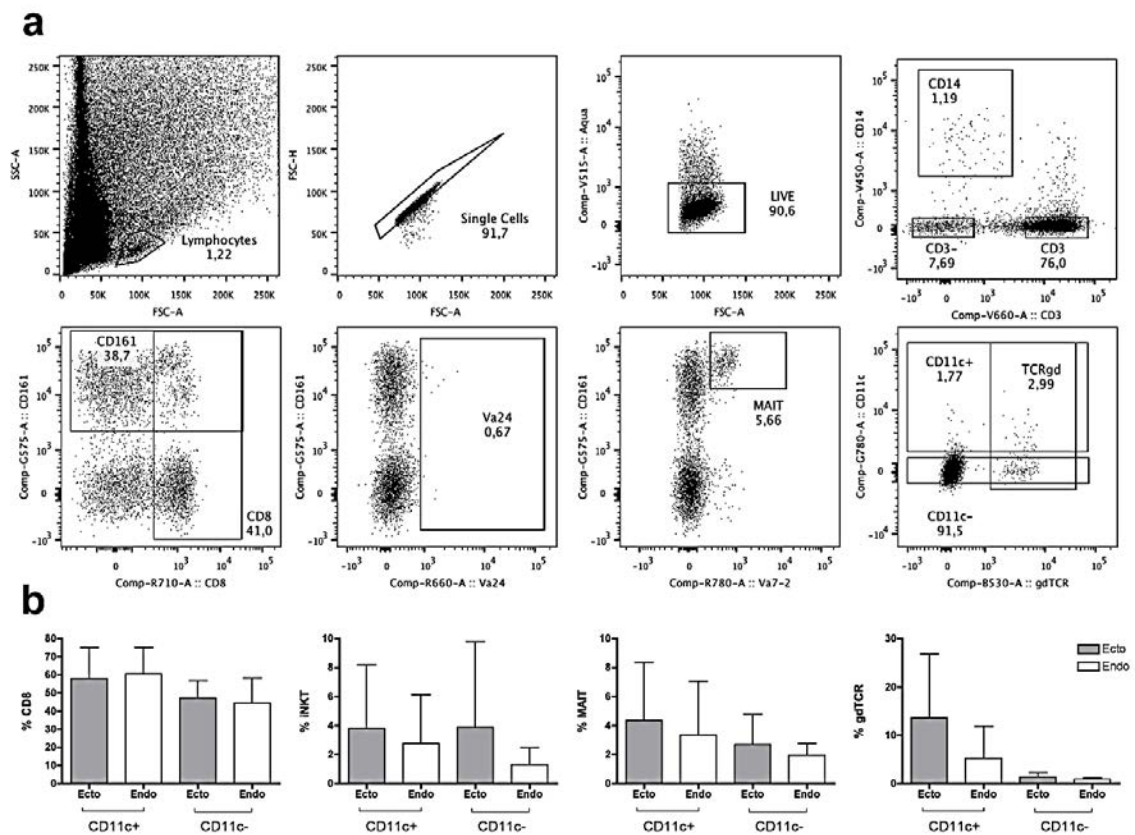

Figure 36. The phenotype of cervically derived T cells from healthy women and analysis by CD11c expression

(a) Representative dot plots from the T cell subsets extracted from the endocervix of healthy women. The top row shows the consecutive general gating strategy to select CD3+ T cells. The bottom row shows different subsets analyzed in the total CD3+ T cells and in the CD11c+ and CD11c- T cell fractions. (b) Frequency of CD8, iNKT (Vα24), MAIT, and $\gamma\delta$T cells by CD11c expression in T cells obtained from cervical tissue. Each bar represents the mean ± SD of the ectocervix and endocervix of each donor (n=5). Data were analyzed using Wilcoxon matched-paired signed-ranked test.

In addition, in 3 samples, CD69/HLA-DR activation markers were analyzed (Figure 37). HLA-DR was highly expressed on cervical T cells with no difference based on CD11c expression; CD69 expression was 86.0 ± 9.5% on CD11c$^+$ vs. 74.5 ± 10.1 % in CD11c$^-$ (p = 0.069; A) (Figure 37; a). Finally, analysis of CD103 frequency in another set of five samples showed no differences based on CD11c expression with values of 25-30% expression (Figure 37; b).
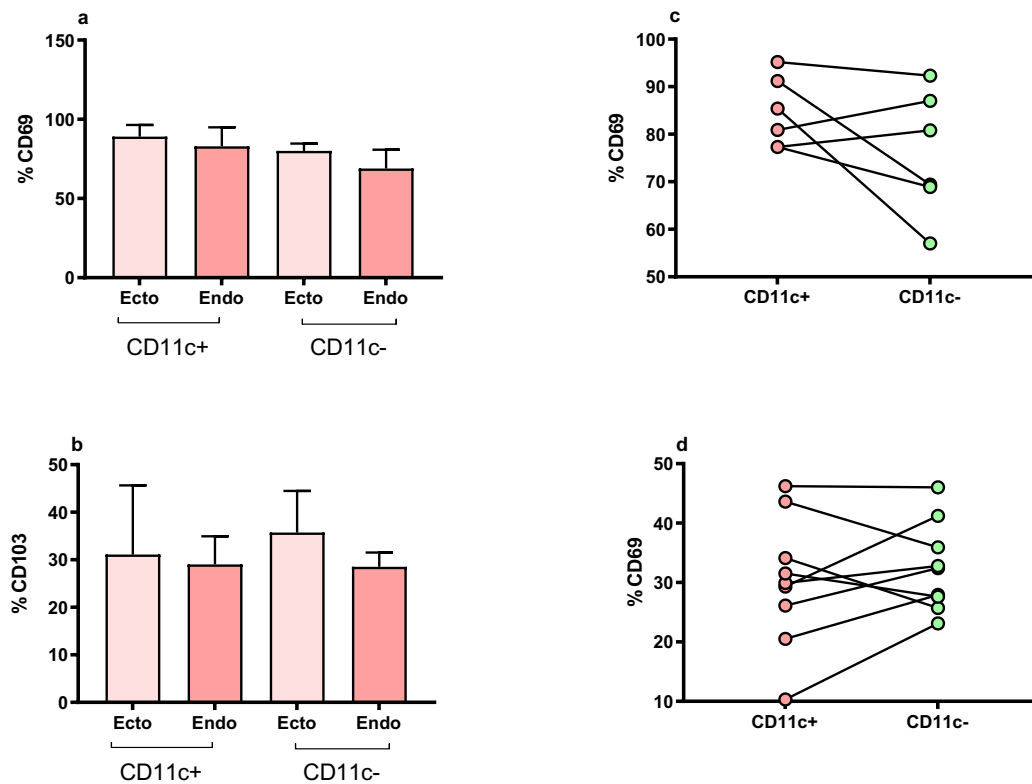

Figure 37. Expression of CD69 and CD103 in cervix from healthy women and analysis by CD11c expression

The frequency of CD69 (a) and CD103 (b) by CD11c expression in T cells obtained from cervical tissue is shown. Each bar represents the mean ± SD of the ectocervix and endocervix of each donor (n = 3–5). A comparison on the frequency of CD69 (c) or CD103 (d) in T cells from the same individual based on CD11c expression is shown for both cervical tissues. Data were analyzed using Wilcoxon matched-paired signed-ranked test.

Compared to blood, γδTCR$^+$ and CD161$^+$ represented smaller populations of total CD3$^+$T cells in women's cervix, while CD8$^+$T cells were enriched. The frequency of CD11c$^+$ in γδT cells was 20.4±10.3% (Figure 38; a), from which 44% were CD161$^+$ and 39% CD8$^+$. CD161 was again similar in γδT cells regardless of CD11c expression (Figure 38; b), while CD8 tended to be enriched in CD11c$^+$ γδTCR$^+$ T cells compared to total CD3$^+$ γδTCR$^+$ T cells (39% vs. 20%; p=0.068; Figure 38; c). Finally, CD11c$^+$ represented 5.8±2.9% of total CD8$^+$ T cells (Figure 38; a), in which CD161 was not significantly different from total CD3$^+$ CD8$^+$ T cells (33-41%; Figure 38; d). Regardless of differences in the percentage of CD8 and other subsets between blood and mucosa in women, similar findings were observed concerning the subsets enriched in CD11c$^+$ T cells.
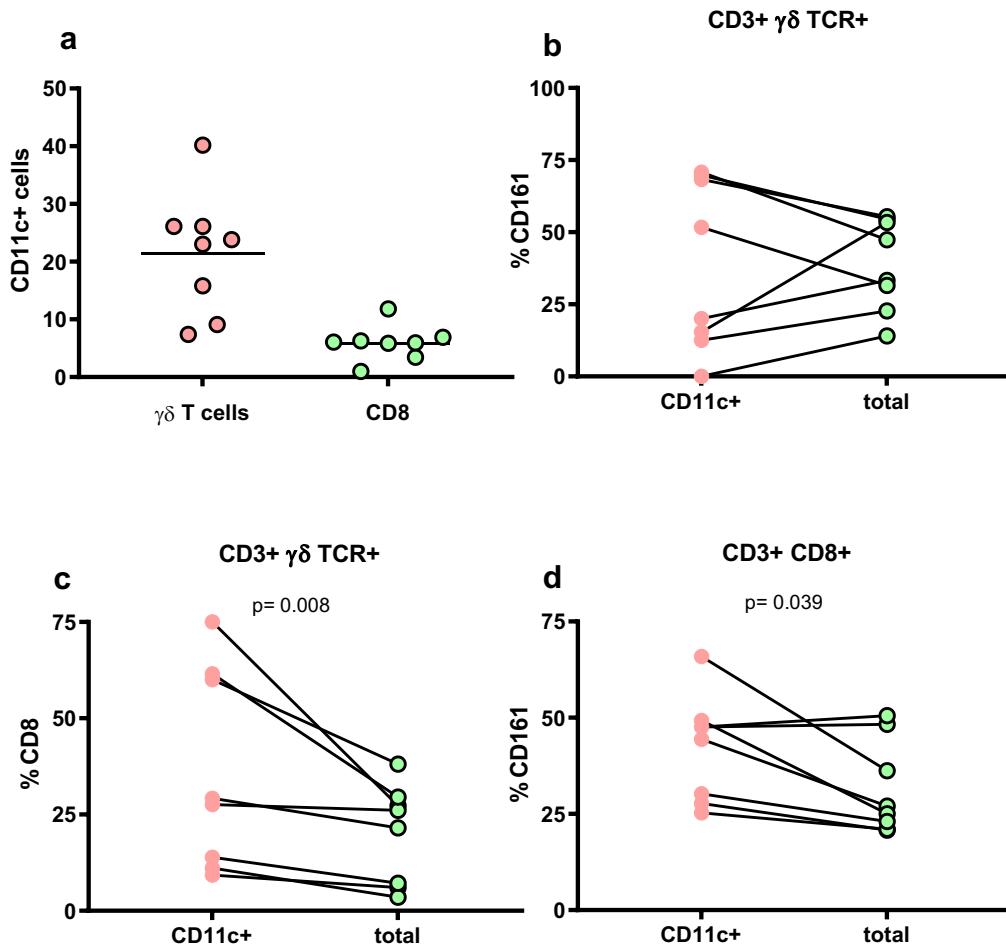
Figure 38. γδTCR+ and CD8+ T cells phenotype based on CD11c expression in GT from healthy women

The percentage of CD11c in γδTCR+ and CD8+ T cells is shown in (a). A comparison on the expression of CD161 and CD8 in CD11c+ γδ T cells vs. total γδ T cells from GT is shown in (b and c). A comparison on the expression of CD161 in CD11c+ CD8+ T cells vs. total CD8+ T cells from GT is shown in (d). Data were analyzed using Wilcoxon matched-paired signed-ranked test.

3.4.4.4   Homing molecules in CD11c T cells

Following the study in section 3.3.1, Homing Molecules During Baseline Conditions, we studied the association of CD11c expression with a variety of cellular adhesion molecules and chemokines receptors in thirteen healthy women. The circulating CD3^{+} CCR7^{-} CD4– population expressing CD11c stood out by the expression of the following markers: CCR2, CCR9, CCR10, CXCR6, α1β1, α4β7 (Figure 39; a and c-g). Additionally, both CXCR3 (18, 7±2.9% vs 4.5±1.89) and α4β1 (37.4±5.2% vs 4.5±1.2%) were also overexpressed (p=0.0002; data not shown). In contrast, CCR5 was higher in the CD11c^{-} fraction (Figure 39; b), while CLA and CD103 did not show differences (data not shown). Regarding activation markers, HLA-DR^{+} and/or CD38^{+} were also significantly increased in CD11c^{+} T cells compared to CD11c– T cells (all p≤0.0006; Figure 39; h and some data not shown)

Thus, compared to the animal model, CD103 was not particularly associated to CD11c^{+} T cells (3.5% vs. 3.8% in CD11c^{-}). Still, and similarly to the mouse data, CCR10 was

enriched in CD11c⁺ TEM cells, as occurred for most of the other chemokine receptors and other adhesion molecules measured, except for CCR5. In conclusion, CD11c⁺ T cells are activated with a high homing potential into different tissues and mucosae. However, they are not exclusive to the FGT, a conclusion already obtained in the other sections.
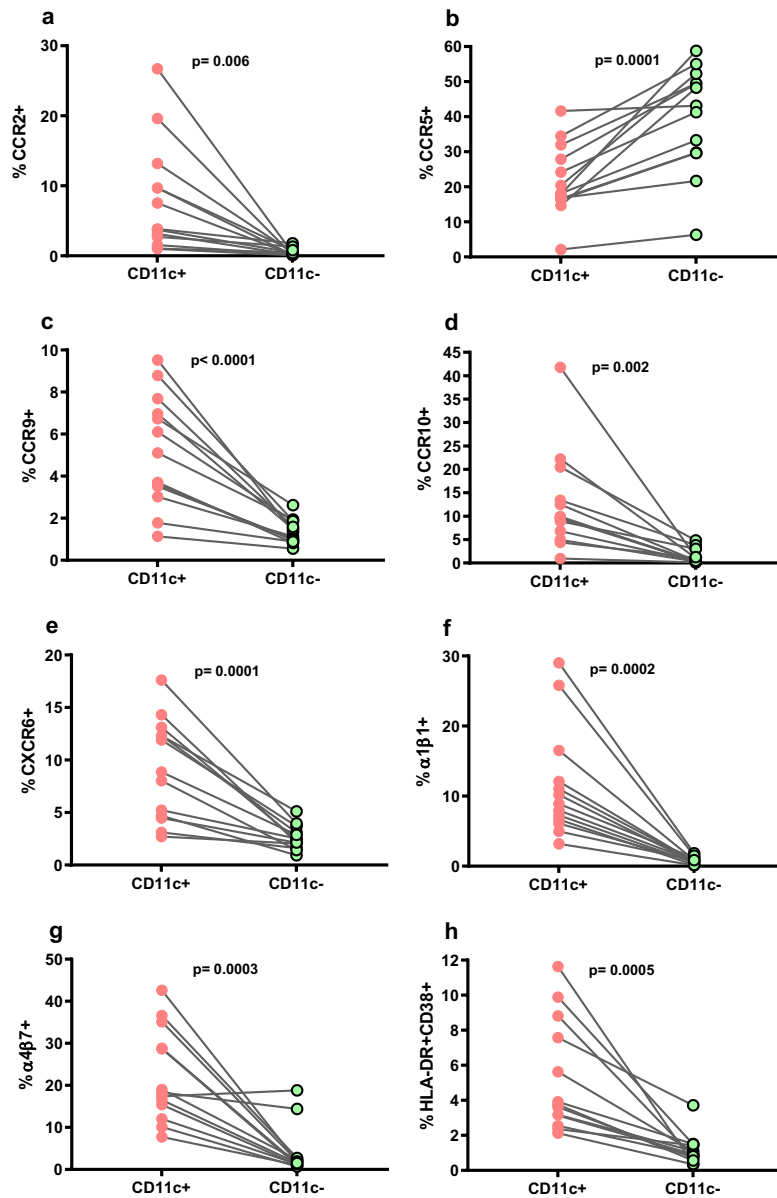

Figure 39. Comparison of adhesion molecule frequencies based on CD11c expression in CD4-TEM cells from healthy women

Comparison of the frequency of (a) CCR2, (b) CCR5, (c) CCR9, (d) CCR10, (e) CXCR6, (f) α1β1, (g) α4β7, (h) HLA-DR+ CD38+ in CD11c+ and CD11c- CD4- CCR7- T cells from the same individual (n=13). The gating strategy consisted of the following consecutive gates: lymphocytes, singlets, live CD3+ T cells, CCR7- CD11c+or CD11c- T cells, CD4- T cells, and expression of the different molecules addressed. Data were analyzed using Wilcoxon matched-paired signed-ranked test.

3.4.4.5   IFN-γ production in CD11c⁺ γδT cells

In the literature, the expression of CD11c in T cells has been associated with effector functions such as high IFNγ production (196,197). Therefore, the capacity of activated γδT

cells for IFNγ secretion was assessed based on CD11c expression. PBMCs were stimulated for 18 hours with HMBPP, which is phosphoantigen from Mycobacterium tuberculosis and other microbes. This compound activates and expands human Vγ2Vδ2 T cells, and the Vγ2Vδ2 TCR recognizes and binds to HMBPP presented by an APC (198). Control unstimulated samples and conventional T cell populations were unable to produce IFNγ (Figure 40; a) . However, 5.9±4.1% of the CD11c⁺ and 3.4 ±2.1% of the CD11c⁻ γδT cells secreted IFNγ after stimulation (Figure 40; a). Furthermore, when samples from the same individual were compared based on CD11c expression, we detected statistical significance in both IFNγ secretion and activation of γδT cells based on this marker (Figure 40; a and b).
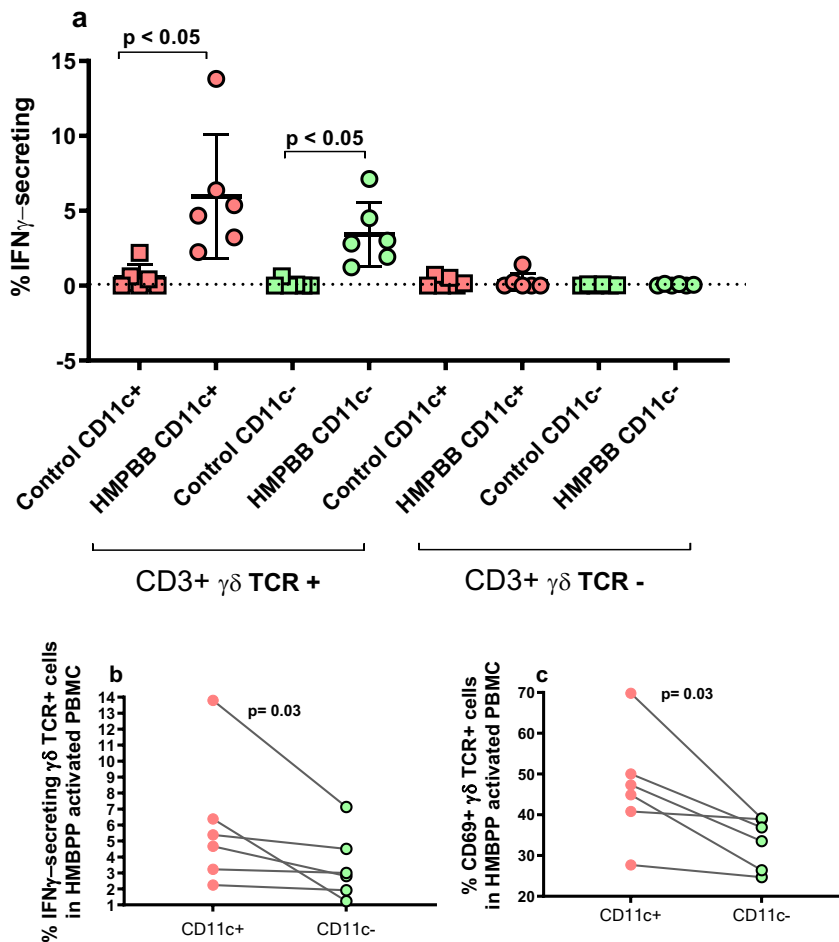

Figure 40. IFN-γ-secreting γδ T cells in PBMC from healthy women after HMBPP activation

(a) Comparison of the frequency of γδTCR+ CD11c+/- and γδTCR- CD11c+/- T cells that secrete IFNγ in PBMC from the same individual (n=6) after 20 hours of (E)-4-hydroxy-3-methyl-but-2-enyl pyrophosphate (HMBPP) activation. The gating strategy consisted of the following consecutive gates: lymphocytes, singlets, CD3+ T cells, γδTCR+/-, CD11c+/-, and IFNγ/CD69+ expression. Each bar represents the mean ± SD of control (squares) and HMBPP-stimulated PBMC (circles) samples. Data were analyzed using the non-parametric Friedman test for repeated measures, with Dunn's multiple comparisons post-hoc test. Graphs below show the comparison in the frequency of (b) IFN-γ-secreting γδT cells and (c) CD69 expression in γδT cells based on CD11c expression in HMBPP-activated PBMC from the same individual (n=6). Data were analyzed using Wilcoxon matched-paired

4 Discussion

The differential expression of adhesion molecules is known to confer site-dependent homing of circulating effector T cells to mucosal tissues. Lymphocytes induced by FGT immunization or infection will traffic transiently in blood, expressing a specific set of homing markers. Thus, specific homing molecules can be measured in the blood as surrogate markers of local immunity (e.g., α4β7 for the gut). By isolating cells from blood soon after mucosal FGT immunization or infection during the brief period in which mucosal lymphocytes recirculate, specific integrins, chemokine receptors, and other molecules responsible for lymphocyte entry into the FGT may be detected (264).

The current study provided solid evidence about the differential expression of proteins and gene transcription of molecules involved in T lymphocyte homing to the FGT in infected mice. As described above, cluster genes related to cellular and immunological functions were analyzed using the DAVID tool. As a result, functions of transcription (11% of genes), cell cycle (7.6% of genes), regulation of programmed cell death (4.7% of genes), and a small fraction of genes related to cytokine signaling (0.9% of genes) were identified. Regarding the immune response, the most significant clusters were signaling via IFN (159 genes), immune response (933 genes), and via cytokines (270 genes). Moreover, distinct genes potentially related to homing were detected, including Ccr5, Itgax, Cxcr6, and Ccr2. These results are consistent with other findings from studies carried out in the C57BL/6 mice model, in which twenty-six chemokine genes expressed in the mice female reproductive tract were identified, many of them expressed in several component tissues, whereas some were restricted or, at least, enriched to a specific tissue. Xcl1 and Ccl28 were restricted to the uterus, while Ccl20 and genes encoding CXCR2 ligands were primarily transcribed in the cervix and vagina (265).

In the current work, expression of Ccr5, Itgax, Cxcr6, and Ccr2 was higher in the VAG group of mice versus the control group. Further, validation in the mouse model demonstrated a significant increase in TEM (CD62L⁻), CD4⁺CD62L-CD44⁺ T, and CD8⁺ T cells CD44⁺ and CD44– after infection in the VAG group. These cells showed a noticeable increase in CCR2, CXCR6, and CD11c 10 and 14 days after infection, while CCR5 only increased ten days post-infection. These results indicate that active bacterial infection may induce upregulation of different genes specifically related to the expression of different chemokines and adhesion molecules facilitating TEM and CD4⁺ and CD8⁺ T cell to be recruited to mucosal effector sites at the GT (167)

Ou results from gene expression analyses detected Ccr5 as a molecule potentially involved in traffic to the genital tract, suggesting an essential role in protecting against infections. In this context, a study published in 2019 reported that the expression of Ccr5 is increased by effector CD4⁺ T cells in Ag-priming sites and vaginal tissue after intranasal immunization (266). The study was focused on determining the role of specific chemokine–receptor interactions in Ag-specific T cells from nasal and genital mucosa after intranasal immunization with live attenuated HSV-2 TK−. The main result was the upregulation of Ccr5 expression in effector CD4⁺ T cells from cervical LNs (as Ag-priming sites) and the vaginal tissue (266). In addition, the CCR5 ligands CCL3, CCL4, and CCL5 were

upregulated in vaginal tissue, and, in particular, CCL5 expression was highly enhanced in the stromal cells of vaginal tissue after nasal immunization. At the same time, intravaginal blockade of CCL5 by neutralizing antibodies diminished the number of HSV-2-specific effector cells in the vagina (266) Last, cells mixture from cervical LNs adoptively transferred from Ccr5-deficient mice failed to migrate into the vaginal tissue, consequently increasing the recipient mice's susceptibility to HSV-2 vaginal infection (266). These results support our finding, confirming that the CCR5–CCL5 chemokine pathway is required to migrate and retain Ag-specific effector cells in the vagina to provide protective immunity against infections (266).

CD11c expression has not been thoroughly studied in the context of T cell immunity. We found a consistent elevation of this molecule in all activated effector CD8$^+$ T cell subsets analyzed. Even though it must be considered that CD11c is not exclusive to genital tract infection, its remarkable increase in response to genital tract disorders places it as a novel surrogate marker of mucosal immunity in women (267). Classically, the α integrin CD11c defines conventional DC, but it is also expressed in populations of NK cells and activated B and T cells. CD8$^+$CD11c$^+$ T cells have been related to antiviral (268) and anti-tumoral activity (269), where they play an essential role in the adaptive immune response, either performing suppressor or effector functions. Although the origins of CD8$^+$CD11c$^+$ T cells are still not well elucidated, there is evidence that activation, development, and expansion of CD8$^+$CD11c$^+$ T cells is closely linked to the activation of the co-stimulatory molecules 41BB (also known as CD137) (269,270). In a mouse tumor model, it has been demonstrated that administration of anti-41BB to mice challenged with B16F10-melanoma cells increases the expansion of CD8$^+$CD11c$^+$ T cells that produced IFNγ and IL-2, correlating with tumor suppression (269). T cell co-stimulatory receptor 41BB, a member of the TNF receptor superfamily, is induced when T cells receive Ag-specific signals. Its ligand, 4-1BBL (CD137L), is also induced in antigen-presenting cells, such as DC, macrophages, and B cells (271). 41BB signaling can promote the transcription of several genes involved in T cell expansion, induce the expression of IL-2 and IFNγ, and co-stimulate T cells through the NF-κB, c-Jun, and p38 pathways, independently of CD28 (272).

As explained above, TEM cell activation was compared among four groups of patients, which had active episodes of psoriasis (PS), ulcerative colitis (UC), bacterial vaginosis (BV), or were healthy (ND). In the PS group, there was an increase in the expression of HLA-DR in CD4$^+$ TEM cells compared to ND, while CD38 and HLA-DR/CD38 double-positive cells increased in the UC group. Indeed, TEM cells are involved in immune response against mucosal infections and disorders, representing an Ag-specific response and particular migratory profile (273). After SARs-CoV-2 mRNA vaccination or natural infection, circulating SARS-CoV-2-specific CD4 T cells lack the expression of CCR7 exhibiting TEM profile and express CXCR3 marker suggesting lung homing (274). More evidence about the importance of TEM cell response in the gut against *Escherichia coli* was shown in a recent study (275). When volunteers were experimentally infected with

Enterotoxigenic Escherichia coli, circulating CD4$^+$ Th17-like cell populations showed a TEM profile with increased expression of activation, gut-homing, and proliferation markers (275). Other than these tissues, TEM cells have been reported in the female reproductive tract after vaccination against HPV in women (276). According to the study, the HPV vaccination response increased HPV-specific CD8 circulating cells with effector phenotype and CXCR3 expression, with an increase in infiltrating HPV-specific CD8 T cells to the cervical mucosa with a TRM phenotype (276).

The full expression of chemokine receptors and adhesion molecules in CD4$^+$ and CD8$^+$ TEM cells differed significantly between women with mucosal disorders and ND. Patients with BV showed significant enrichment of CD11c, CXCR6, and CCR10 expression in CD8$^+$ T cells, while CCR2, CD11c, α4β7, and α4β1 in the same group of patients were enriched in CD4$^+$ T cells. In contrast, in the other groups (PS and UC), the most remarkable molecules were CCR10 expression on CD8$^+$ cells, suggesting that CD11c and CXCR6 expression on T cells could indicate homing to the FGT potentially associated to BV in patients. In addition, circulating CD4$^+$ TEM cells from the BV group expressed CCR5 and α4β1 compared to healthy donors. CCR5 is related to many mucosal infections, especially HIV susceptibility (277). Activated CD4$^+$ T cells expressing CCR5, especially mucosal Th17 cells, appear to be the main HIV target cell during the early phases of the FGT infection (277–279). This finding may explain the association between HIV vaginal infections and BV in women. In many studies (280–285), BV was consistently linked to a higher risk of contracting HIV (281,283–285). A high BV prevalence could lead to a large proportion of HIV infections having BV as their primary cause (280,281,284). BV cause a pro-inflammatory environment in FGT, increasing the damage in the epithelial barrier and the infiltration of CD4$^+$ T cells expressing CCR5 (286).

It has been described that percentages of peripheral blood CD8$^+$ T cells expressing CXCR6 are higher in psoriatic patients than in healthy or atopic individuals (287). In agreement, a consistent increase in CXCR6 expression in total and activated TEM cell subsets from PS patients was observed. A recent study found that CXCR6/CXCL16 signaling axis controls the localization of TRM cells to different lung compartments and maintains airway TRM cells: CXCR6 recruits CD8 TRM cells to the airways, while CXCL16 is localized at the respiratory epithelium (288). CXCR6 expression and IL-15 trans-presentation in the tumoral context are critical for the survival and local expansion of effector-like CTLs in the tumor microenvironment to maximize their anti-tumor activity before progressing to irreversible dysfunction (289,290).

Finally, while CLA expression in total CD4$^+$ TEM cells of the PS group was unexpectedly reduced compared to ND, we detected a higher frequency of CLA on CD8$^+$ HLA-DR$^+$ TEM cells from the BV group. Due to their migration to the skin, CLA$^+$ T cells in the periphery decrease inversely to disease severity during acute psoriasis (291) . Further, CLA interacts with E-selectin expressed on venular endothelial cells not only from inflamed skin but also from oral mucosa and FGT, and genital HSV-specific CD8$^+$ T cells in the peripheral blood express high levels of CLA (291). However, α4β7, another molecule described in

asymptomatic HSV-2-infected patients but not in uninfected patients, was down-regulated in activated TEM cells from BV patients. While this decrease could also indicate selective infiltration of these cells into the infected tissues early after infection, the existence of a mechanism that would down-regulate some of these molecules cannot be discarded.

Overall the differential expression of specific adhesion molecules can induce a site-dependent homing profile that may work together with other generic signals (such as CXCR3, CCR3, CCR5, and CCR6) (267). Previous studies have examined adhesion molecules necessary for homing to the upper genital tract in a mouse model of C. trachomatis infection by directly infecting the uterine horn (292). In this model, CXCR3, CCR5, and α4β1 were required for protective T cells to home to the murine upper genital tract (292). Other homing molecules previously suggested as required for homing to the genital mucosa, such as α4β1 and α4β7 (293) were also differentially expressed in these patients. Thus, samples from women with symptomatic BV confirmed one of these molecules as potentially involved in FGT homing in humans since integrin α4β1 was indeed up-regulated in CD4$^+$ TEM cells, which correlated with high expression of this integrin in the genital mucosa of women. This scenario may be vital for developing mucosal vaccines against BV (292).

Previous studies have reported that CD8$^+$ CD11c$^+$ cells contribute to the clearance of Malaria parasites by secreting IFNγ and are involved in vaccine-stimulated protective immune responses (294). Vaccination with a single dose of genetically attenuated malaria parasites induced sterile protection against sporozoite challenges in the rodent *Plasmodium yoelii* model (294). Vaccine-induced CD8$^+$ T cell phenotype changes are characterized by significant upregulation of CD11c on CD3$^+$ CD8b$^+$ T cells in the liver, spleen, and peripheral blood. CD11c$^+$ CD8$^+$ T cells were predominantly CD11a^{hi} CD44^{hi} CD62L, indicative of Ag-experienced effector cells. Following in vitro restimulation with malaria-infected hepatocytes, CD11c$^+$ CD8$^+$ T cells expressed inflammatory cytokines and cytotoxicity markers, including IFNγ, TNF, IL-2, perforin, and CD107a. In another study (295), coculture of CD11c$^+$, but not CD11c, CD8$^+$ T cells with sporozoite-infected primary hepatocytes significantly inhibited liver-stage parasite development. Tetramer staining for the CSP-specific CD8$^+$ T cell epitope showed that CD11c expression was lost as the CD8$^+$ T cells entered the memory phase. Together, these results suggest that CD11c marks a subset of highly inflammatory, short-lived, Ag-specific effector cells, which may be essential in eliminating infected hepatocytes and are involved in vaccine-induced immune mechanisms.

This thesis showed a clear association between CD11c and NK1.1 expression, which strikingly increased after vaginal infection in mice. Previous work using whole-genome microarray datasets of the Immunological Genome Project demonstrated a close transcriptional relationship between NK and T cells distinguished by their expression of similar signaling functions. Moreover, gene expression analyses of activated CD11c$^+$ TEM cells showed that up-regulation of some effector mechanisms was related to NK properties (296). DX5, NKG2A, and NKp46 markers were examined in the

CD3+CD11c+ T cell population in section 4.3 (results). More than 70% of circulating CD3+CD11c+ T cells under basal conditions expressed DX5 and NKG2A. After infection, the frequency of NKG2A within CD11c+ T cells decreased significantly. NKG2A receptor transduces inhibitory signaling, suppressing NK cytokine secretion and cytotoxicity (297). More recent studies have shown overexpression of NKG2A on CD8+ of COVID-19-infected patients compared to healthy controls (298). NKG2A overexpression functionally exhausts CD8+ cells and NK cells, resulting in a severely compromised innate immune response (298). The literature described the expression of NKG2A by T cells (299–304). A subset of Vδ2 T cells expressing NKG2A was characterized by an intrinsic hyper-responsiveness against tumor cells (301). While a recent study published this year described a human NKG2A+CD8+ T cell population exhibiting elevated IL-12 and IL-18 receptors and low expression of CCR7 with higher cytotoxicity measured by gene expression (304). NKG2A expression on CD8+ T cells is induced by TCR activation in a way that works in concert with cytokines, including IL-12, IL-15, and TGF (299,303,304). As with NK cells, NKG2A engagement inhibits CD8+ T cell effector activities, NKG2A blockage enhances the cytotoxic activity of NKG2A-expressing CD8+ T cells (302,303). Thus in relation to our results, NKG2A may regulate the cytotoxic potential of circulating CD3+CD11c+ T cells.

Although expression of NK1.1 on T cells was first employed to exclusively define NKT cells (305), nowadays, there is sufficient evidence indicating that other subsets of non-conventional and activated T cells express NK1.1 or CD161 in mice and humans, respectively (306,307). CD4+, CD8+, and γδ+ T cells expressing CD161 share a transcriptional profile and exert similar innate immune functions. CD161 functions as a coinhibitory receptor on NK cells but can inhibit or enhance αβ T cell function depending on the co-stimulatory molecules involved (308). As described in section 3.4.3 (results), under basal conditions in mice, the CD3+CD11c+ cell fraction included almost exclusively iNKT cells and high proportions of γδT cells, the latter remaining after infection. However, PI, iNKT cells decreased, especially in the GT. After Chlamydia infection, blood γδT cells expressed higher levels of CD11c, while iNKT cells expressed lower levels. This could be related to the upregulation of the expression of the gene Klrb1b (encoding CD161) (309), although this was not confirmed. Of importance, γδT cells expressing NK1.1 are the main IFNγ-producers among γδT cell populations (310). Thus, CD161 expression on γδ T cells is associated with enhanced IFN-γ and IL-17 production and enhanced endothelial transmigration (310). Additionally, MAIT cells also express CD161. MAIT and CD161+ γδ T produce IFN-γ in response to IL-12/IL-18 stimulation regardless of TCR activation (311). Interestingly, the expression of killer cell lectin-like receptor B1 (KLRB1), the gene encoding the cell surface molecule CD161, is associated with a favorable prognosis in many cancers (307). Recently it was confirmed that CD161 expression and regulation defines rapidly responding effector CD4+ T cells associated with improved survival in HPV16-associated tumors (312).

From all the T cell subsets analyzed, besides CD8+ T cells, the most consistent population expressing CD11c was γδTCR+. γδT cells differ from other unconventional T cell

subpopulations in the expression of the Itgax gene, which encodes the CD11c. Earlier studies have reported functions as APC by γδ T cells in humans (313–315). These cells express CD69⁺ along with various costimulatory and adhesion molecules (including HLA-DR and CD11c respectively) (315). In agreement with these previous findings in this work, γδ T cells expressing CD11c were more activated. Moreover, CD11c⁺ and γδTCR⁺ cells also increased in the GT after infection. Because the expression of CD11c in T cells has previously been associated with effector functions such as high IFNγ production (316,317), the capacity of activated γδT cells for IFNγ secretion was assessed based on CD11c expression. Although a low proportion of the CD11c⁺ and the CD11c⁻ γδT cells secreted IFNγ after stimulation, CD11c⁺ were more activated and secreted more IFNγ compared to the negative fraction from the same individual. Nevertheless, these results are preliminary and further studies may confirm the capacity of CD11c⁺ and CD11c⁻ γδT cells to produce IFNγ in response to Ags and their protective role during genital infections. In human blood, γδ T cells quickly expand after infection in response to microbial metabolites (318). Thus, an increase in these cells would be expected in the context of GT disorders caused by *Chlamydia* or *Gardnerella* spp. Due to the production of these metabolites. The data of this work do not confirm if the increase of CD11c⁺ T cells during bacterial vaginosis in women is due to an augment in γδ T cells. However, CD11c expression was increased in circulating γδ T cells of Chlamydia-infected mice, which was demonstrated by the expansion of CD11c⁺ NK1.1⁺ γδ T cells in the blood seven days after infection.

Beyond this, there was a clear association between CD103 and CD11c expression in mice. CD103 is an αE integrin induced by TGF-β necessary for tissue retention (319,320). CD103⁺CD8⁺ T cells provide critical protection against viral infections due to anatomical privileged location within the epithelium linked to TRM profile (321,322), they exhibit rapid local cytotoxic function, and induction of tissue antiviral state through the production of IFNγ and other pro-inflammatory cytokines (323). Interestingly, inducible TGF-β was upregulated 3-5 fold in CD11c⁺ T cells (187). TRMs' importance in local immunity underlines the therapeutic potential of targeting this population against cancers and infections. These cells are heterogeneous, forming separate effector populations with specific functions at various tissue localizations (324) they are characterized by the expression of CD103 and CD andhe absence of CCR7 (320). In this work, it was observed that in uninfected mice and after infection, the expression of CD103 in blood and GT was restricted to subpopulations expressing CD11c. Therefore, CD11c could potentially be another marker of TRM in mice. Although no differences were observed in the frequency of CD103 expression on CD11c⁺ cells in women's cervix, CD11c⁺ T cells in this tissue may also contain CD8⁺ TRM cells since not all TRM cells express CD103 (325). In this regard, in humans, memory T cells with TRM characteristics have been identified at multiple mucosal surfaces, including the lung, the intestines, and the FGT (326). In the FGT, more than 95% of T cells are effector memory, with a high proportion of T cells expressing CD103 in the vagina, endocervix, ectocervix, and endometrium (327). Previous work has provided evidence indicating that in the genital skin after HSV infection, virus-specific TRM CD8⁺ T cells persist at the epidermal-dermal junction (328). Moreover, cervical

CD103$^+$ T cells and DC numbers declined in postmenopausal women (329). Furthermore, decreased DCs correlated with decreased CD103$^+$ T cells in the endocervix but not the ectocervix. These findings demonstrate previously unrecognized compartmentalization of TRMs in the FRT of postmenopausal women, with loss of TRMs and DCs in the cervix with aging and increased TRMs and DC induction capacity in the endometrium, which may be relevant to understanding immune protection in the FRT and to the design of vaccines for women of all ages (329).

Understanding how TRM functions and responds to infections and cancer at diverse mucosal locations may help shape future vaccination and immunotherapeutic approaches. Numerous murine works have shown that long-lived CD8$^+$ TRMs can be produced during infection and generated through vaccination in the FGT, where they can defend against infectious diseases such as HSV and HPV. Emerging data in the human field suggest that CD8$^+$ TRM expressing higher levels of CD103 and cytotoxic molecules (e.g., Granzyme B) are located near the epithelium, whereas lower levels of CD103 are found on CD8$^+$ TRMs in the stroma, indicating that distinct Ag-specific CD8$^+$ TRM subsets are distributed throughout the human cervix (324,330). In the context of mucosal vaccines, TRM has emerged as a newly recognized memory T cell subset in the last ten years, particularly in the case of respiratory infection biology. Because this cell type is positioned at the site of the pathogen entrance and has distinct transcriptional and functional profiles, it is an excellent candidate for the next generation of vaccines. Multiple human and animal studies have established the role of these cells in disease prevention against viruses such as influenza, respiratory syncytial virus, and the recent SARS-CoV-2 infection (321,331–334).

Our results suggest that the CD11c$^+$ T cells described in this work may be candidates for TRM in the genital mucosa. These results may have significant applications in mucosal vaccines against STIs. Chlamydia trachomatis infection is the most common sexually transmitted disease caused by bacteria, but there is still no vaccine. To develop successful preclinical studies in animals, a CT vaccine composed of ultraviolet light–inactivated Ct (UV-Ct) conjugated to charge-switching synthetic adjuvant nanoparticles (cSAPs) has been described (335). CT infection induced protective immunity that depended on the production of IFN-γ by CD4$^+$ T cells. In contrast, uterine exposure to UV-Ct generated tolerogenic Ct-specific regulatory T cells, exacerbating bacterial burden upon Ct rechallenge. Intrauterine or intranasal vaccination, but not subcutaneous vaccination, stimulated genital protection in both conventional and humanized mice. Regardless of vaccination route, UV-Ct–cSAP always evoked a robust systemic memory T cell response, but only mucosal vaccination induced effector T cells with the capacity to seed the uterine mucosa during the first week after vaccination, which may lead to the establishment of TRM. These Immune mechanisms are schematized in Figure 27 (335). Additionally, preclinical studies on TRM -targeted vaccination against cancer have shown a favorable outcome. Intranasal and mucosal administration of vaccine generated protective T cells resident memory cells in the lung and airway of mice (336).
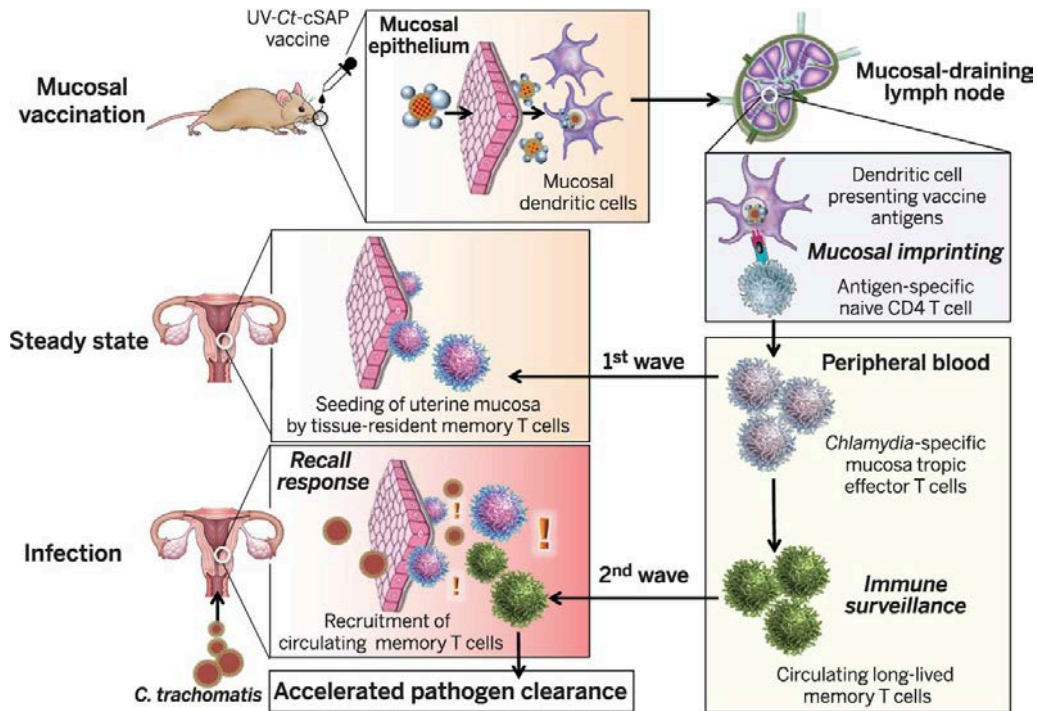
Figure 27. Upon mucosal vaccination, dendritic cells carry UV-Ct–cSAP to LNand stimulate CD4 T cells

Effector T cells are imprinted to traffic to uterine mucosa (first wave) and establish tissue-resident memory cells (TRM cells). Vaccination also generates circulating memory T cells. Upon genital Ct infection, local uterine TRM cells' local reactivation triggers the circulating memory subset (second wave) recruitment. Optimal pathogen clearance requires both waves of memory cells (335).

Overall, many properties that enable T cells to traffic to specific locations are programmed during the early stages of the infection. Thus, to understand the homing patterns and dynamics of the mucosal response associated with vaccination and infection, we need to analyze specific and activated T-cell responses early after activation, which may provide biomarkers for infection and vaccine-response. In summary, in this study, adhesion molecules CD11c, α4β1, CCR5, and CXCR6 were identified as markers associated with an effector T cell mucosal response against STI. Moreover, most of these markers are also associated with TRM profiles. They may thus serve as indicators of TRM precursors, measurable in the blood, during the development and trafficking of the immune response.

5 Conclusions

During this work, we have studied the homing profile of T cells owards certain peripheral tissues, including the FGT in women and mice. We have been able to characterize the response of TEM cells to CT infection through transcriptomic studies in mice with their phenotypic validation in both mice and women. We defined adhesion molecules, namely CCR5, α4β1, and CD11c, which may be desirable to induce for an effective mucosal response in vaccine candidates against STI. Additionally, we have described and characterized the CD11c integrin as a new marker in the context of T cells and mucosal response. Particular attention should be given to this marker in the context of T-cell mucosal immunity in response to genital tract disorders. In summary, we can highlight the following points as the essential finding of this work:

- Blood CD3$^+$ CD62L$^-$ CD44$^+$ T cells overexpress Ccr5, Itgax, Cxcr6, and Ccr2 genes after vaginal infection in mice.
- Selected up-regulated genes were confirmed by protein expression. While CCR2 and CCR5 were only increased in the CD4$^+$ TEM cell subset after vaginal infection, expression of CXCR6 and CD11c was much more abundant in CD8$^+$ TEM cells.
- At least one marker was over-expressed during mucosal disorders compared to ND women in circulating TEM cells from blood.
- The BV group had an increase in CCR5 and α4β1 expression in CD4$^+$ TEM cells and CD11c in CD8$^+$ TEM cells compared to ND.
- Higher circulating CD11c$^+$ CD8$^+$ T cell frequency is detected soon after *Chlamydia* infection in mice.
- CD11c expression increases in human circulating CD8$^+$ TEM during symptomatic vaginosis.
- CD11c expression in blood after vaginal infection correlates with an increase in the genital tract but is not exclusive to infection of the genital tract.
- Murine-activated CD11c$^+$ TEM cells are enriched for NK gene signatures.
- Murine CD11c$^+$ T cells include high frequencies of γδT and iNKT cells.
- CD103 expression is exclusively associated with CD11c$^+$ T cells in mice.
- Circulating T cells expressing CD11c are associated with γδ T cells but not with iNKT cells in women.
- Human cervical tissue contains γδ T cells expressing CD11c.
- CD11c$^+$ T cells are highly enriched for adhesion molecules expression but not for CD103 in women.
- CD11c expression in γδ T cells is associated with higher capacity IFNγ secretion after activation.

6 Supplementary material
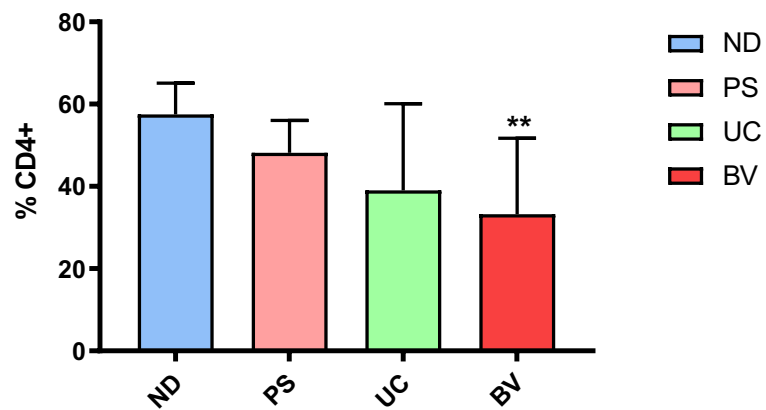
S1: The percentage of CD4+ T cells determined by flow cytometry is shown in Figure 14. for ND and the different groups of patients. General gating strategy is shown in. Each bar represents the median ± interquartile range of healthy young women (ND; white bars, n = 13), women with psoriasis (PS; grey bars, n = 5), ulcerative colitis (UC; checkered bars, n = 4) and bacterial vaginosis (BV; dark bars, n = 5). P value indicates *<0.05.

PLOS | ONE

Adhesion Molecules Associated with Female Genital Tract Infection

Jamal Qualai[1©], Jon Cantero[1©], Lin-Xi Li[2], José Manuel Carrascosa[3], Eduard Cabré[4,5], Olga Dern[6], Lauro Sumoy[7], Gerard Requena[8], Stephen J. McSorley[9], Meritxell Genescà[1]*

1 Mucosal Immunology Unit, Institut d'Investigació en Ciències de la Salut Germans Trias i Pujol (IGTP), AIDS Research Institute IrsiCaixa-HIVACAT, Can Ruti Campus, Badalona, Spain, 2 Department of Microbiology and Immunology, University of Arkansas for Medical Sciences, Little Rock, Arkansas, United States of America, 3 Department of Dermatology, University Hospital "Germans Trias i Pujol," Badalona, Universitat Autònoma de Barcelona, Spain, 4 Department of Gastroenterology, University Hospital "Germans Trias i Pujol," Can Ruti Campus, Badalona, Catalonia, Spain, 5 Centro de Investigación Biomédica en Red de Enfermedades Hepáticas y Digestivas (CIBERehd), Madrid, Spain, 6 Atenció Salut Sexual i Reproductiva (ASSIR), Centre d'Atenció Primària (CAP) Sant Fèlix, Institut Català de la Salut (ICS), Sabadell, Spain, 7 Genomics and Bioinformatics Group, Institute for Predictive and Personalized Medicine of Cancer (IMPPC), Can Ruti Campus, Badalona, Spain, 8 Flow Cytometry Unit, Institut d'Investigació en Ciències de la Salut Germans Trias i Pujol, Badalona, Spain, 9 Center for Comparative Medicine (CCM), Department of Anatomy, Physiology and Cell Biology, School of Veterinary Medicine, University of California Davis, Davis, California, United States of America

© These authors contributed equally to this work.
* mgenesca@igtp.cat (MG)

Abstract

Efforts to develop vaccines that can elicit mucosal immune responses in the female genital tract against sexually transmitted infections have been hampered by an inability to measure immune responses in these tissues. The differential expression of adhesion molecules is known to confer site-dependent homing of circulating effector T cells to mucosal tissues. Specific homing molecules have been defined that can be measured in blood as surrogate markers of local immunity (e.g. $\alpha 4\beta 7$ for gut). Here we analyzed the expression pattern of adhesion molecules by circulating effector T cells following mucosal infection of the female genital tract in mice and during a symptomatic episode of vaginosis in women. While CCR2, CCR5, CXCR6 and CD11c were preferentially expressed in a mouse model of *Chlamydia* infection, only CCR5 and CD11c were clearly expressed by effector T cells during bacterial vaginosis in women. Other homing molecules previously suggested as required for homing to the genital mucosa such as $\alpha 4\beta 1$ and $\alpha 4\beta 7$ were also differentially expressed in these patients. However, CD11c expression, an integrin chain rarely analyzed in the context of T cell immunity, was the most consistently elevated in all activated effector CD8+ T cell subsets analyzed. This molecule was also induced after systemic infection in mice, suggesting that CD11c is not exclusive of genital tract infection. Still, its increase in response to genital tract disorders may represent a novel surrogate marker of mucosal immunity in women, and warrants further exploration for diagnostic and therapeutic purposes.

Introduction

Female genital tract (FGT) infections, including common sexually transmitted infections (STI), seriously compromise the health of women. Worldwide, more than 340 million new cases of treatable STI occur each year and they are estimated to be the leading cause of morbidity in women in developing countries [1]. Furthermore, pre-existing FGT infections affect the development and pathogenesis of other STI, as occurs with the pro-inflammatory environment generated by bacterial vaginosis (BV) and the enhancement of human immunodeficiency virus (HIV) replication [2]. The long-term consequences of STI, including pelvic inflammatory disease, cancer, infertility, stillbirth, etc. not only are highly relevant at the social and health level, but also have a major economic impact.

Although effective vaccines exist for human papilloma virus and hepatitis B virus, efforts to develop vaccines against herpes simplex virus type 2 (HSV-2), HIV and bacterial STI have been hampered by an inability to effectively measure immune responses in the genital tract. Such vaccines need to be able to generate robust immune responses at site of potential exposure in order to provide rapid control of primary infection [3, 4]. Mucosal T cells and, notably, cytotoxic T lymphocytes play a critical role in the clearance of sexually transmitted pathogens [4]. For instance, studies in human have confirmed the association of T cell-mediated immunity with clearance of *Chlamydia* infection [5] and susceptibility to re-infection [6]. Moreover, the presence of antiviral effector CD8$^+$ T cells in the vagina of immunized monkeys correlates with protection from uncontrolled viremia after pathogenic challenge with simian immunodeficiency virus [7]. In these models of genital infection, the induction of effector memory T (T$_{EM}$) cells and antibodies that are able to mount fast responses upon re-challenge is critical to control the pathogen. However, current assays used to understand the magnitude and quality of immune responses in the FGT rely primarily on blood samples and thus provide an incomplete picture of localized immune control.

The capacity of distinct subsets of antigen-experienced lymphocytes to traffic preferentially into specific compartments is termed homing. T$_{EM}$ cell entry into inflamed non-lymphoid tissues is an active process involving members of the integrin, selectin-ligand and chemokine-receptor families, which mediate selective interactions of circulating lymphocytes with the specialized vascular endothelium [8]. While some adhesion molecules are enriched for a given tissue, e.g. α4β7 integrin and CC chemokine receptor CCR9 are associated with homing of T cells to the gut and cutaneous lymphocyte-associated antigen (CLA) and CCR4/CCR10 with T cell homing to the skin, other molecules are specialized for tissue-inflammatory functions to multiple tissues, such as CXCR3 or αLβ2 [9, 10]. Importantly, many properties that enable T cells to traffic to specific locations are programmed during the early stages of the infection [11]. Analysis of blood samples during the primary immune response to yellow fever immunization in humans suggests that human virus-specific CD8$^+$ T cells express a dynamic pattern of homing molecules early after immune activation [12]. Thus, analysis of lymphocytes in blood will not reflect the quantity/quality of non-recirculating resident memory T cells [11], and sampling directly from mucosal surfaces will be required to define correlates of protection after vaccination. However, after activation, there is a window of opportunity to examine circulating lymphocytes in blood as they are homing to a specific mucosal tissue.

In contrast to the gastrointestinal tract or the skin, our understanding of homing receptors that are required for cells migrating to the FGT is limited. α4β7 was proposed to recruit CD4$^+$ T cells to the vaginal mucosa of mice infected with *Chlamydia* [13]. Yet, a recent paper demonstrated that this integrin is not necessary for CD4$^+$ T cell-mediated protection against *Chlamydia trachomatis* infection, while α4β1 appears to drive homing of protective cells into the murine upper genital tract [14]. Other papers using animal models support these findings [15]

and expression of vascular cell adhesion molecule-1, which binds this integrin, has been detected in the human vagina [16, 17]. Nonetheless, another recent paper demonstrated that circulating CD4^{+} T cells from asymptomatic HSV-2-infected patients express higher levels of α4β7 than uninfected patients [18]. Lastly, other investigators have described homing receptors that are shared between immune cells migrating to the skin and the FGT [16, 19]. Here, we hypothesized that defining the homing profiles of lymphocytes migrating towards the genital tract could potentially be used as a surrogate marker of FGT immunity. We found that T_{EM} cells from mice intravaginally-infected with *Chlamydia muridarum* expressed high levels of CCR2, CCR5, CXCR6 and CD11c. When comparing these homing profiles to women with different mucosal or skin disorders, unique features were detected in each of the cohorts, compared to healthy patients. Of particular interest, CD11c was strikingly increased in CD8^{+} T_{EM} cells from patients with BV and thus could serve as a novel indirect marker of FGT immunity.

Materials and Methods

Ethics statement

All mice were maintained in accordance with the recommendations of the Association for Assessment and Accreditation of Laboratory Animal Care International Standards and with the recommendations in the Guide for the Care and Use of Laboratory Animals of the National Institutes of Health. The Institutional Animal Use and Care Committee of the University of California, Davis, approved these experiments (Protocol # 18299).

Informed written consent was obtained from all participants and the study protocol and questionnaire was approved by the University Hospital Germans Trias i Pujol (HUGTP, Badalona, Spain) Clinical Research Ethics Committee (reference # EO-11-074). The study was undertaken in accordance with the Declaration of Helsinki and the requirements of Good Clinical Practice.

Animal model

Chlamydia muridarum strain Weiss was purchased from ATCC (Manassas, VA) and propagated in HeLa 229 cells in Dulbecco's modified Eagle's medium (Life Technologies, Grand Island, NY) supplemented with 10% fetal bovine serum (FBS). *C. muridarum* elementary bodies (EBs) were purified by discontinuous density gradient centrifugation as previously described and stored at -80°C [20]. The number of inclusion-forming units of purified EBs was determined by infection of HeLa 229 cells and enumeration of inclusions that were stained with anti-*Chlamydia* major outer membrane protein antibody (a kind gift from Dr. Harlan Caldwell). Eight weeks old C57BL/6 mice were purchased from The Jackson Laboratory (Bar Harbor, ME). For systemic infection, mice were intravenously (IV) injected in the lateral tail vein with 1×10^5 C. muridarum. For vaginal infection, estrus was synchronized by subcutaneous injection of 2.5 mg medroxyprogesterone acetate (Greenstone, NJ). Seven days after, 1×10^5 C. muridarum in 5μL sucrose/phosphate/glutamate buffer were deposited directly into the vaginal vaults with a blunted pipet tip [21]. Seven, 10 and 14 days post-infection, blood was collected by retro-orbital bleeding. Immediately after collection, blood samples for cell sorting and validation analyses were air-shipped from the laboratory of Dr. McSorley (CCM, UC Davis, CA) to the laboratory of Dr. Genescà (IGTP, Badalona, Spain). Samples arrived refrigerated and in good conditions 48 hours later and were immediately processed.

Cell sorting

Circulating T_{EM} cells were sorted from six 7 days *Chlamydia*-infected mice (VAG group) and six contemporary sham-treated mice (control group). Blood samples (~500μl) were

immediately lysed using an in-house red blood cell lysis buffer. After washing, cells were stained with antibodies against CD3-Vioblue (145-2C11), CD62L-PE (MEL-14-H2.100) and CD44-FITC (IM7.8.1; all from Miltenyi Biotec, Madrid, Spain). Cells suspended in cold FACS flow buffer (0.5% FBS-PBS with 0.5mM EDTA) were immediately sorted into 350µl of chilled RLT buffer (QIAGEN, Valencia, CA) using a BD FACSAria™ Cell Sorter (Flow Cytometry Platform, IGTP). Purity of sorted CD62L$^-$ CD44$^+$ activated T$_{EM}$ cells was >99%. Once sorted, samples were mixed for a minute and after a short spin, the volume of RLT was adjusted (3.5:1 ratio of RLT to sheath fluid) using filtered tips. Samples were mixed and spun again and immediately frozen at -80°C.

Gene expression analyses

Total RNA was isolated from cells using RNA easy Mini kit (QIAGEN). After qualitative assessment of RNA integrity, samples were amplified using Whole Transcriptome Amplification 2 (Sigma-Aldrich, Madrid, Spain). We chose four samples in each group that qualified for microarray analyses, yet one sample from the VAG and control group were discarded after as outliers, thus microarray analyses were performed in n = 3 for the VAG group and n = 3 for the control group (which were actually contemporary samples). The number of sorted cells in each group was similar (15,207 ± 2,339 cells for the VAG group and 20,793 ± 2,443 cells for the control group; not significant).

Affymetrix microarray hybridization was performed using the Mouse Genome 430 PM Strip platform. Images intensities were extracted using GeneAtlas System software (Affymetrix), normalized and summarized using Robust Multi-array Average algorithm. Differential gene expression analysis was assessed by fitting to an empirical Bayesian linear model. Statistical significance in differential gene expression was computed with a false discovery rate multiple testing adjustment correction. For this analysis we used the Limma package and the R statistical programming environment [22]. The 'compute overlaps' function in the 'investigate gene sets web application (http://www.broadinstitute.org/gsea/msigdb/annotate.jsp) of the Molecular Signatures Database v4.0 (MaSigDB) was used to explore functions enriched among the top regulated genes defined as having a nominal (non-adjusted) p-value <0.005. The lists of gene symbols up-regulated and down-regulated in infected versus uninfected samples were scrutinized for significant overlaps with pathway (C2: CP, KEGG) and immunologic signatures (C7) in MaSigDB [23].

Flow cytometry validation analyses in mice

Blood samples (~500µl) were immediately lysed, washed, suspended in PBS and incubated with Aqua vital dye to distinguish live from dead cells (Invitrogen, Burlington, ON, Canada). Following two more washes, cells were suspended in washing and staining buffer (1% bovine serum albumin-PBS) and incubated for 20 minutes with the following cocktail of pre-titrated anti-mouse antibodies: CD3-Vioblue (145-2C11), CD4-APC-H7 (GK1.5), CD62L-PE (MEL-14-H2.100) (Miltenyi Biotec), CD44-Brilliant Violet 570 (IM7; BioLegend, San Diego, CA), CD11c-PE-Cy7 (HL3; BD Biosciences) and CCR5-FITC (CTC5), CXCR6-PerCP (221002) and CCR2-APC (475301) (R&D Systems Inc., Minneapolis, MN). All events were acquired in a BD FACSAria™ Cell Sorter and analyzed with FlowJo vX.0.7 software (TreeStar, Ashland, OR).

Participant enrolment and inclusion criteria for human samples

All participants for this study (20–40 year old women) were classified in the following different cohorts: normal donors (ND, n = 13, median age of 25 years with interquartile range (IQR) of 23–28 years), psoriasis (PS, n = 5, median of 35 with IQR 30–37), ulcerative colitis (UC, n = 4,

median of 26 with IQR 22–38), and BV (n = 5, median of 30 with IQR 25–36). Healthy ND volunteers were recruited from the clinical trials unit of the University Hospital Germans Trias i Pujol (HUGTP, Badalona, Spain). Patient recruitment for the PS and UC cohorts was carried in the corresponding services of Dermatology and Gastroenterology of the HUGTP. BV patients were recruited at the Unit of Attention to Sexual and Reproductive Health from the Primary Health Care centers of Sabadell and Cerdanyola in Catalonia (Spain).

Participants completed a questionnaire in order to detect possible exclusion criteria (other chronic or acute diseases, allergies or infections, immunosuppressive treatment, etc.) and register menstrual cycle and birth control data. Patients included in each cohort presented either an active burst (for PS and UC groups) or symptoms compatible with a recent infection within the last 7 days (for BV group). Inclusion criteria for the PS group consisted on women with acute psoriasis vulgaris that suffered a relapse of less than two weeks, with no treatment for at least six weeks. UC subjects were women with active ulcerative colitis: the extent of pathology was defined based on the Montreal classification [24] and the severity of disease on the Mayo's Disease Activity Index [25]. Only patients with active burst (index >9) off immunosuppressive treatment were included. Lastly, not-treated and symptomatic BV infections defined by Nugent scoring of >7 and suspected of *Gardnerella vaginalis* origin were confirmed by microscopic examination (more than 20% of clue cells). Patients with other STI were excluded.

Human T cell phenotype

Blood was collected and processed within 4 hours maximum. An ammonium chloride-based lysing reagent (BD Pharm Lyse, BD Biosciences) was used for erythrocyte deletion of 1ml of blood. After washing, cells were suspended in PBS and stained with Aqua Dye (Invitrogen) for cell viability. Cells were washed again, suspended in staining buffer and divided in four tubes. The four different panels assessed contained some common and some specific antibodies. Common antibodies were: CD3-eFluor 605, CD4-Alexa700 (eBioscience, San Diego, CA), CCR7-Horizon PE-CF594, CD38-Brillant Violet 421, HLA-DR-PerCP-Cy5.5 and CD11c-PE-Cy7 (BD Biosciences). Specific for each panel were: 1) CCR2-PE, CCR5-APC-Cy7, CXCR6-APC (R&D Systems Inc.) and CXCR3-FITC (BioLegend); 2) CD49d (α4)-FITC, β7-APC, CCR9-PE (BD Biosciences) and CD29 (β1)–APC-Cy7 (BioLegend); 3) CD103-FITC, CD54-APC, CD49a (α1)-PE and CD29–APC-Cy7 (BioLegend); 4) CD18-APC, CLA-FITC (BD Biosciences) and CCR10-PE (BioLegend). Cells were acquired using a BD LSRFortessa SORP flow cytometer (Flow Cytometry Platform, IGTP) and analyzed with FlowJo 9.3.2 software (TreeStar). Gates were drawn based on fluorescence minus one-controls and isotypes, and CD3$^+$ CD4$^-$ phenotype was considered CD8$^+$ T cells.

Tissue processing and flow cytometry

Mouse spleen and iliac lymph nodes were harvested and a single-cell suspension prepared. Peripheral blood was collected by retro-orbital bleeding. Red blood cells were removed by ACK lysing buffer (Life Technologies). Leukocytes were washed with FACS buffer (PBS with 2% FBS) and stored on ice until use. Mouse genital tract were removed and leukocytes isolated as described [26]. Briefly, mouse genital tract (vagina, cervix, uterine horns, oviducts) were minced into small pieces, digested in 500mg/L collagenase IV (Sigma) for 1 hour at 37°C with constant stirring. Leukocytes were purified by percoll density gradient centrifugation (GE Healthcare), washed with FACS buffer and stored on ice until use.

Single cell suspensions from spleen, dLNs, blood and genital tract were prepared in FACS buffer and blocked with Fc block (culture supernatant from the 24G2 hybridoma, 2% mouse serum, 2%, rat serum, and 0.01% sodium azide). Cells were then stained with anti-CD11b,

PLOS ONE

Homing Molecules Associated with Vaginal Infection

F4/80 and B220-FITC together with MHCII PerCP-Cy5.5 (as dump channels), CD4-APC-eFluor780, CD8-Pacific Orange, CD44-Alexa 700 and CD11c-APC. All flow antibodies were obtained from eBiosciences. Samples were acquired on an LSRFortessa flow cytometer and analyzed using FlowJo software (TreeStar).

Statistical Analysis

Data are reported as the median and IQR for each animal group or cohort using Prism 4.0 software (GraphPad Software). Statistical analyses were performed by non-parametric Mann Whitney test to compare single time points between two groups (case *vs.* control) using SPSS software for Windows version 13.0 (Chicago, IL). P value of <0.05 was considered significant.

Accession codes

Microarray data presented in this article are deposited into the Gene Expression Omnibus (http://www.ncbi.nlm.nih.gov/geo/) under accession number GSE67147.

Results

Differentially expressed genes after genital tract infection in mice

To address the homing profile of T_{EM} cells shortly after vaginal infection, blood $CD3^+$ $CD62L^-$ $CD44^+$ T cells were sorted from *Chlamydia*-infected mice (VAG group) and sham-treated mice (control group) 7 days post-infection in a pilot experiment. After qualitative assessment of the sample RNA integrity and amplification, we chose three samples in each group that qualified for microarray analyses. We detected highly significant differences in genes involved in interferon signaling, synthesis of DNA, cell cycle and activation of the immune system between the two groups (Table 1). Regarding adhesion molecules, several chemokine receptors and integrin genes were significantly up-regulated in infected animals compared to the control group and the four most significant genes were selected for further validation: *Ccr5*, *Itgax*, *Cxcr6* and *Ccr2* (Fig 1).

Higher frequency of circulating $CD11c^+$ $CD8^+$ T cells is detected early after Chlamydia infection

In order to confirm the expression of these molecules, we analyzed a 10-color panel by flow cytometry at 7, 10 and 14 days post-infection. In general, the percentage of CCR2, CCR5, CXCR6 and CD11c (*Itgax*) in live $CD4^+$ or $CD4^-$ (putative $CD8^+$) T cells peaked 10 days after infection, when in most cases their total frequency was significantly higher than in the control group (S1 Fig). Of note, there was a significant increase in the frequency of T_{EM} cells ($CD62L^-$) in the VAG groups compared to control animals. While $CD4^+$ T cells only had a significant increase in the percentage of $CD44^+$ activated T_{EM} cells (S1e Fig), $CD8^+$ T cells demonstrated a significant increase in both, $CD44^+$ and $CD44^-$ subsets after infection (S1e and S1f Fig). When analyzing the expression of the selected homing molecules in the activated T_{EM} cell subset, there was a higher percentage of CCR5, CCR2 and CD11c in the $CD4^+$ $CD44^+$ T_{EM} cells at 10 and/or 14 days post-infection than in the control group (Fig 2a, 2g, 2e and 2c). In contrast, we detected a higher percentage of CXCR6 seven days after infection and of CD11c at all-time points in the $CD8^+$ $CD44^+$ T_{EM} cells compared to the control group (Fig 2e and 2g). Although expression of these markers was also increased in the non-activated fraction of both T_{EM} cell subsets, the magnitude of expression was much lower (Fig 2b, 2d, 2f and 2h). Thus, all the selected up-regulated genes were confirmed by protein expression. While CCR2 and CCR5

Table 1. Functions enriched among the top up-regulated genes in activated effector T cells from *Chlamydia*-infected vs. uninfected mouse samples with Canonical pathways.

Gene Set Name	# Genes in Gene Set (K)[a]	Description	# Genes in overlap (k)[b]	k/K[c]	FDR[d] q-value
REACTOME_SYNTHESIS_OF_DNA	92	Genes involved in Synthesis of DNA	7	0.0761	7.02E-05
REACTOME_INTERFERON_SIGNALING	159	Genes involved in Interferon Signaling	8	0.0503	7.02E-05
REACTOME_ANTIVIRAL_MECHANISM_BY_IFN_STIM._GENES	66	Genes involved in Antiviral mechanism by IFN-stimulated genes	6	0.0909	7.02E-05
REACTOME_S_PHASE	109	Genes involved in S Phase	7	0.0642	7.02E-05
REACTOME_IMMUNE_SYSTEM	933	Genes involved in Immune System	16	0.0171	1.33E-04
PID_TCPTP_PATHWAY	43	Signaling events mediated by TCPTP	5	0.1163	1.33E-04
REACTOME_CELL_CYCLE	421	Genes involved in Cell Cycle	11	0.0261	1.33E-04
REACTOME_CYTOKINE_SIGNALING_IN_IMMUNE_SYSTEM	270	Genes involved in Cytokine Signaling in Immune system	9	0.0333	1.69E-04
REACTOME_CELL_CYCLE_MITOTIC	325	Genes involved in Cell Cycle, Mitotic	9	0.0277	6.65E-04
REACTOME_DNA_STRAND_ELONGATION	30	Genes involved in DNA strand elongation	4	0.1333	6.65E-04
REACTOME_ACTIVATION_OF_THE_PRE_REPLICATIVE_COMPLEX	31	Genes involved in Activation of the pre-replicative complex	4	0.129	6.92E-04
REACTOME_DNA_REPLICATION	192	Genes involved in DNA Replication	7	0.0365	1.02E-03

[a] K indicates the number of genes in the set from MSigDB.
[b] k indicates the number of genes in the intersection of the query set with a set from MSigDB.
[c] k/K indicates the proportion of gene set genes present in the query set.
[d] FDR corresponds to false discovery rate.

doi:10.1371/journal.pone.0156605.t001

were only increased in the CD4$^+$ T$_{EM}$ cell subset after infection, expression of CXCR6 and CD11c was much more abundant in CD8$^+$ T$_{EM}$ cells.

CD11c expression increases in human circulating CD8$^+$ T$_{EM}$ during symptomatic vaginosis

We next addressed the expression of these and other potentially relevant mucosal homing molecules in peripheral blood T$_{EM}$ cells from healthy young women (ND) in comparison to women with psoriasis (PS), ulcerative colitis (UC) and BV. First, we analyzed the expression of the different molecules by CD4$^+$ and CD4$^-$ (putative CD8$^+$) T cells in CCR7$^-$ T$_{EM}$ cells from thirteen ND, as shown in the general gating strategy (Fig 3 and S2 Fig). All these molecules were also analyzed based on the activation markers included (CD38/HLA-DR) in order to detect associations between them. We observed a higher percentage of circulating CCR7$^-$ CD4$^+$ T cells expressing the CCR2, CCR9 and CCR10 chemokine receptors compared to CD8$^+$ T cells, while there was a higher percentage of circulating CD8$^+$ T$_{EM}$ cells expressing CCR5 and CXCR6 compared to CD4$^+$ T$_{EM}$ cells (Fig 4). Regarding integrins and other molecules, the frequency of α1β1, α4β7 and CLA was in general higher in CD4$^+$ T$_{EM}$ cells than in CD8$^+$, while the frequency of α4β1 and CD11c was higher in CD8$^+$ T$_{EM}$ cells (Fig 4). Finally, the frequency

Probe Set ID	Gene Symbol	Gene Title	Fold Change	P.Value	adj.P.Val
1422259_PM_a_at	Ccr5	chemokine (C-C motif) receptor 5	3.64	0.01	0.56
1419128_PM_at	Itgax	integrin alpha X	2.93	0.02	0.58
1422612_PM_at	Cxcr6	chemokine (C-X-C motif) receptor 6	2.62	0.01	0.56
1421188_PM_at	Ccr2	chemokine (C-C motif) receptor 2	2.46	0.00	0.54

Fig 1. Adhesion molecule related genes overexpressed in circulating activated T$_{EM}$ cells from vaginally *Chlamydia*-infected mice. Median centered log 2 intensity values derived from Affymetrix microarray hybridization experiments comparing non-infected control mice (n = 3, x symbol) vs. vaginally-infected mice (n = 3, • symbol) for the *Ccr5, Itgax, Cxcr6* and *Ccr2* genes are shown. Fold change: Average fold change of vaginally-infected vs. control mice. P value: Nominal p-value. Adj p val: false discovery rate adjusted p-value.

of CXCR3 did not show any differences between these subsets, while CD103 was only higher in the HLA-DR$^+$ fraction of circulating CCR7$^-$ CD4$^+$ T cells compared to CD8$^+$ T cells (S4 Fig).

Next we compared the expression of these adhesion molecules in ND with their expression in different mucosal and skin disorders. Of note, there was an overall decrease of the percentage of CD4$^+$ T cells in the different groups of patients that was only significant for the BV cohort (S5 Fig). When analyzing the T$_{EM}$ cell fractions, we detected a significant increase in at least one of the activation markers in each cohort, which denoted the pathological condition of the patients (Fig 5). The comparison on the expression of the different adhesion molecules was performed in the T$_{EM}$ cell fraction as a total (S6 Fig), as well as in each of the activated fractions (S7 and S8 Figs). The main findings in total fractions were a general decrease on the frequency of CCR2 in CD4$^+$ T$_{EM}$ cells and an increase on the frequency of CCR10 in CD8$^+$ T$_{EM}$ cells from all groups of patients (S6 Fig). Also, there was a significant increase on the percentage of α1β1 expression in CD4$^+$ T$_{EM}$ cells from the PS group and a decrease on the percentage of CLA in the same cells compared to ND (S6c Fig). The UC group presented an increase on the percentage of α1β1 expression in CD8$^+$ T$_{EM}$ cells (S6d Fig), while the BV group had an increase on CCR5 and α4β1 expression in CD4$^+$ T$_{EM}$ cells and of CD11c in CD8$^+$ T$_{EM}$ cells when compared to ND (S6 Fig).

Since activated T$_{EM}$ cells more likely contain specific T cells migrating towards the inflamed tissues [27], we focused on the differences detected in the double activated fraction (Fig 6). This way, the only significant changes within CD38$^+$ HLA-DR$^+$ T$_{EM}$ cells from the PS group compared to ND were: increased frequency of CCR9 in CD8 T$_{EM}$ cells, increased frequency of α1β1 in CD4$^+$ T$_{EM}$ cells, and a significant decrease of α4β1 and α4β7 in CD8$^+$ T$_{EM}$ cells
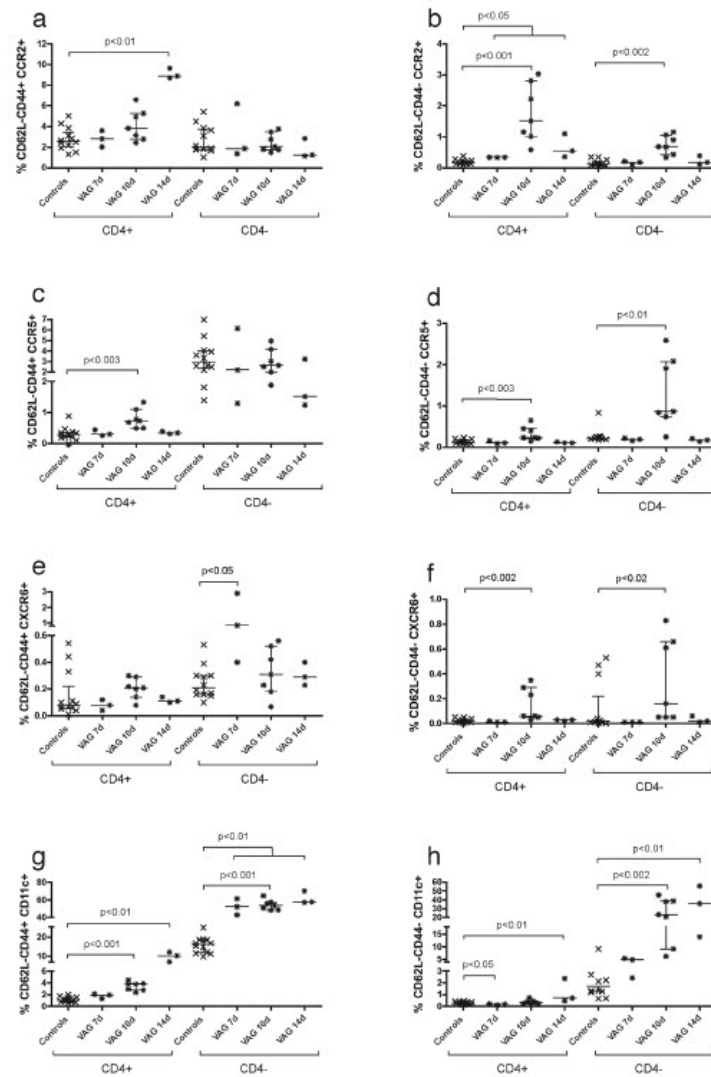
Fig 2. Kinetics of CCR2, CCR5, CXCR6 and CD11c frequency after vaginal *Chlamydia* infection in mice. The frequency of CCR5 (a, b), CCR2 (c, d), CXCR6 (e, f) and CD11c (g, h) was determined in activated CD44+ (left graphs) and CD44- (right graphs) effector memory T (T_EM) cells from blood by flow cytometry at 7, 10 and 14 days after vaginal infection with *C. muridarum* in mice. After gating on live CD3+ cells and CD4+ or CD4- (putative CD8+) T cells, the frequency of CCR5, CCR2, CXCR6 and CD11c was quantified in the CD62L-

CD44+/CD44- T cell subsets. Each time point represents the median ± interquartile range of three or seven infected animals and all controls (n = 12).

doi:10.1371/journal.pone.0156605.g002
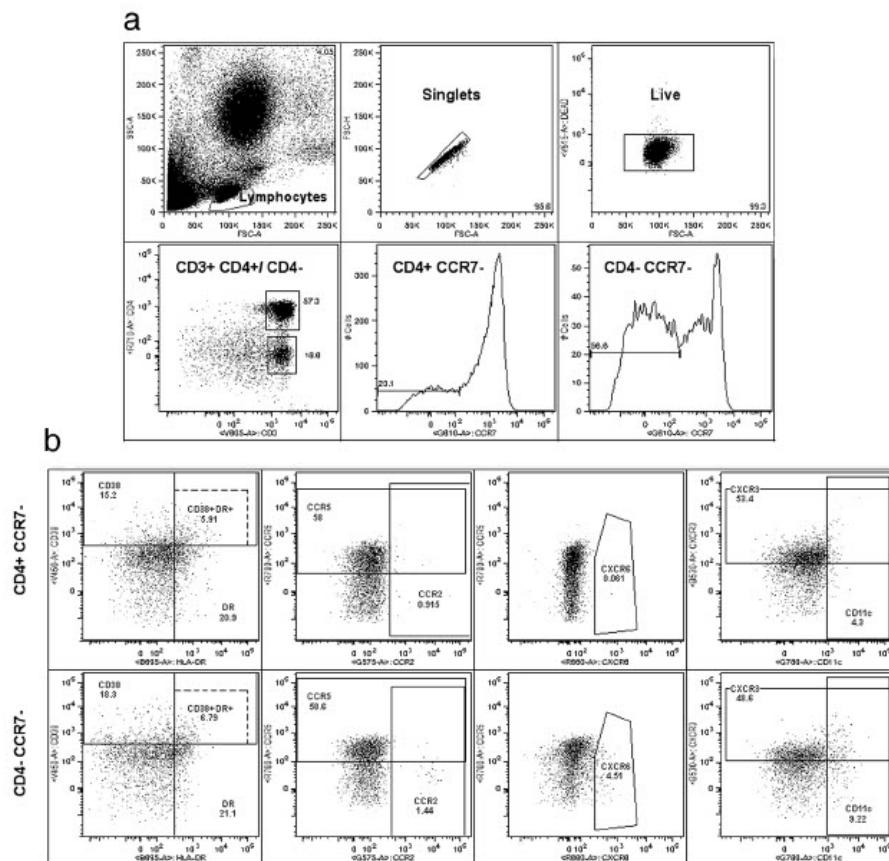
Fig 3. Gating strategy and representative plots of adhesion molecule analysis in circulating T$_{EM}$ cells from women. The overall gating strategy for a representative single normal donor is shown. (a) General gating strategy for effector memory T (T$_{EM}$) cells consist of the following consecutive gates: lymphocytes, singlets and live CD3+ T cells (top row); CD4+ and CD4- (putative CD8+) T cells, and the effector CCR7- fraction for each of these subsets (bottom row). (b) Representative plots of molecules analyzed in T$_{EM}$ cells in one of the panels are shown: activated CD38 and/or HLA-DR T$_{EM}$ cells, expression of CCR5 and CCR2, expression of CXCR6, and expression of CXCR3 and CD11c for CD4+ T$_{EM}$ cells (top row) and CD8+ T$_{EM}$ cells (bottom row). Isotype controls are shown in S3 Fig.

doi:10.1371/journal.pone.0156605.g003
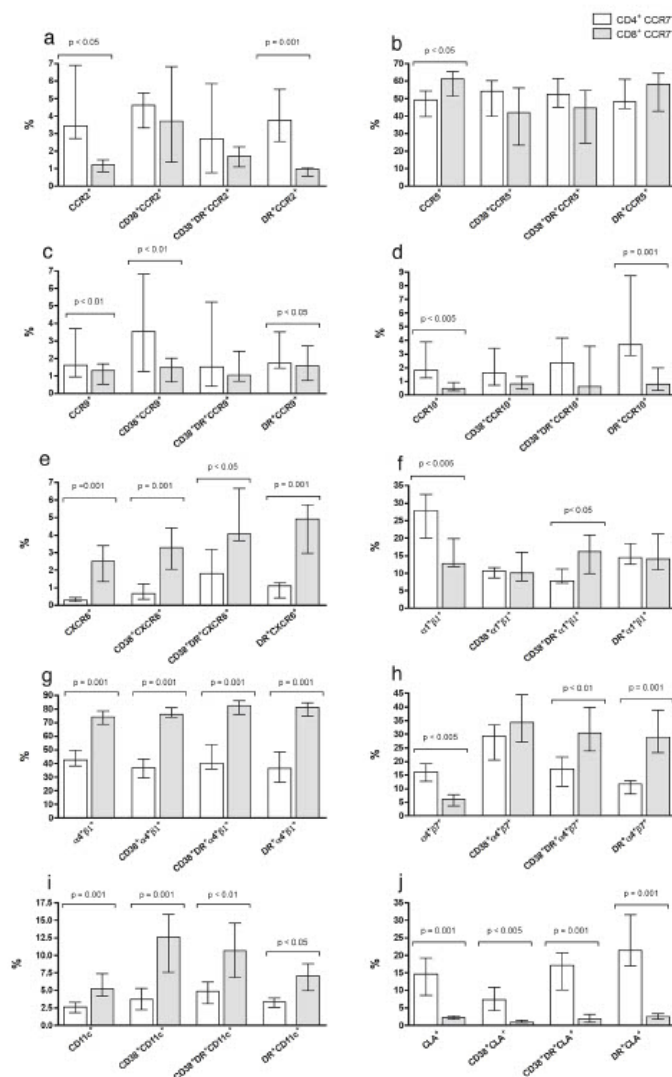
Fig 4. Comparison of adhesion molecule frequency in CD4 and CD8 T_{EM} cells from healthy women. A comparison between the frequency of (a) CCR5, (b) CCR2, (c) CCR9, (d) CCR10, (e) CXCR6, (f) α1β1, (g) α4β1, (h) α4β7, (i) CD11c and (j) CLA in CD4 (white bars) and CD8 (grey bars) effector memory T (T_{EM}) cells was determined by flow cytometry. The frequency of each molecule was analyzed in total CD3$^+$ T_{EM} cells and CD38$^+$, CD38$^+$ HLA-DR$^+$ or HLA-DR$^+$ activated fractions. General gating strategy is shown in Fig 3 and S2 Fig. Each bar represents the median ± interquartile range of the mean of healthy young women (n = 13).

doi:10.1371/journal.pone.0156605.g004
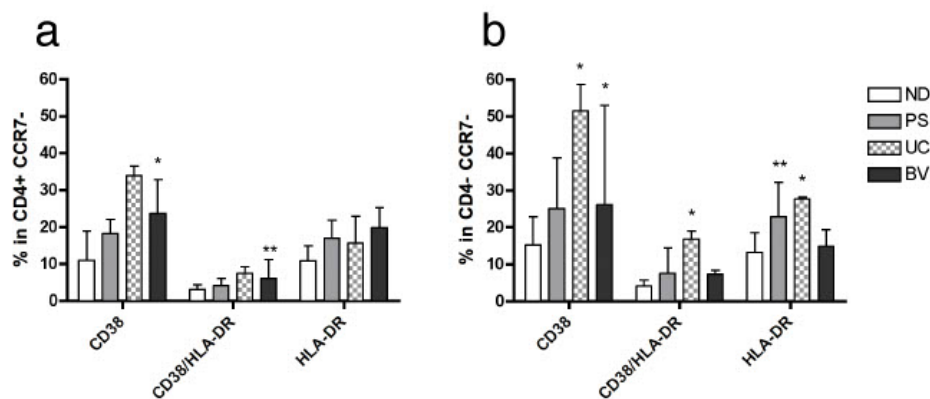
Fig 5. Comparison of activation markers frequency in T_EM cells from different conditions affecting women. The frequency of activated CD38^{+}, CD38^{+} HLA-DR^{+} or HLA-DR^{+} CD4^{+} (a) and CD8^{+} (b) effector memory T (T_EM) cells determined by flow cytometry is shown for normal donors (ND) and the different groups of patients. General gating strategy is shown in Fig 3 and S2 Fig. Each bar represents the median ± interquartile range of healthy young women (ND; white bars, n = 13), women with psoriasis (PS; grey bars, n = 5), ulcerative colitis (UC; checkered bars, n = 4) and bacterial vaginosis (BV; dark bars, n = 5). P values indicate: *<0.05; **<0.01.

doi:10.1371/journal.pone.0156605.g005

(Fig 6). In fact, the decrease of α4β7 in CD8^{+} T_EM cells was a general observation in all groups of patients (Fig 6d), which was predominantly significant in the CD38^{+} fraction (S7 Fig). UC group characteristic profile in CD38^{+} HLA-DR^{+} T_EM cells was an increase of α1β1 percentage in CD4^{+} T_EM cells (as occurred in the PS group) (Fig 6c). Lastly, the BV group shared the decrease in the percentage of α4β7 expression in CD8^{+} T_EM cells with the PS group. As for the unique features in BV patients, we detected higher frequency of CCR5 and α4β1 in CD4^{+} T_EM cells with a concomitant decrease in the frequency of α4β7 in these cells, and also exclusive high percentage of CD11c in CD8^{+} T_EM cells (Fig 6). In summary, increased expression of CCR5 and CD11c on CD4^{+} and CD8^{+} T_EM cells respectively was confirmed in women with symptomatic BV.

CD11c expression in blood after vaginal infection correlates with an increase in the genital tract but is not exclusive of infection in these tissues

Considering that CD11c was the most striking and novel marker of genital tract condition in both, mice and women, we performed additional experiments to address if this increase was exclusive of productive infection in these tissues or, in contrast, was a consequence of bacterial infection in general. Therefore, we performed a new set of animal experiments in which we included an intravenously (IV) *Chlamydia*-infected group. It is important to note that IV infection induces bacterial replication in different systemic and also mucosal tissues, including spleen and lung [21]. Interestingly, seven days post-infection the frequency of CD11c^{+} cells on blood T cells was much higher in the IV group (median: 13.1% [IQR: 10.9–16.3]) than in any other group (median: 1.51%, [IQR: 0.9–2.2] in the controls or median: 5.23% [IQR: 3.4–8.4] in the VAG group) (Fig 7). In the control and the VAG groups we obtained cell suspensions from the genital tract to determine the frequency of CD11c^{+} T cells. As shown (Fig 7), seven days after infection, the total frequency of CD3^{+} CD11c^{+} in genital tract increased from a median of

高
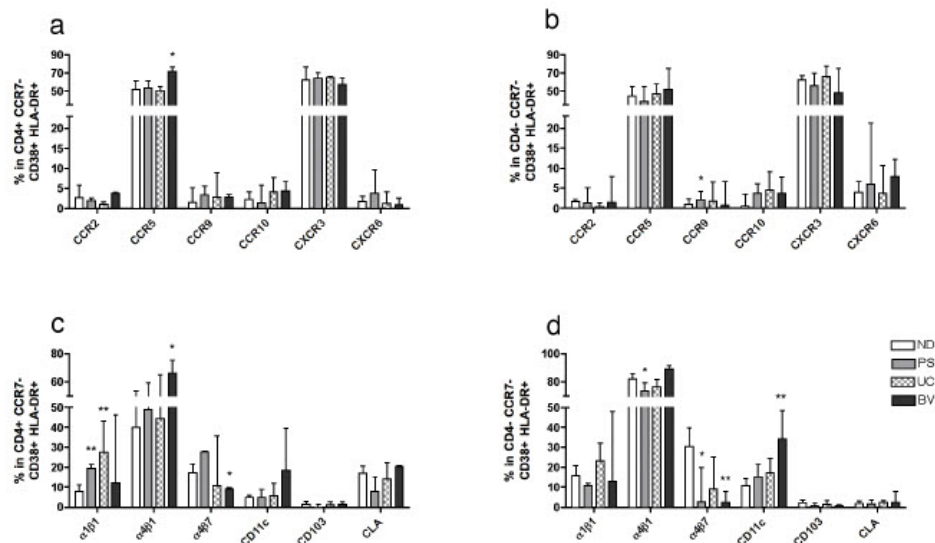
Fig 6. Frequency of adhesion molecules in CD38⁺ HLA-DR⁺ T$_{EM}$ cells from different conditions affecting women. Percentages of the expression of chemokine receptors in CD38⁺ HLA-DR⁺ (a) CD4⁺ effector memory T (T$_{EM}$) cells and (b) CD8⁺ T$_{EM}$ cells determined by flow cytometry are shown for normal donors (ND) and the different groups of patients. Percentages of the expression of integrins and other adhesion molecules in CD38⁺HLA-DR⁺ (c) CD4⁺ T$_{EM}$ and (d) CD8⁺ T$_{EM}$ cells determined by flow cytometry are shown for ND and the different groups of patients. General gating strategy is shown in Fig 3 and S2 Fig. Each bar represents the median ± interquartile range of healthy young women (ND; white bars, n = 13), women with psoriasis (PS; grey bars, n = 5), ulcerative colitis (UC; checkered bars, n = 4) and bacterial vaginosis (BV; dark bars, n = 5). P values indicate: *<0.05; **<0.01.

doi:10.1371/journal.pone.0156605.g006

0.46% [IQR: 0.28–0.74] in the control group to a median of 4.43% [IQR: 2.68–5.33] in the VAG group. Additional assessment of the expansion of CD11c⁺ CD44⁺ cells in different tissues, including spleen, draining lymph nodes (dLNs), blood and genital tract of the VAG infected animals 14 days post-infection demonstrated that most of these cells are CD8⁺ that expand in spleen, blood and, mainly, in the genital tract (Fig 8). This way, while CD11c⁺ CD44⁺ represented 0.37% [IQR: 0.47–0.85] of the CD4⁺ cells in spleen, 0.61% [IQR: 0.40–0.82] in dLNs, 0.83% [IQR: 0.17–0.41] in blood and 4.2% [IQR: 2.3–4.7] in genital tract of the VAG-infected mice, these CD11c⁺ CD44⁺ cells were more frequent in the CD8⁺ cell fraction from all these tissues: 6.4% [IQR: 6.3–10] in the spleen, 1.9% [IQR: 1.5–2.1] in the dLNs, 23% [IQR: 15–42] in blood and 53% [IQR: 46–53] in the genital tract. Thus, 7 and 14 days after infection, CD11c expression increases in the genital tract of mice correlating with the increase observed in blood. However, CD11c increased expression is not specific to infection in the genital tract, since systemic infection also expands this subset.

Discussion

We interrogated the expression of multiple adhesion molecules in circulating T$_{EM}$ cells from different groups of women with disorders affecting primarily peripheral tissues. We report for the first time that women with BV have higher frequency of CD8⁺ T$_{EM}$ expressing CD11c. This
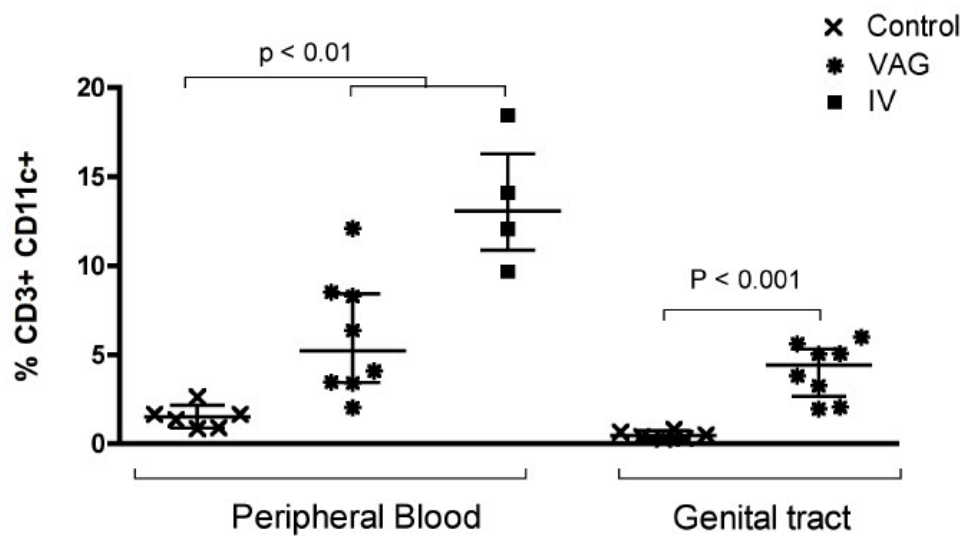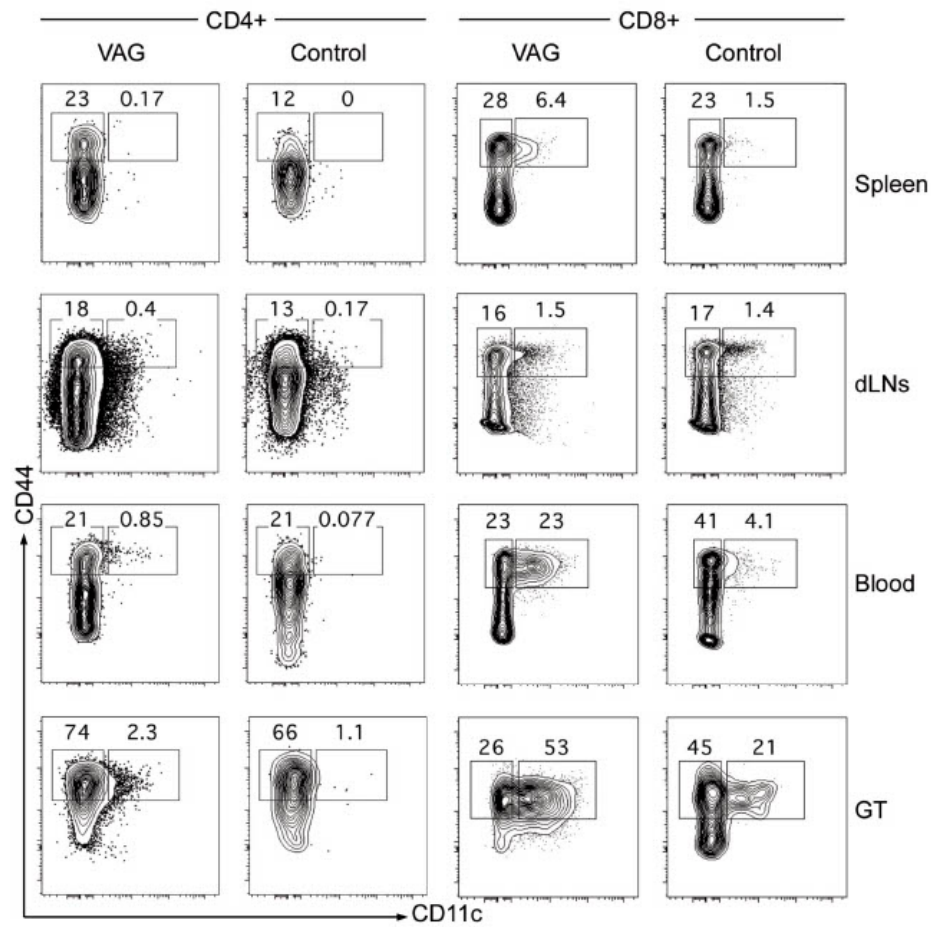
Fig 7. CD11c expression in T cells from blood and genital tract after vaginal or systemic *Chlamydia* infection. The frequency of CD11c in CD3⁺ T cells was determined by flow cytometry 7 days after vaginal (VAG) or intravenous (IV) infection with *C. muridarum* in blood or genital tract from mice. Each time point represents the median ± interquartile range of controls (n = 6), VAG-infected animals (n = 8) and IV-infected animals (n = 4).

doi:10.1371/journal.pone.0156605.g007

increase was not observed during inflammatory pathologies affecting the gastrointestinal tract or the skin. Importantly, we also detected an increase in CD11c gene and protein expression in a mouse model of *Chlamydia* reproductive tract infection in both, blood and genital tract. Other patterns of integrin and chemokine receptor expression were also observed in patients with BV. In particular, the expression of CCR5 and $\alpha 4\beta 1$ was increased in circulating CD4⁺ T_{EM} cells of these women compared to healthy donors.

The increased expression of CD11c in T_{EM} cell subsets soon after vaginal infection or during an episode of vaginosis was a strong and consistent finding in mice and women. Although the expression of CD11c has been classically used to identify dendritic cells, this α-chain integrin is also expressed in other myeloid cells, NK cells and populations of activated T and B cells [28]. Specifically within the activated T cell fraction, CD11c expression has been associated to effector and regulatory T cells in different mouse models [29–33], as well as with intraephitelial lymphocytes in the small gut [34, 35]. More recently, some authors have described the existence of a unique subset in mice and importantly, in humans, that combine key features of T and dendritic cells [36]. These cells are positive for T cell receptor, major histocompatibility complex II and CD11c⁺ and, regardless of their lymphocyte morphology, posses antigen presenting cell and innate-like properties [36]. However, to our knowledge, no specific report on expression of CD11c in human T cells in association to a mucosal condition has ever been published.

A considerable constraint in our study is the comparison between the cohorts evaluated. Although all these disorders have a clear Th1 component [37–39], they have very different

Fig 8. CD11c expression in activated CD4 /CD8 cells from different tissues after vaginal *Chlamydia* infection in mice. The frequency of CD44+ CD11c+ in CD4+ (left panels) and CD8+ cells (right panels) was determined by flow cytometry 14 days after vaginal (VAG) infection with *C. muridarum* in spleen, draining lymph nodes (dLNs), blood and genital tract (GT) from mice. Examples from one infected and one control animal are shown.

doi:10.1371/journal.pone.0156605.g008

origins and associated inflammation, and no other mucosal disorder with a bacterial component could be compared to the BV group. This fact, the *Chlamydia* systemic infection experiment results (Fig 7) and supporting animal models that demonstrate CD11c expression in T cells after systemic vaccination and infection [29–33], indicates that CD11c expression is not specific to genital tract infection, rather indicative of activation and recirculation in general.

Moreover, there was a trend towards higher percentage of CD11c$^+$ in T cells from patients with UC that was significant in the HLA-DR fraction (S8 Fig). Although we acknowledge the limitation of the sample size for the cohorts included in the study, the present results represent a unique comparison between peripheral tissue alterations that provide adhesion molecules of interest for each of the different disorders to further explore. In any case, this is the first report demonstrating enhanced CD11c expression in CD8$^+$ T$_{EM}$ cells after intravaginal *Chlamydia* infection in mice and symptomatic BV in women, and we are currently working on defining the phenotype and role of these cells in these models.

The differential expression of certain adhesion molecules can induce a site-dependent homing profile that may work together with some other generic signals (such as CXCR3, CCR3, CCR5 and CCR6) [10]. Previous studies have examined adhesion molecules necessary for homing to the upper genital tract in a mouse model of *C. trachomatis* infection by directly infecting the uterine horns [14, 40]. In this model, CXCR3, CCR5 and α4β1 are required for homing of protective T cells to the murine upper genital tract [14, 40]. Interestingly, samples from women with symptomatic BV, confirmed two of these molecules as potentially involved in FGT homing in humans. The frequency of integrin α4β1 was indeed up regulated in CD4$^+$ T$_{EM}$ cells, which correlates with high expression of this integrin in the genital mucosa of women [41]. Moreover, BV patients did also showed a higher percentage of CCR5 expression in their CD4$^+$ T$_{EM}$ cells compared to ND, indicating that CCR5 might indeed be necessary for FGT homing as suggested [40]. Asymptomatic genital HSV-2 infection is also associated with increased expression of CCR5 by endocervical CD4$^+$ T cells and similar trends were observed in circulating CD4$^+$ T cells [18]. Further, a live-attenuated vaccine that continuously replicates in systemic and mucosal tissues in macaques also induces increased frequency of peripheral CD4$^+$ T cells expressing CCR5, and the two animals with the highest percentage of this population had the highest number of specific T cells in the genital tract [42]. However, a recent report on the effect of vaginal immunization in women showed a clear down-regulation of CCR5 on CD4$^+$ T cells after immunization [43]. Nevertheless, the first time-point analyzed in that study was 4 weeks post-immunization, when major recirculation and infiltration of T cells may have already occurred [12]. Of great importance is the fact that this increment is detected in the CD4$^+$ T$_{EM}$ cell population, since CCR5 is a co-receptor for HIV and thus could have highly detrimental effects favoring HIV infection susceptibility [44, 45]. If higher numbers of CCR5 expressing CD4$^+$ T$_{EM}$ cells are indeed infiltrated in the genital tissue during BV episodes, this could partially explain its association with higher risk of HIV-1 acquisition [46].

Finally, while CLA expression in total CD4$^+$ T$_{EM}$ cells of the PS group was unexpectedly reduced compared to ND (S1c Fig), we detected higher frequency of CLA on CD8$^+$ HLA-DR$^+$ T$_{EM}$ cells from the BV group (S8d Fig). Due to their migration to skin, the number of CLA$^+$ T cells in the periphery decreases inversely to disease severity during acute psoriasis [47]. Further, CLA interacts with E-selectin expressed on venular endothelial cells not only from inflamed skin, but also from oral mucosa and FGT, and genital HSV-specific CD8$^+$ T cells in the peripheral blood express high levels of CLA [16, 19]. Yet α4β7, another molecule described in asymptomatic HSV-2-infected patients but not in uninfected patients [18], was down regulated in activated T$_{EM}$ cells from BV patients (Fig 6). While this decrease could also indicate selective infiltration of these cells into the infected tissues early after infection, the existence of a mechanism that would actually down-regulate some of these molecules cannot be discarded.

Many properties that enable T cells to traffic to specific locations are programmed during the early stages of the infection [11]. Thus, in order to understand the homing patterns and dynamics of the mucosal response associated to vaccination and infection, we need to analyze specific and activated T cells responses early after activation [4, 12]. In summary, in this study we define adhesion molecules, namely CCR5, α4β1 and CD11c, which may be desirable to

induce in order to generate an effective mucosal response in vaccine candidates against STI. Special attention should be given to CD11c as a novel marker of T cell mucosal immunity in response to genital tract disorders.

Supporting Information

S1 Fig. Kinetics of the frequency of adhesion molecules and effector T cells after vaginal infection in mice. The frequency of CCR5 (a), CCR2 (b), CXCR6 (c), CD11c (d), $CD62L^-$ $CD44^+$ (e) and $CD62L^-$ $CD44^-$ (f) was determined in T cells from blood by flow cytometry at 7, 10 and 14 days after vaginal infection with *C. muridarum* in mice. After gating on live $CD3^+$ cells and $CD4^+$ or $CD4^-$ (putative $CD8^+$) T cells, the frequency of CCR5, CCR2, CXCR6, CD11c, $CD62L^-$ $CD44^+$ and $CD62L^-$ $CD44^-$ was quantified. Each time point represents the median ± interquartile range of three or seven infected animals and all controls (n = 12). (TIF)

S2 Fig. Representative plots of adhesion molecule analysis in circulating T_{EM} cells from women. The overall gating strategy for a representative single normal donor is shown in Fig 3. Representative plots of molecules analyzed in T_{EM} cells in each of the panels are shown for $CD4^+$ T_{EM} cells (top row) and $CD8^+$ T_{EM} cells (bottom row): (a) expression of CCR9, α4 and β7; (b) expression of α1, β1 and CD103 and (c) expression of CCR10 and CLA. Isotype controls are shown in S3 Fig. (TIF)

S3 Fig. Isotype controls for the molecules analyzed in circulating $CD4^-$ T_{EM} cells from women. The cut-off determined by the isotype control for each adhesion or activation molecule analyzed is shown in zebra plots for the $CD4^-$ $CCR7^-$ T cells. (TIF)

S4 Fig. Comparison of CXCR3 and CD103 frequencies in CD4 and CD8 T_{EM} cells from healthy women. A comparison between the frequency of (a) CXCR3 and (b) CD103 in CD4 (white bars) and CD8 (grey bars) effector memory T (T_{EM}) cells was determined by flow cytometry. The frequency of each molecule was analyzed in total $CD3^+$ T_{EM} cells and $CD38^+$, $CD38^+$ $HLA-DR^+$ or $HLA-DR^+$ activated fractions. General gating strategy is shown in Fig 3 and S2 Fig. Each bar represents the median ± interquartile range of healthy young women (n = 13). (TIF)

S5 Fig. Frequency of $CD4^+$ T cells during different conditions affecting peripheral tissues in women. The percentage of $CD4^+$ T cells determined by flow cytometry is shown for ND and the different groups of patients. General gating strategy is shown in Fig 3. Each bar represents the median ± interquartile range of healthy young women (ND; white bars, n = 13), women with psoriasis (PS; grey bars, n = 5), ulcerative colitis (UC; checkered bars, n = 4) and bacterial vaginosis (BV; dark bars, n = 5). P value indicates: * <0.05. (TIF)

S6 Fig. Frequency of adhesion molecules in T_{EM} cells from different conditions affecting women. Percentages of the expression of chemokine receptors in total (a) $CD4^+$ effector memory T (T_{EM}) cells and (b) $CD8^+$ T_{EM} cells determined by flow cytometry are shown for normal donors (ND) and the different groups of patients. Percentages of the expression of integrins and other adhesion molecules in total (c) $CD4^+$ T_{EM} and (d) $CD8^+$ T_{EM} cells determined by flow cytometry is shown for ND and the different groups of patients. General gating strategy is shown in Fig 3 and S2 Fig. Each bar represents the median ± interquartile range of healthy

young women (ND; white bars, n = 13), women with psoriasis (PS; grey bars, n = 5), ulcerative colitis (UC; checkered bars, n = 4) and bacterial vaginosis (BV; dark bars, n = 5). P values indicate: $^*<0.05$; $^{**}<0.01$; $^{***}<0.001$.
(TIF)

S7 Fig. Frequency of adhesion molecules in CD38$^+$ T$_{EM}$ cells from different conditions affecting women. Percentages of the expression of chemokine receptors in CD38$^+$ (a) CD4$^+$ effector memory T (T$_{EM}$) cells and (b) CD8$^+$ T$_{EM}$ cells determined by flow cytometry are shown for normal donors (ND) and the different groups of patients. Percentages of the expression of integrins and other adhesion molecules in CD38$^+$ (c) CD4$^+$ T$_{EM}$ and (d) CD8$^+$ T$_{EM}$ cells determined by flow cytometry are shown for ND and the different groups of patients. General gating strategy is shown in Fig 3 and S2 Fig. Each bar represents the median ± interquartile range of healthy young women (ND; white bars, n = 13), women with psoriasis (PS; grey bars, n = 5), ulcerative colitis (UC; checkered bars, n = 4) and bacterial vaginosis (BV; dark bars, n = 5). P values indicate: $^*<0.05$; $^{**}<0.01$; $^{***}<0.001$.
(TIF)

S8 Fig. Frequency of adhesion molecules in HLA-DR$^+$ T$_{EM}$ cells from different conditions affecting women. Percentages of the expression of chemokine receptors in HLA-DR$^+$ (a) CD4$^+$ effector memory T (T$_{EM}$) cells and (b) CD8$^+$ T$_{EM}$ cells determined by flow cytometry are shown for normal donors (ND) and the different groups of patients. Percentages of the expression of integrins and other adhesion molecules in HLA-DR$^+$ (c) CD4$^+$ T$_{EM}$ and (d) CD8$^+$ T$_{EM}$ cells determined by flow cytometry are shown for ND and the different groups of patients. General gating strategy is shown in Fig 3 and S2 Fig. Each bar represents the median ± interquartile range of healthy young women (ND; white bars, n = 13), women with psoriasis (PS; grey bars, n = 5), ulcerative colitis (UC; checkered bars, n = 4) and bacterial vaginosis (BV; dark bars, n = 5). P values indicate: $^*<0.05$; $^{**}<0.01$; $^{***}<0.001$.
(TIF)

Acknowledgments

Author Contributions

Conceived and designed the experiments: JQ LL SJM MG. Performed the experiments: JQ LL JC GR MG. Analyzed the data: JQ JC LL LS MG. Contributed reagents/materials/analysis tools: JMC EC OD. Wrote the paper: JQ JC LL SJM MG.

References

1. Lewis DA, Latif AS, Ndowa F. WHO global strategy for the prevention and control of sexually transmitted infections: time for action. Sexually transmitted infections. 2007; 83(7):508–9. doi: 10.1136/sti. 2007.028142 PMID: 18024710; PubMed Central PMCID: PMC2598641.

2. Ghosh M, Fahey JV, Shen Z, Lahey T, Cu-Uvin S, Wu Z, et al. Anti-HIV activity in cervical-vaginal secretions from HIV-positive and -negative women correlate with innate antimicrobial levels and IgG antibodies. PLoS One. 2010; 5(6):e11366. Epub 2010/07/09. doi: 10.1371/journal.pone.0011366 PMID: 20614007; PubMed Central PMCID: PMC2894072.

PLOS ONE

Homing Molecules Associated with Vaginal Infection

3. Genesca M. Characterization of an Effective CTL Response against HIV and SIV Infections. J Biomed Biotechnol. 2011; 2011:103924. Epub 2011/10/07. doi: 10.1155/2011/103924 PMID: 21976964; PubMed Central PMCID: PMC3184421.

4. Iwasaki A. Antiviral immune responses in the genital tract: clues for vaccines. Nat Rev Immunol. 2010; 10(10):699–711. Epub 2010/09/11. nri2836 [pii]doi: 10.1038/nri2836 PMID: 20829886.

5. Miyairi I, Ramsey KH, Patton DL. Duration of untreated chlamydial genital infection and factors associated with clearance: review of animal studies. J Infect Dis. 2010; 201 Suppl 2:S96–103. Epub 2010/05/28. doi: 10.1086/652393 PMID: 20470047.

6. Ficarra M, Ibana JS, Poretta C, Ma L, Myers L, Taylor SN, et al. A distinct cellular profile is seen in the human endocervix during Chlamydia trachomatis infection. Am J Reprod Immunol. 2008; 60(5):415–25. Epub 2008/09/19. AJI639 [pii]doi: 10.1111/j.1600-0897.2008.00639.x PMID: 18798835; PubMed Central PMCID: PMC2574558.

7. Genesca M, Skinner PJ, Hong JJ, Li J, Lu D, McChesney MB, et al. With minimal systemic T-cell expansion, CD8+ T Cells mediate protection of rhesus macaques immunized with attenuated simian-human immunodeficiency virus SHIV89.6 from vaginal challenge with simian immunodeficiency virus. J Virol. 2008; 82(22):11181–96. Epub 2008/09/13. JVI.01433-08 [pii]doi: 10.1128/JVI.01433-08 PMID: 18787003; PubMed Central PMCID: PMC2573271.

8. Marelli-Berg FM, Fu H, Vianello F, Tokoyoda K, Hamann A. Memory T-cell trafficking: new directions for busy commuters. Immunology. 2010; 130(2):158–65. Epub 2010/04/23. IMM3278 [pii]doi: 10.1111/j.1365-2567.2010.03278.x PMID: 20408895; PubMed Central PMCID: PMC2878460.

9. Agace WW. Tissue-tropic effector T cells: generation and targeting opportunities. Nature reviews Immunology. 2006; 6(9):682–92. Epub 2006/08/26. doi: 10.1038/nri1869 PMID: 16932753.

10. Ferguson AR, Engelhard VH. CD8 T cells activated in distinct lymphoid organs differentially express adhesion proteins and coexpress multiple chemokine receptors. J Immunol. 2010; 184(8):4079–86. Epub 2010/03/10. jimmunol.0901903 [pii]doi: 10.4049/jimmunol.0901903 PMID: 20212096; PubMed Central PMCID: PMC2887738.

11. Cauley LS, Lefrancois L. Guarding the perimeter: protection of the mucosa by tissue-resident memory T cells. Mucosal Immunol. 2013; 6(1):14–23. Epub 2012/11/08. mi201296 [pii]doi: 10.1038/mi.2012.96 PMID: 23131785.

12. Masopust D, Choo D, Vezys V, Wherry EJ, Duraiswamy J, Akondy R, et al. Dynamic T cell migration program provides resident memory within intestinal epithelium. J Exp Med. 2010; 207(3):553–64. Epub 2010/02/17. jem.20090858 [pii]doi: 10.1084/jem.20090858 PMID: 20156972; PubMed Central PMCID: PMC2839151.

13. Kelly KA, Chan AM, Butch A, Darville T. Two Different Homing Pathways Involving Integrin beta7 and E-selectin Significantly Influence Trafficking of CD4 Cells to the Genital Tract Following Chlamydia muridarum Infection. Am J Reprod Immunol. 2009. Epub 2009/04/28. AJI704 [pii]doi: 10.1111/j.1600-0897.2009.00704.x PMID: 19392981; PubMed Central PMCID: PMC2888875.

14. Davila SJ, Olive AJ, Starnbach MN. Integrin alpha4beta1 is necessary for CD4+ T cell-mediated protection against genital Chlamydia trachomatis infection. J Immunol. 2014; 192(9):4284–93. doi: 10.4049/jimmunol.1303238 PMID: 24659687; PubMed Central PMCID: PMC3995848.

15. Goodsell A, Zhou F, Gupta S, Singh M, Malyala P, Kazzaz J, et al. Beta7-integrin-independent enhancement of mucosal and systemic anti-HIV antibody responses following combined mucosal and systemic gene delivery. Immunology. 2008; 123(3):378–89. Epub 2007/10/20. IMM2702 [pii]doi: 10.1111/j.1365-2567.2007.02702.x PMID: 17944930; PubMed Central PMCID: PMC2433338.

16. Johansson EL, Rudin A, Wassen L, Holmgren J. Distribution of lymphocytes and adhesion molecules in human cervix and vagina. Immunology. 1999; 96:272–7. PMID: 10233705.

17. Youn H, Hong K, Yoo JW, Lee CH. ICAM-1 expression in vaginal cells as a potential biomarker for inflammatory response. Biomarkers. 2008; 13(3):257–69. Epub 2008/04/17. 789981735 [pii]doi: 10.1080/13547500701843338 PMID: 18415799.

18. Shannon B, Yi TJ, Thomas-Pavanel J, Chieza L, Janakiram P, Saunders M, et al. Impact of asymptomatic herpes simplex virus type 2 infection on mucosal homing and immune cell subsets in the blood and female genital tract. J Immunol. 2014; 192(11):5074–82. doi: 10.4049/jimmunol.1302916 PMID: 24760150.

19. Koelle DM, Liu Z, McClurkan CM, Topp MS, Riddell SR, Pamer EG, et al. Expression of cutaneous lymphocyte-associated antigen by CD8(+) T cells specific for a skin-tropic virus. J Clin Invest. 2002; 110(4):537–48. doi: 10.1172/JCI15537 PMID: 12189248; PubMed Central PMCID: PMC150419.

20. Scidmore MA. Cultivation and Laboratory Maintenance of Chlamydia trachomatis. Current protocols in microbiology. 2005; Chapter 11:Unit 11A 1. doi: 10.1002/9780471729259.mc11a01s00 PMID: 18770550.

PLOS | ONE

21. Li LX, McSorley SJ. B cells enhance antigen-specific CD4 T cell priming and prevent bacteria dissemination following Chlamydia muridarum genital tract infection. PLoS pathogens. 2013; 9(10):e1003707. doi: 10.1371/journal.ppat.1003707 PMID: 24204262; PubMed Central PMCID: PMC3814678.

22. Smyth GK. Limma: linear models for microarray data. In: Gentleman R, Carey V, Dudoit S, Irizarry R, Huber W, editors. Bioinformatics and Computational Biology Solutions Using R and Bioconductor. New York: Springer; 2005. p. 397–420.

23. Subramanian A, Tamayo P, Mootha VK, Mukherjee S, Ebert BL, Gillette MA, et al. Gene set enrichment analysis: a knowledge-based approach for interpreting genome-wide expression profiles. Proc Natl Acad Sci U S A. 2005; 102(43):15545–50. doi: 10.1073/pnas.0506580102 PMID: 16199517; PubMed Central PMCID: PMC1239896.

24. Silverberg MS, Satsangi J, Ahmad T, Arnott ID, Bernstein CN, Brant SR, et al. Toward an integrated clinical, molecular and serological classification of inflammatory bowel disease: report of a Working Party of the 2005 Montreal World Congress of Gastroenterology. Canadian journal of gastroenterology = Journal canadien de gastroenterologie. 2005; 19 Suppl A:5A–36A. PMID: 16151544.

25. Schroeder KW, Tremaine WJ, Ilstrup DM. Coated oral 5-aminosalicylic acid therapy for mildly to moderately active ulcerative colitis. A randomized study. N Engl J Med. 1987; 317(26):1625–9. doi: 10.1056/NEJM198712243172603 PMID: 3317057.

26. Schenkel JM, Fraser KA, Vezys V, Masopust D. Sensing and alarm function of resident memory CD8 (+) T cells. Nat Immunol. 2013; 14(5):509–13. doi: 10.1038/ni.2568 PMID: 23542740; PubMed Central PMCID: PMC3631432.

27. Adekambi T, Ibegbu CC, Cagle S, Kalokhe AS, Wang YF, Hu Y, et al. Biomarkers on patient T cells diagnose active tuberculosis and monitor treatment response. J Clin Invest. 2015; 125(5):1827–38. doi: 10.1172/JCI77990 PMID: 25822019.

28. Tan SM. The leucocyte beta2 (CD18) integrins: the structure, functional regulation and signalling properties. Bioscience reports. 2012; 32(3):241–69. doi: 10.1042/BSR20110101 PMID: 22458844.

29. Kubota K, Kadoya Y. Innate IFN-gamma-producing cells in the spleen of mice early after Listeria monocytogenes infection: importance of microenvironment of the cells involved in the production of innate IFN-gamma. Front Immunol. 2011; 2:26. Epub 2011/01/01. doi: 10.3389/fimmu.2011.00026 PMID: 22566816; PubMed Central PMCID: PMC3341966.

30. Cooney LA, Gupta M, Thomas S, Mikolajczak S, Choi KY, Gibson C, et al. Short-lived effector CD8 T cells induced by genetically attenuated malaria parasite vaccination express CD11c. Infect Immun. 2013; 81(11):4171–81. Epub 2013/08/28. IAI.00871-13 [pii]doi: 10.1128/IAI.00871-13 PMID: 23980113; PubMed Central PMCID: PMC3811835.

31. Beyer M, Wang H, Peters N, Doths S, Koerner-Rettberg C, Openshaw PJ, et al. The beta2 integrin CD11c distinguishes a subset of cytotoxic pulmonary T cells with potent antiviral effects in vitro and in vivo. Respir Res. 2005; 6:70. Epub 2005/07/14. 1465-9921-6-70 [pii]doi: 10.1186/1465-9921-6-70 PMID: 16011799; PubMed Central PMCID: PMC1184101.

32. Chen Z, Han Y, Gu Y, Liu Y, Jiang Z, Zhang M, et al. CD11c(high)CD8+ regulatory T cell feedback inhibits CD4 T cell immune response via Fas ligand-Fas pathway. J Immunol. 2013; 190(12):6145–54. Epub 2013/05/17. jimmunol.1300060 [pii]doi: 10.4049/jimmunol.1300060 PMID: 23677464.

33. Fujiwara D, Chen L, Wei B, Braun J. Small intestine CD11c+ CD8+ T cells suppress CD4+ T cell-induced immune colitis. Am J Physiol Gastrointest Liver Physiol. 2011; 300(6):G939–47. Epub 2011/03/26. ajpgi.00032.2010 [pii]doi: 10.1152/ajpgi.00032.2010 PMID: 21436319; PubMed Central PMCID: PMC3119121.

34. Egan CE, Craven MD, Leng J, Mack M, Simpson KW, Denkers EY. CCR2-dependent intraepithelial lymphocytes mediate inflammatory gut pathology during Toxoplasma gondii infection. Mucosal Immunol. 2009; 2(6):527–35. doi: 10.1038/mi.2009.105 PMID: 19741601; PubMed Central PMCID: PMC2860785.

35. Huleatt JW, Lefrancois L. Antigen-driven induction of CD11c on intestinal intraepithelial lymphocytes and CD8+ T cells in vivo. J Immunol. 1995; 154(11):5684–93. PMID: 7751620.

36. Kuka M, Munitic I, Ashwell JD. Identification and characterization of polyclonal alphabeta-T cells with dendritic cell properties. Nature communications. 2012; 3:1223. doi: 10.1038/ncomms2223 PMID: 23187623; PubMed Central PMCID: PMC3528357.

37. Puleston J, Cooper M, Murch S, Bid K, Makh S, Ashwood P, et al. A distinct subset of chemokines dominates the mucosal chemokine response in inflammatory bowel disease. Alimentary pharmacology & therapeutics. 2005; 21(2):109–20. doi: 10.1111/j.1365-2036.2004.02262.x PMID: 15679760.

38. Teraki Y, Miyake A, Takebayashi R, Shiohara T. Homing receptor and chemokine receptor on intraepidermal T cells in psoriasis vulgaris. Clinical and experimental dermatology. 2004; 29(6):658–63. doi: 10.1111/j.1365-2230.2004.01638.x PMID: 15550147.

PLOS | ONE

39. Anton G, Rid J, Mylonas I, Friese K, Weissenbacher ER. Evidence of a TH1-shift of local vaginal inflammatory response during bacterial vaginosis. Infection. 2008; 36(2):147–52. doi: 10.1007/s15010-007-7152-2 PMID: 18330506.

40. Olive AJ, Gondek DC, Starnbach MN. CXCR3 and CCR5 are both required for T cell-mediated protection against C. trachomatis infection in the murine genital mucosa. Mucosal Immunol. 2011; 4(2):208–16. Epub 2010/09/17. mi201058 [pii]doi: 10.1038/mi.2010.58 PMID: 20844481; PubMed Central PMCID: PMC3010299.

41. Hladik F, Lentz G, Delpit E, McElroy A, McElrath MJ. Coexpression of CCR5 and IL-2 in human genital but not blood T cells: implications for the ontogeny of the CCR5+ Th1 phenotype. J Immunol. 1999; 163 (4):2306–13. PMID: 10438976.

42. Genesca M, Skinner PJ, Bost KM, Lu D, Wang Y, Rourke TL, et al. Protective attenuated lentivirus immunization induces SIV-specific T cells in the genital tract of rhesus monkeys. Mucosal Immunol. 2008; 1(3):219–28. doi: 10.1038/mi.2008.6 PMID: 19079181; PubMed Central PMCID: PMC3401012.

43. Lewis DJ, Wang Y, Huo Z, Giemza R, Babaahmady K, Rahman D, et al. Effect of vaginal immunization with HIVgp140 and HSP70 on HIV-1 replication and innate and T cell adaptive immunity in women. J Virol. 2014; 88(20):11648–57. doi: 10.1128/JVI.01621-14 PMID: 25008917; PubMed Central PMCID: PMC4178755.

44. Hladik F, Sakchalathorn P, Ballweber L, Lentz G, Fialkow M, Eschenbach D, et al. Initial events in establishing vaginal entry and infection by human immunodeficiency virus type-1. Immunity. 2007; 26 (2):257–70. doi: 10.1016/j.immuni.2007.01.007 PMID: 17306567; PubMed Central PMCID: PMC1885958.

45. Joag VR, McKinnon LR, Liu J, Kidane ST, Yudin MH, Nyanga B, et al. Identification of preferential CD4 (+) T-cell targets for HIV infection in the cervix. Mucosal Immunol. 2016; 9(1):1–12. doi: 10.1038/mi.2015.28 PMID: 25872482.

46. Mitchell C, Marrazzo J. Bacterial vaginosis and the cervicovaginal immune response. Am J Reprod Immunol. 2014; 71(6):555–63. doi: 10.1111/aji.12264 PMID: 24832618; PubMed Central PMCID: PMC4128638.

47. Ferran M, Gimenez-Arnau AM, Bellosillo B, Pujol RM, Santamaria-Babi LF. Circulating CLA+ T cell subsets inversely correlate with disease severity and extension in acute psoriasis but not in chronic plaque psoriasis. European journal of dermatology: EJD. 2008; 18(6):647–50. doi: 10.1684/ejd.2008.0513 PMID: 18955198.

PLOS ONE

Expression of CD11c Is Associated with Unconventional Activated T Cell Subsets with High Migratory Potential

Jamal Qualai[1☉], Lin-Xi Li[2☉], Jon Cantero[1], Antoni Tarrats[3], Marco Antonio Fernández[4], Lauro Sumoy[5], Annie Rodolosse[6], Stephen J. McSorley[7], Meritxell Genescà[1*]

1 Mucosal Immunology Unit, Institut d'Investigació en Ciències de la Salut Germans Trias i Pujol, AIDS Research Institute IrsiCaixa-HIVACAT, Can Ruti Campus, Badalona, Spain, 2 Department of Microbiology and Immunology, University of Arkansas for Medical Sciences, Little Rock, Arkansas, United States of America, 3 Department of Obstetrics and Gynecology, University Hospital "Germans Trias i Pujol," Can Ruti Campus, Badalona, Spain, 4 Flow Cytometry Unit, Institut d'Investigació en Ciències de la Salut Germans Trias i Pujol, Badalona, Spain, 5 Genomics and Bioinformatics Group, Institute for Predictive and Personalized Medicine of Cancer (IMPPC), Can Ruti Campus, Badalona, Spain, 6 Functional Genomics Core, Institute for Research in Biomedicine (IRB Barcelona), Barcelona, Spain, 7 Center for Comparative Medicine, Department of Anatomy, Physiology and Cell Biology, School of Veterinary Medicine, University of California, Davis, California, United States of America

☉ These authors contributed equally to this work.
* mgenesca@igtp.cat

Abstract

CD11c is an α integrin classically employed to define myeloid dendritic cells. Although there is little information about CD11c expression on human T cells, mouse models have shown an association of CD11c expression with functionally relevant T cell subsets. In the context of genital tract infection, we have previously observed increased expression of CD11c in circulating T cells from mice and women. Microarray analyses of activated effector T cells expressing CD11c derived from naïve mice demonstrated enrichment for natural killer (NK) associated genes. Here we find that murine CD11c+ T cells analyzed by flow cytometry display markers associated with non-conventional T cell subsets, including γδ T cells and invariant natural killer T (iNKT) cells. However, in women, only γδ T cells and CD8+ T cells were enriched within the CD11c fraction of blood and cervical tissue. These CD11c+ cells were highly activated and had greater interferon (IFN)-γ secretory capacity than CD11c- T cells. Furthermore, circulating CD11c+ T cells were associated with the expression of multiple adhesion molecules in women, suggesting that these cells have high tissue homing potential. These data suggest that CD11c expression distinguishes a population of circulating T cells during bacterial infection with innate capacity and mucosal homing potential.

Introduction

The ability to assess ongoing mucosal immune responses is critical for understanding host-pathogen responses and would assist mucosal vaccine development. In the case of the female

PLOS ONE

genital tract (GT) immune responses, assays to determine the magnitude and quality of the immune response in mucosal tissues largely rely on sampling of peripheral blood. Measuring antigen-specific T cell responses directly is not always technically or economically feasible, therefore methods that provide an indirect measure of the immune response are essential.

We previously detected an increase in the expression of α chain integrin (αX, CD11c molecule) when analyzing blood samples from mice with lower GT *Chlamydia* infection and women with symptomatic bacterial vaginosis (*J. Qualai et al., submitted for publication*). Integrins are widely expressed cell surface molecules, composed of non-covalently linked α and β subunits that allow cell-extracellular matrix and cell-cell interactions [1]. Among these integrins, CD11c/CD18 is one of the four members of the β2 leukocyte integrin family [1]. CD11c is also referred to as complement receptor 4, since it can mediate phagocytosis of inactivated complement C3b-opsonized particles, demonstrating a wider role in host defense than cell-cell adhesion [2]. There are a wide variety of ligands described for CD11c, including other adhesion molecules, bacterial cell wall components (including lipopolysaccharide), complement proteins, and matrix proteins [2]. The CD11c/CD18 complex is also reported to bind denatured proteins, perhaps acting as a danger signal in the context of innate immune defense [3].

CD11c is typically considered to be a marker of conventional dendritic cells (DC) [4], and is not often considered in the context of T cell responses [5]. Yet, CD11c can be expressed on NK cells and populations of activated T and B cells [6]. Indeed, studies in several different mouse models have associated CD11c expression with effector memory and regulatory T cell subsets (T$_{EM}$/T$_{regs}$) [7–12], small gut intra-epithelial lymphocytes [13, 14], and the development of experimental autoimmune encephalomyelitis [15]. The exact role of CD11c is unclear but was found to correlate with increased cytotoxicity, effector, or regulatory function (*reviewed in* [16]). CD11c expression has also been associated with activated antigen-specific T cells expanded in response to infection or vaccination, and has been correlated with the potential of these cells to secrete IFN-γ [9, 12]. Recent reports have also described a unique cellular subset in mice and humans that contains key features of both T cells and DCs [17]. Interestingly, these unusual cells are characterized by the expression of T cell receptor (TCR), major histocompatibility complex (MHC) II, and CD11c [17].

Our hypothesis is that increased CD11c expression in circulating T cells during bacterial infection of the GT indicates the activation and migration of innate-like T cells. Here, we have examined the phenotype of T cells expressing CD11c in the blood and GT of mice and women. We find that in addition to CD8⁺ T cells, γδ T cells represent an unconventional T cell subset that expresses CD11c under physiological conditions. These innate populations should be considered when evaluating mucosal immune responses to infection.

Materials and Methods

Ethics statement

All animal procedures were approved and supervised by the Animal Care Committee of the Germans Trias i Pujol Health Science Research Institute (IGTP) and by the Department of Environment of the Catalan Government (approval number # 7066).

Informed written consent was obtained from all participants and the study protocols and questionnaires were approved by the University Hospital Germans Trias i Pujol (HUGTP, Badalona, Spain) Clinical Research Ethics Committee (reference numbers # EO-11-074 and # PI-14-070). The study was undertaken in accordance with the Declaration of Helsinki and the requirements of Good Clinical Practice.

Samples for differential gene expression analysis

Six to eight week-old female C57BL/6 mice were bred in house. Mice were kept in ventilated cages with sterile food and water *ad libitum*, under specific-pathogen-free conditions at the animal facility for experimental models of the IGTP, Spain. A group of six females were treated subcutaneously with 3mg of Depo-Provera six days prior to euthanizing in order to homogenize the endocrine effects on immunity by synchronizing the menstrual cycle. All mice were euthanized with isoflurane (inhalation excess) and blood was immediately obtained by cardiac puncture.

Blood samples (~500µl) were immediately lysed, washed, suspended in PBS and incubated with Aqua vital dye to distinguish dead cells (Invitrogen, Burlinguh, ON, Canada). Cells were suspended in staining buffer (1% BSA-PBS) and incubated with CD3-Vioblue, CD4-APC-H7, CD62L-PE (Miltenyi Biotec, Madrid, Spain), CD44-Brilliant Violet 570 (BioLegend, San Diego, CA) and CD11c-PE-Cy7 (HL3) (BD Biosciences, San Jose, CA). Cells were suspended in cold FACS-flow buffer (1% FBS-PBS with 0.5mM EDTA) and immediately sorted into $CD3^+$ $CD62L^-$ $CD44^{high}$ $CD11c^+$ and $CD3^+$ $CD62L^-CD44^{high}$ $CD11c^-$ using a BD FACSAria™ Cell Sorter. Purity of sorted cells was >99%. Each sample was sorted by collecting 300 cells directly into refrigerated lysis buffer [18], immediately spun, heated at 65°C for 15 minutes and kept at 4°C until delivery to the Institute for Research in Biomedicine (IRB, Barcelona, Spain).

Differential gene expression and gene set enrichment analysis

Microarray gene expression profiling with Mouse Genome 430 PM Strip arrays was performed following manufacturer recommendations (Affymetrix Inc, Santa Clara, CA) with specific adaptations based on the picoprofiling method [18]. Image intensities were extracted with Affymetrix GeneAtlas System software, normalized and summarized by RMA and analyzed for differential gene expression by Limma [19] with false discovery rate multiple testing significance correction. NK-related γδTCR, iNKT $CD4^+$ and iNKT $CD4^-$ cells specific gene sets [20] were tested by Gene Set Enrichment Analysis (GSEA) [21] for significant enrichment in $CD11c^+$ T cells.

Animal model

Chlamydia muridarum elementary bodies were purified by discontinuous density gradient centrifugation and the number of inclusion-forming units were determined as previously described [22, 23]. Eight week-old C57BL/6 mice were purchased from The Jackson Laboratory (Bar Harbor, ME). All mice were maintained in accordance with University of California Davis Research Animal Resource guidelines, USA. Estrus was synchronized and 7 days after, $1x10^5$ C. muridarum in 5µL sucrose/phosphate/glutamate buffer were deposited directly into the vaginal vaults with a blunted pipet tip [23].

Tissue processing

Blood was collected by retro-orbital bleeding and erythrocytes were immediately removed by ACK lysing buffer (Life Technologies). Leukocytes were washed with FACS buffer (PBS with 2% FBS) and stored on ice until use. Mouse GT were removed and leukocytes isolated as described [24]. Briefly, vagina, cervix, uterine horns and oviducts were minced into small pieces, digested in 500mg/L collagenase IV (Sigma) for 1 hour at 37°C with constant stirring. Leukocytes were purified by percoll density gradient centrifugation (GE Healthcare), washed with FACS buffer and stored on ice until use.

T cell subset analyses in mouse tissues

Leukocytes from blood and GT were harvested from naïve or infected mice as described above. Single cell suspensions were prepared in FACS buffer and blocked with Fc block (culture supernatant from the 24G2 hybridoma, 2% mouse serum, 2% rat serum and 0.01% sodium azide). Cells were stained with different panels of antibodies including: FITC-CD4 (GK1.5), CD8 (53–6.7), NKp46 (29A1.4; Biolegend), PE-CD49b (DX5), CD103 (2E7), NK1.1 (PK136), γδTCR (eBioGL3), PerCP-Cy5.5-CD11c (N418), Alexa Fluor 700-CD3 (eBio500A2), eFluor 450-CD8 (53–6.7), NK1.1; APC-CD19 (MB19-1), CD159a (16A11) (Biolegend), CCR10 (248918; R&D Systems, MN) and APC labeled mCD1d PBS-57 tetramer (NIH Tetramer Core Facility). All antibodies were obtained from eBiosciences (San Diego, CA) unless otherwise noted. Flow data was acquired on an LSRFortessa flow cytometer and analyzed using FlowJo vX.0.7 software (Tree Star, Ashland, OR). Because of the low number of CD3$^+$ events in the GT of naïve animals, we analyzed some of the frequencies as % of the total number of events (i.e. CD3$^+$ or CD3$^+$ CD11c$^+$); while others, like the expression of certain molecules within the CD3$^+$ CD11c$^{+/-}$ fractions, were analyzed as the % of the parent as we did for blood (i.e. CD3$^+$ CD11c$^{+/-}$ TCRγδ$^+$). Boolean gating strategy was used for simultaneous expression of different molecules, which were represented visually using Pestle (v1.7) and Spice (v5.3) softwares (provided by the National Institutes of Health) [25].

Phenotyping of human blood

Healthy normal donors (ND) were recruited from the clinical trials unit of the HUGTP. For unconventional T cell subset phenotyping (n = 10, 27±4 years old), 1ml of blood was lysed by ammonium Lysis Buffer (BD Pharm Lyse, BD Biosciences) and processed for staining. Leftover blood (~9ml) was used to isolate peripheral blood mononuclear cells (PBMC) by density gradient centrifugation over Ficoll gradient (Biochrom AG, Berlin, Germany). Both cell suspensions were stained with: CD3-eFluor 605 (OKT3, eBiosciences), CD14-V450 (MØP9), CD19-V450 (HIB19), CD11c-PE-Cy7 (B-ly6), CCR7-Horizon PE-CF594 (150503), CD8-V500 (RPA-T8) (BD Biosciences), NK1.1-PE (191B8), γδTCR-FITC (11F2), Vα7.2-APC-H7 (REA179) (Miltenyi Biotec) and Vα24-APC (6B11) (BioLegend).

For adhesion molecules phenotyping, samples (n = 13, 26±3 years old) were analyzed as described (J. Qualai et al., submitted for publication). Briefly, after erythrocyte depletion from 1ml of blood, cells were stained with Aqua Dye (Invitrogen), washed again, suspended in staining buffer and divided into four tubes. Common antibodies to each panel were: CD3-eFluor 605, CD4-Alexa700 (eBioscience), CCR7-Horizon PE-CF594, CD38-Brillant Violet 421, HLA-DR-PerCP-Cy5.5 and CD11c-PE-Cy7 (BD Biosciences). Specific for each panel were: 1) CCR2-PE, CCR5-APC-Cy7, CXCR6-APC (R&D Systems Inc.) and CXCR3-FITC (BioLegend); 2) CD49d (α4)-FITC, β7-APC, CCR9-PE (BD Biosciences) and CD29 (β1)–APC-Cy7 (BioLegend); 3) CD103-FITC, CD54-APC, CD49a (α1)-PE and CD29 (β1)–APC-Cy7 (all from BioLegend); 4) CD18-APC, CLA-FITC (both from BD Biosciences) and CCR10-PE (BioLegend). For both analyses cells were acquired using a BD LSRFortessa SORP flow cytometer (Flow Cytometry Platform, IGTP) and analyzed with FlowJo vX.0.7 software (TreeStar). Gates were drawn based on fluorescence minus one-controls.

Cervical tissue digestion and flow cytometry

Human cervical tissue was obtained from two sets of five healthy women (age range 42–47 years old) undergoing hysterectomy for benign indication at HUGTP. After confirmation of healthy tissue status by the Pathological Anatomy Service, a piece from ecto and endocervix separated by anatomical localization was delivered to the laboratory in refrigerated RPMI 1640

medium (Cellgro, Manassas, VA) containing 10% FBS (Lonza, Basel, Switzerland), 500U/mL penicillin, 500μg/mL streptomycin, 5μg/mL fungizone and 1μg/mL gentamycin (Life Technologies). Tissue was processed within the next 12 h after surgery, and 8-mm³ block-dissection was performed as described [26]. Tissue digestion of 5–9 pieces of ecto or endocervix with collagenase IV (Invitrogen) was immediately executed as described [26]. Tissue blocks were then dissociated manually with a disposable pellet pestle and filtered through a 70μm-cell strainer (BD Biosciences). After centrifugation, pellet was suspended in staining buffer (1% mouse serum, 1% goat serum in PBS) and stained with different combinations of CD3-eFluor 605 (eBiosciences), CD14-V450, CD11c-PE-Cy7, CD8-V500, HLA-DR-PerCP-Cy5.5, CD69-Horizon PE-CF594 (BD Biosciences), NK1.1-PE, γδTCR-FITC, Vα7.2-APC-H7 (Miltenyi Biotec), CD103-FITC and Vα24-APC (BioLegend). Data were acquired and analyzed as described for blood.

PBMC activation and intracellular cell staining

PBMC were cultured in RPMI 1640 supplemented with 10% FBS and 40μg/ml gentamycin. Stimulation was performed with 1μl (E)-4-hydroxy-3-methyl-but-2-enyl pyrophosphate (HMBPP, Sigma). After 18 h of activation, Brefeldin A (GolgiPlug, BD Biosciences) was added. Five hours later, cells were stained with CD3-PerCP (OKT3), CD11c-PE-Cy7 (B-ly6), HLA-DR-PerCP-Cy5.5 (G46-6), CD69-Horizon PE-CF594 (FN50) (BD Biosciences) and γδTCR-PE (11F2) (Miltenyi Biotec). After surface staining cells were fixed and permeabilized with Fix/Perm Kit and intracellularly stained with IFN-γ-Alexa700 (B27) (Invitrogen). Data were acquired and analyzed as described for blood.

Statistical Analysis

Data are reported as the mean and the standard deviation (SD) for each group using Prism 4.0 software (GraphPad Software). For animal samples, statistical analyses were performed by Student's t test or by Paired T test when comparing the positive and negative fraction of the same sample. For all the other analyses in human samples, which did not pass normality test ($p < 0.05$), non-parametric tests were employed. A p value of <0.05 was considered significant.

Accession codes

Microarray data presented in this article are deposited into the Gene Expression Omnibus (http://www.ncbi.nlm.nih.gov/geo/) under accession number GSE68934.

Results

Murine activated CD11c⁺ T_EM cells are enriched for NK gene signatures

In order to characterize circulating CD11c⁺ T cells, we initially analyzed gene expression in activated CD3⁺ CD62L⁻ CD44⁺ CD11c⁺ and CD3⁺ CD62L⁻ CD44⁺ CD11c⁻ T_{EM} cells recovered from naïve female mice. Multiple related genes were expressed two to eight fold higher in CD11c⁺ than CD11c⁻ T cells (Table 1). Many of these genes are expressed in NK and non-conventional memory T cell subsets but are not highly expressed in conventional αβ T cells [20]. Gene Set Enrichment Analysis revealed significant enrichment for γδT, NK and CD4⁻ iNKT cells when looking at the entire dataset (S1 Fig). Thus, CD11c expressing circulating T cells display a gene signature similar to γδ T and CD4⁻ iNKT cells.

Table 1. Example of up-regulated genes in activated effector CD11c⁺ vs. CD11c⁻ T cells in naive mice.

Gene Symbol	Gene Title	Log Fold Change	Adjusted p Value
C3ar1	complement component 3a receptor 1	6.20	0.0081
C5ar1	complement component 5a receptor 1	5.80	0.0132
Ccl3	chemokine (C-C motif) ligand 3	7.04	0.0050
Ccl4	chemokine (C-C motif) ligand 4	5.23	0.0055
Ccl6	chemokine (C-C motif) ligand 6	7.19	0.0055
Ccl9	chemokine (C-C motif) ligand 9	6.39	0.0050
Cd244	CD244 natural killer cell receptor 2B4	3.75	0.0081
Cd8a	CD8 antigen, alpha chain	2.36	0.0490
Csf1	colony stimulating factor 1 (macrophage)	5.98	0.0156
Csf1r	colony stimulating factor 1 receptor	5.95	0.0077
Csf2ra	colony stimulating factor 2 receptor, alpha, low-affinity (granulocyte-macrophage)	4.69	0.0240
Csf2rb	colony stimulating factor 2 receptor, beta, low-affinity (granulocyte-macrophage)	7.74	0.0055
Csf2rb2	colony stimulating factor 2 receptor, beta 2, low-affinity (granulocyte-macrophage)	6.66	0.0055
Csf3r	colony stimulating factor 3 receptor (granulocyte)	2.36	0.0300
Gzma	granzyme A	3.66	0.0055
Gzmb	granzyme B	2.93	0.0490
H2-Aa	histocompatibility 2, class II antigen A, alpha	8.91	0.0050
H2-Ab1	histocompatibility 2, class II antigen A, beta 1	6.86	0.0065
H2-DMa	histocompatibility 2, class II, locus DMa	3.63	0.0063
H2-DMb1 /// H2-DMb2	histocompatibility 2, class II, locus Mb1 /// histocompatibility 2, class II, locus Mb2	4.46	0.0055
H2-DMb2	histocompatibility 2, class II, locus Mb2	4.76	0.0225
H2-Eb1	histocompatibility 2, class II antigen E beta	5.93	0.0121
Ifitm1	interferon induced transmembrane protein 1	6.42	0.0050
Ifitm2 /// LOC631287	interferon induced transmembrane protein 2 /// interferon-induced transmembrane protein	5.09	0.0063
Ifitm3	interferon induced transmembrane protein 3	6.20	0.0276
Klra2	killer cell lectin-like receptor, subfamily A, member 2	3.45	0.0258
Klrb1b	killer cell lectin-like receptor subfamily B member 1B	3.43	0.0253
Tgfbi	transforming growth factor, beta induced	5.69	0.0050
Tlr7	toll-like receptor 7	2.47	0.0450
Tlr9	toll-like receptor 9	2.95	0.0065

doi:10.1371/journal.pone.0154253.t001

Murine CD11c⁺ T cells express high levels of NK1.1 in blood after vaginal infection

Next, we performed flow cytometry analyses of blood and GT obtained from C57BL/6 mice vaginally infected with *Chlamydia muridarum*. Seven days after infection, the frequency of T cells expressing CD11c⁺ in peripheral blood increased from 1.53% to 6.04% as reported *(J. Qualai et al., submitted for publication)*. Within this fraction we analyzed the expression of several NK-associated molecules (NK1.1, DX5, NKG2A, NKp46), specific T cell phenotypes (CD8α, CD1d-restricted iNKT cells, γδTCR) and adhesion molecules (CD103, CCR10). Part of the gating strategy is shown in S2 Fig. The frequency of CD11c⁺ T cells expressing CD8α in blood was similar before and after infection, while NK1.1 expression increased markedly following infection (Fig 1A and 1B). Before infection, a significant fraction of CD3⁺ CD11c⁺ T cells also expressed DX5 and NKG2A (Fig 2), but these markers either decreased or remained the same after infection (Fig 2).
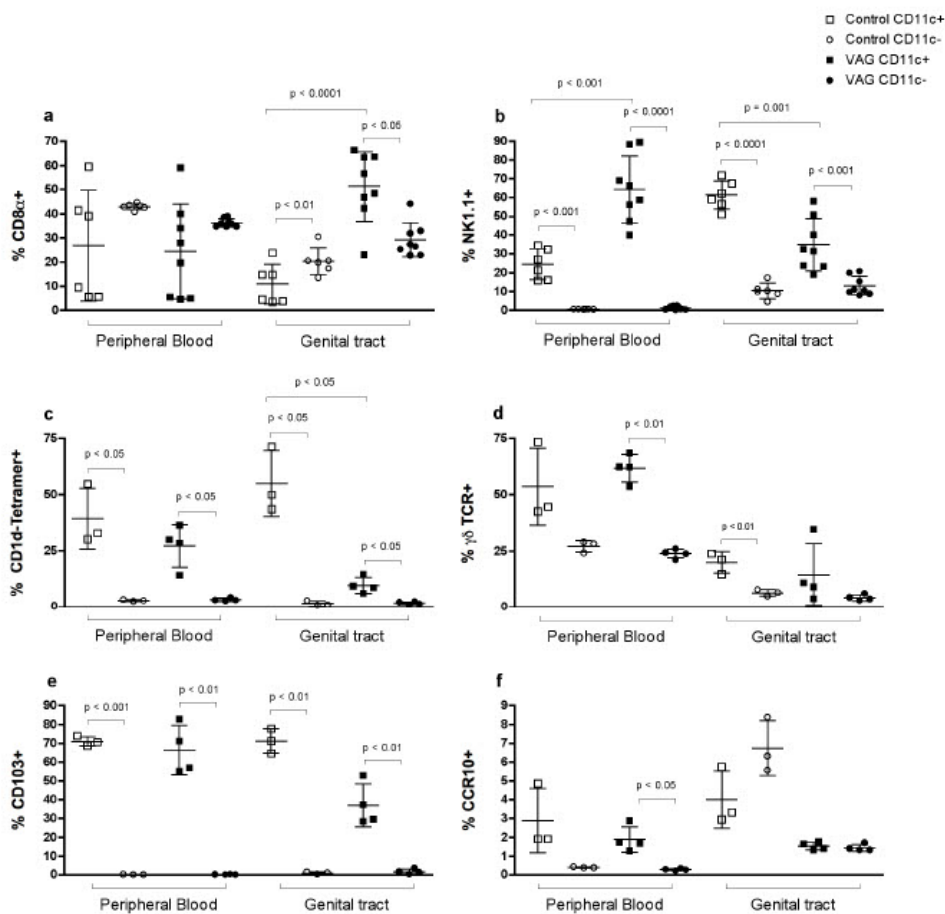
Fig 1. T cell phenotypes in blood and genital tract of mice by CD11c expression. Comparison on the frequency of (a) NK1.1, (b) CD8α, (c) CD1d-tetramer, (d) γδTCR, (e) CD103 and (f) CCR10 in CD11c⁺ (squares) and CD11c⁻ (circles) T cells from the same individual. Gating strategy consisted on a lymphocyte gate based on FSC vs. SSC, followed by doublet exclusion and a CD3⁺ T cells gate. After gating on CD11c⁺ or CD11c⁻ T cells, surface expression of the different markers was quantified (see S2 Fig for further details). Each bar represents the mean ± SD of control (white; n = 3 or n = 6) or vaginally (VAG)-infected mice (black; n = 4 or n = 8) seven days after infection. Data were analyzed using the paired Student's t-test.

doi:10.1371/journal.pone.0154253.g001

The frequency of $CD3^+ CD11c^+$ T cells within the GT increased from 0.5±0.2% to 4.1±1.6% seven days after infection (p = 0.0001). In marked contrast to blood, the expression of CD8 by $CD11c^+$ T cells strikingly increased in these tissues after *Chlamydia* infection (Fig 1A). NK1.1 was expressed at high levels by GT $CD11c^+$ T cells before infection and significantly decreased after infection (Fig 1B). The expression of DX5 and NKG2A was less frequent at baseline in
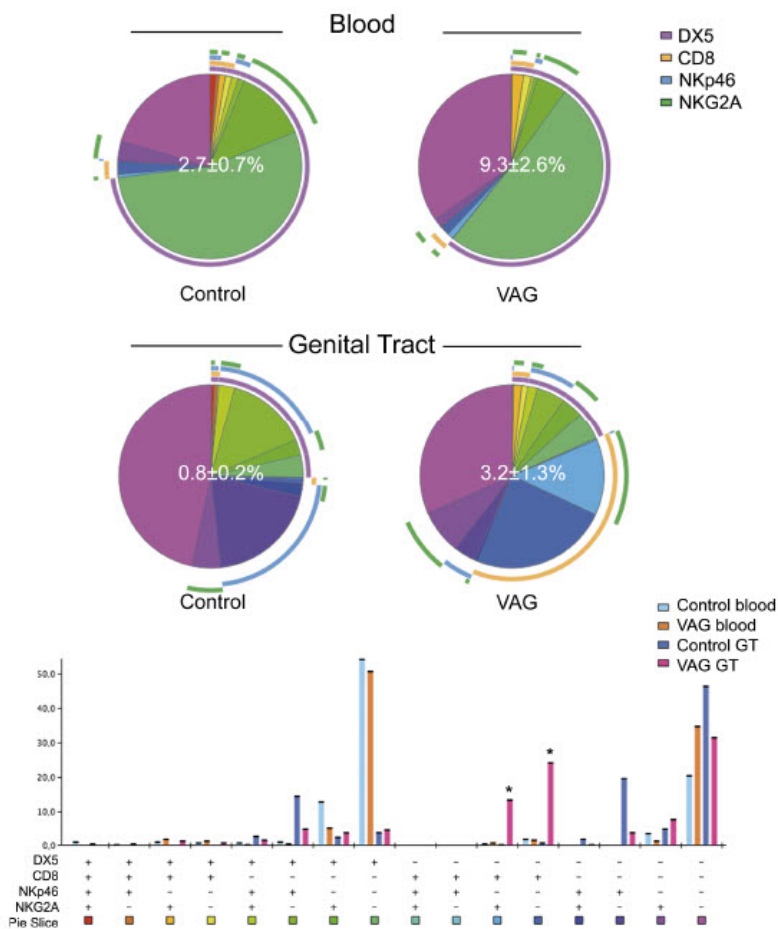
Fig 2. NK phenotypes included in the CD11c⁺ T cell fraction after vaginal Chlamydia infection in mice. The frequency of the different subsets obtained from combining DX5, CD8α, NKp46 and NKG2A expression is displayed for each group as a pie chart and as a complementary bar graph. Gating strategy was performed as described in Fig 1 and in Materials and Methods. The frequency of CD11c positive cells in the T cell fraction as the mean ± SD is shown as a white number in the center of the pie chart for each group in blood (top) and genital tract (GT, bottom). Each colored portion of a pie chart indicates the percentage of a specific subset detailed in the bar chart below. The arcs around the pie show the molecule or combination of molecules to which those proportions correspond (see color legend indicating DX5, CD8α, NKp46 and NKG2A). *Indicates p<0.05 by Student's t test analyses only for values >5% of the total CD11c⁺ T cells in vaginally (VAG)-infected mice seven days after infection (n = 4) compared to control (n = 3) animals.

GT CD11c⁺ T cells compared to blood, while the activating receptor NKp46 was expressed by approximately 40% of cells (Fig 2). After infection, the frequency of NKG2A expression by CD11c⁺ T cells significantly increased (p = 0.006), while NKp46 decreased (p = 0.0009) (Fig 2).

Thus, CD3$^+$ CD11c$^+$ T cells increase in both blood and GT after vaginal infection and express different patterns of surface markers within these compartments.

Murine CD11c$^+$ T cells include high frequencies of γδ T cells and iNKT cells

The total frequency of iNKT or γδ T cells in blood did not change after vaginal infection; however, it did increase in the GT of the infected mice (p<0.003; data not shown). When comparing CD11c$^+$ and CD11c$^-$ subsets, there was a clear enrichment of these unconventional T cells within the CD11c$^+$ fraction in both tissues (Fig 1C and 1D). Thus, under physiological conditions, CD11c$^+$ T cells included almost exclusively all iNKT cells and high proportions of γδ T cells. Of CD3$^+$ CD11c$^+$ T cells in the blood, 27–39% of them were iNKT and 50–60% were γδ T cells and this frequency did not change after vaginal infection (Fig 1C and 1D). Nevertheless the frequency of CD1d-tetramer$^+$ cells in the CD11c$^+$ T cell fraction decreased in the GT after infection (Fig 1C). Actually, when performing the analysis in combination with CD8 and NK1.1 expression, it was clear that while NK1.1$^+$ γδ T cells characterized the major subset expanding in blood, a single CD8$^+$ phenotype was the major contributor to the increment of CD11c$^+$ T cells observed in the GT (Fig 3).

CD103 expression is exclusively associated to CD11c$^+$ T cells in mice

Previous work in a mouse model of colitis determined that CD11c$^+$ CD8$^+$ T$_{regs}$ are CD8α$^+$ CD103$^+$ NK1.1$^-$ in the small intestine, but CD8α$^-$ CD103$^-$ NK1.1$^+$ in the colon [10]. We analyzed the expression of these molecules and included CCR10, which could indicate migration of CD11c$^+$ T cells into the GT. The ligand for this chemokine, CC-chemokine ligand 28, is expressed in the genital tract, and B cells homing there express CCR10 [27]. Co-expression of CD103 and CD11c was high in the blood and GT of uninfected mice (Fig 1E). Additionally, among circulating T cells, CCR10 expression was found almost exclusively associated with the CD11c$^+$ subset (Fig 1F). This chemokine receptor represented a small fraction of CD11c$^+$ T cells, but expression was clearly enriched in CD11c$^+$ cells after infection (Fig 1F).

To summarize, it appears that the majority of CD11c$^+$ T cells in blood under homeostatic conditions are CCR10$^-$ CD8α$^-$ CD103$^+$ NK1.1$^-$, but this phenotype is less frequent in the GT (Fig 4). After vaginal infection, CD103$^+$ NK1.1$^+$ CD8α$^-$ cells expand among circulating CD11c$^+$ T cells and CD8α$^+$ CD103$^-$ NK1.1$^-$ are elevated in the GT (Fig 4). Thus, none of these phenotypes illustrated the T$_{regs}$ described in the colitis model [10].

Circulating T cells expressing CD11c are associated with γδ T cells but not iNKT cells in women

Next, we examined CD11c expression in CD3$^+$ CD4$^{+/-}$ and CCR7$^{+/-}$ T cells from healthy young women (normal donors, ND), and found an enrichment of this marker in the CCR7$^-$ CD4$^-$ fraction (Fig 5). We then analyzed subsets studied in the mouse model and examined Vα7.2 expression to determine mucosal associated invariant T (MAIT) cells, which are characterized by high CD161 expression (NK1.1 human homolog) [28]. We also adressed iNKT populations via expression of the invariant TCR α chain (Vα24-Jα18). We analyzed each phenotype in circulating CD3$^+$ CCR7$^-$ T cells, and compared their expression in CD11c$^+$ (1.9±0.7%) vs. CD11c$^-$ (35.4±10.0%) cells using a non-parametric paired T test (Fig 6A and S3 Fig left). The gating strategy used for these analyses excluded CD19$^+$ and CD14$^+$ cells, which marginally contaminated CD11c$^+$ T cells. The only subsets significantly enriched in the positive fraction were CD8$^+$ and γδTCR$^+$ (Fig 6A). In contrast, MAIT cells (Vα7.2$^+$ CD161^h) and iNKT cells were lower in the positive than in the
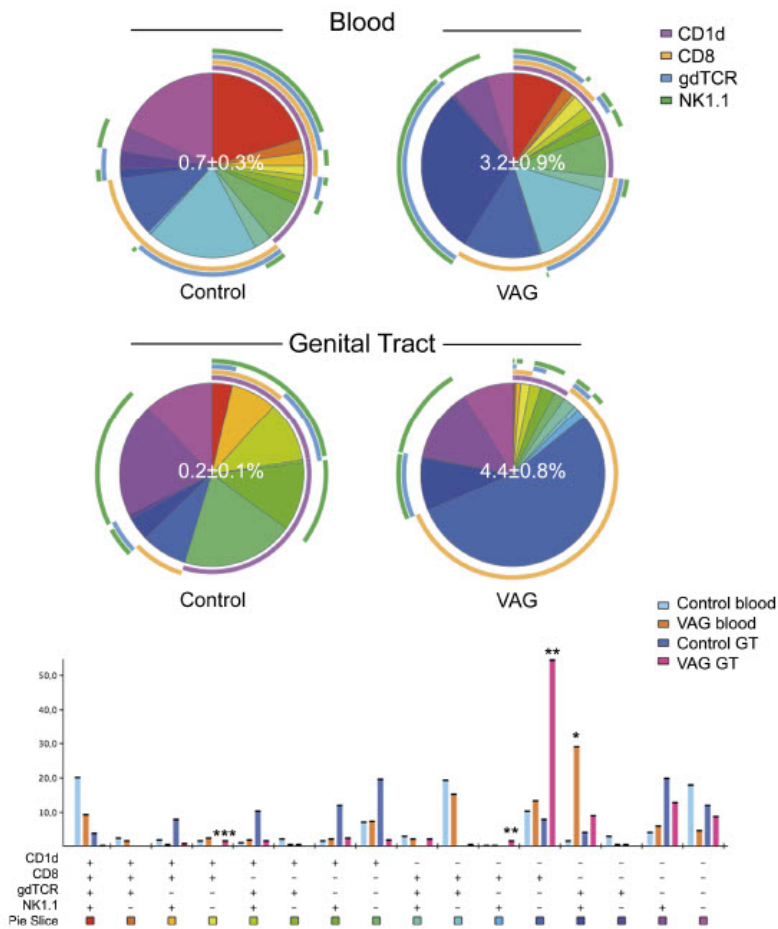
Fig 3. Unconventional phenotypes included in the CD11c⁺ T cell fraction after vaginal Chlamydia infection in mice. The frequency of the different subsets obtained from combining CD1d-tetramer, CD8α, γδTCR and NK1.1 expression is displayed for each group as a pie chart and as a complementary bar graph. Gating strategy was performed as described in Fig 1 and in Materials and Methods. The frequency of CD11c positive cells in the T cell fraction as the mean ± SD is shown as a white number in the center of the pie chart for each group in blood (top) and genital tract (GT, bottom). Each colored portion of a pie chart indicates the percentage of a specific subset detailed in the bar chart below. The arcs around the pie show the molecule or combination of molecules to which those proportions correspond (see color legend indicating CD1d-tetramer, CD8α, γδTCR and NK1.1). *Indicates p<0.05 by Student's t test analyses only for values >5% of the total CD11c⁺ T cells in vaginally (VAG)-infected mice seven days after infection (n = 4) compared to control (n = 3) animals.

doi:10.1371/journal.pone.0154253.g003

negative fraction (Fig 6A). Of note, γδ T cells represented 5.7±2.7% of the total CD3⁺ T cells in blood, and the frequency of CCR7⁻ CD11c⁺ in this subset was of ~10% (S4A Fig), from which

Fig 4. Adhesion molecules included in the CD11c⁺ T cell fraction after vaginal Chlamydia infection in mice. The frequency of the different subsets obtained from combining CCR10, CD8α, CD103 and NK1.1 expression is displayed for each group as a pie chart and as a complementary bar graph. Gating strategy was performed as described in Fig 1 and in Materials and Methods. The frequency of CD11c positive cells in the T cell fraction as the mean ± SD is shown as a white number in the center of the pie chart for each group in blood (top) and genital tract (GT, bottom). Each colored portion of a pie chart indicates the percentage of a specific subset detailed in the bar chart below. The arcs around the pie show the molecule or combination of molecules to which those proportions correspond (see color legend indicating CCR10, CD8α, CD103 and NK1.1). *Indicates p<0.05 by Student's t test analyses only for values >5% of the total CD11c⁺ T cells in vaginally (VAG)-infected mice seven days after infection (n = 4) compared to control (n = 3) animals.

~78% were CD161⁺ and ~18% were CD8⁺. In fact, CD161 was similarly high in γδ T cells regardless of CD11c expression (S4B Fig), but CD8 expression was doubled in the CCR7 CD11c⁺ fraction of γδT cells compared to total CD3⁺ γδTCR⁺ T cells (S4C Fig). Regarding CD8⁺ T cells,

PLOS ONE
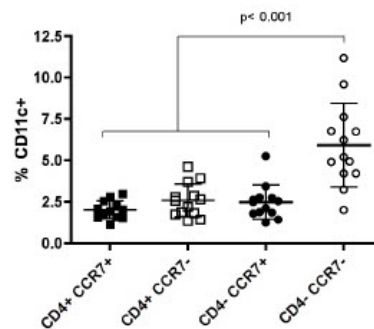
Fig 5. CD11c expression in circulating T cells from healthy young women. CD11c+ cells were analyzed by flow cytometry in the CD4+ CCR7+/- and CD4- CCR7+/- CD3+ T cell subsets. Gating strategy consisted on the following consecutive gates: lymphocytes, singlets, live CD3+ T cells, CD4+ or CD4- T cells, CCR7+ or CCR7- and lastly CD11c+. Each bar represents the mean ± SD of normal donors (n = 13). Data were analyzed by Kruskall-Wallis test with Bonferroni post-test correction.

doi:10.1371/journal.pone.0154253.g005

which represented 28.8±7.7% of the T cells, only about 3.5% of them were CCR7- CD11c+ (S4A Fig), in which CD161 was enhanced compared to total CD3+ CD8+ T cells (S4D Fig).

In six of these donors, we analyzed the expression of these markers after obtaining PBMC to determine if this process affected any of the T cell phenotypes determined. The overall differences between CD11c+ and CD11c- T_{EM} cells were mostly maintained, yet MAIT and iNKT significances were lost (Fig 6B and S3 Fig right). Thus, circulating CD11c+ T_{EM} cells represented at least two different populations in healthy women: a subset of γδ T cells with their constitutive high expression of CD161 and enriched CD8 expression, and a subset of CD8+ T cells with enhanced CD161, yet not belonging to the MAIT or iNKT lineages.

Human cervical tissue contains γδ T cells expressing CD11c

The same subsets were determined by flow cytometry in cervical samples from healthy women. First, we evaluated the impact of tissue digestion on the detection of these phenotypes in PBMC, since it has been reported that other markers are affected by collagenase treatment [29]. While we confirmed the loss of CD56 expression, we also detected a dramatic reduction on CD19, CD20 and CCR7 protein expression. However, expression of CD3/CD8/CD14/CD16/CD161/αβTCR/γδTCR/Vα7.2/Vα24/CD11c/HLA-DR was not modified. Thus, we analyzed the same subsets without considering CCR7 expression, since most CD3+ T cells in these tissues were CCR7- (>95%). Following the gating strategy shown in Fig 7A, CD11c expression on CD3+ CD14- T cells represented an average of 3.3±1.5% for ectocervix and 3.7±2.5% for endocervix. Since there were no differences between any of the subsets analyzed in the ecto and endocervix (Fig 7B), we pooled both tissues in order to strengthen the statistical power of the analysis. This way, the proportion of γδTCR was of >9% in CD11c+ vs. ~1% in CD11c- and the proportion of CD8 was of 59% in CD11c+ vs. 46% in CD11c- (p<0.006 for both). In three of these samples, we also analyzed the activation marker CD69, which expression was of 86.0±9.5% in CD11c+ vs. 74.5±10.1% in CD11c- (S5A Fig). Finally, the analysis of the frequency of CD103 in another set of five samples demonstrated no differences based on CD11c expression (S5B Fig).

Characterization of T Cell Subsets Expressing CD11c
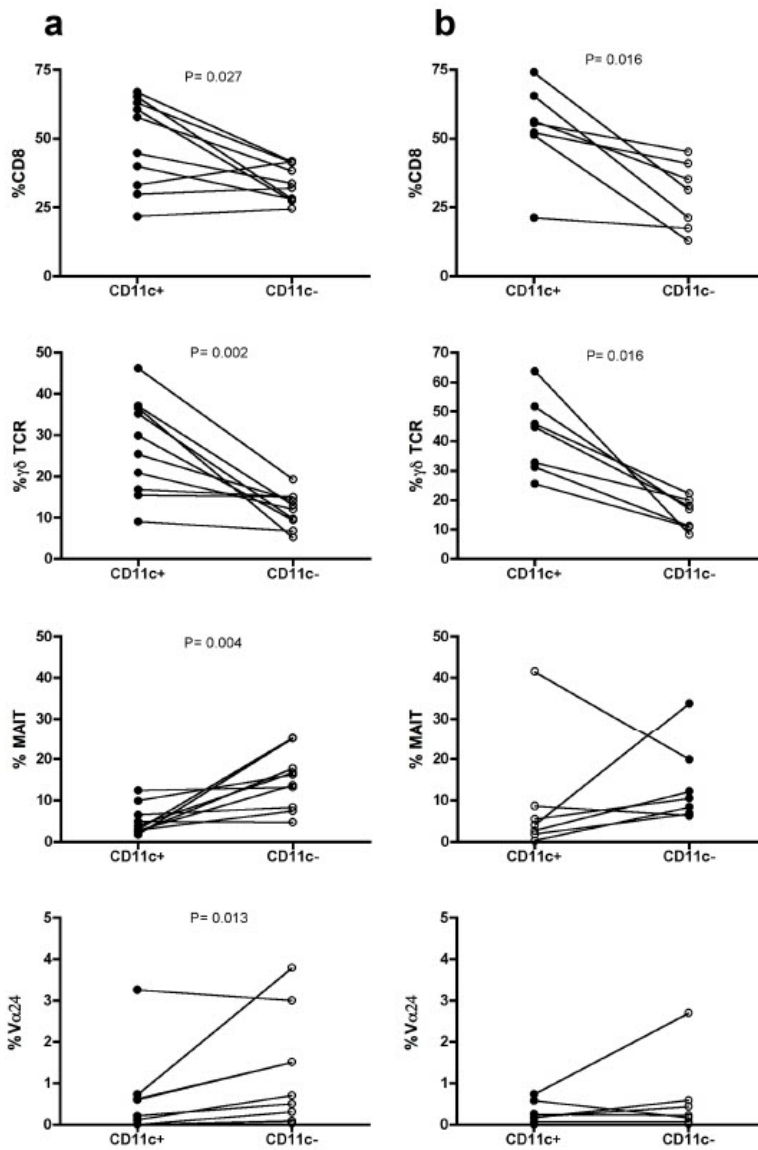
Fig 6. Comparison of specific phenotype frequencies based on CD11c expression in blood samples from healthy women. Comparison of the frequency of CD8, γδTCR, MAIT and iNKT (Vα24) in CD11c⁺ and CD11c⁻, CCR7⁻ CD3⁺ T cells from the same individual. (a) Fresh blood (n = 10) and (b) PBMC (n = 6). Gating strategy consisted on the following consecutive gates: lymphocytes, singlets, live CD14⁻ CD19⁻ CD3⁺ T cells and CCR7⁻ CD11c⁺or CD11c⁻ T cells (see S3 Fig for further details). Data were analyzed using the paired Student's t-test.

Compared to blood, γδTCR⁺ and CD161⁺ represented smaller populations of total CD3⁺ T cells in the cervix, while CD8⁺ T cells were clearly enriched in this tissue. The mean frequency of CD11c⁺ in γδ T cells was of over 20% (S4E Fig), from which CD161 was again independent of CD11c expression (S4F Fig), while CD8 was significantly enriched compared to total CD3⁺ γδTCR⁺ T cells (S4G Fig). Finally, CD11c⁺ represented 5.8±2.9% of total CD8⁺ T cells (S4E Fig), in which CD161 was also significantly different from total CD3⁺ CD8⁺ T cells (S4H Fig). Regardless of differences in the percentage of CD8 and other subsets between blood and mucosa in women, similar findings were observed concerning the subsets enriched in CD11c⁺ T cells.
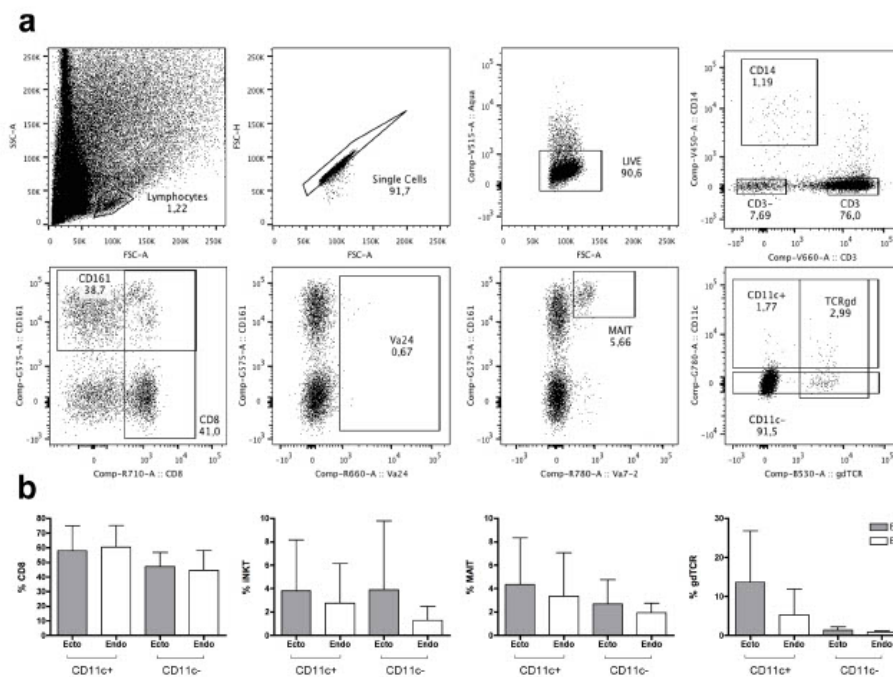
Fig 7. Phenotype of cervically derived T cells from healthy women and analysis by CD11c expression. (a) Representative dot plots from the T cell subsets extracted from the endocervix of healthy women. Top row shows the consecutive general gating strategy to select CD3⁺ T cells. Bottom row shows different subsets analyzed in the total CD3⁺ T cells and in the CD11c⁺ and CD11c⁻ T cell fractions. (b) Frequency of CD8, iNKT (Vα24), MAIT, and γδT cells by CD11c expression in T cells obtained from cervical tissue. Each bar represents the mean ± SD of the ectocervix and endocervix of each donor (n = 5). Data were analyzed using Wilcoxon matched-paired signed-ranked test.

CD11c$^+$ T cells are highly enriched for adhesion molecules expression but not CD103 in women

Additionally, we studied the association of CD11c expression with a variety of cellular adhesion molecules in thirteen ND from a previous homing study (*J. Qualai et al., submitted for publication*). We observed that many of these molecules were enriched for the CD11c-positive fraction of circulating CCR7$^-$ CD4$^-$ T cells: CCR2, CCR9, CCR10, CXCR6, α1β1, α4β7 (Fig 8A and 8C–8G), as well as CXCR3 (18.7±2.9% vs. 4.5±1.89) and α4β1 (37.4±5.2% vs. 4.5±1.2%) (p = 0.0002; data not shown). In contrast, expression of CCR5 was higher in the negative fraction compared to the positive (Fig 8B), while cutaneous lymphocyte antigen and CD103 were not different between these two subsets (data not shown). Additionally, activation markers HLA-DR$^+$ and/or CD38$^+$ were also significantly increased in CD11c$^+$ compared to CD11c$^-$ T cells (all p≤0.0006; Fig 8H and data not shown). Thus, compared to the animal model, CD103 was not particularly expressed in CD11c$^+$ T cells. Still, and similarly to the mouse data, CCR10 was enriched in CD11c$^+$ T$_{EM}$ cells, as occurred for most of the other chemokine receptors and other adhesion molecules measured, except for CCR5. This suggests that subsets of T cells expressing CD11c$^+$ are activated T cells with high homing potential to a variety of tissues and mucosal compartments.

CD11c expression in γδ T cells is associated with higher IFNγ secretion after activation

CD11c expression in T cells has been associated with multiple effector functions, such as increased IFN-γ secretion [9, 12]. In order to address if activated γδ T cells also differ in their capacity to secrete IFN-γ based on CD11c expression, we stimulated PBMC for 18 hours with HMBPP and then determined IFN-γ secretion and activation. HMBPP is an intermediate of the 2-C-methyl-D-erythritol-4-phosphate pathway of isoprenoid biosynthesis used by many pathogens, and represents the most potent stimulant known of the major γδ T cell population in human peripheral blood [30]. No IFN-γ secretion was detected in conventional T cells or
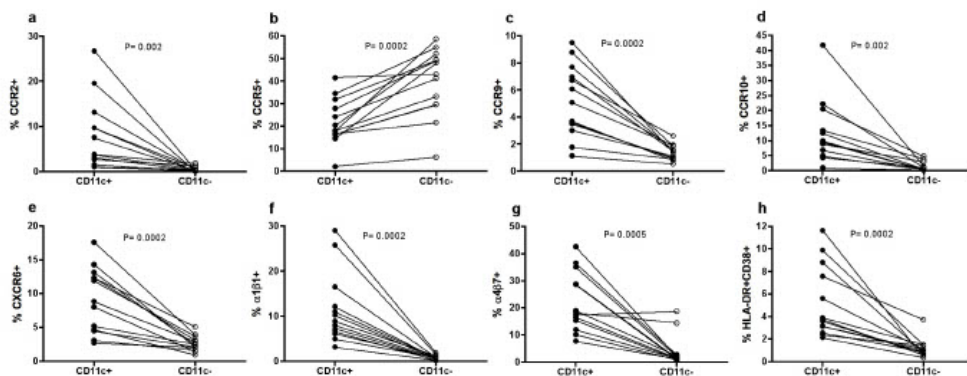
Fig 8. Comparison of adhesion molecule frequencies based on CD11c expression in CD4$^-$ T$_{EM}$ cells from healthy women. Comparison of the frequency of (a) CCR2, (b) CCR5, (c) CCR9, (d) CCR10, (e) CXCR6, (f) α1β1, (g) α4β7, (h) HLA-DR$^+$ CD38$^+$ in CD11c$^+$ and CD11c$^-$ CD4$^-$ CCR7$^-$ T cells from the same individual (n = 13). Gating strategy consisted on the following consecutive gates: lymphocytes, singlets, live CD3$^+$ T cells, CCR7$^-$ CD11c$^+$ or CD11c$^-$ T cells, CD4$^-$ T cells and expression of the different molecules addressed. Data were analyzed using Wilcoxon matched-paired signed-ranked test.

doi:10.1371/journal.pone.0154253.g008

control samples, while 5.9±4.1% of the CD11c$^+$ and 3.4 ±2.1% of the CD11c$^-$ γδ T cells secreted IFN-γ after stimulation (Fig 9A). When samples from the same individual were compared based on CD11c expression we detected significant differences in both, IFN-γ secretion and activation of γδ T cells based on this marker (Fig 9B and 9C).
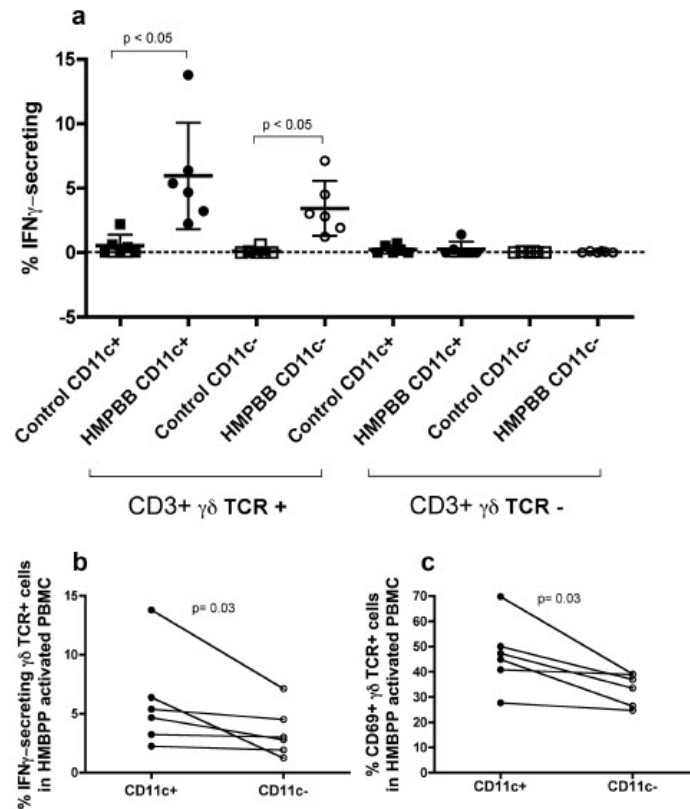
Fig 9. IFN-γ-secreting γδ T cells in PBMC from healthy women after HMBPP activation. (a) Comparison of the frequency of γδTCR$^+$ CD11c$^+$/$^-$ and γδTCR$^-$ CD11c$^+$/$^-$ T cells that secrete IFNγ in PBMC from the same individual (n = 6) after 20 hours of (E)-4-hydroxy-3-methyl-but-2-enyl pyrophosphate (HMBPP) activation. Gating strategy consisted on the following consecutive gates: lymphocytes, singlets, CD3$^+$ T cells, γδTCR$^+$/$^-$, CD11c$^+$/$^-$ and IFNγ/CD69$^+$ expression. Each bar represents the mean ± SD of control (squares) and HMBPP-stimulated PBMC (circles) samples. Data were analyzed using the non-parametric Friedman test for repeated measures, with Dunn's multiple comparisons post-hoc test. Graphs below show the comparison in the frequency of (b) IFN-γ-secreting γδ T cells and (c) CD69 expression in γδ T cells based on CD11c expression in HMBPP-activated PBMC from the same individual (n = 6). Data were analyzed using Wilcoxon matched-paired signed-ranked test.

doi:10.1371/journal.pone.0154253.g009

Discussion

We have attempted to characterize the cellular subsets found in murine and human circulating and GT T cells marked by CD11c expression. While NK1.1 and CD103 expression was tightly associated with CD11c expression in T cells from female mice, these markers were not common in CD11c⁺ T cells isolated from women. Furthermore, although both iNKT and γδ T cell populations were enriched in this fraction in the blood and GT of mice, only the second subset was consistently found in CD11c⁺ T cells from women. These cells are highly activated, express high levels of adhesion molecules, and secrete higher levels of IFN-γ upon activation, when compared to CD11c⁻ T cells. Thus, considering that CD11c⁺ T cells increase after infection or vaccination in different mouse models [9, 12], but also during symptomatic vaginosis (*J. Qualai et al., submitted for publication*), we need to reconsider CD11c⁺ T cells in the context of mucosal immune responses.

In murine models of viral infection and graft-versus-host disease, TCR stimulation induces CD11c up-regulation in CD8⁺ T cells [14, 16]. CD11c expression has been associated with gain of effector function, identification of antigen-specific T cells during infection or vaccination (9, 12), and specific T_{regs} [16]. Protection provided by these cells derives from high IFN-γ secretion and up-regulation of effector mechanisms (i.e. granzyme), which account for both effector and regulatory functions [9, 16]. Gene expression analyses of activated CD11c⁺ T_{EM} cells revealed up-regulation of some of these effector mechanisms to be highly related to NK properties [20, 31]. Our data show a clear association between CD11c and NK1.1 expression, which strikingly increases after vaginal infection in mice. Although expression of this molecule on T cells was first employed to exclusively define NKT cells [32], it is now clear that other subsets of non-conventional and activated T cells express NK1.1 or CD161 in mice and humans, respectively [28]. In mice, two different genes encoding proteins with opposite functions share the NK1.1 epitope, namely *Klrb1b* and *Klrb1c* [33]. According to the gene expression analyses we performed, only *Klrb1b* was significantly up-regulated in blood, which would suggest an inhibitory function, although this was not confirmed. However, γδ T cells expressing NK1.1 are the main IFNγ-producers among γδ T cell populations [12] and, as occurred for other NK markers addressed here, differences in the expression of activator (i.e. NKp46) or inhibitory (NKG2A) molecules between blood and tissue could also exist for this epitope. Similarly, in humans, CD161⁺ γδ T cells are efficient producers of IFN-γ but not of interleukin (IL)-17A [34]. In healthy women, we also detected an enrichment of CD161 expression in CD11c⁺ CD8⁺ T cells from blood and cervix; while in γδ T cells, this marker was already high. Although the role of this molecule as inhibitory or co-stimulatory has not yet been fully defined, CD161⁺ T cells, including MAIT and CD161⁺ γδ T cells, have been shown to commonly respond in an innate-like manner to IL-12/IL-18 stimulation independent of TCR activation [28].

Several potential mechanisms could also contribute to the expression of CD11c on T cells. In particular, protein or RNA transfer from activated antigen presenting cells via trogocytosis or external vesicles/exosomes during infection have been described [35, 36]. Although further research should clarify the role of these processes here, the fact that these differences exist during baseline physiological conditions suggest constitutive expression of CD11c by T cells, as others have observed [7]. From all the T cell-subsets analyzed, besides CD8⁺ T cells, the most consistent population expressing CD11c was γδTCR⁺. Indeed, one of the genes that differentiates γδ T cells from other non-conventional T cell subsets is *Itgax*, which encodes the αX integrin [20]. About 10 years ago, Brandes et al. described antigen presenting cell functions by γδ T cells in humans [37]. These cells have signs of pre-activation (CD69⁺) along with up-regulation of a variety of co-stimulatory and adhesion molecules (including HLA-DR and CD11c) [37]. Similarly we found that γδ T cells expressing CD11c are more activated, while CD11c⁺ CD3⁺

T_{EM} cells expressed increased levels of HLA-DR/CD38 and of most of the cellular adhesion molecules addressed compared to CD11c⁻ T cells.

In human blood, γδ T cells and specifically Vγ2Vδ2⁺ T cells, quickly expand after infection in response to microbial metabolites [31, 37]. Thus, we could expect an increase on these cells in the context of GT disorders caused by *Chlamydia* or *Gardnerella spp.* due to production of these metabolites [30]. Although we have not yet been able to confirm if the increment of CD11c⁺ T cells during bacterial vaginosis is due to an increase on this subset, CD11c expression increased in circulating γδ T cells of *Chlamydia*-infected mice, which demonstrated expansion of CD11c⁺ NK1.1⁺ γδ T cells in blood seven days after infection (Fig 3). Moreover, CD11c⁺ and γδTCR⁺ cells also increased in the GT after infection. The role of γδ T cells during *C. trachomatis* infection was examined in a knockout model of pneumonia by Rank´s group [38]. Although these cells were protective during the first 3–7 days post-infection, they were potentially deleterious at later stages [38]. As suggested, the diversity of their cytotoxic and regulatory effects may impact differently on the course of various inflammatory processes [38]. Additionally, based on the level of CD11c expression, a regulatory (CD11c^{high}) and an effector (CD11c^{low}) subset have been described for CD11c⁺ CD8⁺ T cells in mice [8]. Future investigations should elucidate if all CD11c⁺ T cell subsets, including γδ T cells, can be similarly distinguished, even in humans.

Further, there was a clear association between CD103 and CD11c expression in mice. CD103 is an αE integrin induced by transforming growth factor (TGF)-β necessary for tissue retention [31, 39]. Interestingly, inducible TGF-β was up-regulated >3–5 times in CD11c⁺ T cells (Table 1). CD103 expression, together with the absence of CCR7 and expression of CD69, is one of the hallmarks of tissue-resident memory (T_{RM}) CD8⁺ T cells [39]. In naïve mice, only T cells expressing CD11c expressed CD103 in blood and GT, and this association was maintained after infection. Therefore, CD11c could potentially be another marker for T_{RM} in mice. Although no differences were observed in the frequency of CD103 expression based on CD11c expression in the cervix of women, CD11c⁺ T cells in this tissue may also contain CD8⁺ T_{RM} cells, since not all T_{RM} cells express CD103⁺ [40]. Undoubtedly, the relationship between these different phenotypes needs further clarification.

Intraepithelial CD103⁺ CD11c⁺ T cells with an activated phenotype that mediate inflammatory gut pathology during infection have also been described in mice [13]. These cells, composed of ~50% γδ T and αβ T cells, depend on CCR2 for recruitment and, actually, CD11c⁺ T cells express higher levels of CCR2 than CD11c⁻ T cells [13]. In other models, expression of adhesion molecules such as α4β1 on γδ T cells control trafficking into tissue [41]. We determined CCR2 and α4β1 expression in CCR7⁻ CD4⁻ T cells, among other adhesion molecules, and found that during physiological conditions CD11c⁺ are almost exclusively associated with expression of most of these molecules. Likewise, CD161⁺⁺ CD8⁺ T cells, including different unconventional phenotypes, have been proposed to possess critical functions in diverse tissues because of their specific tissue-homing expression patterns [42].

In summary, several animal models evidence that CD11c⁺ CD8⁺/CD11c⁺ NK1.1⁺ T cells are functionally more potent than the ones not expressing CD11c [7, 9–12]. Following respiratory syncytial virus infection, only CD11c⁺ CD8⁺ T cells show signs of recent activation, including up-regulation of CD11b/CD69, and are recruited preferentially to the lung [7]. The characterization of the major subsets included in CD11c⁺ T cells during physiological and infection conditions performed here may recapitulate similar findings described in the literature for these related phenotypes. In humans, this may include the recent description of αβ T cells with DC properties [17], as reported before for γδ T cells [37], and possibly even CD8⁺ T_{RM} [39, 40]. Further research on the role of the different subsets included in this phenotype during mucosal infection is warranted.

Supporting Information

S1 Fig. Significant gene set enrichment of NK biomarkers among differentially up-regulated genes in CD11c positive versus CD11c negative cells. A signal-to-noise ratio (SNR) statistic was computed by GSEA software for each gene in a gene set compared to the rank list of the genes assayed on the microarray ranked according to their correlation with CD11c^{+}, this means positively correlated with log2 expression ratios. Significantly enriched gene sets cluster in the up-regulated end of the ranked list have positive enrichment scores of the gene set used for the comparison (red). The graph on the bottom of each panel represents the non-redundant list of genes ranked by differential gene expression between the CD11c^{+} and CD11c^{-} T cells. On each panel, the vertical black lines indicate the position of each of the genes of the studied in the gene set of interest within the rank ordered, non-redundant data set. The green curve corresponds to the ES (enrichment score) curve, which is the running sum of the weighted enrichment score generated by the GSEA software. Shown below are the normalized enrichment scores (NES) for each plot, which are equivalent to the value of the ES curve at the leading edge of the curve (where the statistic reaches its maximum value for a particular gene set). Results show that genes up-regulated in CD11c^{+} cells are significantly enriched for all four gene sets, as judged by the density of hits (black vertical bars) localized at the tip of the blue region with $p < 0.05$ and false discovery rate (FDR) <0.25, but show more significant enrichment in γδ T and iNKT CD4^{+} than in iNKT CD4^{-} cells.
(TIF)

S2 Fig. Flow cytometry gating strategy in T cells from peripheral blood and genital tract based on CD11c expression. Representative dot plots showing the frequency of CD11c^{+} in CD3^{+} T cells of: (a) peripheral blood of a control animal, (b) peripheral blood and (c) genital tract (GT) of a vaginally (VAG)-infected animal. For each of these subsets (CD11c^{+} top row, CD11c^{-} bottom row) expression of TCRγδ and CD8α or NK1.1 and CD103 is shown.
(TIF)

S3 Fig. Gating strategy of specific T cell phenotypes by CD11c expression in blood and PBMC from healthy women. Example of the frequency of CD161, CD8, Vα24, MAIT and γδTCR in the CD11c^{+} and CD11c^{-}, CCR7^{-} CD3^{+} T cell fractions on fresh blood (left) and processed PBMC (right) from the same individual.
(TIF)

S4 Fig. γδTCR^{+} and CD8^{+} T cells phenotype based on CD11c expression in blood and genital tract from healthy women. The percentage of CD11c in γδTCR^{+} and CD8^{+} T cells is shown for blood (a) and genital tract (GT) (e) from healthy women. A comparison on the expression of CD161 and CD8 in CD11c^{+} γδ T cells vs. total γδ T cells from blood (b and c) and genital tract (f and g) is shown. A comparison on the expression of CD161 in CD11c^{+} CD8^{+} T cells vs. total CD8^{+} T cells from blood (d) and genital tract (h) is shown. Data were analyzed using Wilcoxon matched-paired signed-ranked test.
(TIF)

S5 Fig. Expression of CD69 and CD103 in cervix from healthy women and analysis by CD11c expression. The frequency of CD69 (a) and CD103 (b) by CD11c expression in T cells obtained from cervical tissue is shown. Each bar represents the mean ± SD of the ectocervix and endocervix of each donor (n = 3–5). A comparison on the frequency of CD69 (c) or CD103 (d) in T cells from the same individual based on CD11c expression is shown for both cervical tissues. Data were analyzed using Wilcoxon matched-paired signed-ranked test.
(TIF)

PLOS ONE

Characterization of T Cell Subsets Expressing CD11c

Acknowledgments

Author Contributions

Conceived and designed the experiments: JQ LL SJM MG. Performed the experiments: JQ LL JC MG. Analyzed the data: JQ LL JC LS MG. Contributed reagents/materials/analysis tools: AT MAF AR. Wrote the paper: JQ LL SJM MG.

References

1. Tan SM. The leucocyte beta2 (CD18) integrins: the structure, functional regulation and signalling properties. Bioscience reports. 2012; 32(3):241–69. doi: 10.1042/BSR20110101 PMID: 22458844.

2. Sadhu C, Ting HJ, Lipsky B, Hensley K, Garcia-Martinez LF, Simon SI, et al. CD11c/CD18: novel ligands and a role in delayed-type hypersensitivity. Journal of leukocyte biology. 2007; 81(6):1395–403. doi: 10.1189/jlb.1106680 PMID: 17389580.

3. Vorup-Jensen T, Carman CV, Shimaoka M, Schuck P, Svitel J, Springer TA. Exposure of acidic residues as a danger signal for recognition of fibrinogen and other macromolecules by integrin alphaX-beta2. Proc Natl Acad Sci U S A. 2005; 102(5):1614–9. doi: 10.1073/pnas.0409057102 PMID: 15665082; PubMed Central PMCID: PMC547869.

4. Ganguly D, Haak S, Sisirak V, Reizis B. The role of dendritic cells in autoimmunity. Nat Rev Immunol. 2013; 13(8):566–77. doi: 10.1038/nri3477 PMID: 23827956; PubMed Central PMCID: PMC4160805.

5. Moon JJ, Chu HH, Hataye J, Pagan AJ, Pepper M, McLachlan JB, et al. Tracking epitope-specific T cells. Nat Protoc. 2009; 4(4):565–81. doi: 10.1038/nprot.2009.9 PMID: 19373228; PubMed Central PMCID: PMC3517879.

6. Arakelyan A, Fitzgerald W, Grivel JC, Vanpouille C, Margolis L. Histocultures (tissue explants) in human retrovirology. Methods in molecular biology. 2014; 1087:233–48. doi: 10.1007/978-1-62703-670-2_19 PMID: 24158827.

7. Beyer M, Wang H, Peters N, Doths S, Koerner-Rettberg C, Openshaw PJ, et al. The beta2 integrin CD11c distinguishes a subset of cytotoxic pulmonary T cells with potent antiviral effects in vitro and in vivo. Respir Res. 2005; 6:70. Epub 2005/07/14. 1465-9921-6-70 [pii] doi: 10.1186/1465-9921-6-70 PMID: 16011799; PubMed Central PMCID: PMC1184101.

8. Chen Z, Han Y, Gu Y, Liu Y, Jiang Z, Zhang M, et al. CD11c(high)CD8+ regulatory T cell feedback inhibits CD4 T cell immune response via Fas ligand-Fas pathway. J Immunol. 2013; 190(12):6145–54. Epub 2013/05/17. jimmunol.1300060 [pii] doi: 10.4049/jimmunol.1300060 PMID: 23677464.

9. Cooney LA, Gupta M, Thomas S, Mikolajczak S, Choi KY, Gibson C, et al. Short-lived effector CD8 T cells induced by genetically attenuated malaria parasite vaccination express CD11c. Infect Immun. 2013; 81(11):4171–81. Epub 2013/08/28. IAI.00871-13 [pii] doi: 10.1128/IAI.00871-13 PMID: 23980113; PubMed Central PMCID: PMC3811835.

10. Fujiwara D, Chen L, Wei B, Braun J. Small intestine CD11c+ CD8+ T cells suppress CD4+ T cell-induced immune colitis. Am J Physiol Gastrointest Liver Physiol. 2011; 300(6):G939–47. Epub 2011/03/26. ajpgi.00032.2010 [pii] doi: 10.1152/ajpgi.00032.2010 PMID: 21436315; PubMed Central PMCID: PMC3119121.

11. Kim YH, Seo SK, Choi BK, Kang WJ, Kim CH, Lee SK, et al. 4-1BB costimulation enhances HSV-1-specific CD8+ T cell responses by the induction of CD11c+CD8+ T cells. Cellular immunology. 2005; 238(2):76–86. doi: 10.1016/j.cellimm.2006.01.004 PMID: 16524567.

12. Kubota K, Kadoya Y. Innate IFN-gamma-producing cells in the spleen of mice early after Listeria monocytogenes infection: importance of microenvironment of the cells involved in the production of innate IFN-gamma. Front Immunol. 2011; 2:26. Epub 2011/01/01. doi: 10.3389/fimmu.2011.00026 PMID: 22566816; PubMed Central PMCID: PMC3341966.

13. Egan CE, Craven MD, Leng J, Mack M, Simpson KW, Denkers EY. CCR2-dependent intraepithelial lymphocytes mediate inflammatory gut pathology during Toxoplasma gondii infection. Mucosal Immunol. 2009; 2(6):527–35. doi: 10.1038/mi.2009.105 PMID: 19741601; PubMed Central PMCID: PMC2860785.

14. Huleatt JW, Lefrancois L. Antigen-driven induction of CD11c on intestinal intraepithelial lymphocytes and CD8+ T cells in vivo. J Immunol. 1995; 154(11):5684–93. PMID: 7751620.

PLOS | ONE

15. Bullard DC, Hu X, Adams JE, Schoeb TR, Barnum SR. p150/95 (CD11c/CD18) expression is required for the development of experimental autoimmune encephalomyelitis. The American journal of pathology. 2007; 170(6):2001–8. Epub 2007/05/26. S0002-9440(10)61408-3 [pii] doi: 10.2353/ajpath.2007. 061016 PMID: 17525267; PubMed Central PMCID: PMC1899456.

16. Tsai S, Clemente-Casares X, Santamaria P. CD8(+) Tregs in autoimmunity: learning "self"-control from experience. Cellular and molecular life sciences: CMLS. 2011; 68(23):3781–95. doi: 10.1007/s00018-011-0738-y PMID: 21671120.

17. Kuka M, Munitic I, Ashwell JD. Identification and characterization of polyclonal alphabeta-T cells with dendritic cell properties. Nature communications. 2012; 3:1223. doi: 10.1038/ncomms2223 PMID: 23187623; PubMed Central PMCID: PMC3528357.

18. Gonzalez-Roca E, Garcia-Albeniz X, Rodriguez-Mulero S, Gomis RR, Kornacker K, Auer H. Accurate expression profiling of very small cell populations. PLoS One. 2010; 5(12):e14418. Epub 2011/01/05. doi: 10.1371/journal.pone.0014418 PMID: 21203435; PubMed Central PMCID: PMC3010985.

19. Smyth GK. Limma: linear models for microarray data. In: Gentleman R, Carey V, Dudoit S, Irizarry R, Huber W, editors. Bioinformatics and Computational Biology Solutions Using R and Bioconductor. New York: Springer; 2005. p. 397–420.

20. Bezman NA, Kim CC, Sun JC, Min-Oo G, Hendricks DW, Kamimura Y, et al. Molecular definition of the identity and activation of natural killer cells. Nat Immunol. 2012; 13(10):1000–9. PubMed Central PMCID: PMC3572860. doi: 10.1038/ni.2395 PMID: 22902830

21. Del Campo J, Lindqvist M, Cuello M, Backstrom M, Cabrerra O, Persson J, et al. Intranasal immunization with a proteoliposome-derived cochleate containing recombinant gD protein confers protective immunity against genital herpes in mice. Vaccine. 2010; 28(5):1193–200. doi: 10.1016/j.vaccine.2009. 11.035 PMID: 19945418.

22. Denucci CC, Mitchell JS, Shimizu Y. Integrin function in T-cell homing to lymphoid and nonlymphoid sites: getting there and staying there. Critical reviews in immunology. 2009; 29(2):87–109. PMID: 19496742; PubMed Central PMCID: PMC2744463.

23. Li LX, McSorley SJ. B cells enhance antigen-specific CD4 T cell priming and prevent bacteria dissemination following Chlamydia muridarum genital tract infection. PLoS pathogens. 2013; 9(10):e1003707. doi: 10.1371/journal.ppat.1003707 PMID: 24204262; PubMed Central PMCID: PMC3814678.

24. Fuller JM, Raghupathi KR, Ramireddy RR, Subrahmanyam AV, Yesilyurt V, Thayumanavan S. Temperature-sensitive transitions below LCST in amphiphilic dendritic assemblies: host-guest implications. Journal of the American Chemical Society. 2013; 135(24):8947–54. doi: 10.1021/ja402019c PMID: 23692369; PubMed Central PMCID: PMC3706455.

25. Roederer M, Nozzi JL, Nason MC. SPICE: exploration and analysis of post-cytometric complex multivariate datasets. Cytometry Part A: the journal of the International Society for Analytical Cytology. 2011; 79(2):167–74. doi: 10.1002/cyto.a.21015 PMID: 21265010; PubMed Central PMCID: PMC3072288.

26. Grivel JC, Margolis L. Use of human tissue explants to study human infectious agents. Nat Protoc. 2009; 4(2):256–69. doi: 10.1038/nprot.2008.245 PMID: 19197269; PubMed Central PMCID: PMC3427853.

27. Lycke N. Recent progress in mucosal vaccine development: potential and limitations. Nat Rev Immunol. 2012; 12(8):592–605. doi: 10.1038/nri3251 PMID: 22828912.

28. Fergusson JR, Smith KE, Fleming VM, Rajoriya N, Newell EW, Simmons R, et al. CD161 defines a transcriptional and functional phenotype across distinct human T cell lineages. Cell reports. 2014; 9 (3):1075–88. doi: 10.1016/j.celrep.2014.09.045 PMID: 25437561; PubMed Central PMCID: PMC4250839.

29. Trifonova RT, Lieberman J, van Baarle D. Distribution of immune cells in the human cervix and implications for HIV transmission. Am J Reprod Immunol. 2014; 71(3):252–64. doi: 10.1111/aji.12198 PMID: 24410939; PubMed Central PMCID: PMC3943534.

30. Eberl M, Hintz M, Reichenberg A, Kollas AK, Wiesner J, Jomaa H. Microbial isoprenoid biosynthesis and human gammadelta T cell activation. FEBS Lett. 2003; 544(1–3):4–10. PMID: 12782281.

31. Pennington DJ, Vermijlen D, Wise EL, Clarke SL, Tigelaar RE, Hayday AC. The integration of conventional and unconventional T cells that characterizes cell-mediated responses. Advances in immunology. 2005; 87:27–59. doi: 10.1016/S0065-2776(05)87002-6 PMID: 16102571.

32. Godfrey DI, MacDonald HR, Kronenberg M, Smyth MJ, Van Kaer L. Opinion—NKT cells: what's in a name? Nature Reviews Immunology. 2004; 4(3):231–7. doi: 10.1038/Nri11309 PMID: WOS:000189345200017.

33. Ljutic B, Carlyle JR, Filipp D, Nakagawa R, Julius M, Zuniga-Pflucker JC. Functional requirements for signaling through the stimulatory and inhibitory mouse NKR-P1 (CD161) NK cell receptors. J Immunol. 2005; 174(8):4789–96. PMID: 15814704.

34. Haas JD, Gonzalez FH, Schmitz S, Chennupati V, Fohse L, Kremmer E, et al. CCR6 and NK1.1 distinguish between IL-17A and IFN-gamma-producing gammadelta effector T cells. Eur J Immunol. 2009; 39(12):3488–97. doi: 10.1002/eji.200939922 PMID: 19830744.

35. Romagnoli PA, Premenko-Lanier MF, Loria GD, Altman JD. CD8 T Cell Memory Recall Is Enhanced by Novel Direct Interactions with CD4 T Cells Enabled by MHC Class II Transferred from APCs. PLoS One. 2013; 8(2). ARTN e56999 doi: 10.1371/journal.pone.0056999 PMID: WOS:000315159200086.

36. Qureshi OS, Zheng Y, Nakamura K, Attridge K, Manzotti C, Schmidt EM, et al. Trans-Endocytosis of CD80 and CD86: A Molecular Basis for the Cell-Extrinsic Function of CTLA-4. Science. 2011; 332 (6029):600–3. doi: 10.1126/science.1202947 PMID: WOS:000289991100052.

37. Brandes M, Willimann K, Moser B. Professional antigen-presentation function by human gammadelta T Cells. Science. 2005; 309(5732):264–8. doi: 10.1126/science.1110267 PMID: 15933162.

38. Williams DM, Grubbs BG, Kelly K, Pack E, Rank RG. Role of gamma-delta T cells in murine Chlamydia trachomatis infection. Infect Immun. 1996; 64(9):3916–9. PMID: 8751950; PubMed Central PMCID: PMC174314.

39. Cauley LS, Lefrancois L. Guarding the perimeter: protection of the mucosa by tissue-resident memory T cells. Mucosal Immunol. 2013; 6(1):14–23. Epub 2012/11/08. mi201296 [pii] doi: 10.1038/mi.2012.96 PMID: 23131785.

40. Farber DL, Yudanin NA, Restifo NP. Human memory T cells: generation, compartmentalization and homeostasis. Nat Rev Immunol. 2014; 14(1):24–35. doi: 10.1038/nri3567 PMID: 24336101; PubMed Central PMCID: PMC4032067.

41. Paul S, Shilpi, Lal G. Role of gamma-delta (gammadelta) T cells in autoimmunity. Journal of leukocyte biology. 2015; 97(2):259–71. doi: 10.1189/jlb.3RU0914-443R PMID: 25502468.

42. Billerbeck E, Kang YH, Walker L, Lockstone H, Grafmueller S, Fleming V, et al. Analysis of CD161 expression on human CD8+ T cells defines a distinct functional subset with tissue-homing properties. Proc Natl Acad Sci U S A. 2010; 107(7):3006–11. Epub 2010/02/06. 0914839107 [pii] doi: 10.1073/pnas.0914839107 PMID: 20133607; PubMed Central PMCID: PMC2840308.

References

1. Schröder K, Bosch TC. The origin of mucosal immunity: lessons from the holobiont Hydra. mBio. 2016;7(6):e01184-16.

2. Russell MW, Mestecky J, Strober W, Lambrecht BN, Kelsall BL, Cheroutre H. Overview: The Mucosal Immune System. The Mucosal Immune System. In: Mucosal Immunology: Fourth Edition. 2015. p. 3–8.

3. Holmgren J, Czerkinsky C. Mucosal immunity and vaccines. Nat Med. 2005;11(4):S45–53.

4. Kelsall BL, Strober W. Overview: Inductive and Effector Cells and Tissues of the Mucosal Immune System. In: Mucosal Immunology: Fourth Edition. 2015. p. 487–8.

5. Russell MW, Mestecky J, Strober W, Lambrecht BN, Kelsall BL, Cheroutre H. Overview: The Mucosal Immune System. In: Mucosal Immunology: Fourth Edition. 2015. p. 3–8.

6. Holmgren J, Czerkinsky C. Mucosal immunity and vaccines. Nat Med. 2005;11(4S):S45.

7. Mikhak Z, Agace WW, Luster AD. Lymphocyte Trafficking to Mucosal Tissues [Internet]. Fourth Edi. Vols. 1–2, Mucosal Immunology: Fourth Edition. Elsevier; 2015. 805–830 p. Available from: http://dx.doi.org/10.1016/B978-0-12-415847-4.00040-9

8. Brandtzaeg P. Overview of the mucosal immune system. Curr Top Microbiol Immunol. 1989;146:13–25.

9. Zeissig S, Mayer L, Blumberg RS. Role of Epithelial Cells in Antigen Presentation [Internet]. Fourth Edi. Vols. 1–2, Mucosal Immunology: Fourth Edition. Elsevier; 2015. 557–570 p. Available from: http://dx.doi.org/10.1016/B978-0-12-415847-4.00027-6

10. Larsen SB, Cowley CJ, Fuchs E. Epithelial cells: liaisons of immunity. Curr Opin Immunol [Internet]. 2020 Feb 1 [cited 2023 May 21];62:45. Available from: /pmc/articles/PMC7067656/

11. Laiosa C V., Stadtfeld M, Graf T. DETERMINANTS OF LYMPHOID-MYELOID LINEAGE DIVERSIFICATION. https://doi.org/101146/annurev.immunol24021605090742 [Internet]. 2006 Mar 21 [cited 2023 May 21];24:705–38. Available from: https://www.annualreviews.org/doi/abs/10.1146/annurev.immunol.24.021605.090742

12. Iwasaki H, Akashi K. Myeloid Lineage Commitment from the Hematopoietic Stem Cell. Immunity. 2007 Jun 22;26(6):726–40.

13. De Kleer I, Willems F, Lambrecht B, Goriely S, Kollmann TR, Zwirner NW. Ontogeny of myeloid cells. 2014; Available from: www.frontiersin.org

14. Weiskopf K, Schnorr PJ, Pang WW, Chao MP, Chhabra A, Seita J, et al. Myeloid Cell Origins, Differentiation, and Clinical Implications. 2016; Available from: https://journals.asm.org/journal/spectrum

15. Kapellos TS, Bonaguro L, Gemünd I, Reusch N, Saglam A, Hinkley ER, et al. Human monocyte subsets and phenotypes in major chronic inflammatory diseases. Front Immunol. 2019 Aug 30;10(AUG):2035.

16. Guermonprez P, Jung S, Kapellos TS, Schultze JL, Bonaguro L, Gemünd I, et al. Human Monocyte Subsets and Phenotypes in Major Chronic Inflammatory Diseases. Chronic Inflammatory Diseases Front Immunol [Internet]. 2019;1:2035. Available from: www.frontiersin.org

17. Ożańska A, Szymczak D, Rybka J. Pattern of human monocyte subpopulations in health and disease. Scand J Immunol. 2020;92(1).

18. Laiosa C V., Stadtfeld M, Graf T. DETERMINANTS OF LYMPHOID-MYELOID LINEAGE   DIVERSIFICATION. https://doi.org/101146/annurev.immunol24021605090742 [Internet]. 2006 Mar 21 [cited 2023 May 21];24:705–38. Available from: https://www.annualreviews.org/doi/abs/10.1146/annurev.immunol.24.021605.0 90742

19. Fayette J, Dubois B, Vandenabeele S, Bridon JM, Vanbervliet B, Durand I, et al. Human dendritic cells skew isotype switching of CD40-activated naive B cells towards IgA1 and IgA2. J Exp Med. 1997 Jun 2;185(11):1909–18.

20. Soto JA, Gálvez NMS, Andrade CA, Pacheco GA, Bohmwald K, Berrios R V., et al. The Role of Dendritic Cells During Infections Caused by Highly Prevalent Viruses. Front Immunol. 2020 Jul 16;11:1513.

21. Cabeza-Cabrerizo M, Cardoso A, Minutti CM, Pereira da Costa M, Reis Sousa C. Annual Review of Immunology Dendritic Cells Revisited. 2021; Available from: https://doi.org/10.1146/annurev-immunol-061020-

22. Soltani S, Mahmoudi M, Farhadi E. Dendritic Cells Currently under the Spotlight; Classification and Subset Based upon New Markers. Immunol Invest [Internet]. 2021;50(6):646–61.   Available   from: https://doi.org/10.1080/08820139.2020.1783289

23. Collin M, Mcgovern N, Haniffa M. Human dendritic cell subsets. Immunology [Internet]. 2013 Sep [cited 2023 May 21];140(1):22. Available from: /pmc/articles/PMC3809702/

24. Germic N, Ziva Frangez •, Yousefi S, Simon • Hans-Uwe. Regulation of the innate immune system by autophagy: monocytes, macrophages, dendritic cells and antigen presentation. Cell Death Differ [Internet]. 2019;26:715–27. Available from: https://doi.org/10.1038/s41418-019-0297-6

25. Hovav AH. Dendritic cells of the oral mucosa. Mucosal Immunology 2014 7:1 [Internet]. 2013 Jun 12 [cited 2023 May 21];7(1):27–37. Available from: https://www.nature.com/articles/mi201342

26. Nijmeijer BM, Langedijk CJM, Geijtenbeek TBH. Mucosal Dendritic Cell Subsets Control HIV-1's Viral Fitness. https://doi.org/101146/annurev-virology-020520-025625 [Internet]. 2020 Sep 29 [cited 2023 May 21];7:385–402. Available from: https://www.annualreviews.org/doi/abs/10.1146/annurev-virology-020520-025625

27. Hovav AH. Dendritic cells of the oral mucosa. Mucosal Immunology 2014 7:1 [Internet]. 2013 Jun 12 [cited 2023 May 21];7(1):27–37. Available from: https://www.nature.com/articles/mi201342

28. Rodriguez-Garcia M, Connors K, Ghosh M. HIV Pathogenesis in the Human Female Reproductive Tract HHS Public Access. 2021;18(2):139–56.

29. Yunna C, Mengru H, Lei W, Weidong C. Macrophage M1/M2 polarization. Eur J Pharmacol [Internet]. 2020;877(November 2019):173090. Available from: https://doi.org/10.1016/j.ejphar.2020.173090

30. Sreejit G, Fleetwood AJ, Murphy AJ, Nagareddy PR. Origins and diversity of macrophages in health and disease. Clin Transl Immunology. 2020;9(12):1–19.

31. Chávez-Galán L, Olleros ML, Vesin D, Garcia I. Much more than M1 and M2 macrophages, there are also CD169+ and TCR+ macrophages. Front Immunol. 2015 May 26;6(MAY):263.

32. Fitzgerald KA, Kagan JC. Toll-like Receptors and the Control of Immunity. Vol. 180, Cell. 2020. p. 1044–66.

33. Dennis EA, Robinson TO, Smythies LE, Smith PD. Characterization of human blood monocytes and intestinal macrophages. Curr Protoc Immunol. 2017 Aug 1;2017:14.3.1-14.3.14.

34. Yao X, Dong G, Zhu Y, Yan F, Zhang H, Ma Q, et al. Leukadherin-1-Mediated activation of CD11b Inhibits LPS-Induced pro-inflammatory response in macrophages and protects mice against endotoxic shock by blocking LPS-TLR4 interaction. Front Immunol. 2019 Feb 12;10(FEB):215.

35. Smith PD, Smythies LE, Shen R, Greenwell-Wild T, Gliozzi M, Wahl SM. Intestinal macrophages and response to microbial encroachment. Mucosal Immunol [Internet]. 2010 Oct 20 [cited 2023 Jun 5];4(1):31–42. Available from: https://www.ncbi.nlm.nih.gov/pmc/articles/pmid/20962772/?tool=EBI

36. Krishnaswamy JK, Alsén S, Yrlid U, Eisenbarth SC, Williams A. Determination of T Follicular Helper Cell Fate by Dendritic Cells. Front Immunol. 2018 Sep 27;9.

37. Mousset CM, Hobo W, Woestenenk R, Preijers F, Dolstra H, van der Waart AB. Comprehensive Phenotyping of T Cells Using Flow Cytometry. Cytometry Part A

[Internet]. 2019 Jun 1 [cited 2023 May 27];95(6):647–54. Available from: https://onlinelibrary.wiley.com/doi/full/10.1002/cyto.a.23724

38. Jameson SC, Masopust D. Understanding Subset Diversity in T Cell Memory. Immunity [Internet]. 2018;48(2):214–26. Available from: https://doi.org/10.1016/j.immuni.2018.02.010

39. Farber DL, Yudanin NA, Restifo NP. Human memory T cells: generation, compartmentalization and homeostasis. Nat Rev Immunol [Internet]. 2014 Jan [cited 2023 Jun 6];14(1):24. Available from: /pmc/articles/PMC4032067/

40. Miron M, Meng W, Rosenfeld AM, Dvorkin S, Poon MML, Lam N, et al. Maintenance of the human memory T cell repertoire by subset and tissue site. Genome Med. 2021;13(1):1–14.

41. Mami-Chouaib F, Tartour E. Editorial: Tissue resident memory T cells. Front Immunol. 2019 May 27;10(MAY):1018.

42. Yenyuwadee S, Sanchez-Trincado Lopez JL, Shah R, Rosato PC, Boussiotis VA. The evolving role of tissue-resident memory T cells in infections and cancer. Sci Adv [Internet]. 2022 Aug 19 [cited 2023 May 27];8(33):5871. Available from: https://www.science.org/doi/10.1126/sciadv.abo5871

43. Golubovskaya V, Wu L. Different Subsets of T Cells, Memory, Effector Functions, and CAR-T Immunotherapy. Cancers (Basel) [Internet]. 2016 Mar 15 [cited 2023 May 27];8(3). Available from: /pmc/articles/PMC4810120/

44. Seder RA, Ahmed R. Similarities and differences in CD4+ and CD8+ effector and memory T cell generation. Nature Immunology 2003 4:9 [Internet]. 2003 Sep 1 [cited 2023 May 27];4(9):835–42. Available from: https://www.nature.com/articles/ni969

45. Appay V, Van Lier RAW, Sallusto F, Roederer M. Phenotype and function of human T lymphocyte subsets: Consensus and issues. Cytometry Part A [Internet]. 2008 Nov 1 [cited 2023 May 27];73A(11):975–83. Available from: https://onlinelibrary.wiley.com/doi/full/10.1002/cyto.a.20643

46. Martin MD, Badovinac VP. Defining memory CD8 T cell. Front Immunol. 2018;9(NOV):1–10.

47. Radulovic K, Rossini V, Manta C, Holzmann K, Kestler HA, Niess JH. The Early Activation Marker CD69 Regulates the Expression of Chemokines and CD4 T Cell Accumulation in Intestine. PLoS One [Internet]. 2013 Jun 12 [cited 2023 Jun 6];8(6):e65413. Available from: https://journals.plos.org/plosone/article?id=10.1371/journal.pone.0065413

48. Cibrián D, Sánchez-Madrid F. CD69: from activation marker to metabolic gatekeeper. Eur J Immunol [Internet]. 2017 Jun 1 [cited 2023 Jun 6];47(6):946. Available from: /pmc/articles/PMC6485631/

49. Younas M, Psomas C, Reynes J, Corbeau P. Immune activation in the course of HIV-1 infection: Causes, phenotypes and persistence under therapy. HIV Med. 2016 Feb 1;17(2):89–105.

50. Cezar R, Winter A, Desigaud D, Pastore M, Kundura L, Dupuy AM, et al. Identification of distinct immune activation profiles in adult humans. Scientific Reports 2020 10:1 [Internet]. 2020 Nov 30 [cited 2023 Jun 6];10(1):1–14. Available from: https://www.nature.com/articles/s41598-020-77707-6

51. Xie G, Luo X, Ma T, Frouard J, Neidleman J, Hoh R, et al. Characterization of HIV-induced remodeling reveals differences in infection susceptibility of memory CD4+ T cell subsets in vivo. Cell Rep [Internet]. 2021;35(4):109038. Available from: https://doi.org/10.1016/j.celrep.2021.109038

52. Sabat R, Wolk K, Loyal L, Döcke WD, Ghoreschi K. T cell pathology in skin inflammation. Seminars in Immunopathology 2019 41:3 [Internet]. 2019 Apr 26 [cited 2023 May 27];41(3):359–77. Available from: https://link.springer.com/article/10.1007/s00281-019-00742-7

53. Sallusto F, Geginat J, Lanzavecchia A. Central memory and effector memory T cell subsets: function, generation, and maintenance. Annu Rev Immunol [Internet]. 2004 [cited 2023 May 27];22:745–63. Available from: https://pubmed.ncbi.nlm.nih.gov/15032595/

54. Taniuchi I. CD4 Helper and CD8 Cytotoxic T Cell Differentiation. Annu Rev Immunol [Internet]. 2018 Apr 26 [cited 2023 May 20];36:579–601. Available from: https://pubmed.ncbi.nlm.nih.gov/29677476/

55. Tuzlak S, Dejean AS, Iannacone M, Quintana FJ, Waisman A, Ginhoux F, et al. Repositioning TH cell polarization from single cytokines to complex help. Nature Immunology 2021 22:10 [Internet]. 2021 Sep 20 [cited 2023 May 20];22(10):1210–7. Available from: https://www.nature.com/articles/s41590-021-01009-w

56. Serafini N, Di Santo JP. Effector Cells of the Mucosal Immune System: Innate Lymphoid Cells [Internet]. Fourth Edi. Vols. 1–2, Mucosal Immunology: Fourth Edition. Elsevier; 2015. 787–804 p. Available from: http://dx.doi.org/10.1016/B978-0-12-415847-4.00039-2

57. Maynard CL, Weaver CT. Effector CD4+ T Cells in the Intestines [Internet]. Fourth Edi. Vols. 1–2, Mucosal Immunology: Fourth Edition. Elsevier; 2015. 721–732 p. Available from: http://dx.doi.org/10.1016/B978-0-12-415847-4.00034-3

58. Campbell DJ, Debes GF, Johnston B, Wilson E, Butcher EC. Targeting T cell responses by selective chemokine receptor expression. Semin Immunol. 2003;15(5):277–86.

59. Lieberman J. The ABCs of granule-mediated cytotoxicity: New weapons in the arsenal. Vol. 3, Nature Reviews Immunology. 2003. p. 361–70.

60. St. Paul M, Ohashi PS. The Roles of CD8+ T Cell Subsets in Antitumor Immunity. Trends Cell Biol [Internet]. 2020;30(9):695–704. Available from: https://doi.org/10.1016/j.tcb.2020.06.003

61. Willinger T, Freeman T, Hasegawa H, McMichael AJ, Callan MFC. Molecular signatures distinguish human central memory from effector memory CD8 T cell subsets. J Immunol [Internet]. 2005 Nov 1 [cited 2023 May 27];175(9):5895–903. Available from: https://pubmed.ncbi.nlm.nih.gov/16237082/

62. Fuchs A, Colonna M. Natural killer (NK) and NK-like cells at mucosal epithelia: Mediators of anti-microbial defense and maintenance of tissue integrity. Eur J Microbiol Immunol (Bp). 2011;1(4):257–66.

63. Kurashima Y, Goto Y, Kiyono H. Mucosal innate immune cells regulate both gut homeostasis and intestinal inflammation. Eur J Immunol. 2013;43(12):3108–15.

64. Ivanova D, Krempels R, Ryfe J, Weitzman K, Stephenson D, Gigley JP. NK cells in mucosal defense against infection. Biomed Res Int. 2014;2014.

65. Kronenberg M, Lantz O. Mucosal-Resident T Lymphocytes with Invariant Antigen Receptors. In: Mucosal Immunology: Fourth Edition. 2015. p. 749–64.

66. Nguyen P V., Kafka JK, Ferreira VH, Roth K, Kaushic C. Innate and adaptive immune responses in male and female reproductive tracts in homeostasis and following HIV infection. Cell Mol Immunol. 2014;11(5):410–27.

67. Constantinides MG, Belkaid Y. Early-life imprinting of unconventional T cells and tissue homeostasis. Science [Internet]. 2021 Dec 12 [cited 2023 May 21];374(6573):eabf0095. Available from: /pmc/articles/PMC8697520/

68. Dunne MR, Wagener J, Loeffler J, Doherty DG, Rogers TR. Unconventional T cells – New players in antifungal immunity. Clinical Immunology. 2021 Jun 1;227:108734.

69. Ataide MA, Knöpper K, Cruz de Casas P, Ugur M, Eickhoff S, Zou M, et al. Lymphatic migration of unconventional T cells promotes site-specific immunity in distinct lymph nodes. Immunity [Internet]. 2022 Oct 11 [cited 2023 May 21];55(10):1813-1828.e9. Available from: http://www.cell.com/article/S1074761322003545/fulltext

70. Ashkar AA, Rosenthal KL. Interleukin-15 and Natural Killer and NKT Cells Play a Critical Role in Innate Protection against Genital Herpes Simplex Virus Type 2 Infection. J Virol. 2003;77(18):10168–71.

71. Middendorp S, Nieuwenhuis EES. NKT cells in mucosal immunity. Mucosal Immunol. 2009;2(5):393–402.

72. Kronenberg M, Lantz O. Mucosal-Resident T Lymphocytes with Invariant Antigen Receptors. In: Mucosal Immunology: Fourth Edition. 2015. p. 749–64.

73. Ashkar AA, Rosenthal KL. Interleukin-15 and Natural Killer and NKT Cells Play a Critical Role in Innate Protection against Genital Herpes Simplex Virus Type 2 Infection. J Virol. 2003;77(18):10168–71.

74. Middendorp S, Nieuwenhuis EES. NKT cells in mucosal immunity. Mucosal Immunol. 2009;2(5):393–402.

75. Le Bourhis L, Martin E, Péguillet I, Guihot A, Froux N, Coré M, et al. Antimicrobial activity of mucosal-associated invariant T cells. Nat Immunol. 2010;11(8):701–8.

76. Dusseaux M, Martin E, Serriari N, Péguillet I, Premel V, Louis D, et al. Human MAIT cells are xenobiotic-resistant, tissue-targeted, CD161 hi IL-17-secreting T cells. Blood. 2011;117(4):1250–9.

77. McCarthy NE, Eberl M. Human γδ T-cell control of mucosal immunity and inflammation. Front Immunol. 2018;9(MAY).

78. Hayday A, Deban L. Mucosal T Cell Receptor γδ Intraepithelial T Cells. In: Mucosal Immunology: Fourth Edition. 2015. p. 765–76.

79. McCarthy NE, Eberl M. Human γδ T-cell control of mucosal immunity and inflammation. Front Immunol. 2018;9(MAY).

80. Sheridan BS, Romagnoli PA, Pham QM, Fu HH, Alonzo F, Schubert WD, et al. γδ T Cells Exhibit Multifunctional and Protective Memory in Intestinal Tissues. Immunity. 2013;39(1):184–95.

81. Kumar A, Singh B, Tiwari R, Singh VK, Singh SS, Sundar S, et al. Emerging role of γδ T cells in protozoan infection and their potential clinical application. Infection, Genetics and Evolution. 2022 Mar 1;98:105210.

82. Tuero I, Venzon D, Robert-Guroff M. Mucosal and Systemic γδ + T Cells Associated with Control of Simian Immunodeficiency Virus Infection. The Journal of Immunology. 2016;197(12):4686–95.

83. Mikhak Z, Agace WW, Luster AD. Lymphocyte Trafficking to Mucosal Tissues. In: Mucosal Immunology: Fourth Edition. 2015. p. 805–30.

84. Campbell DJ, Debes GF, Johnston B, Wilson E, Butcher EC. Targeting T cell responses by selective chemokine receptor expression. Semin Immunol. 2003;15(5):277–86.

85. Hart AL, Ng SC, Mann E, Al-Hassi HO, Bernardo D, Knight SC. Homing of immune cells: Role in homeostasis and intestinal inflammation. Inflamm Bowel Dis. 2010;16(11):1969–77.

86. Stagg AJ, Kamm MA, Knight SC. Intestinal dendritic cells increase T cell expression of α4β7 integrin. Eur J Immunol. 2002;32(5):1445–54.

87. Mikhak Z, Agace WW, Luster AD. Lymphocyte Trafficking to Mucosal Tissues. In: Mucosal Immunology: Fourth Edition. 2015. p. 805–30.

88. Krummel MF, Bartumeus F, Gérard A. T cell migration, search strategies and mechanisms. Nat Rev Immunol [Internet]. 2016;16(3):193–201. Available from: http://dx.doi.org/10.1038/nri.2015.16

89. Gasteiger G, Ataide M, Kastenmüller W. Lymph node - An organ for T-cell activation and pathogen defense. Immunol Rev. 2016;271(1):200–20.

90. Arasa J, Collado-diaz V, Halin C. Structure and immune function of afferent lymphatics and their mechanistic contribution to dendritic cell and t cell trafficking. Cells. 2021;10(5).

91. Hunter MC, Teijeira A, Halin C. T cell trafficking through lymphatic vessels. Front Immunol. 2016;7(DEC):613.

92. Krummel MF, Bartumeus F, Gérard A. T cell migration, search strategies and mechanisms. Nature Reviews Immunology 2016 16:3 [Internet]. 2016 Feb 8 [cited 2023 Jun 14];16(3):193–201. Available from: https://www.nature.com/articles/nri.2015.16

93. Hunter MC, Teijeira A, Halin C. T cell trafficking through lymphatic vessels. Front Immunol. 2016;7(DEC).

94. Bousso P. T-cell activation by dendritic cells in the lymph node: lessons from the movies. Nature Reviews Immunology 2008 8:9 [Internet]. 2008 Sep [cited 2023 Jun 14];8(9):675–84. Available from: https://www.nature.com/articles/nri2379

95. Albelda SM, Smith CW, Ward PA. Adhesion molecules and inflammatory injury. The FASEB Journal. 1994 May;8(8):504–12.

96. Hunter MC, Teijeira A, Halin C. T cell trafficking through lymphatic vessels. Front Immunol. 2016;7(DEC).

97. Anderson LR, Owens TW, Naylor MJ. Structural and mechanical functions of integrins. Biophys Rev [Internet]. 2014 [cited 2023 Jun 8];6(2):203. Available from: /pmc/articles/PMC5418412/

98. Walling BL, Kim M. LFA-1 in T cell migration and differentiation. Front Immunol. 2018 May 3;9(MAY).

99. Jankowska KI, Williamson EK, Roy NH, Blumenthal D, Chandra V, Baumgart T, et al. Integrins modulate T cell receptor signaling by constraining actin flow at the immunological synapse. Front Immunol. 2018 Jan 18;9(JAN):25.

100. Zhang Y, Wang H. Integrin signalling and function in immune cells. Vol. 135, Immunology. 2012. p. 268–75.

101. Zlotnik A, Yoshie O. Chemokines: A new classification system and their role in immunity. J Cult Herit. 2000;1(2):121–7.

102. Cuesta-Gomez N, Graham GJ, Campbell JDM. Chemokines and their receptors: predictors of the therapeutic potential of mesenchymal stromal cells. J Transl Med. 2021;19(1).

103. Cuesta-Gomez N, Graham GJ, Campbell JDM. Chemokines and their receptors: predictors of the therapeutic potential of mesenchymal stromal cells. J Transl Med. 2021;19(1).

104. Tang P, Wang J. Chemokines: the past, the present and the future. Cell Mol Immunol. 2017;15:4.

105. Picker L, Terstappen LWMM, Rott LS, Streeter PR, Stein H, Butcher EC. Differential expression of homing-associated adhesion molecules by T cell subsets in man. Journal of Immunology. 1990;145(10).

106. Luster AD, Alon R, von Andrian UH. Immune cell migration in inflammation: Present and future therapeutic targets. Nat Immunol. 2005;6(12):1182–90.

107. Nourshargh S, Alon R. Leukocyte Migration into Inflamed Tissues. Immunity [Internet]. 2014;41(5):694–707. Available from: http://dx.doi.org/10.1016/j.immuni.2014.10.008

108. Weninger W, Biro M, Jain R. Leukocyte migration in the interstitial space of non-lymphoid organs. Nat Rev Immunol [Internet]. 2014;14(4):232–46. Available from: http://dx.doi.org/10.1038/nri3641

109. Rose DM, Alon R, Ginsberg MH. Integrin modulation and signaling in leukocyte adhesion and migration. Immunol Rev. 2007;218(1):126–34.

110. Kinashi T, Aker M, Sokolovsky-Eisenberg M, Grabovsky V, Tanaka C, Shamri R, et al. LAD-III, a leukocyte adhesion deficiency syndrome associated with defective Rap1 activation and impaired stabilization of integrin bonds. Blood. 2004;103(3):1033–6.

111. Hamann A, Syrbe U. T-cell trafficking into sites of inflammation. Rheumatology [Internet]. 2000 Jul 1 [cited 2023 Jun 8];39(7):696–9. Available from: https://dx.doi.org/10.1093/rheumatology/39.7.696

112. Sakai Y, Kobayashi M. Lymphocyte "homing" and chronic inflammation. Pathol Int [Internet]. 2015 Jul 1 [cited 2023 Jun 8];65(7):344–54. Available from: https://pubmed.ncbi.nlm.nih.gov/25831975/

113. Etzioni A. Adhesion Molecules-Their Role in Health and Disease. Pediatr Res. 1996;39(2):191–8.

114. Luster AD, Alon R, von Andrian UH. Immune cell migration in inflammation: Present and future therapeutic targets. Nat Immunol. 2005;6(12):1182–90.

115. Wiendl M, Becker E, Müller TM, Voskens CJ, Neurath MF, Zundler S. Targeting Immune Cell Trafficking – Insights From Research Models and Implications for Future IBD Therapy. Front Immunol. 2021;12.

116. Overstreet MG, Gaylo A, Angermann BR, Hughson A, Hyun YM, Lambert K, et al. Inflammation-induced interstitial migration of effector CD4+ T cells is dependent on integrin α v. Nat Immunol. 2013;14(9):949–58.

117. Dai B, Hackney JA, Ichikawa R, Nguyen A, Elstrott J, Orozco LD, et al. Dual targeting of lymphocyte homing and retention through α4β7 and αEβ7 inhibition in inflammatory bowel disease. Cell Rep Med. 2021;2(8).

118. Dai B, Hackney JA, Ichikawa R, Nguyen A, Elstrott J, Orozco LD, et al. Dual targeting of lymphocyte homing and retention through α4β7 and αEβ7 inhibition in inflammatory bowel disease. Cell Rep Med. 2021;2(8).

119. Wang X, Xu H, Gill AF, Pahar B, Kempf D, Rasmussen T, et al. Monitoring α4β7 integrin expression on circulating CD4+ T cells as a surrogate marker for tracking intestinal CD4+ T-cell loss in SIV infection. Mucosal Immunol. 2009;2(6):518–26.

120. Wang X, Xu H, Gill AF, Pahar B, Kempf D, Rasmussen T, et al. Monitoring α4β7 integrin expression on circulating CD4+ T cells as a surrogate marker for tracking intestinal CD4+ T-cell loss in SIV infection. Mucosal Immunol. 2009;2(6):518–26.

121. Santamaria-Babí LF. CLA+ T cells in cutaneous diseases. European Journal of Dermatology. 2004;14(1):13–8.

122. Santamaria-Babí LF. CLA+ T cells in cutaneous diseases. European Journal of Dermatology. 2004;14(1):13–8.

123. Sabat R, Wolk K, Loyal L, Döcke WD, Ghoreschi K. T cell pathology in skin inflammation. Semin Immunopathol. 2019;41(3):359–77.

124. Sabat R, Wolk K, Loyal L, Döcke WD, Ghoreschi K. T cell pathology in skin inflammation. Semin Immunopathol. 2019;41(3):359–77.

125. Rivino L, Kumaran EA, Thein TL, Too CT, Gan VCH, Hanson BJ, et al. Virus-specific T lymphocytes home to the skin during natural dengue infection. Sci Transl Med. 2015;7(278).

126. Zimmer CL, Cornillet M, Solà-Riera C, Cheung KW, Ivarsson MA, Lim MQ, et al. NK cells are activated and primed for skin-homing during acute dengue virus infection in humans. Nat Commun. 2019;10(1).

127. Rivino L, Kumaran EA, Thein TL, Too CT, Gan VCH, Hanson BJ, et al. Virus-specific T lymphocytes home to the skin during natural dengue infection. Sci Transl Med. 2015;7(278).

128. Bordon Y. Air miles for T cells. Nat Rev Immunol. 2013;13(10):705–705.

129. Alon R, Sportiello M, Kozlovski S, Kumar A, Reilly EC, Zarbock A, et al. Leukocyte trafficking to the lungs and beyond: lessons from influenza for COVID-19. Nature Reviews Immunology 2020 21:1 [Internet]. 2020 Nov 19 [cited 2022 Jun 27];21(1):49–64. Available from: https://www.nature.com/articles/s41577-020-00470-2

130. Ssemaganda A, Nguyen HM, Nuhu F, Jahan N, Card CM, Kiazyk S, et al. Expansion of cytotoxic tissue-resident CD8+ T cells and CCR6+CD161+ CD4+ T cells in the nasal mucosa following mRNA COVID-19 vaccination. Nature Communications 2022 13:1 [Internet]. 2022 Jun 10 [cited 2022 Jun 27];13(1):1–9. Available from: https://www.nature.com/articles/s41467-022-30913-4

131. Hoft SG, Sallin MA, Kauffman KD, Sakai S, Ganusov V V., Barber DL. The rate of CD4 T cell entry into the lungs during mycobacterium tuberculosis infection is determined by partial and opposing effects of multiple chemokine receptors. Infect Immun [Internet]. 2019 [cited 2022 Jun 27];87(6). Available from: https://journals.asm.org/doi/full/10.1128/IAI.00841-18

132. Pejoski D, Ballester M, Auderset F, Vono M, Christensen D, Andersen P, et al. Site-Specific DC Surface Signatures Influence CD4+ T Cell Co-stimulation and Lung-Homing. Front Immunol. 2019;10(JULY).

133. Danilova E, Skrindo I, Gran E, Hales BJ, Smith WA, Jahnsen J, et al. A role for CCL28–CCR3 in T-cell homing to the human upper airway mucosa. Mucosal Immunology 2015 8:1 [Internet]. 2014 Jun 11 [cited 2022 Jun 27];8(1):107–14. Available from: https://www.nature.com/articles/mi201446

134. Bordon Y. Air miles for T cells. Nature Reviews Immunology 2013 13:10 [Internet]. 2013 Sep 16 [cited 2022 Jun 27];13(10):705–705. Available from: https://www.nature.com/articles/nri3537

135. Pejoski D, Ballester M, Auderset F, Vono M, Christensen D, Andersen P, et al. Site-Specific DC Surface Signatures Influence CD4+ T Cell Co-stimulation and Lung-Homing. Front Immunol. 2019;10(JULY).

136. Nguyen P V., Kafka JK, Ferreira VH, Roth K, Kaushic C. Innate and adaptive immune responses in male and female reproductive tracts in homeostasis and following HIV infection. Cell Mol Immunol. 2014;11(5):410–27.

137. Nguyen P V., Kafka JK, Ferreira VH, Roth K, Kaushic C. Innate and adaptive immune responses in male and female reproductive tracts in homeostasis and following HIV infection. Cell Mol Immunol [Internet]. 2014;11(5):410–27. Available from: http://dx.doi.org/10.1038/cmi.2014.41

138. Weissenbacher ER. Immunology of the female genital tract. Vol. 9783642149, Immunology of the Female Genital Tract. 2014. 1–262 p.

139. Monin L, Whettlock EM, Male V. Immune responses in the human female reproductive tract. Immunology. 2020;160(2):106–15.

140. Agostinis C, Mangogna A, Bossi F, Ricci G, Kishore U, Bulla R. Uterine immunity and microbiota: A shifting paradigm. Front Immunol. 2019;10(OCT).

141. Rodriguez Garcia M, Patel M V., Shen Z, Fahey J V., Biswas N, Mestecky J, et al. Mucosal Immunity in the Human Female Reproductive Tract [Internet]. Fourth Edi. Vols. 2–2, Mucosal Immunology: Fourth Edition. Elsevier; 2015. 2097–2124 p. Available from: http://dx.doi.org/10.1016/B978-0-12-415847-4.00108-7

142. Duluc D, Gannevat J, Anguiano E, Zurawski S, Carley M, Boreham M, et al. Functional diversity of human vaginal APC subsets in directing T-cell responses. Mucosal Immunol. 2013;6(3):626–38.

143. Weinberg A, Enomoto L, Marcus R, Canniff J. Effect of menstrual cycle variation in female sex hormones on cellular immunity and regulation. J Reprod Immunol [Internet]. 2011;89(1):70–7. Available from: http://dx.doi.org/10.1016/j.jri.2010.11.009

144. Weissenbacher ER. Immunology of the female genital tract. Vol. 9783642149, Immunology of the Female Genital Tract. 2014. 1–262 p.

145. Rodriguez Garcia M, Patel M V., Shen Z, Fahey J V., Biswas N, Mestecky J, et al. Mucosal Immunity in the Human Female Reproductive Tract. In: Mucosal Immunology: Fourth Edition. 2015. p. 2097–124.

146. Woodward Davis AS, Vick SC, Pattacini L, Voillet V, Hughes SM, Lentz GM, et al. The human memory T cell compartment changes across tissues of the female reproductive tract. Mucosal Immunol. 2021;14(4):862–72.

147. Rodriguez Garcia M, Patel M V., Shen Z, Fahey J V., Biswas N, Mestecky J, et al. Mucosal Immunity in the Human Female Reproductive Tract. In: Mucosal Immunology: Fourth Edition. 2015. p. 2097–124.

148. Johansson EL, Rudin A, Wassén L, Holmgren J. Distribution of lymphocytes and adhesion molecules in human cervix and vagina. Immunology. 1999;96(2):272–7.

149. Johansson EL, Rudin A, Wassén L, Holmgren J. Distribution of lymphocytes and adhesion molecules in human cervix and vagina. Immunology. 1999;96(2):272–7.

150. Lee SK, Kim CJ, Kim DJ, Kang J hyun. Immune Cells in the Female Reproductive Tract. Immune Netw. 2015;15(1):16.

151. Monin L, Whettlock EM, Male V. Immune responses in the human female reproductive tract. Immunology. 2020;160(2):106–15.

152. Weissenbacher ER. Immunology of the female genital tract. Vol. 9783642149, Immunology of the Female Genital Tract. 2014. 1–262 p.

153. Duluc D, Gannevat J, Anguiano E, Zurawski S, Carley M, Boreham M, et al. Functional diversity of human vaginal APC subsets in directing T-cell responses. Mucosal Immunol. 2013;6(3):626–38.

154. Lee SK, Kim CJ, Kim DJ, Kang J hyun. Immune Cells in the Female Reproductive Tract. Immune Netw. 2015;15(1):16.

155. Poppe WAJ, Drijkoningen M, Ide PS, Lauweryns JM, Van Assche FA. Lymphocytes and dendritic cells in the normal uterine cervix. An immunohistochemical study. European Journal of Obstetrics and Gynecology and Reproductive Biology. 1998;81(2):277–82.

156. Monin L, Whettlock EM, Male V. Immune responses in the human female reproductive tract. Immunology. 2020;160(2):106–15.

157. Duluc D, Gannevat J, Anguiano E, Zurawski S, Carley M, Boreham M, et al. Functional diversity of human vaginal APC subsets in directing T-cell responses. Mucosal Immunol. 2013;6(3):626–38.

158. Chambers M, Rees A, Cronin JG, Nair M, Jones N, Thornton CA. Macrophage Plasticity in Reproduction and Environmental Influences on Their Function. Front Immunol. 2021;11(January):1–16.

159. Nagamatsu T, Schust DJ. REVIEW ARTICLE: The Contribution of Macrophages to Normal and Pathological Pregnancies. American Journal of Reproductive Immunology [Internet]. 2010 Jun 1 [cited 2023 Jun 10];63(6):460–71. Available from: https://onlinelibrary.wiley.com/doi/full/10.1111/j.1600-0897.2010.00813.x

160. Duluc D, Gannevat J, Anguiano E, Zurawski S, Carley M, Boreham M, et al. Functional diversity of human vaginal APC subsets in directing T-cell responses. Mucosal Immunology 2013 6:3 [Internet]. 2012 Nov 7 [cited 2023 Jun 10];6(3):626–38. Available from: https://www.nature.com/articles/mi2012104

161. Iijima N, Thompson JM, Iwasaki A. Dendritic cells and macrophages in the genitourinary tract. Mucosal Immunol [Internet]. 2008 [cited 2023 Jun 10];1(6):451. Available from: /pmc/articles/PMC2684461/

162. Lee SK, Kim CJ, Kim DJ, Kang J hyun. Immune Cells in the Female Reproductive Tract. Immune Netw [Internet]. 2015 [cited 2023 Jun 10];15(1):16. Available from: /pmc/articles/PMC4338264/

163. Monin L, Whettlock EM, Male V. Immune responses in the human female reproductive tract. Immunology [Internet]. 2020 Jun 1 [cited 2023 Jun 10];160(2):106–15. Available from: https://onlinelibrary.wiley.com/doi/full/10.1111/imm.13136

164. Vicetti Miguel RD, Harvey SAK, LaFramboise WA, Reighard SD, Matthews DB, Cherpes TL. Human Female Genital Tract Infection by the Obligate Intracellular

Bacterium Chlamydia trachomatis Elicits Robust Type 2 Immunity. PLoS One [Internet]. 2013 Mar 13 [cited 2023 Jun 10];8(3):e58565. Available from: https://journals.plos.org/plosone/article?id=10.1371/journal.pone.0058565

165. Lee SK, Kim CJ, Kim DJ, Kang J hyun. Immune Cells in the Female Reproductive Tract. Immune Netw. 2015;15(1):16.

166. Cantero-Pérez J, Grau-Expósito J, Serra-Peinado C, Rosero DA, Luque-Ballesteros L, Astorga-Gamaza A, et al. Resident memory T cells are a cellular reservoir for HIV in the cervical mucosa. Nat Commun [Internet]. 2019;10(1). Available from: http://dx.doi.org/10.1038/s41467-019-12732-2

167. Woodward Davis AS, Vick SC, Pattacini L, Voillet V, Hughes SM, Lentz GM, et al. The human memory T cell compartment changes across tissues of the female reproductive tract. Mucosal Immunol. 2021;14(4):862–72.

168. Yüzen D, Arck PC, Thiele K. Tissue-resident immunity in the female and male reproductive tract. Seminars in Immunopathology 2022 44:6 [Internet]. 2022 Apr 29 [cited 2023 Jun 11];44(6):785–99. Available from: https://link.springer.com/article/10.1007/s00281-022-00934-8

169. Wira CR, Rodriguez-Garcia M, Patel M V. The role of sex hormones in immune protection of the female reproductive tract. Nat Rev Immunol [Internet]. 2015;15(4):217–30. Available from: http://dx.doi.org/10.1038/nri3819

170. Woodward Davis AS, Vick SC, Pattacini L, Voillet V, Hughes SM, Lentz GM, et al. The human memory T cell compartment changes across tissues of the female reproductive tract. Mucosal Immunol [Internet]. 2021;14(4):862–72. Available from: http://dx.doi.org/10.1038/s41385-021-00406-6

171. Collins MK, McCutcheon CR, Petroff MG. Impact of Estrogen and Progesterone on Immune Cells and Host–Pathogen Interactions in the Lower Female Reproductive Tract. The Journal of Immunology [Internet]. 2022 Oct 15 [cited 2023 Jun 10];209(8):1437–49. Available from: https://dx.doi.org/10.4049/jimmunol.2200454

172. Bagri P, Ghasemi R, McGrath JJC, Thayaparan D, Yu E, Brooks AG, et al. Estradiol Enhances Antiviral CD4+ Tissue-Resident Memory T Cell Responses following Mucosal Herpes Simplex Virus 2 Vaccination through an IL-17-Mediated Pathway. J Virol [Internet]. 2021 Dec 9 [cited 2023 Jun 10];95(1). Available from: /pmc/articles/PMC7737739/

173. Ssemaganda A, Cholette F, Perner M, Kambaran C, Adhiambo W, Wambugu PM, et al. Endocervical Regulatory T Cells Are Associated With Decreased Genital Inflammation and Lower HIV Target Cell Abundance. Front Immunol. 2021 Sep 23;12:726472.

174. Yüzen D, Arck PC, Thiele K. Tissue-resident immunity in the female and male reproductive tract. Semin Immunopathol. 2022;

175. Lange J, Rivera-Ballesteros O, Buggert M. Human mucosal tissue-resident memory T cells in health and disease. Mucosal Immunol. 2022;15(3):389–97.

176. Woodward Davis AS, Vick SC, Pattacini L, Voillet V, Hughes SM, Lentz GM, et al. The human memory T cell compartment changes across tissues of the female reproductive tract. Mucosal Immunol. 2021;14(4):862–72.

177. Marks E, Helgeby A, Andersson JO, Schön K, Lycke NY. CD4+ T-cell immunity in the female genital tract is critically dependent on local mucosal immunization. Eur J Immunol. 2011;41(9):2642–53.

178. McKinnon LR, Nyanga B, Chege D, Izulla P, Kimani M, Huibner S, et al. Characterization of a Human Cervical CD4+ T Cell Subset Coexpressing Multiple Markers of HIV Susceptibility. The Journal of Immunology [Internet]. 2011 Dec 1 [cited 2023 Jun 11];187(11):6032–42. Available from: https://dx.doi.org/10.4049/jimmunol.1101836

179. Cantero-Pérez J, Grau-Expósito J, Serra-Peinado C, Rosero DA, Luque-Ballesteros L, Astorga-Gamaza A, et al. Resident memory T cells are a cellular reservoir for HIV in the cervical mucosa. Nature Communications 2019 10:1 [Internet]. 2019 Oct 18 [cited 2022 Jul 8];10(1):1–16. Available from: https://www.nature.com/articles/s41467-019-12732-2

180. Yüzen D, Arck PC, Thiele K. Tissue-resident immunity in the female and male reproductive tract. Seminars in Immunopathology 2022 44:6 [Internet]. 2022 Apr 29 [cited 2023 Jun 10];44(6):785–99. Available from: https://link.springer.com/article/10.1007/s00281-022-00934-8

181. Shanmugasundaram U, Critchfield JW, Pannell J, Perry J, Giudice LC, Smith-Mccune K, et al. Phenotype and functionality of CD4+ and CD8+ T cells in the upper reproductive tract of healthy premenopausal women. Am J Reprod Immunol [Internet]. 2014 Feb [cited 2023 Jun 12];71(2):95. Available from: /pmc/articles/PMC3947236/

182. Pattacini L, Woodward Davis A, Czartoski J, Mair F, Presnell S, Hughes SM, et al. A pro-inflammatory CD8+ T-cell subset patrols the cervicovaginal tract. Mucosal Immunol [Internet]. 2019 Sep 1 [cited 2023 Jun 12];12(5):1118. Available from: /pmc/articles/PMC6717561/

183. Rodriguez-Garcia M, Shen Z, Fortier JM, Wira CR. Differential Cytotoxic Function of Resident and Non-resident CD8+ T Cells in the Human Female Reproductive Tract Before and After Menopause. Front Immunol [Internet]. 2020 Jun 4 [cited 2023 Jun 12];11:1096. Available from: /pmc/articles/PMC7287154/

184. Yüzen D, Arck PC, Thiele K. Tissue-resident immunity in the female and male reproductive tract. Semin Immunopathol. 2022;

185. Anipindi VC, Bagri P, Dizzell SE, Jiménez-Saiz R, Jordana M, Snider DP, et al. IL-17 Production by γδ + T Cells Is Critical for Inducing T h 17 Responses in the Female Genital Tract and Regulated by Estradiol and Microbiota. Immunohorizons. 2019;3(7):317–30.

186. Alcaide ML, Strbo N, Romero L, Jones DL, Rodriguez VJ, Arheart K, et al. Bacterial vaginosis is associated with loss of gamma delta T cells in the female reproductive tract in women in the Miami Women Interagency HIV Study (WIHS): A cross sectional study. PLoS One. 2016;11(4).

187. Anipindi VC, Bagri P, Dizzell SE, Jiménez-Saiz R, Jordana M, Snider DP, et al. IL-17 Production by γδ + T Cells Is Critical for Inducing T h 17 Responses in the Female Genital Tract and Regulated by Estradiol and Microbiota. Immunohorizons. 2019;3(7):317–30.

188. Cisternas IS, Salazar JC, García-Angulo VA. Overview on the bacterial iron-riboflavin metabolic axis. Front Microbiol. 2018;9(JUL).

189. Gibbs A, Leeansyah E, Introini A, Paquin-Proulx D, Hasselrot K, Andersson E, et al. MAIT cells reside in the female genital mucosa and are biased towards IL-17 and IL-22 production in response to bacterial stimulation. Mucosal Immunol. 2017;10(1):35–45.

190. Meermeier EW, Harriff MJ, Karamooz E, Lewinsohn DM. MAIT cells and microbial immunity. Immunol Cell Biol [Internet]. 2018 Jul 1 [cited 2023 Jun 14];96(6):607–17. Available from: https://onlinelibrary.wiley.com/doi/full/10.1111/imcb.12022

191. Gibbs A, Leeansyah E, Introini A, Paquin-Proulx D, Hasselrot K, Andersson E, et al. MAIT cells reside in the female genital mucosa and are biased towards IL-17 and IL-22 production in response to bacterial stimulation. Mucosal Immunology 2017 10:1 [Internet]. 2016 Apr 6 [cited 2023 Jun 14];10(1):35–45. Available from: https://www.nature.com/articles/mi201630

192. Yüzen D, Arck PC, Thiele K. Tissue-resident immunity in the female and male reproductive tract. Seminars in Immunopathology 2022 44:6 [Internet]. 2022 Apr 29 [cited 2023 Jun 14];44(6):785–99. Available from: https://link.springer.com/article/10.1007/s00281-022-00934-8

193. Gibbs A, Leeansyah E, Introini A, Paquin-Proulx D, Hasselrot K, Andersson E, et al. MAIT cells reside in the female genital mucosa and are biased towards IL-17 and IL-22 production in response to bacterial stimulation. Mucosal Immunol [Internet]. 2017;10(1):35–45. Available from: http://dx.doi.org/10.1038/mi.2016.30

194. Bister J, Crona Guterstam Y, Strunz B, Dumitrescu B, Haij Bhattarai K, Özenci V, et al. Human endometrial MAIT cells are transiently tissue resident and respond to Neisseria gonorrhoeae. Mucosal Immunol. 2021;14(2):357–65.

195. Kaipe H, Raffetseder J, Ernerudh J, Solders M, Tiblad E. MAIT Cells at the Fetal-Maternal Interface During Pregnancy. Front Immunol. 2020 Aug 19;11:567785.

196. Boyson JE, Rybalov B, Koopman LA, Exley M, Balk SP, Racke FK, et al. CD1d and invariant NKT cells at the human maternal-fetal interface. Proc Natl Acad Sci U S A. 2002;99(21):13741–6.

197. Armitage CW, Carey AJ, Bryan ER, Kollipara A, Trim LK, Beagley KW. Pathogenic NKT cells attenuate urogenital chlamydial clearance and enhance infertility. Scand J Immunol. 2023;(October 2022):1–16.

198. Shekhar S, Joyee AG, Yang X. Dynamics of NKT-cell responses to chlamydial infection. Front Immunol. 2015;6(MAY):1–8.

199. WHO. Sexually transmitted infections (STIs). 2022.

200. ECDC. Surveillance Atlas of Infectious Diseases. 2022.

201. López de Munain J. Epidemiology and current control of sexually transmitted infections. The role of STI clinics. Enferm Infecc Microbiol Clin. 2019;37(1):45–9.

202. Piñeiro L, Galán JC, Vall-Mayans M. Infecciones por Chlamydia trachomatis (incluye linfogranuloma venéreo) y Mycoplasma genitalium. Enfermedades Infecciosas y Microbiología Clínicaf. 2019;37(8):525–34.

203. WHO. Sexually transmitted infections (STIs). 2022.

204. ECDC. Surveillance Atlas of Infectious Diseases. 2022.

205. López de Munain J. Epidemiology and current control of sexually transmitted infections. The role of STI clinics. Enferm Infecc Microbiol Clin. 2019;37(1):45–9.

206. Piñeiro L, Galán JC, Vall-Mayans M. Infecciones por Chlamydia trachomatis (incluye linfogranuloma venéreo) y Mycoplasma genitalium. Enfermedades Infecciosas y Microbiología Clínicaf. 2019;37(8):525–34.

207. Observatorio de ITS en Mujeres Españolas | Bloom [Internet]. [cited 2023 Jun 14]. Available from: https://bebloomers.com/observatorio-its-mujeres-espana/

208. Sexually transmitted infections (STIs) [Internet]. [cited 2022 Jul 13]. Available from: https://www.who.int/news-room/fact-sheets/detail/sexually-transmitted-infections-(stis)

209. Ahmed SM, Al-Doujaily H, Johnson MA, Kitchen V, Reid WMN, Poulter LW. Immunity in the female lower genital tract and the impact of HIV infection. Scand J Immunol. 2001;54(1–2):225–38.

210. Lowndes CM, Fenton KA. Surveillance systems for STIs in the European Union: Facing a changing epidemiology. Sex Transm Infect. 2004;80(4):264–71.

211. Ahmed SM, Al-Doujaily H, Johnson MA, Kitchen V, Reid WMN, Poulter LW. Immunity in the female lower genital tract and the impact of HIV infection. Scand J Immunol. 2001;54(1–2):225–38.

212. Murray SM, McKay PF. Chlamydia trachomatis: Cell biology, immunology and vaccination. Vaccine. 2021;39(22):2965–75.

213. Häcker G. Biology of chlamydia. Springer; 2018.

214. Murray SM, McKay PF. Chlamydia trachomatis: Cell biology, immunology and vaccination. Vaccine. 2021;39(22):2965–75.

215. Häcker G. Biology of chlamydia. Springer; 2018.

216. De Clercq E, Kalmar I, Vanrompay D. Animal models for studying female genital tract infection with chlamydia trachomatis. Infect Immun. 2013;81(9):3060–7.

217. Hafner L, Beagley K, Timms P. Chlamydia trachomatis infection: Host immune responses and potential vaccines. Mucosal Immunol. 2008;1(2):116–30.

218. Agrawal T, Vats V, Salhan S, Mittal A. The mucosal immune response to Chlamydia trachomatis infection of the reproductive tract in women. J Reprod Immunol. 2009;83(1–2):173–8.

219. De Clercq E, Kalmar I, Vanrompay D. Animal models for studying female genital tract infection with chlamydia trachomatis. Infect Immun. 2013;81(9):3060–7.

220. Marks E, Tam MA, Lycke NY. The female lower genital tract is a privileged compartment with IL-10 producing dendritic cells and poor Th1 immunity following Chlamydia trachomatis infection. PLoS Pathog. 2010;6(11).

221. Reddy BS, Rastogi S, Das B, Salhan S, Verma S, Mittal A. Cytokine expression pattern in the genital tract of Chlamydia trachomatis positive infertile women - Implication for T-cell responses. Clin Exp Immunol. 2004;137(3):552–8.

222. Vasilevsky S, Greub G, Nardelli-Haefliger D, Baud D. Genital Chlamydia trachomatis: Understanding the roles of innate and adaptive immunity in vaccine research. Clin Microbiol Rev. 2014;27(2):346–70.

223. Hafner L, Beagley K, Timms P. Chlamydia trachomatis infection: Host immune responses and potential vaccines. Mucosal Immunol. 2008;1(2):116–30.

224. Agrawal T, Vats V, Salhan S, Mittal A. The mucosal immune response to Chlamydia trachomatis infection of the reproductive tract in women. J Reprod Immunol. 2009;83(1–2):173–8.

225. De La Maza LM, Zhong G, Brunham RC. Update on Chlamydia trachomatis Vaccinology. Clinical and Vaccine Immunology [Internet]. 2017 Apr 1 [cited 2023

Aug 15];24(4). Available from: https://journals.asm.org/doi/10.1128/CVI.00543-16

226. Mitchell C, Marrazzo J. Bacterial Vaginosis and the Cervicovaginal Immune Response. American Journal of Reproductive Immunology. 2014;71(6):555–63.

227. Łaniewski P, Herbst-Kralovetz MM. Bacterial vaginosis and health-associated bacteria modulate the immunometabolic landscape in 3D model of human cervix. NPJ Biofilms Microbiomes. 2021;7(1).

228. Chen X, Lu Y, Chen T, Li R. The Female Vaginal Microbiome in Health and Bacterial Vaginosis. Front Cell Infect Microbiol. 2021 Apr 7;11:631972.

229. Mwatelah R, McKinnon LR, Baxter C, Abdool Karim Q, Abdool Karim SS. Mechanisms of sexually transmitted infection-induced inflammation in women: implications for HIV risk. J Int AIDS Soc. 2019;22(S6).

230. Hearps AC, Tyssen D, Srbinovski D, Bayigga L, Diaz DJD, Aldunate M, et al. Vaginal lactic acid elicits an anti-inflammatory response from human cervicovaginal epithelial cells and inhibits production of pro-inflammatory mediators associated with HIV acquisition. Mucosal Immunol. 2017;10(6):1480–90.

231. WHO. HIV/AIDS. 2022.

232. Rebbapragada A, Howe K, Wachihi C, Pettengell C, Sunderji S, Huibner S, et al. Bacterial vaginosis in HIV-infected women induces reversible alterations in the cervical immune environment. J Acquir Immune Defic Syndr (1988). 2008;49(5):520–2.

233. Schellenberg JJ, Card CM, Ball TB, Mungai JN, Irungu E, Kimani J, et al. Bacterial vaginosis, HIV serostatus and T-cell subset distribution in a cohort of East African commercial sex workers: Retrospective analysis. AIDS. 2012;26(3):387–93.

234. Delgado-Diaz DJ, Tyssen D, Hayward JA, Gugasyan R, Hearps AC, Tachedjian G. Distinct Immune Responses Elicited From Cervicovaginal Epithelial Cells by Lactic Acid and Short Chain Fatty Acids Associated With Optimal and Non-optimal Vaginal Microbiota. Front Cell Infect Microbiol. 2020;9.

235. Mitchell C, Marrazzo J. Bacterial Vaginosis and the Cervicovaginal Immune Response. American Journal of Reproductive Immunology. 2014;71(6):555–63.

236. Bartkevičienė D, Dumalakienė I, Šilkūnas M, Drąsutienė G, Arlauskienė A, Zakarevičienė J. Bacterial vaginosis : risk factors and vaginal. epublications.vu.lt. 2011;21(6):10–5.

237. Mwatelah R, McKinnon LR, Baxter C, Abdool Karim Q, Abdool Karim SS. Mechanisms of sexually transmitted infection-induced inflammation in women: implications for HIV risk. J Int AIDS Soc. 2019;22(S6).

238. Rebbapragada A, Howe K, Wachihi C, Pettengell C, Sunderji S, Huibner S, et al. Bacterial vaginosis in HIV-infected women induces reversible alterations in the cervical immune environment. J Acquir Immune Defic Syndr (1988). 2008;49(5):520–2.

239. WHO. HIV/AIDS. 2022.

240. Amabebe E, Anumba DOC. Mechanistic Insights into Immune Suppression and Evasion in Bacterial Vaginosis. Curr Microbiol. 2022;79(3).

241. Borgdorff H, Gautam R, Armstrong SD, Xia D, Ndayisaba GF, Van Teijlingen NH, et al. Cervicovaginal microbiome dysbiosis is associated with proteome changes related to alterations of the cervicovaginal mucosal barrier. Mucosal Immunol. 2016;9(3):621–33.

242. Łaniewski P, Herbst-Kralovetz MM. Bacterial vaginosis and health-associated bacteria modulate the immunometabolic landscape in 3D model of human cervix. NPJ Biofilms Microbiomes. 2021;7(1).

243. Schellenberg JJ, Card CM, Ball TB, Mungai JN, Irungu E, Kimani J, et al. Bacterial vaginosis, HIV serostatus and T-cell subset distribution in a cohort of East African commercial sex workers: Retrospective analysis. AIDS. 2012;26(3):387–93.

244. de Clercq E, Kalmar I, Vanrompay D. Animal Models for Studying Female Genital Tract Infection with Chlamydia trachomatis. Infect Immun [Internet]. 2013 [cited 2022 Aug 29];81(9):3060. Available from: /pmc/articles/PMC3754237/

245. Rank RG, Whittum-Hudson JA. Protective Immunity to Chlamydial Genital Infection: Evidence from Animal Studies. J Infect Dis [Internet]. 2010 Jun 15 [cited 2022 Aug 29];201(Supplement_2):S168–77. Available from: https://academic.oup.com/jid/article/201/Supplement_2/S168/806569

246. Taylor-Robinson D, Thomas BJ. The role of Chlamydia trachomatis in genital-tract and associated diseases. J Clin Pathol. 1980;33(3):205–33.

247. Dockterman J, Coers J. Immunopathogenesis of genital Chlamydia infection: insights from mouse models. Pathog Dis [Internet]. 2021 Apr 5 [cited 2022 Aug 29];79(4):12. Available from: https://academic.oup.com/femspd/article/79/4/ftab012/6128668

248. de Clercq E, Kalmar I, Vanrompay D. Animal models for studying female genital tract infection with chlamydia trachomatis. Infect Immun [Internet]. 2013 [cited 2022 Aug 29];81(9):3060–7. Available from: https://journals.asm.org/doi/10.1128/IAI.00357-13

249. Sturdevant GL, Caldwell HD. Innate immunity is sufficient for the clearance of Chlamydia trachomatis from the female mouse genital tract. Pathog Dis [Internet]. 2014 Oct 1 [cited 2022 Aug 29];72(1):70–3. Available from: https://academic.oup.com/femspd/article/72/1/70/540814

250. Morrison SG, Su H, Caldwell HD, Morrison RP. Immunity to murine Chlamydia trachomatis genital tract reinfection involves B cells and CD4+ T cells but not CD8+ T cells. Infect Immun [Internet]. 2000 [cited 2022 Aug 29];68(12):6979–87. Available from: https://journals.asm.org/doi/10.1128/IAI.68.12.6979-6987.2000

251. Russell MW, Mestecky J, Strober W, Lambrecht BN, Kelsall BL, Cheroutre H. Overview: The Mucosal Immune System. In: Mucosal Immunology: Fourth Edition. 2015. p. 3–8.

252. Le Bourhis L, Martin E, Péguillet I, Guihot A, Froux N, Coré M, et al. Antimicrobial activity of mucosal-associated invariant T cells. Nat Immunol. 2010;11(8):701–8.

253. Dusseaux M, Martin E, Serriari N, Péguillet I, Premel V, Louis D, et al. Human MAIT cells are xenobiotic-resistant, tissue-targeted, CD161 hi IL-17-secreting T cells. Blood. 2011;117(4):1250–9.

254. Hayday A, Deban L. Mucosal T Cell Receptor γδ Intraepithelial T Cells. In: Mucosal Immunology: Fourth Edition. 2015. p. 765–76.

255. Sheridan BS, Romagnoli PA, Pham QM, Fu HH, Alonzo F, Schubert WD, et al. γδ T Cells Exhibit Multifunctional and Protective Memory in Intestinal Tissues. Immunity. 2013;39(1):184–95.

256. Stagg AJ, Kamm MA, Knight SC. Intestinal dendritic cells increase T cell expression of α4β7 integrin. Eur J Immunol. 2002;32(5):1445–54.

257. Adekambi T, Ibegbu CC, Cagle S, Kalokhe AS, Wang YF, Hu Y, et al. Biomarkers on patient T cells diagnose active tuberculosis and monitor treatment response. J Clin Invest [Internet]. 2015 May 1 [cited 2023 May 29];125(5):1827–38. Available from: https://pubmed.ncbi.nlm.nih.gov/25822019/

258. Li LX, McSorley SJ. B Cells Enhance Antigen-Specific CD4 T Cell Priming and Prevent Bacteria Dissemination following Chlamydia muridarum Genital Tract Infection. PLoS Pathog [Internet]. 2013 Oct [cited 2023 May 29];9(10):e1003707. Available from: https://journals.plos.org/plospathogens/article?id=10.1371/journal.ppat.1003707

259. GSEA | MSigDB.

260. GSEA [Internet]. [cited 2022 Aug 10]. Available from: http://www.gsea-msigdb.org/gsea/index.jsp

261. Fujiwara D, Chen L, Wei B, Braun J. Small intestine CD11c+ CD8+ T cells suppress CD4+ T cell-induced immune colitis. Am J Physiol Gastrointest Liver Physiol. 2011;300(6):939–47.

262. Fergusson JR, Smith KE, Fleming VM, Rajoriya N, Newell EW, Simmons R, et al. CD161 defines a transcriptional and functional phenotype across distinct human T cell lineages. Cell Rep. 2014;9(3):1075–88.

263. Grivel JC, Margolis L. Use of human tissue explants to study human infectious agents. Nature Protocols 2009 4:2 [Internet]. 2009 Feb 5 [cited 2023 Jul 27];4(2):256–69. Available from: https://www.nature.com/articles/nprot.2008.245

264. Qualai J, Cantero J, Li LX, Carrascosa JM, Cabré E, Dern O, et al. Adhesion molecules associated with female genital tract infection. PLoS One. 2016;11(6).

265. Menzies FM, Oldham RS, Waddell C, Nelson SM, Nibbs RJB. A Comprehensive Profile of Chemokine Gene Expression in the Tissues of the Female Reproductive Tract in Mice. Immunol Invest. 2020 Apr 2;49(3):264–86.

266. Joo S, Suwanto A, Sato A, Nakahashi-Ouchida R, Mori H, Uchida Y, et al. A role for the CCR5–CCL5 interaction in the preferential migration of HSV-2-specific effector cells to the vaginal mucosa upon nasal immunization. Mucosal Immunol. 2019;12(6):1391–403.

267. Qualai J, Cantero J, Li LX, Carrascosa JM, Cabré E, Dern O, et al. Adhesion molecules associated with female genital tract infection. PLoS One. 2016 Jun 1;11(6).

268. Lin Y, Roberts TJ, Sriram V, Cho S, Brutkiewicz RR. Myeloid marker expression on antiviral CD8+ T cells following an acute virus infection. Eur J Immunol. 2003;33(10):2736–43.

269. Ju SA, Park SM, Lee SC, Kwon BS, Kim BS. Marked expansion of CD11c+CD8+ T-cells in melanoma-bearing mice induced by anti-4-1BB monoclonal antibody. Mol Cells. 2007;24(1):132–8.

270. Vinay DS, Kim CH, Choi BK, Kwon BS. Origins and functional basis of regulatory CD11c+CD8+ T cells. Eur J Immunol. 2009;39(6):1552–63.

271. Won EY, Cha K, Byun JS, Kim DU, Shin S, Ahn B, et al. The structure of the trimer of human 4-1BB ligand is unique among members of the tumor necrosis factor superfamily. Journal of Biological Chemistry. 2010;285(12):9202–10.

272. Parker BS, Rautela J, Hertzog PJ. Antitumour actions of interferons: Implications for cancer therapy. Nat Rev Cancer. 2016 Mar 1;16(3):131–44.

273. Tokura Y, Phadungsaksawasdi P, Kurihara K, Fujiyama T, Honda T. Pathophysiology of Skin Resident Memory T Cells. Front Immunol. 2021 Feb 3;11.

274. Pieren DKJ, Kuguel SG, Rosado J, Robles AG, Rey-Cano J, Mancebo C, et al. Limited induction of polyfunctional lung-resident memory T cells against SARS-CoV-2 by mRNA vaccination compared to infection. Nature Communications 2023 14:1 [Internet]. 2023 Apr 5;14(1):1887. Available from: https://www.nature.com/articles/s41467-023-37559-w

275. Rim S, Sakkestad ST, Zhou F, Gullaksen SE, Skavland J, Chauhan SK, et al. Dynamics of circulating lymphocytes responding to human experimental enterotoxigenic Escherichia coli infection. Eur J Immunol [Internet]. 2023 Apr 27

[cited 2023 Jun 26];2250254. Available from: https://onlinelibrary.wiley.com/doi/full/10.1002/eji.202250254

276. Maldonado L, Teague JE, Morrow MP, Jotova I, Wu TC, Wang C, et al. Intramuscular therapeutic vaccination targeting HPV16 induces T cell responses that localize in mucosal lesions. Sci Transl Med [Internet]. 2014 Jan 1 [cited 2023 Jun 26];6(221):221ra13-221ra13. Available from: https://www.ncbi.nlm.nih.gov/pmc/articles/pmid/24477000/?tool=EBI

277. Ellwanger JH, Secchi M, Aliberti J, Vangelista L. Editorial: CCR5: A receptor at the center stage in infection. Front Immunol. 2022 Oct 18;13:1054430.

278. Ellwanger JH, Kulmann-Leal B, Kaminski V de L, Rodrigues AG, Bragatte MA de S, Chies JAB. Beyond HIV infection: Neglected and varied impacts of CCR5 and CCR5Δ32 on viral diseases. Virus Res. 2020 Sep 1;286:198040.

279. Mohamed H, Gurrola T, Berman R, Collins M, Sariyer IK, Nonnemacher MR, et al. Targeting CCR5 as a Component of an HIV-1 Therapeutic Strategy. Front Immunol. 2022 Jan 20;12:816515.

280. McKinnon LR, Achilles SL, Bradshaw CS, Burgener A, Crucitti T, Fredricks DN, et al. The Evolving Facets of Bacterial Vaginosis: Implications for HIV Transmission. AIDS Res Hum Retroviruses [Internet]. 2019 Mar 1 [cited 2023 Jul 7];35(3):219–28. Available from: https://www.liebertpub.com/doi/10.1089/aid.2018.0304

281. Atashili J, Poole C, Ndumbe PM, Adimora AA, Smith JS. Bacterial vaginosis and HIV acquisition: A meta-analysis of published studies. AIDS [Internet]. 2008 Jul 7 [cited 2023 Jul 7];22(12):1493. Available from: /pmc/articles/PMC2788489/

282. Mirmonsef P, Krass L, Landay A, Spear GT. The Role of Bacterial Vaginosis and Trichomonas in HIV Transmission Across The Female Genital Tract. Curr HIV Res [Internet]. 2012 Nov 11 [cited 2023 Jul 7];10(3):202. Available from: /pmc/articles/PMC3788616/

283. Nava-Memije K, Hernández-Cortez C, Ruiz-González V, Saldaña-Juárez CA, Medina-Islas Y, Dueñas-Domínguez RA, et al. Bacterial Vaginosis and Sexually Transmitted Infections in an HIV-Positive Cohort. Frontiers in Reproductive Health. 2021 Apr 12;3:660672.

284. Cohen CR, Lingappa JR, Baeten JM, Ngayo MO, Spiegel CA, Hong T, et al. Bacterial Vaginosis Associated with Increased Risk of Female-to-Male HIV-1 Transmission: A Prospective Cohort Analysis among African Couples. PLoS Med [Internet]. 2012 [cited 2023 Jul 7];9(6):e1001251. Available from: https://journals.plos.org/plosmedicine/article?id=10.1371/journal.pmed.1001251

285. Foessleitner P, Petricevic L, Boerger I, Steiner I, Kiss H, Rieger A, et al. HIV infection as a risk factor for vaginal dysbiosis, bacterial vaginosis, and candidosis in pregnancy: A matched case-control study. Birth [Internet]. 2021 Mar 1 [cited 2023

Jul 7];48(1):139–46. Available from: https://onlinelibrary.wiley.com/doi/full/10.1111/birt.12526

286. Prabhu VM, Padwal V, Velhal S, Salwe S, Nagar V, Patil P, et al. Vaginal Epithelium Transiently Harbours HIV-1 Facilitating Transmission. Front Cell Infect Microbiol. 2021 Mar 17;11:634647.

287. Saczonek AO, Krajewska-Włodarczyk M, Kasprowicz-Furmańczyk M, Placek W. Immunological memory of psoriatic lesions. Vol. 21, International Journal of Molecular Sciences. 2020.

288. Wein AN, McMaster SR, Takamura S, Dunbar PR, Cartwright EK, Hayward SL, et al. CXCR6 regulates localization of tissue-resident memory CD8 T cells to the airways. Journal of Experimental Medicine. 2019;216(12):2748–62.

289. Di Pilato M, Kfuri-Rubens R, Pruessmann JN, Ozga AJ, Messemaker M, Cadilha BL, et al. CXCR6 positions cytotoxic T cells to receive critical survival signals in the tumor microenvironment. Cell [Internet]. 2021;184(17):4512-4530.e22. Available from: https://doi.org/10.1016/j.cell.2021.07.015

290. Mabrouk N, Tran T, Sam I, Pourmir I, Gruel N, Granier C, et al. CXCR6 expressing T cells: Functions and role in the control of tumors. Front Immunol. 2022;13(October):1–9.

291. Ho AW, Kupper TS. T cells and the skin: from protective immunity to inflammatory skin disorders. Vol. 19, Nature Reviews Immunology. 2019. p. 490–502.

292. Davila SJ, Olive AJ, Starnbach MN. Integrin α 4 β 1 Is Necessary for CD4 + T Cell–Mediated Protection against Genital Chlamydia trachomatis Infection. The Journal of Immunology. 2014;192(9):4284–93.

293. Perciani CT, Jaoko W, Farah B, Ostrowski MA, Anzala O, MacDonald KS. αeβ7, α4β7 and α4β1 integrin contributions to T cell distribution in blood, cervix and rectal tissues: Potential implications for HIV transmission. PLoS One. 2018 Feb 1;13(2).

294. Cooney LA, Gupta M, Thomas S, Mikolajczak S, Choi KY, Gibson C, et al. Short-lived effector CD8 T cells induced by genetically attenuated malaria parasite vaccination express CD11c. Infect Immun. 2013 Nov;81(11):4171–81.

295. Cooney LA, Gupta M, Thomas S, Mikolajczak S, Choi KY, Gibson C, et al. Short-lived effector CD8 T cells induced by genetically attenuated malaria parasite vaccination express CD11c. Infect Immun. 2013;81(11):4171–81.

296. Bezman NA, Kim CC, Sun JC, Min-Oo G, Hendricks DW, Kamimura Y, et al. ImmGen Report: Molecular definition of Natural Killer cell identity and activation. Nat Immunol. 2012;13(10):1000–9.

297. Gutiérrez-Hoya A, Soto-Cruz I. NK cell regulation in cervical cancer and strategies for immunotherapy. Vol. 10, Cells. Multidisciplinary Digital Publishing Institute; 2021. p. 3104.

298. Moll-Bernardes R, Fortier SC, Sousa AS, Lopes RD, Vera N, Conde L, et al. NKG2A Expression among CD8 Cells Is Associated with COVID-19 Progression in Hypertensive Patients: Insights from the BRACE CORONA Randomized Trial. J Clin Med [Internet]. 2022 Jul 1 [cited 2023 Jul 31];11(13):3713. Available from: /pmc/articles/PMC9267446/

299. McMahon CW, Raulet DH. Expression and function of NK cell receptors in CD8+ T cells. Curr Opin Immunol. 2001;13(4):465–70.

300. Roy Chowdhury R, Valainis JR, Dubey M, von Boehmer L, Sola E, Wilhelmy J, et al. NK-like CD8+ γδ T cells are expanded in persistent Mycobacterium tuberculosis infection. Sci Immunol [Internet]. 2023 Mar 1 [cited 2023 Jul 10];8(81):eade3525. Available from: https://www.science.org/doi/10.1126/sciimmunol.ade3525

301. Cazzetta V, Bruni E, Terzoli S, Carenza C, Franzese S, Piazza R, et al. NKG2A expression identifies a subset of human Vδ2 T cells exerting the highest antitumor effector functions. Cell Rep. 2021 Oct 19;37(3):109871.

302. Borst L, Sluijter M, Sturm G, Charoentong P, Santegoets SJ, van Gulijk M, et al. NKG2A is a late immune checkpoint on CD8 T cells and marks repeated stimulation and cell division. Int J Cancer [Internet]. 2022 Feb 15 [cited 2023 Jul 10];150(4):688–704. Available from: https://onlinelibrary.wiley.com/doi/full/10.1002/ijc.33859

303. Koh JY, Kim DU, Moon BH, Shin EC. Human CD8+ T-Cell Populations That Express Natural Killer Receptors. Immune Netw [Internet]. 2023 [cited 2023 Jul 10];23(1). Available from: /pmc/articles/PMC9995994/

304. Choi SJ, Koh JY, Rha MS, Seo IH, Lee H, Jeong S, et al. KIR+CD8+ and NKG2A+CD8+ T cells are distinct innate-like populations in humans. Cell Rep [Internet]. 2023 Mar 28 [cited 2023 Jul 10];42(3). Available from: http://www.cell.com/article/S2211124723002474/fulltext

305. Godfrey D, MacDonald H. NKT cells: what's in a name? Nat Rev Immunol. 2004;4(3):231–7.

306. Fergusson JR, Smith KE, Fleming VM, Rajoriya N, Newell EW, Simmons R, et al. CD161 Defines a Transcriptional and Functional Phenotype across Distinct Human T Cell Lineages. Cell Rep [Internet]. 2014 Nov 11 [cited 2023 Jul 10];9(3):1075. Available from: /pmc/articles/PMC4250839/

307. Konduri V, Oyewole-Said D, Vazquez-Perez J, Weldon SA, Halpert MM, Levitt JM, et al. CD8+CD161+ T-Cells: Cytotoxic Memory Cells With High Therapeutic Potential. Front Immunol. 2021 Feb 1;11:613204.

308. Konduri V, Oyewole-Said D, Vazquez-Perez J, Weldon SA, Halpert MM, Levitt JM, et al. CD8+CD161+ T-Cells: Cytotoxic Memory Cells With High Therapeutic Potential. Front Immunol. 2021 Feb 1;11.

309. Fergusson JR, Smith KE, Fleming VM, Rajoriya N, Newell EW, Simmons R, et al. CD161 Defines a Transcriptional and Functional Phenotype across Distinct Human T Cell Lineages. Cell Rep. 2014 Nov 6;9(3):1075–88.

310. Karunathilaka A, Halstrom S, Price P, Holt M, Lutzky VP, Doolan DL, et al. CD161 expression defines new human γδ T cell subsets. Immunity and Ageing. 2022 Dec 1;19(1):1–8.

311. Provine NM, Binder B, FitzPatrick MEB, Schuch A, Garner LC, Williamson KD, et al. Unique and common features of innate-like human Vδ2+ γδT cells and mucosal-associated invariant T cells. Front Immunol. 2018 Apr 23;9(APR):756.

312. Duurland CL, Santegoets SJ, Abdulrahman Z, Loof NM, Sturm G, Wesselink TH, et al. CD161 expression and regulation defines rapidly responding effector CD4+ T cells associated with improved survival in HPV16-associated tumors. J Immunother Cancer. 2022;10(1).

313. Li Y, Li G, Zhang J, Wu X, Chen X. The Dual Roles of Human γδ T Cells: Anti-Tumor or Tumor-Promoting. Front Immunol. 2021;11(February):1–13.

314. Lawand M, Déchanet-Merville J, Dieu-Nosjean MC. Key features of gamma-delta T-cell subsets in human diseases and their immunotherapeutic implications. Front Immunol. 2017;8(JUN).

315. Brandes M, Willimann K, Moser B. Immunology: Professional antigen-presentation function by human γδ cells. Science (1979). 2005;309(5732):264–8.

316. Smythies LE, Denning TL, Smith PD. Mucosal Macrophages in Defense and Regulation. In: Mucosal Immunology: Fourth Edition. 2015. p. 543–56.

317. Maynard CL, Weaver CT. Effector CD4+ T Cells in the Intestines. In: Mucosal Immunology: Fourth Edition. 2015. p. 721–32.

318. Davey MS, Lin CY, Roberts GW, Heuston S, Brown AC, Chess JA, et al. Human neutrophil clearance of bacterial pathogens triggers anti-microbial γδ T cell responses in early infection. PLoS Pathog. 2011 May;7(5).

319. Pennington DJ, Vermijlen D, Wise EL, Clarke SL, Tigelaar RE, Hayday AC. The integration of conventional and unconventional T cells that characterizes cell-mediated responses. Vol. 87, Advances in Immunology. 2005. p. 27–59.

320. Cauley LS, Lefrançois L. Guarding the perimeter: Protection of the mucosa by tissue-resident memory T cells. Vol. 6, Mucosal Immunology. 2013. p. 14–23.

321. Nelson SA, Sant AJ. Potentiating Lung Mucosal Immunity Through Intranasal Vaccination. Front Immunol. 2021 Dec 14;12.

322. Hassert M, Harty JT. Tissue resident memory T cells- A new benchmark for the induction of vaccine-induced mucosal immunity. Front Immunol [Internet]. 2022 Oct 4 [cited 2023 May 22];13. Available from: /pmc/articles/PMC9581298/

323. Rosato PC, Beura LK, Masopust D. Tissue resident memory T cells and viral immunity. Vol. 22, Current Opinion in Virology. 2017. p. 44–50.

324. Lange J, Rivera-Ballesteros O, Buggert M. Human mucosal tissue-resident memory T cells in health and disease. Mucosal Immunology 2021 15:3 [Internet]. 2021 Nov 6 [cited 2023 May 20];15(3):389–97. Available from: https://www.nature.com/articles/s41385-021-00467-7

325. Farber DL, Yudanin NA, Restifo NP. Human memory T cells: Generation, compartmentalization and homeostasis. Vol. 14, Nature Reviews Immunology. 2014. p. 24–35.

326. Thome JJC, Farber DL. Emerging concepts in tissue-resident T cells: Lessons from humans. Vol. 36, Trends in Immunology. 2015. p. 428–35.

327. Moylan DC, Goepfert PA, Kempf MC, Saag MS, Richter HE, Mestecky J, et al. Diminished cd103 (αeβ7) expression on resident t cells from the female genital tract of hiv-positive women. Pathog Immun. 2016;1(2):371–89.

328. Zhu J, Koelle DM, Cao J, Vazquez J, Meei LH, Hladik F, et al. Virus-specific CD8+ T cells accumulate near sensory nerve endings in genital skin during subclinical HSV-2 reactivation. Journal of Experimental Medicine. 2007;204(3):595–603.

329. Rodriguez-Garcia M, Fortier JM, Barr FD, Wira CR. Aging impacts CD103+CD8+ T cell presence and induction by dendritic cells in the genital tract. Aging Cell. 2018 Jun 1;17(3):e12733.

330. Mami-Chouaib F, Tartour E. Editorial: Tissue resident memory T cells. Front Immunol. 2019 May 27;10(MAY):1018.

331. Hassert M, Harty JT. Tissue resident memory T cells- A new benchmark for the induction of vaccine-induced mucosal immunity. Front Immunol. 2022 Oct 4;13:5964.

332. Kaech SM, Wherry EJ, Ahmed R. Effector and memory T-cell differentiation: implications for vaccine development. Nature Reviews Immunology 2002 2:4 [Internet]. 2002 [cited 2023 May 20];2(4):251–62. Available from: https://www.nature.com/articles/nri778

333. Lavelle EC, Ward RW. Mucosal vaccines – fortifying the frontiers. Nature Reviews Immunology 2021 22:4 [Internet]. 2021 Jul 26 [cited 2023 May 20];22(4):236–50. Available from: https://www.nature.com/articles/s41577-021-00583-2

334. Fraser R, Orta-Resendiz A, Mazein A, Dockrell DH. Upper respiratory tract mucosal immunity for SARS-CoV-2 vaccines. Trends Mol Med [Internet]. 2023 Apr 1 [cited

2023 May 20];29(4):255–67. Available from: http://www.cell.com/article/S1471491423000175/fulltext

335. Stary G, Olive A, Radovic-Moreno AF, Gondek D, Alvarez D, Basto PA, et al. A mucosal vaccine against Chlamydia trachomatis generates two waves of protective memory T cells. Science (1979). 2015 Jun 19;348(6241).

336. Nizard M, Roussel H, Diniz MO, Karaki S, Tran T, Voron T, et al. Induction of resident memory T cells enhances the efficacy of cancer vaccine. Nat Commun. 2017 May 24;8.